RESEARCH

UDOT

Keeping Utah Moving

Utah Department of Transportation - Research Division
4501 South 2700 West - P.O. Box 148410 - SLC,UT 84114-8410

Report No. UT-20.28

DEVELOPMENT OF A MANAGEMENT GUIDE FOR CONCRETE BRIDGE DECKS IN UTAH

Prepared For:

Utah Department of Transportation
Research & Innovation Division

Final Report
December 2020

DISCLAIMER

The authors alone are responsible for the preparation and accuracy of the information, data, analysis, discussions, recommendations, and conclusions presented herein. The contents do not necessarily reflect the views, opinions, endorsements, or policies of the Utah Department of Transportation or the U.S. Department of Transportation. The Utah Department of Transportation makes no representation or warranty of any kind, and assumes no liability therefore. The authors also make no warranty, express or implied, regarding the suitability of findings documented in this report for a particular purpose and shall not be held liable under any circumstances for any direct, consequential, or other damages with respect to claims by users of any findings documented in this report, including claims based on allegations of errors, omissions, or negligence.

ACKNOWLEDGMENTS

The authors acknowledge the Utah Department of Transportation for funding this research. The authors also acknowledge the many members of the Brigham Young University (BYU) Materials and Pavements Research Group who assisted with data collection. The authors specifically recognize Amy L. McElwee, project manager for the BYU Materials and Pavements Research Group for her time and effort in helping to prepare Chapter 2 of this report.

TECHNICAL REPORT ABSTRACT

1. Report No. UT-20.28	2. Government Accession No. N/A	3. Recipient's Catalog No. N/A
4. Title and Subtitle DEVELOPMENT OF A MANAGEMENT GUIDE FOR CONCRETE BRIDGE DECKS IN UTAH		5. Report Date December 2020 6. Performing Organization Code N/A
7. Author(s) Tenli Waters Emery, Hannah Polanco, W. Spencer Guthrie, Ph.D.		8. Performing Organization Report No. N/A
9. Performing Organization Name and Address Brigham Young University Department of Civil and Environmental Engineering 430 Engineering Building Provo, UT 84602		10. Work Unit No. 5H08419H 11. Contract or Grant No. 15-8775
12. Sponsoring Agency Name and Address Utah Department of Transportation 4501 South 2700 West P.O. Box 148410 Salt Lake City, UT 84114-8410		13. Type of Report & Period Covered Final, December 2015 to November 2020 14. Sponsoring Agency Code PIC No. UT14.403
15. Supplementary Notes Prepared in cooperation with the Utah Department of Transportation and the U.S. Department of Transportation, Federal Highway Administration		

16. Abstract

The objectives of this research were to 1) investigate bridge deck condition assessment methods used in the field and laboratory, methods of managing bridge decks, and methods for estimating remaining bridge deck service life using computer models through a comprehensive literature review on these subjects; 2) collect and analyze field data from representative concrete bridge decks in Utah; and 3) develop a decision tree for concrete bridge deck management in Utah. Based on the results of field work and statistical analyses, placing an overlay within a year after construction is recommended. Removing SIPMFs after a deck age greater than 18 years is not likely to be effective at reversing the adverse effects of the SIPMFs on bridge deck condition and is not recommended. Bridge deck construction using internally cured concrete is not recommended for protecting against rebar corrosion. To the extent that excluding an automatic deck deicing system does not compromise public safety, automatic deck deicing systems are not recommended. To supplement the typical corrosion initiation threshold of 2.0 lb Cl^-/yd^3 of concrete for black bar, a corrosion initiation threshold of 8.0 lb Cl^-/yd^3 of concrete is recommended in this research for bridge decks with intact epoxy-coated rebar. For chloride concentrations less than 20 lb Cl^-/yd^3 of concrete as measured between reinforcing bars, an increase of up to 70 percent should be applied to estimate the corresponding chloride concentration of the concrete in direct contact with the rebar. The decision tree developed in this research includes 10 junctions and seven recommended treatments. The junctions require the user to address questions about surface type, degree of protection against water and chloride ion ingress, degree of deterioration, and years of additional service life needed; the answers lead to selection of treatment options ranging from repairing an overlay to full-depth bridge deck reconstruction.

17. Key Words Bridge deck management, chloride concentration, concrete bridge deck, condition assessment, corrosion, decision tree, preservation, rehabilitation		18. Distribution Statement Not restricted. Available through: UDOT Research & Innovation Div. 4501 South 2700 West P.O. Box 148410 Salt Lake City, UT 84114-8410 www.udot.utah.gov/go/research		23. Registrant's Seal N/A
19. Security Classification (of this report) Unclassified	20. Security Classification (of this page) Unclassified	21. No. of Pages 250	22. Price N/A	

TABLE OF CONTENTS

LIST OF TABLES

LIST OF FIGURES

LIST OF ACRONYMS

AASHTO	American Association of State Highway and Transportation Officials
ABC	accelerated bridge construction
ASCE	American Society of Civil Engineers
ASTM	American Society for Testing and Materials
BIR	bridge inspection report
BMS	bridge management system
BPT	British pendulum test
BYU	Brigham Young University
CH	calcium hydroxide
CSE	copper-copper sulfate reference electrode
C-S-H	calcium silicate hydrate
DOT	department of transportation
FHWA	Federal Highway Administration
GPM	galvanostatic pulse measurement
GPR	ground-penetrating radar
HCP	half-cell potential
HMWM	high-molecular-weight methacrylate
HPC	high-performance concrete
I-80	Interstate 80
I-215	Interstate 215
LMC	latex-modified concrete
LWFA	lightweight fine aggregate
MSC	microsilica concrete
NBI	National Bridge Inventory
PIA	petrographic image analysis
PPC	polyester polymer concrete
RCP	rapid chloride permeability
SIPMF	stay-in-place metal form
SN	skid number
SR-85	State Route 85

SR-190	State Route 190
UDOT	Utah Department of Transportation
UPRR	Union Pacific railroad
USW	ultrasonic waves
VEI	vertical electrical impedance

EXECUTIVE SUMMARY

The objectives of this research were to 1) investigate bridge deck condition assessment methods used in the field and laboratory, methods of managing bridge decks, and methods for estimating remaining bridge deck service life using computer models through a comprehensive literature review on these subjects; 2) collect and analyze field data from representative concrete bridge decks in Utah; and 3) develop a decision tree for concrete bridge deck management in Utah. As a result of the literature review performed for objective 1, a synthesis of existing information about condition assessment, bridge deck preservation and rehabilitation, bridge deck reconstruction, and estimating remaining service life using computer models was compiled. For objective 2, 15 bridge decks were strategically selected for testing in this research. Five bridge decks had bare concrete surfaces, five bridge decks had asphalt overlays, and five bridge decks had polymer overlays. Bridge deck testing included site layout, cover depth measurement, chloride concentration testing, chain dragging, half-cell potential testing, Schmidt rebound hammer testing, impact-echo testing, and vertical electrical impedance testing. Two-sample *t*-tests were performed to investigate the effects of selected bridge deck features, including polymer overlay application, deck age at polymer overlay application, overlay age, asphalt overlay application with and without a membrane, stay-in-place metal forms (SIPMFs), SIPMF removal, internally cured concrete, and use of an automatic deck deicing system. For objective 3, condition assessment methods were described in terms of test type, factors evaluated, equipment cost, data collection speed, required expertise, and traffic control for each method. Unit costs, expected treatment service life estimates, and factors addressed for the preservation, rehabilitation, and reconstruction methods most commonly used by the Utah Department of Transportation (UDOT) were also summarized. Bridge deck testing results were supplemented with information about current bridge deck management practices and treatment costs obtained from UDOT, as well as information about condition assessment and expected treatment service life, to develop a decision tree for concrete bridge deck management.

Based on the results of field work and statistical analyses, placing an overlay within a year after construction is recommended. Removing SIPMFs after a deck age greater than 18 years is not likely to be effective at reversing the adverse effects of the SIPMFs on bridge deck condition and is not recommended. Bridge deck construction using internally cured concrete is

not recommended for protecting against rebar corrosion. To the extent that excluding an automatic deck deicing system does not compromise public safety, automatic deck deicing systems are not recommended. To supplement the typical corrosion initiation threshold of 2.0 lb Cl^-/yd^3 of concrete for black bar, a corrosion initiation threshold of 8.0 lb Cl^-/yd^3 of concrete is recommended in this research for bridge decks with intact epoxy-coated rebar. For chloride concentrations less than 20 lb Cl^-/yd^3 of concrete as measured between reinforcing bars, an increase of up to 70 percent should be applied to estimate the corresponding chloride concentration of the concrete in direct contact with the rebar. The decision tree developed in this research includes 10 junctions and seven recommended treatments. The junctions require the user to address questions about surface type, degree of protection against water and chloride ion ingress, degree of deterioration, and years of additional service life needed; the answers lead to selection of treatment options ranging from repairing an overlay to full-depth bridge deck reconstruction. Revisions to the decision tree should be incorporated as additional methods, data, treatments, or other relevant information become available.

1.0 INTRODUCTION

1.1 Problem Statement

Concrete bridge deck deterioration is a continuous and gradual process that is affected by traffic loading, environmental factors, current deck condition, bridge design, and material properties (Mauch and Madanat 2001). The main cause of deck deterioration in northern and coastal regions is the corrosion of steel reinforcement due to salt exposure, which can lead to both severe damage and premature failure (Melhem and Cheng 2003, Tuttle 2005). Chloride ions from deicing salts diffuse into the bridge deck and eventually reach the depth of the reinforcement. Chloride ions can destroy the passive oxide film on steel and initiate corrosion (Mindess et al. 2003). Because corrosion products are expansive, the corrosion process leads to the development of tensile stresses in the concrete, eventually causing cracking, delamination, spalling, and potholes.

Despite many efforts to mitigate chloride-induced corrosion in concrete bridge decks, the rate of structural deterioration of bridge decks throughout the United States appears to be increasing, most likely due to the expanding use of deicing salts in cold regions; nationwide salt usage has increased from fewer than 1 million tons per year in the 1950s to approximately 27 million tons per year in 2014 (Bolen 2016). The corrosion epidemic yields two major objectives for bridge managers: 1) slow the rate of corrosion that will eventually result in costly repairs and 2) prioritize individual bridges so that they are repaired before costly rehabilitation or reconstruction is required (Carter 1989).

To address these and other bridge management problems, bridge management systems (BMSs) have been created (Hema et al. 2004, Hudson et al. 1987). The overall aim of a BMS is to maximize the average service life of bridges in a given network, where the service life of a bridge is the time between construction and replacement. A BMS allows decision-makers at all bridge management levels to select optimum solutions from a variety of cost-effective alternatives that should deliver the desired level of service while minimizing the overall life-cycle cost of a bridge (Hema et al. 2004). The steps and objectives of a BMS include the following (Hudson et al. 1987):

- Collect and record inventory data
- Define bridge conditions through condition assessment
- Determine funding needs for preservation and reconstruction projects
- Identify and prioritize bridges for preservation and reconstruction projects
- Recommend and account for preservation and reconstruction actions
- Forecast future conditions
- Maintain an appropriate database of information

While the importance of BMSs has been understood for some time (Hudson et al. 1987), implementation of BMSs has still not fully occurred nationwide (FHWA 2010). A 2010 questionnaire survey conducted of state departments of transportation (DOTs) by the Federal Highway Administration (FHWA) reported that many state agencies used a BMS only for storing information. Less than 30 percent of respondents used a BMS for making preservation, rehabilitation, and reconstruction decisions. As many as 37 percent of respondents used no products, methods, or tools to predict future deterioration of bridge elements, and 21 percent of respondents used no products, methods, or tools to identify preservation, rehabilitation, and reconstruction practices and strategies. The most commonly used measure of performance was the national bridge inventory (NBI) rating, from which the number of structurally deficient bridges can be determined, and 31 percent of respondents did not collect any data other than NBI ratings. A staggering 58 percent of respondents did not have a bridge preservation policy, and 46 percent did not document bridge management practices.

As evidence of a continuing national need for more effective bridge management, the American Society of Civil Engineers (ASCE) reported a grade of C+ for bridges in the United States in 2017 and indicated that approximately 9 percent of bridges in the United States were structurally deficient, with nearly 40 percent of all bridges being older than 50 years (ASCE 2017). Of particular interest to this research, Utah ranked fifth from the top by both number and percentage of structurally deficient bridges, with 3.1 percent being rated structurally deficient (ASCE 2017).

Although useful information has been published about selected aspects of bridge deck management (Gucunski et al. 2013, Hema et al. 2004, Manning 1985, Sprinkel et al. 1993,

Stratfull et al. 1975, Weyers et al. 1994), a comprehensive guide describing bridge deck management processes is not currently available in the industry. Furthermore, the effects of specific deck treatment types and timing on bridge deck performance have not been fully quantified. Given the continuing challenges of preserving concrete bridge decks in cold regions, such as Utah, the Utah Department of Transportation (UDOT) requested development of a concrete bridge deck management guide specific to the design, construction, environmental conditions, and deterioration mechanisms typical of concrete bridge decks in Utah.

1.2 Objectives

Three research objectives were developed to assist in the overarching purpose of creating a concrete bridge deck management guide:

1. Investigate bridge deck condition assessment methods used in the field and laboratory, methods of managing bridge decks, and methods for estimating remaining bridge deck service life using computer models through a comprehensive literature review on these subjects.
2. Collect and analyze field data from representative concrete bridge decks in Utah.
3. Develop a decision tree for concrete bridge deck management in Utah.

These three objectives were necessarily completed in numerical order; information about possible condition assessment methods was required before bridge deck testing was completed. Additionally, information about possible preservation and rehabilitation methods, as well as the results from bridge deck testing, were required to inform the development of the decision tree and test the efficacy of the recommended treatments.

1.3 Scope

The scope of the research therefore included a comprehensive literature review and synthesis of numerous references, extensive field and laboratory testing and analysis to determine the condition of 15 typical concrete bridge decks in Utah, and development of a decision tree for concrete bridge deck management. The 15 bridge decks included five bare

decks, five decks with an asphalt overlay, and five decks with polymer overlays, each strategically selected to evaluate specific bridge deck features.

1.4 Outline of Report

Five chapters are included in this report. Chapter 1 gives the problem statement and outlines the objectives of this research. Chapters 2, 3, and 4 address research objectives 1, 2, and 3, respectively. Chapter 5 gives conclusions and recommendations based on the research findings.

2.0 LITERATURE REVIEW

2.1 Overview

This chapter addresses objective 1 of this research, for which bridge deck condition assessment methods used in the field and laboratory, methods of managing bridge decks, and methods for estimating remaining bridge deck service life using computer models were investigated through a comprehensive literature review on these subjects. The following sections describe condition assessment methods; bridge deck preservation and rehabilitation methods; bridge deck reconstruction methods; and estimating remaining service life using computer models. This research is not intended to promote any specific product or manufacturer; prices and performance may vary among the available options.

2.2 Condition Assessment Methods

Before an informed decision can be made about a preservation treatment, rehabilitation treatment, or reconstruction, the condition of the bridge deck must be known. Various methods, both destructive and nondestructive, are available to evaluate the condition of a bridge deck and determine appropriate preservation, rehabilitation, and reconstruction actions. The following sections describe some of the available condition assessment methods and tools, which are presented in alphabetical order for convenience, including chain dragging, chloride concentration testing, coring, cover depth measurement, dye penetration testing, embedded sensor monitoring, galvanostatic pulse measurement (GPM), ground-penetrating radar (GPR) scanning, half-cell potential (HCP) testing, hammer sounding, impact-echo testing, infrared thermography scanning, linear polarization testing, petrographic analysis, radiography, rapid chloride permeability (RCP) testing, resistivity testing, Schmidt rebound hammer testing, skid resistance testing, ultrasonic pulse echo testing, ultrasonic surface waves (USW) measurement, vertical electrical impedance (VEI) testing, and visual inspection. For each method, information about theory, procedures, data interpretation, and additional considerations is presented.

2.2.1 Chain Dragging

Chain dragging is one of the most widely used methods in the United States for assessing the condition of bridge decks. A relatively simple, inexpensive, and nondestructive test, it involves manually dragging a chain across the surface of a bridge deck. The sound produced by the chain is used to identify areas where delamination may be present (Gucunski et al. 2013, Manning 1985). Figure 2-1 shows chain dragging being performed on a bridge deck.

2.2.1.1 *Theory*

Chain dragging is the process of dragging a steel chain across a bridge deck surface and listening to changes in the acoustic response (Scott et al. 2003). Delaminations within the deck produce a different frequency than intact concrete, allowing the human ear to identify delaminated portions of the bridge deck (Gucunski et al. 2013). Good-quality concrete will produce a clear ringing sound (Henderson et al. 1999). When delaminations are present, however, the acoustic response is a dull, hollow sound resulting from flexural oscillations within the deck (Gucunski et al. 2013, Henderson et al. 1999, Stratfull 1973a). These flexural

Figure 2-1 Chain dragging of a concrete bridge deck.

oscillations occur after some form of impact, such as chain dragging or sounding with a hammer or rod, and it typically manifests as a sound from 1 to 3 kHz (Guthrie et al. 2019a).

2.2.1.2 *Procedures*

The procedure for chain dragging is outlined in American Society for Testing and Materials (ASTM) D4580 (Measuring Delaminations in Concrete Bridge Decks by Sounding). The bridge deck should be prepared for chain dragging by clearing away any accumulated debris and marking the surface in a grid system to more easily map any detected delaminations. Preparation of the bridge deck can be time-consuming, especially for larger bridges. After preparation, the bridge deck is surveyed by dragging chains over the entire surface. Areas identified as being delaminated should be marked on the deck surface for plotting and evaluation. Chain dragging by a single team can require 4 to 6 hours for a typical deck. More time is required to complete testing for bridge decks with a large number and/or area of delaminations than for bridge decks with fewer and/or smaller delaminations. Chain dragging requires stationary traffic control.

2.2.1.3 *Data Interpretation*

According to ASTM D4580, after a bridge deck has been surveyed, delaminated areas should be plotted on a map of the bridge deck using the grid system previously marked on the deck surface. The total area of identified delaminations should be calculated, divided by the total interrogated area of the bridge deck, and multiplied by 100 to determine the percentage of the bridge deck that is delaminated.

2.2.1.4 *Considerations*

Chain dragging is typically used as a preliminary investigative tool to identify areas of a bridge deck to be more thoroughly assessed using other techniques. This method is relatively inexpensive and provides immediate results, although it can be very time-consuming (Manning 1985).

Although chain dragging is widely used, several limitations apply to this condition assessment method. Chain dragging requires an experienced technician to detect meaningful changes in the acoustic response, thereby introducing subjectivity into the test, as different

operators can hear the same sound differently (Henderson et al. 1999, Scott et al. 2003). To one technician the acoustic response may sound clear, while to another the sound may seem dull (Robison and Tanner 2012).

The accuracy of chain-dragging can also be affected by technician fatigue since ambient noise tends to reduce the technician's sensitivity to changes in the acoustic response (Manning 1985). The fatigue of the technician is an important source of variability in this test (Henderson et al. 1999, Scott et al. 2003).

Although chain dragging provides valuable information about the presence and location of delaminations, it can only do so after delaminations have progressed to the point where major rehabilitation is required (Gucunski et al. 2000). Initial delamination produces flexural oscillations that are outside of the audible range of the human ear; therefore, chain dragging is not effective in identifying initial delamination (Gucunski et al. 2013).

Another limitation is that, while chain dragging can locate delaminations, it is not a reliable method for directly identifying areas of corroding reinforcement. Different deterioration processes, such as freezing and thawing, can also result in delaminations (Stratfull 1973a); therefore, the operator should not automatically assume that the presence of delaminated concrete is a manifestation of corroding reinforcing steel. Additionally, the accuracy of chain-drag surveys is unsatisfactory on asphalt-overlaid decks and decks with other thick overlays (Gucunski et al. 2013, Manning 1985). Furthermore, on decks with thin overlays, chain-dragging cannot readily distinguish between a corrosion-induced delamination and an area where an overlay has debonded from the concrete bridge deck surface.

2.2.2 Chloride Concentration Testing

Chloride concentration testing is among the most common techniques for evaluating the condition of a concrete bridge deck (ASTM 1978). This is a destructive test, typically performed on pulverized concrete samples, that is used to determine if chloride concentrations may be high enough to initiate corrosion of the reinforcing steel. Concrete is extracted from the bridge deck either as a core or as powder and then tested for chloride concentration. Figure 2-2 shows collection of concrete powder for chloride concentration testing using a rotary hammer drill.

Figure 2-2 Concrete powder sampling for chloride concentration testing.

2.2.2.1 *Theory*

As soon as chloride-based deicing salts come in contact with water on the surface of a bridge deck, dissolution begins, and chloride ions can start to penetrate the concrete by traveling through the pore water in a process called diffusion (Arora et al. 1997). Diffusion is characterized by the movement of ions from areas of high concentration to areas of low concentration (Birdsall et al. 2007). Chloride ions also penetrate the concrete through cracks that may exist in the deck. Repeated deicing salt applications over time and continued downward chloride ion movement cause chloride concentrations to be highest at the deck surface and decrease with increasing concrete depth. Through chloride concentration testing, a chloride concentration profile can be created and analyzed to determine the condition of a concrete bridge deck with respect to corrosion (Montgomery 2014).

2.2.2.2 *Procedures*

Chloride concentration testing involves collection of concrete samples from the bridge deck and subsequent analysis of the samples. Two methods are available for collecting concrete samples. The first collection method is extracting core samples to be sectioned, pulverized, and tested in a laboratory (Manning 1985). The second collection method is pulverizing and

collecting concrete powder directly from the deck to be tested in a laboratory (Grover and Jackson 1996, Manning 1985, Stratfull et al. 1975). Figure 2-2 demonstrates the method of pulverizing the sample in the field with a rotary hammer drill. For a trained technician, extracting a core sample can take approximately 20 minutes per core, which must later be sectioned into samples and pulverized in the laboratory, while pulverizing and collecting concrete powder directly from the deck can take approximately 5 minutes per sample. Both methods of chloride concentration collection require stationary traffic control.

For both collection methods, samples are ideally obtained at multiple locations on a bridge deck. At each of these locations, samples collected from various depths are evaluated to produce chloride concentration profiles. The number of samples should be minimized to avoid excessive costs, disruptive traffic control, and the potential for compromising the structural integrity of the deck with unnecessary sampling (Montgomery 2014).

Whether core samples are collected to be pulverized later or the rotary hammer method is used to collect pulverized concrete in the field, the options for laboratory test methods are the same. All samples must pass a No. 50 (0.0118-in.) screen before laboratory tests can be conducted (Manning 1985), and the sample weight must be 0.022 lb according to ASTM C1218 (Standard Test Method for Water-Soluble Chloride in Mortar and Concrete) or 0.007 lb according to the American Association of State Highway Transportation Officials (AASHTO) T260 (Standard Method of Test for Sampling and Testing for Chloride Ion in Concrete and Concrete Raw Materials).

Two laboratory methods of chloride concentration testing, differing in the chloride ion extraction technique, have been standardized. In the acid-soluble chloride testing method, a powdered sample of the concrete is dissolved in dilute nitric acid, as described in the ASTM C1152 (Standard Test Method for Acid-Soluble Chloride in Mortar and Concrete). A silver nitrate solution is then used to conduct a potentiometric titration of the chloride ions. Figure 2-3 shows the titration portion of chloride concentration testing. This method measures both the free and chemically bound chloride ions in concrete. Consequently, the results contain measurements of chloride ions that do not contribute to corrosion of the reinforcement. The second laboratory method of determining the chloride concentration in concrete is the water-soluble chloride

Figure 2-3 Chloride concentration testing.

testing method. This method uses water to extract the chloride ions, as described in ASTM C1218. The test duration and the temperature of the water to which the concrete sample is exposed determine the amount of chloride ions extracted. Generally, the samples are boiled for 5 minutes and then cooled for a period of 24 hours. The water-soluble test measures both the free chloride ions and a portion of the chemically bound ions. Therefore, neither of the tests has a clear advantage over the other.

2.2.2.3 *Data Interpretation*

Chloride concentration is usually reported in pounds of chloride per cubic yard of concrete. At the depth of the reinforcing steel, concentrations greater than the corrosion initiation threshold value of 2.0 lb Cl^-/yd^3 of concrete can initiate corrosion of uncoated reinforcing steel within the concrete (Mindess et al. 2003). Epoxy-coated reinforcing steel is estimated to be able to withstand chloride concentrations up to 4.6 times higher than uncoated reinforcing steel before

corrosion is initiated (Bentz et al. 2014). Consideration of chloride concentration profiles can also indicate relative rates of chloride ion diffusion through the deck.

2.2.2.4 *Considerations*

Chloride concentration testing is typically used to quantify corrosion potential or evaluate the benefit of surface treatments on concrete bridge decks and can be performed at any time during the life of a bridge deck. One limitation of chloride concentration testing is that only trained personnel should perform the testing because of the sensitivity of the test to even small procedural errors and the possibility of inadvertent sample contamination.

2.2.3 Coring

Coring is a destructive test used to extract a cylindrical sample from a concrete bridge deck. Extracting a concrete core and performing a simple visual inspection or petrographic analysis can be useful to determine the general condition of the concrete. A concrete core can also be used to determine qualities such as compressive strength, permeability, chloride concentration, and delamination depth.

2.2.3.1 *Theory*

Coring, as described in ASTM C42 (Standard Test Method for Obtaining and Testing Drilled Cores and Sawed Beams of Concrete), is performed to extract cylindrical samples from concrete elements. Core analysis is a reliable way of determining the condition of in-place concrete down to a certain depth. It allows the concrete beneath the surface to be inspected and analyzed in detail. Figure 2-4 demonstrates the coring procedure.

2.2.3.2 *Procedures*

Concrete specimens are extracted perpendicular to the concrete surface in areas of desired testing, through or between reinforcing bars in the deck. Although typical core diameters are 2.0 to 6.0 in., depending on the purpose of the core, samples having up to an 18-in. diameter can be cored using diamond-impregnated bits attached to a core barrel. In all cases, the depth of coring must be controlled to ensure that the bit does not penetrate the full thickness of the bridge deck, which would allow the core to fall below the deck. If taken for petrographic analyses, cores

Figure 2-4 Coring of a concrete bridge deck.

should be sampled in accordance with ASTM C856 (Standard Practice for Petrographic Examination of Hardened Concrete).

For a trained technician, extracting a concrete core sample can take approximately 20 minutes; however, additional time may be required when a thick asphalt overlay is present or when the concrete comprises silica fume or other admixtures leading to much higher strength. Given that additional time is needed for installation and curing of concrete patches, coring can be a relatively time-consuming method. For personnel safety and quality control, lane closures are required during the coring, patching, and curing processes (Hema et al. 2004).

2.2.3.3 *Data Interpretation*

While cores can be used to perform various tests, the most common is visual inspection. For example, visual inspection of a core is useful for evaluating concrete uniformity, concrete consolidation quality, overlay thickness and bond quality, occurrence and depth of delamination, and other similar properties.

2.2.3.4 *Considerations*

Coring can be performed at any time during the life of a bridge deck. Properly trained personnel are needed to extract cores from the bridge deck and perform the laboratory testing (Hema et al. 2004). One limitation of coring is the difficulty of extracting some cores when the concrete does not crack along the bottom of the core; this is most common for shallow cores, including cores through delaminations. Additionally, because the top and bottom mats of reinforcement are not typically aligned, the depth of coring may be limited to the bottom mat when cutting through rebar is not allowed.

2.2.4 Cover Depth Measurement

The cover meter, also known as a pachometer, is a simple, nondestructive tool that measures the depth of the reinforcing steel from the deck surface. It also allows reinforcing steel configurations to be identified, which in turn facilitates coring or drilling deliberately through or between reinforcing bars (Newman and Choo 2003). Figure 2-5 shows a cover meter in use.

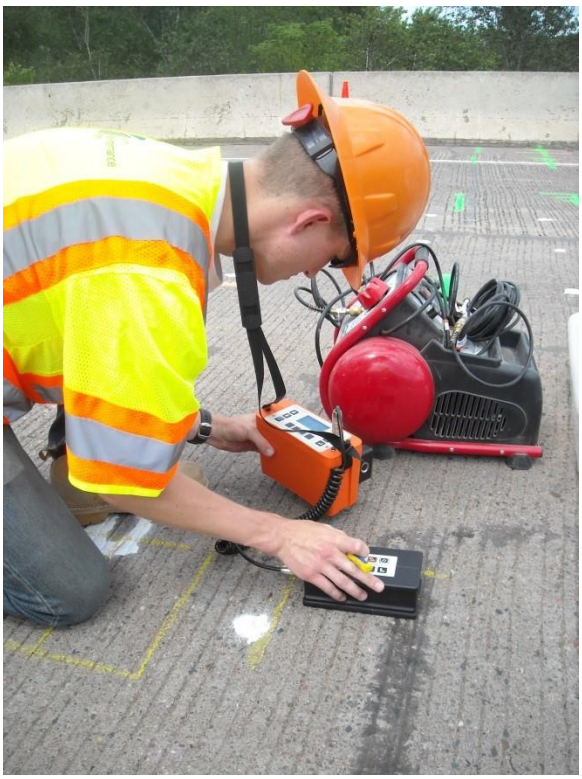

Figure 2-5 Concrete cover measurement using a cover meter.

2.2.4.1 *Theory*

The majority of cover meters are based on one of two electromagnetic principles, magnetic induction or eddy currents (Alldred 1995, Barnes and Zheng 2008, Hoki 2011, IAEA 2002, Shohet et al. 2002, Snell et al. 1985). Cover meters based on magnetic induction produce a magnetic field in the concrete and measure the degree to which nearby objects embedded in the concrete become magnetized. Because reinforcing steel can become magnetized when placed in a magnetic field, it responds to the magnetic field and can thus be detected. Decreasing the distance between the meter and the steel and/or increasing the amount of steel within the magnetic field leads to higher magnetic induction and a larger signal reported by the cover meter. For this reason, knowing the size of the rebar is often important for accurately estimating its depth. The presence of other magnetic materials, including other steel reinforcement, can influence the measurement.

Cover meters based on eddy currents produce an alternating magnetic field that generates electrical currents, known as eddy currents, within nearby electrically conductive materials. These electrical currents generate magnetic fields in opposition to the applied alternating magnetic field. The opposing magnetic fields can be sensed by the cover meter and thereby allow detection of nearby conductive materials. While any conductive material within the alternating magnetic field will generate eddy currents, the magnitude of the eddy currents depends on the conductivity, volume, shape, and orientation of the material; cover meters are designed specifically to detect steel reinforcement.

Many brands of cover meters are available, and each manufacturer has a unique standard of precision. Furthermore, some meters have both a deep-scan antenna and a shallow-scan antenna, and the calibration of these antennas and the depth of investigation can also vary between manufacturers. Currently, the only requirements for cover meter precision are found in British Standards Institution 1881-204 (Recommendations on the Use of Electromagnetic Covermeters), which gives a relatively large interval of acceptance.

2.2.4.2 *Procedures*

If possible, a copy of the reinforcement detail from the bridge deck plans should be obtained to determine the rebar size, spacing, and orientation for at least the upper mat of

reinforcement in the bridge deck in both the longitudinal and transverse directions. The cover meter should then be set to the size of rebar being interrogated, and the appropriate antenna should be chosen. Antenna selection is dependent on the depth and spacing of the rebar.

The lane(s) where readings are being taken should be closed to traffic during measurements. Debris should be removed from the test area. To avoid interference, conductive metal rings, watches, and other articles should not be worn by the person operating the antenna. The meter should be calibrated per the manufacturer's instructions.

To perform the test, the antenna should be placed on the deck surface, with the longitudinal axis of the antenna parallel to the longitudinal axis of the bridge. The technician should then slowly sweep the antenna across the deck surface, perpendicular to the longitudinal axis of the bridge deck. During this process, the meter readings should be constantly monitored.

Local minimums in the cover meter reading typically indicate rebar locations. These locations should be marked, and the readings should be recorded. Obtaining and averaging two or three readings along the same rebar are recommended. Individual readings can typically be obtained in less than a minute. This process should then be repeated for the transverse direction, as desired. Cover depth measurement testing requires stationary traffic control.

2.2.4.3 *Data Interpretation*

The recorded data should include reinforcing steel depths, the rebar orientation (longitudinal or transverse), and the assumed rebar size. If multiple locations are tested, an average for the deck can be calculated, or values can be compared to design depths or actual depths measured during coring or drilling.

2.2.4.4 *Considerations*

The cover meter is a useful tool that can be used at any time during the service life of a bridge deck. However, some limitations include the need for the instrument to be in physical contact with the deck surface and the possibility of not being able to accurately determine cover depth on decks covered with thick asphalt overlays. The maximum measurable cover depth depends on the bar spacing, bar diameter, and cover meter manufacturer, but typically a cover

meter cannot accurately measure deeper than about 3.5 in. (Barnes and Zheng 2008, Shohet et al. 2002).

The chief limitation of the eddy-current method in comparison to the magnetic-induction method is that, since the driving current in the search coil operates at frequencies over 1.0 kHz, the probe is affected by any metal that will conduct electricity, such as metal rings or steel-toed shoes, within the effective zone of interrogation of the probe (Tam 1977).

2.2.5 Dye Penetration Testing

Dye penetration testing is a nondestructive method primarily utilized for detecting surface defects in concrete that are not detected during a visual inspection (Larson 2002). Penetration dyes help to establish an observable contrast between discontinuities and the surrounding intact concrete (Gamidi 2009, Hayes 1998).

2.2.5.1 *Theory*

A penetration dye is a fluid with low surface tension that is used to penetrate a concrete surface through capillary action (Gamidi 2009). A dye may be either fluorescent, which requires an ultraviolet light to identify flaws, or nonfluorescent, which is visible to the human eye in normal lighting (Gamidi 2009, Larson 2002).

2.2.5.2 *Procedures*

Penetration dyes are applied by dipping, spraying, or brushing the dye onto clean concrete surfaces. The dye is then allowed to seep into surface discontinuities and open voids (Gamidi 2009, Hayes 1998). After the appropriate penetrant dwell time, or the time required for the dye to fully penetrate any flaws, has passed, excess dye is washed from the surface; minimum dwell times can vary from 5 to 60 minutes, depending on the dye manufacturer (Larson 2002). After the excess dye is removed, a white developer is applied to the concrete surface. Several types of developers exist, including non-aqueous wet developers, dry powder developers, water-suspendable developers, and water-soluble developers (Gamidi 2009). In each case, the developer acts as a blotter, drawing the dye out from the discontinuities. Upon contact, the dye stains the developer, marking the location of surface defects. A white or blank surface indicates an absence of cracks or other surface defects. Figure 2-6 shows the process of a dye

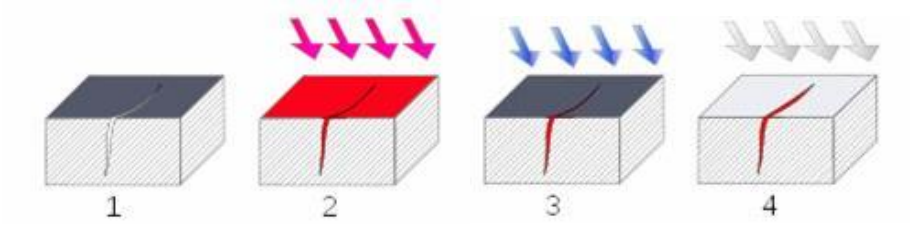

Figure 2-6 Dye penetration testing (Gamidi 2009).

penetration test. Step 1 of the sequence in Figure 2-6 shows a crack in a concrete surface before any dye has been applied. Step 2 shows the dye being applied and penetrating the crack. The surface is then cleaned as illustrated in step 3, and then the white developer is applied as shown in step 4.

Successful use of penetration dyes requires a concrete surface that is free of any contaminants that may impede the migration of penetrants into discontinuities. Following the inspection process, penetrant materials are removed from the concrete surface using specified cleaning procedures, especially as required in the field prior to the placement of a surface treatment (Gamidi 2009). Dye penetration testing requires stationary traffic control.

2.2.5.3 *Data Interpretation*

Once the flaws are identified, they can be recorded via a sketch, photograph, or map. Crack lengths and widths can also be measured.

2.2.5.4 *Considerations*

Penetration dyes are used when surface defects that are not visible to the human eye, such as fine cracks in concrete, require evaluation. One limitation of fluorescent dyes is that field inspections must be performed at night when a black light can be used effectively (Larson 2002). Neither non-fluorescent nor fluorescent dyes can determine the depth of cracking (Gamidi 2009).

Surface roughness and porosity can limit the use of penetration dyes. Rough surfaces tend to trap more penetrant in the various tool marks, scratches, and pits in the deck surface. Removing the penetrant from the surface of the rough area is more difficult (Larson 2002).

Another limitation of penetration dyes is that the chemicals can become contaminated or degrade over time. Also, human interpretation of results is susceptible to variability (Larson 2002).

2.2.6 Embedded Sensor Monitoring

Embedded sensors, which are typically small enough to fit between longitudinal and transverse reinforcing steel, can be used to nondestructively monitor internal concrete properties on bridge decks (Guthrie and Yaede 2013). Figure 2-7 shows the placement of embedded sensors prior to new deck construction.

2.2.6.1 *Theory*

Many of the main factors that influence the corrosion of reinforcing steel in a concrete structure can be measured using embedded sensors (Cain et al. 2003). Embedded sensors are intended to monitor such factors so that the condition of the bridge deck can be evaluated and tracked. Sensors are specifically available for measuring temperature, moisture content, electrical conductivity, relative humidity, chloride concentration levels, resistivity, polarization resistance, and open-circuit potential (Carkhuff and Cain 2003, Fortner 2003, Giatec 2020, Guthrie et al. 2015, Meter Group 2017, Watters 2003).

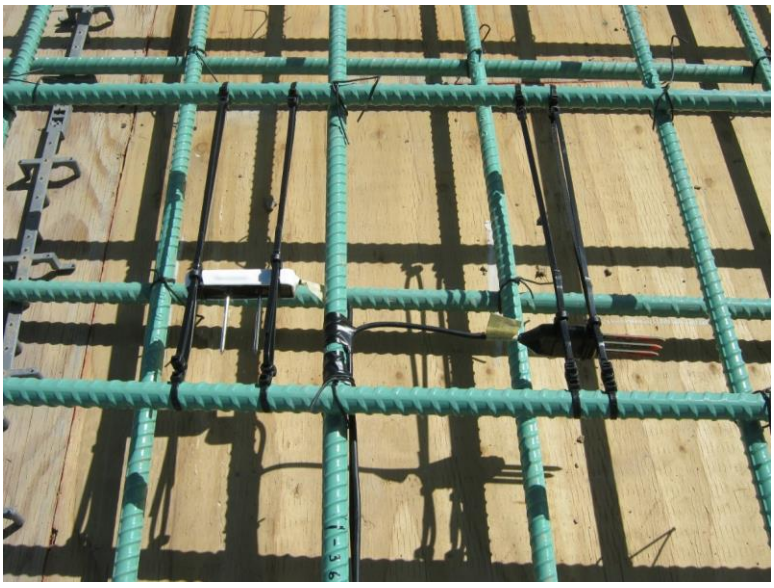

Figure 2-7 Placement of sensors to be embedded in a new concrete bridge deck.

Data collection is influenced by the type of sensor, wired or wireless, and the type of sensing, active or passive. Although wired systems are often more time-consuming to install than wireless sensors, they allow for active sensing through continuous monitoring or automated data transmission at specified time intervals (Ceylan et al. 2011). Wireless sensors are powered remotely, usually through the use of a radio frequency identification chip, and are generally passive, relaying information only when activated by an interrogation unit (Fortner 2003, Watters 2003). Some sensors require visits to the site for data collection, which is performed automatically using a high-speed data collection vehicle or manually using a handheld data collection device (Cain et al. 2003, Carkhuff and Cain 2003), while other sensors can be connected to a data logger for real-time data collection (Ceylan et al. 2011).

2.2.6.2 *Procedures*

The basic procedure for obtaining data from embedded sensors involves sensor installation and data acquisition. Regarding installation, sensors can be placed in a bridge deck during or after construction. When placed during construction, sensors are often mounted on or between reinforcing bars where corrosion, for example, may be a concern (Carkhuff and Cain 2003). The sensors must then be carefully protected during concrete placement to avoid being damaged. When placed after construction, sensors are typically inserted into a drilled hole or sawn slot, which is then backfilled using grout, which may influence the sensor readings (Watters et al. 2003). While cables for wired sensors can be fastened below reinforcing steel prior to concrete placement, embedment of cables in the deck is not normally a viable option after construction; instead, a small hole is drilled from the intended sensor location through the bottom of the deck, and the cable is routed through the hole and into conduit, as needed, that conveys it to the desired location.

In general, regarding data acquisition, sensors are either plugged into a reader or wirelessly interrogated from a moving platform, such as a specially equipped vehicle, that passes over the bridge deck. A reader may be a data logger permanently mounted on, under, or near the bridge deck, or it may be a handheld device that is carried by the inspector from bridge to bridge (Cain et al. 2003, Guthrie et al. 2015). When permanent power is required, such as for active sensing, the sensors may be connected to the power grid or a battery; in the latter case, a rechargeable battery may be used in conjunction with a solar panel to extend battery life. When

frequent data acquisition is important, especially at remote sites, readers can be equipped with a cellular connection to enable remote downloads of the collected data (Guthrie and Yaede 2013). When data are acquired using a moving platform, the rate of communication between the platform and the embedded sensor governs the maximum allowable speed of the platform (Watters et al. 2003). Ideally, traffic control is not necessary for data acquisition.

2.2.6.3 *Data Interpretation*

Over time, individual readings from an embedded sensor can be plotted for analysis. As an example, the output of two embedded sensors is shown in Figure 2-8. These particular sensors recorded the moisture content of two bridge decks, one with conventional concrete and one with internally cured concrete, on 1-hour intervals beginning at the time of deck construction (Guthrie and Yaede 2013). If a bridge deck has multiple embedded sensors, maps of the bridge deck can be created for a given time.

2.2.6.4 *Considerations*

Placing embedded sensors in bridge decks can allow for continuous, long-term, nondestructive monitoring. The intended application should be considered before the type of sensor is selected. Spatial constraints can limit the size of the sensor, construction constraints can require a specific sensor installation method, trafficking and/or site location can necessitate a

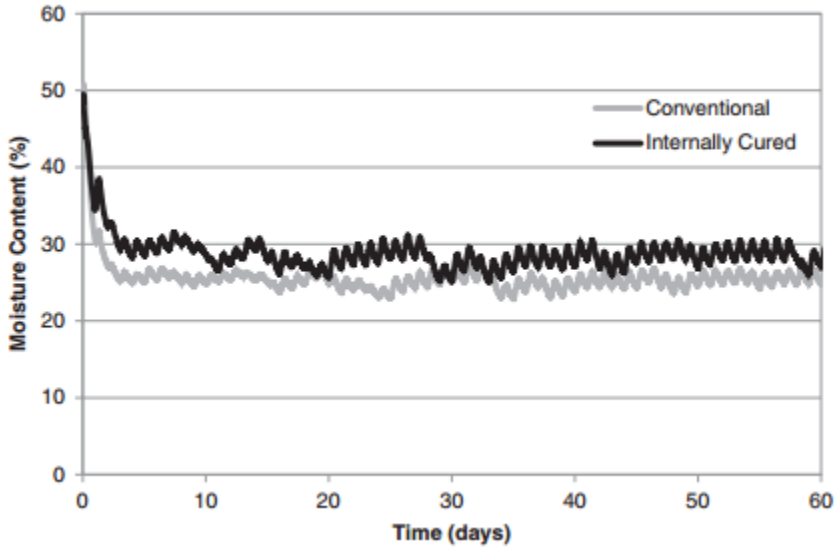

Figure 2-8 Moisture content data from sensors embedded in a concrete bridge deck (Guthrie and Yaede 2013).

specific type of sensor access, desired deck coverage can require multiple sensors, and the frequency and duration of data collection can govern the power requirements (Ceylan et al. 2011). Each sensor has a limited life span and eventually stops providing information, even if the power source is still active. Some sensors have a projected lifetime of 50 years (Ceylan et al. 2011), while others have failed after only a few years (Guthrie et al. 2015). The reliability of embedded sensors is limited by a number of factors, including sensor durability, installation quality, and environmental conditions (Ceylan et al. 2011).

2.2.7 Galvanostatic Pulse Measurement

GPM is a rapid, nondestructive, electrochemical test used to estimate the rate of rebar corrosion (Gucunski et al. 2013). After applying a short current pulse to the reinforcement, the change in potential is measured, recorded, and used to estimate the corrosion rate of the rebar (Frølund et al. 2002, Sathiyanarayanan et al. 2006). This method is similar to HCP testing, which is discussed in a later section.

2.2.7.1 *Theory*

In the GPM method, corrosion assessment is based on the measurement of the current required to change the potential difference between the reinforcement and a reference electrode. A short-duration anodic current pulse is applied to the reinforcement galvanostatically, or with constant current, from a counter electrode placed on the concrete surface together with a reference electrode (FHWA 2015, Frølund et al. 2002, Sathiyanarayanan et al. 2006). Both the counter electrode and the reference electrode are electrically coupled to the concrete surface using a moistened sponge. The applied current is normally in the range of 5 to 400 μA, and the typical pulse duration is up to 10 seconds (Frølund et al. 2002). The small anodic current results in a change of reinforcement potential, which is recorded as a function of testing time. The corrosion rate is proportional to the amount of current required to change the potential. Non-corroding reinforcement has a high polarization resistance and therefore a low corrosion rate (FHWA 2015). Figure 2-9 demonstrates the GPM testing process, in which the counter electrode and reference electrodes are concentrically configured for the testing.

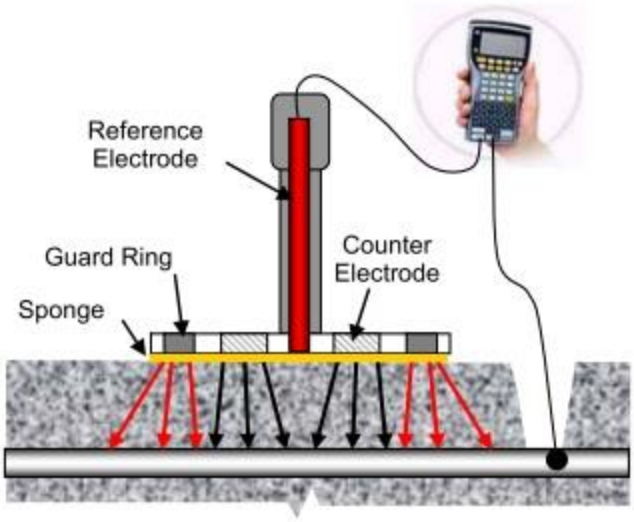

Figure 2-9 GPM testing (Germann Instruments 2016).

2.2.7.2 *Procedures*

Before the GPM method is performed, the electrical resistance of the reinforcing steel within the test area should be determined. This measurement is achieved by tapping the reinforcing steel at two locations on the deck, preferably in opposing corners of the accessible test area so that multiple longitudinal and transverse bars will be tested. After connecting each tap to a lead of a multimeter, the electrical resistance of the reinforcing steel can be measured.

The GPM method requires a digital voltmeter to measure the HCP of the rebar and a pulse generator to initiate the current in the rebar (Elsener et al. 1997). Once the rebar is exposed and tapped, a short, anodic current pulse, typically lasting up to 10 seconds, is sent to the reinforcement. The reinforcement is polarized, and the change of reinforcement potential is measured with the voltmeter and recorded as a function of polarization time (Frølund et al. 2002). Measurements can be obtained in a grid pattern to facilitate drawing of equipotential lines on a two-dimensional contour map (FHWA 2015). GPM requires stationary traffic control.

2.2.7.3 *Data Interpretation*

After readings have been obtained across the area of interest, contour maps can be generated to delineate areas of high and low electrical resistance and corrosion rate. The corrosion rate can be further correlated to the steel cross-section loss. A corrosion rate of $1x10^{-5}$ $A/in.^2$ corresponds to a cross section loss of about 0.71 mil/year (FHWA 2015).

2.2.7.4 *Considerations*

The GPM test is useful for evaluating the occurrence of reinforcing steel corrosion (Gucunski et al. 2013, Sathiyanarayanan et al. 2006). One limitation of this test is that the GPM can be adversely affected when the concrete cover has high electrical resistivity, which can lead to unstable measurements. To potentially minimize this effect, pre-wetting of the concrete surface is recommended prior to performing the measurements. The first reading should be taken a few minutes after wetting the surface to avoid any potential shifts in the reading caused by the wetting (Gucunski et al. 2013).

2.2.8 Ground-Penetrating Radar Scanning

GPR is a nondestructive geophysical method that can be used to locate reinforcing steel, contaminated concrete, inadequate concrete cover, changes in overlay thickness, or delaminations on a concrete bridge deck (Gucunski et al. 2013). Available in both ground-coupled and air-coupled configurations, GPR can be utilized to map subsurface features at relatively shallow depths (Sharma 1997). An example of ground-coupled GPR testing equipment is shown in Figure 2-10. In an air-coupled configuration, the equipment is often mounted above the ground at the front or rear of a high-speed vehicle.

Figure 2-10 GPR testing of a bridge deck.

2.2.8.1 *Theory*

Most GPR systems designed for scanning reinforced concrete use electromagnetic waves in the frequency band of 1.0 to 2.5 GHz (Saarenketo and Soderqvist 1994) to map subsurface characteristics of bridge decks, including objects buried within the structure (Gucunski et al. 2013). Radar waves are emitted into the bridge deck from a surface antenna that may be in contact with the deck or positioned above the deck (Maser et al. 2001, Shin and Grivas 2003). When radar waves traveling through the bridge deck come in contact with an electrical interface, such as a boundary between two materials having different dielectric values, they are transmitted or reflected to various degrees depending on the dielectric contrast between the two materials forming the interface (Hugenschmidt and Mastrangelo 2006, Maser et al. 2001). Typically, a small portion of the radar wave is reflected back to the surface antenna, while the remainder of the wave continues through the bridge deck. The travel times and amplitudes of reflected radar waves are recorded and processed, as shown in Figure 2-11 (Hugenschmidt and Mastrangelo 2006, Maser et al. 2001, Shin and Grivas 2003).

2.2.8.2 *Procedures*

GPR scanning involves data collection and analysis. For easier data collection, GPR units are typically mounted to a small cart, as shown in Figure 2-10, or to a high-speed vehicle (Barnes and Trottier 2000, Maser and Rawson 1992, Sharma 1997, Shin and Grivas 2003). As the unit is moved over a bridge deck, the GPR transmitter emits electromagnetic energy that is reflected back to a receiving antenna for later data analysis (Barnes and Trottier 2000, Shin and Grivas

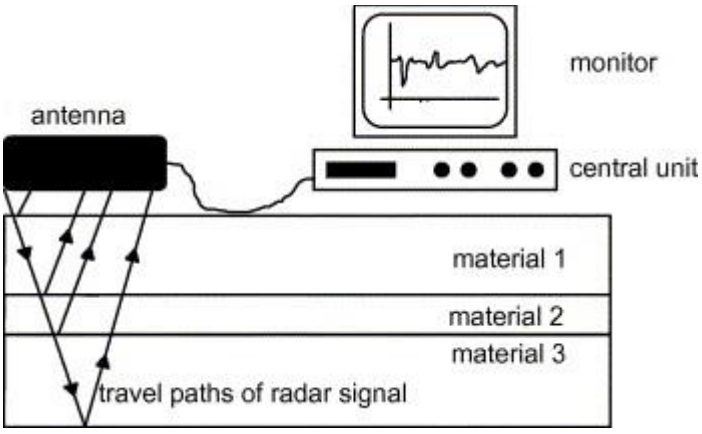

Figure 2-11 GPR wave paths (Hugenschmidt and Mastrangelo 2006).

2003). GPR scans of entire bridge decks can be completed relatively quickly, although stationary traffic control is necessary when antennas are not mounted to a high-speed vehicle.

2.2.8.3 *Data Interpretation*

Radar data are usually analyzed with specialized software (Sharma 1997). Output from such a software program can include contour maps of rebar depth or dielectric value (Shin and Grivas 2003). Typically, the final result of a GPR analysis is a percentage of the total bridge deck area that has contaminated concrete or delaminations (Barnes and Trottier 2000, Maser and Rawson 1992, Shin and Grivas 2003), which is then used to determine bridge deck condition.

2.2.8.4 *Considerations*

The results of GPR scanning can provide information about potential bridge deck performance problems over a wide range of deck conditions. The type of antenna used affects the quality of GPR surveys since the resolution of a GPR unit is directly proportional to the operating frequency (GeoModel, Inc. 2014). In bridge deck surveys, higher frequencies, such as 1.0 to 2.5 GHz, are necessary to achieve the increased resolution required to identify smaller objects such as reinforcing steel (Saarenketo and Soderqvist 1994).

The depths to which a GPR unit can effectively and accurately scan vary with the electrical conductivity of the surface and subsurface materials. Generally, the depth of penetration decreases with increasing electrical conductivity. Since concrete is primarily composed of sand and gravel, which both have low electrical conductivity values, a concrete bridge deck can be an ideal environment for GPR surveys (Sharma 1997).

Cold weather conditions and the use of deicing salts can adversely affect the results of GPR scanning. In cold weather conditions, moisture that freezes in a bridge deck can no longer be detected by GPR. When deicing salts are applied, their dissolution and diffusion into the concrete can lead to high electrical conductivity values that significantly reduce the depth of penetration (Gucunski et al. 2013).

Advanced training is required to accurately interpret GPR results (Barnes and Trottier 2004). Nondestructive evaluation methods and limited destructive sampling, such as core

sampling or chloride concentration testing, are generally required to supplement and/or calibrate GPR results (Gucunski et al. 2013).

2.2.9 Half-Cell Potential Testing

The HCP test is a rapid, nondestructive, electrochemical method used to determine the activity of reinforcing steel corrosion in concrete (Finch et al. 1998, Gucunski et al. 2013, Stratfull et al. 1975). HCP measurements provide a classification of the corrosion activity of the steel and indicate locations where the steel is potentially corroding (Stratfull et al. 1975). Figure 2-12 shows HCP testing.

2.2.9.1 *Theory*

The objective of HCP testing is to measure the voltage, or potential difference, between the reinforcing steel and a half-cell, normally a copper-copper sulfate ($Cu\text{-}CuSO_4$) reference

Figure 2-12 HCP testing.

electrode (CSE) (Pinkerton 2007). The CSE is placed in a bottle of electrolytic solution with a sponge attached to the bottom, which is then placed on the surface of the concrete above the steel reinforcement. Current passes from the CSE to the concrete surface through the sponge soaked with the electrolytic solution (Pinkerton 2007). In the HCP setup, the CSE behaves as the cathode and the reinforcing steel behaves as the anode, as copper is higher in the galvanic series than steel (Broomfield 1997). The CSE is connected to the positive end of a high-input-impedance voltmeter that is connected to a data-logging device. The negative end of the voltmeter is connected to the reinforcing steel by drilling into the concrete to expose the steel and tapping into the reinforcing steel with a screw so that a good electrical connection is made (Elsener 2001, Stratfull 1973b).

Through the circuit created, the potential difference is measured. With the CSE acting as the cathode and being connected to the positive terminal of the voltmeter, measured HCP values have a negative value. An HCP measurement results from the multiplication of the reinforcement corrosion potential by the ratio of the internal resistance of the voltmeter to the sum of the internal resistance of the voltmeter and the resistance of the concrete (Gu and Beaudoin 1998). As the concentration of chloride ions increases, the rate at which the reinforcing steel corrodes significantly increases, resulting in a shift toward more negative HCP readings (Gu and Beaudoin 1998).

2.2.9.2 *Procedures*

Before HCP testing is performed, the electrical resistance of the reinforcing steel within the test area should be determined. This measurement is achieved by tapping the reinforcing steel at two locations on the deck, preferably in opposing corners of the accessible test area so that multiple longitudinal and transverse bars will be tested. After connecting each tap to a lead of a voltmeter, the electrical resistance of the reinforcing steel can be measured.

HCP testing should be performed in accordance with ASTM C876 (Standard Test Method for Corrosion Potentials of Uncoated Reinforcing Steel in Concrete). The HCP apparatus is connected to the tap and can be used at any location on the bridge that is electrically continuous with the tap location. Numerous measurements across the bridge may be quickly taken with a single tap to create a detailed map of the deck condition.

In order to reduce the occurrence of HCP values that are erroneously low in magnitude or incorrectly shifted toward less negative readings, the surface of the concrete should be wetted prior to testing. Wetting the concrete surface reduces the resistance of the concrete (Frølund et al. 2003, Gu and Beaudoin 1998, Stratfull 1973b). HCP testing requires stationary traffic control.

2.2.9.3 *Data Interpretation*

After readings have been obtained across the area of interest, contour maps can be generated to delineate areas of corrosion (Stratfull 1973b). Surface potential measurements are a reliable indicator of the corrosion activity of reinforcing steel. Although the rate of corrosion cannot be quantified using surface potential measurements, the amount of corrosion can be inferred. In general, an extensive area of potentials more negative than -0.35 V suggests a high probability that corrosion is occurring (Stratfull 1973a, Stratfull et al. 1975). Table 2-1 shows the HCP measurements with the associated probability of corrosion, as specified in ASTM C876.

2.2.9.4 *Considerations*

The HCP test is useful for evaluating the occurrence of reinforcing steel corrosion (Gucunski et al. 2013). A wide range of factors influence corrosion potentials, including concrete moisture content, concrete resistivity, chloride concentration, concrete cover thickness, temperature, polarization, and presence or condition of epoxy coating on the reinforcing steel (Gu and Beaudoin 1998, Gucunski et al. 2013, NEA 2002, Stratfull 1973b). Additionally, the presence of zinc components in electrical contact with the reinforcing steel can influence HCP readings, causing significantly lower, or more negative, readings.

2.2.10 Hammer Sounding

Hammer sounding is a simple, inexpensive, and nondestructive test, similar to chain dragging, that is used to identify areas where delamination may be present (Gucunski et al. 2013,

Table 2-1 Interpretation of HCP Measurements

Potential (V)	Probability
More negative than -0.35	> 90% that corrosion is occurring
-0.20 to -0.35	Uncertain
More positive than -0.20	> 90% that corrosion is not occurring

Henderson et al. 1999). Striking a hammer on delaminated concrete produces a different sound than that produced by striking intact concrete.

2.2.10.1 *Theory*

Hammer sounding involves using a hammer to strike a bridge deck surface, as shown in Figure 2-13, and listening to changes in the acoustic response (Moore 1975). Delaminations within the deck produce a different frequency of sound than that produced by intact concrete, allowing the human ear to identify delaminated portions of the bridge deck (Gucunski et al. 2013). Good-quality concrete produces a clear ringing sound (Henderson et al. 1999). When delaminations are present, however, the acoustic response is a dull, hollow sound resulting from flexural oscillations within the deck (Gucunski et al. 2013, Henderson et al. 1999). These flexural oscillations are typically in the range of 1 to 3 kHz (Guthrie et al. 2019a).

2.2.10.2 *Procedures*

The procedure for hammer sounding is outlined in ASTM D4580 (Measuring Delaminations in Concrete Bridge Decks by Sounding). The bridge deck should be prepared for

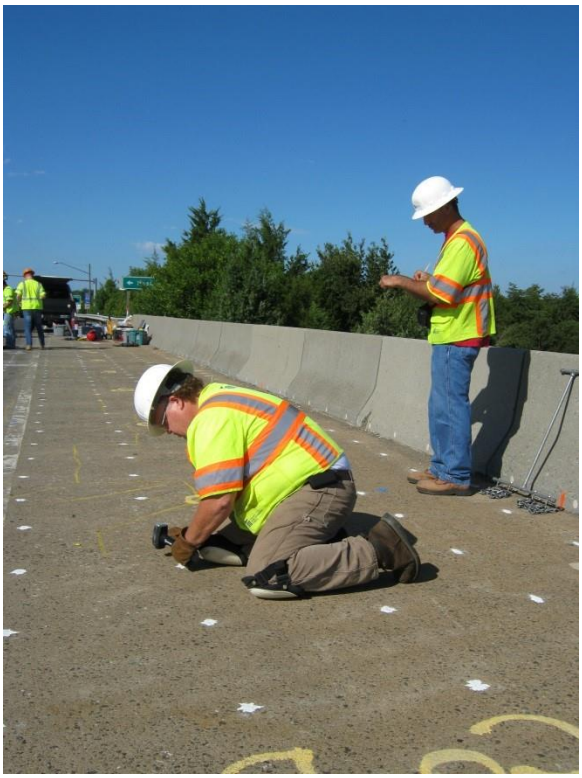

Figure 2-13 Bridge deck sounding with a hammer.

hammer sounding by clearing away any accumulated debris and marking the surface in a grid system to more easily map any detected delaminations. Preparation of the bridge deck can be time-consuming, especially for larger bridges. After preparation, the bridge deck is then surveyed by tapping a hammer on the surface and listening for changes in the sound. As an alternative to a standard hammer, an upright iron bar dropped on its end has also been used (Manning 1985), as shown in Figure 2-14. Areas determined to be delaminated are marked on the deck surface and mapped for evaluation. Hammer sounding requires stationary traffic control.

2.2.10.3 *Data Interpretation*

According to ASTM D4580, after a bridge deck has been surveyed, delaminated areas should be plotted on a map of the bridge deck using the grid system previously marked on the deck surface. The total area of identified delaminations should be calculated, divided by the total interrogated area of the bridge deck, and multiplied by 100 to determine the percentage of the bridge deck that is delaminated.

2.2.10.4 *Considerations*

Hammer sounding is typically used as a preliminary investigative tool to identify areas of a bridge deck to be more thoroughly assessed using other techniques. This method is relatively

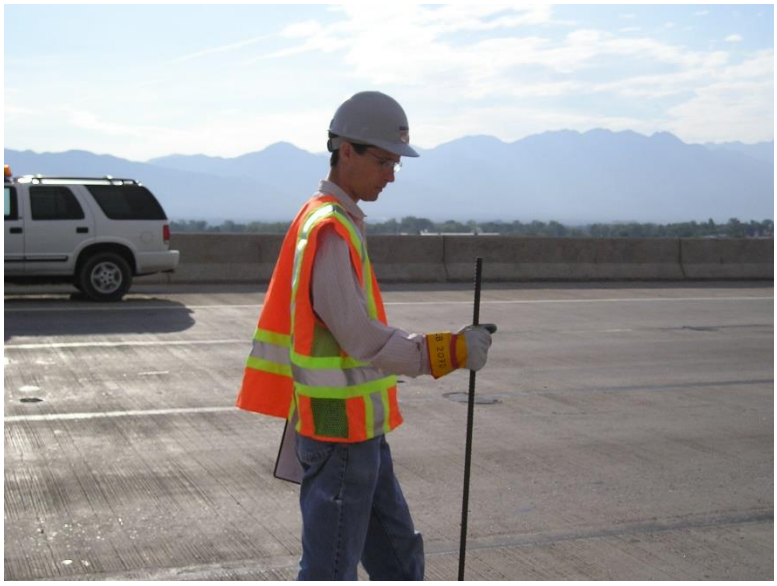

Figure 2-14 Bridge deck sounding with an iron bar.

inexpensive and provides immediate results, although it can be very time-consuming (Gucunski et al. 2013). Hammer sounding is sometimes performed in conjunction with a chain-dragging survey to more definitively mark the edges of a delamination.

The same limitations that apply to chain dragging apply to hammer sounding. For example, hammer sounding on decks with asphalt overlays do not produce accurate results (Gucunski et al. 2013, Manning 1985). Furthermore, the results are affected by the subjective judgment and hearing sense of the technician, as well as by the ambient noise (Manning 1985, Moore 1975). Because hammer sounding is slower than chain dragging, it is more appropriate for evaluating smaller areas of concrete (Manning 1985).

2.2.11 Impact-Echo Testing

The impact-echo method is a nondestructive test method based on the use of seismic or stress waves for detecting defects in concrete, primarily delaminations (Sansalone and Carino 1989). Other defects that can be detected using impact-echo testing include voids, honeycombing, and cracks in reinforced and post-tensioned concrete decks (Impact-Echo Instruments 2004).

Historically, impact-echo testing has not been successfully automated; however, researchers have recently developed fully automated prototypes that have been employed on a number of projects (Guthrie et al. 2014, Popovics 2010, Rutgers 2018). Figures 2-15 and 2-16 show two multi-channel devices that can perform impact-echo testing from a continuously moving platform (Guthrie et al. 2019b, Larsen et al. 2020); these devices, which have both been commercialized, are expected to enable the more frequent use of impact-echo testing for condition assessment of concrete bridge decks.

2.2.11.1 *Theory*

In impact-echo testing, a low-frequency stress wave, typically less than 80 kHz, is generated by mechanically impacting the surface of the concrete (Impact-Echo Instruments 2004, Scott et al. 2003). The stress wave propagates through the concrete at a velocity that is characteristic of the material. Stress waves are reflected by discontinuities in the concrete and travel back toward the source, where they are detected by a contact or contactless sensor (Guthrie

Figure 2-15 Mallet-based multi-channel impact-echo scanner.

Figure 2-16 Tire-based multi-channel impact-echo scanner.

et al. 2019a, Guthrie et al. 2019b, Impact-Echo Instruments 2004, Larsen et al. 2020, Scott et al. 2003).

Contact sensors use transducers for digitizing the reflected information, after which the data are usually recorded on a computer. Wave velocity is determined by measuring the travel time of a stress wave between two transducers separated by a known distance, while the wave frequency is obtained using accelerometers. The resulting frequencies constitute a response

spectrum (Impact-Echo Instruments 2004). The peaks in the reflection spectrum designate dominant frequencies, which are associated with reflections of stress waves or with flexural vibrations in thin or delaminated layers (Gucunski et al. 2000). The structural integrity of the concrete affects the frequency of the reflection waves by causing a shift in the response spectrum. Good-quality concrete creates a peak in the response spectrum at comparatively low frequencies. However, for delaminated bridge decks, for example, the reflection waves return from depths much less than the deck thickness, causing higher frequencies that are marked by a peak farther to the right in the response spectrum. When a delamination is just beginning, the high-frequency peak may be accompanied by a second peak of lower frequency, corresponding to reflections from the bottom of the deck slab. As separation of the delaminated concrete increases, however, wave transmission across the delamination is prohibited so that only the higher-frequency peak appears.

Contactless sensors use microphones suspended above the test surface and can produce results similar to those obtained using contact sensors (Guthrie et al. 2019a, Larsen et al. 2020). Instead of directly measuring the pressure waves that propagate within the concrete, the microphones capture leaky surface waves or, perhaps more imperfectly in the case of concrete, flexural modes of the concrete that transmit acoustic energy through the air. This process is analogous to traditional sounding in that the inspector excites these flexural modes with a hammer or chain and interprets the acoustic response by ear. This method of detection works best for delaminations with a horizontal length-to-thickness ratio greater than five (Oh 2012). When the effective horizontal length is significantly greater than the thickness of the delamination, the flexural modes dominate the acoustic response of the concrete, and the delamination can be detected more easily. In general, the flexural modes for a delamination resonate with a dominant frequency between 1.0 and 3.5 kHz, while for intact concrete they resonate at a frequency around 10 kHz (Kee and Gucunski 2016). When an inspector performs a typical chain drag of a bridge deck, the difference in sound produced by intact and delaminated concrete is related to this difference in frequency. This difference in frequency is also the basis for quantitative classification schemes that allow automated algorithms to rapidly classify an area of concrete as either delaminated or intact.

2.2.11.2 *Procedures*

Three versions of the impact-echo method are available. The first is a manual method used for point-by-point data collection (Olson Instruments 2015), the second is a low-speed, automated method for scanning a full lane width (Guthrie et al. 2014, Popovics 2010, Rutgers 2018, Tinkey et al. 2011), and the third is a high-speed, automated method for scanning a full lane width (Guthrie et al. 2019b).

The manual method of impact-echo testing involves the use of a handheld device for testing individual points, usually on a grid marked on the bridge deck surface. The device applies the impact with a solenoid impactor and measures the response with an integrated displacement transducer. The test results are recorded on the device (Olson Instruments 2015). This method of impact-echo testing requires stationary traffic control.

The low-speed impact-echo method involves the use of an automated scanner that is self-propelled or towed by a vehicle across a bridge deck at a speed of up to 2.0 ft per second (Guthrie et al. 2014, Popovics 2010, Rutgers 2018). Vehicle-towed scanners can typically assess a full lane width, while self-propelled scanners assess a smaller area. As impacts to a deck surface are applied, generally with mallets, the acoustic response is recorded using microphones, and the relative energy of the echo or return frequency is calculated from the response and used to create a heat map and/or to identify delaminations along the length of the bridge deck (Gucunski et al. 2013, Guthrie et al. 2014). This method of impact-echo testing requires traffic control.

The high-speed impact-echo method involves the use of an automatic scanner that is towed by a vehicle across a bridge deck at a speed of 25 to 40 mph (Guthrie et al. 2019b). This scanner can assess a full lane width, applying impacts to a deck surface through the contact of chain links fastened to tires that roll along the deck and recording acoustic responses using microphones. Methods of calculation are similar to those utilized for the low-speed methods (Guthrie et al. 2019b). This method of impact-echo testing does not require traffic control.

2.2.11.3 *Data Interpretation*

After data are collected, they are plotted, typically in the form of a heat map, to show the locations of delaminations. Figure 2-17 shows a heat map from a highly delaminated bridge deck, with the delaminations shown in dark red (Guthrie et al. 2014). The percentage of deck area that is delaminated can then be calculated.

2.2.11.4 *Considerations*

Impact-echo testing is typically used to identify delaminations, voids, honeycombing, and cracks on concrete bridge decks before a preservation or rehabilitation project. Although the impact-echo method can be used to detect delaminations in decks with portland cement concrete overlays, detection of delaminations in decks with asphalt overlays is more difficult. Furthermore, impact-echo testing cannot generally be used to distinguish between a corrosion-induced delamination and an area where an overlay has debonded from the concrete bridge deck surface.

Data must be collected on a very dense grid in order to accurately define the boundaries of delaminated areas, and hand-operated hammers are commonly used for this purpose. When using impact-echo testing near the edge of a bridge deck, boundary effects should be taken into consideration; reflections from the boundaries may distort the response (Gucunski et al. 2013).

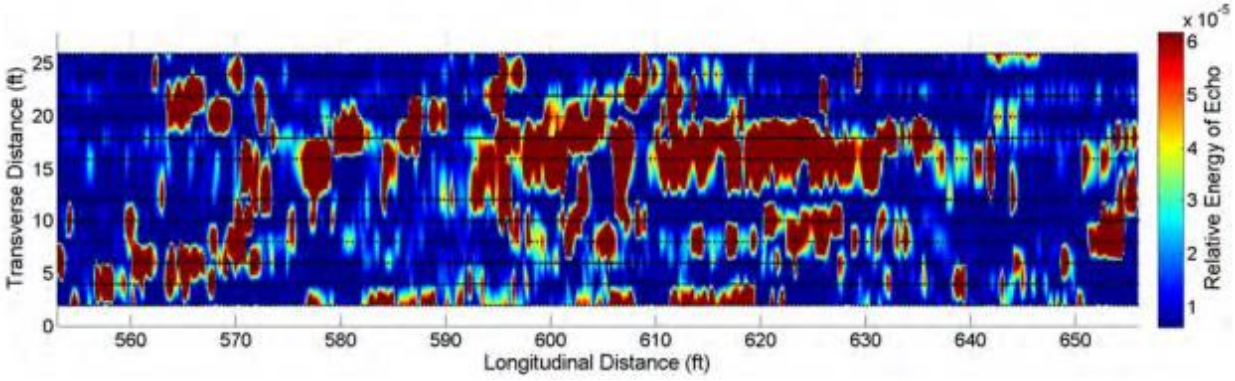

Figure 2-17 Impact-echo map of a highly delaminated concrete bridge deck (Guthrie et al. 2014).

2.2.12 Infrared Thermography Scanning

Infrared thermography scanning is a nondestructive method used to detect delaminations in bridge structures (Gucunski et al. 2013, Maser et al. 2001). Because intact and delaminated concrete typically exhibit different surface temperatures when a bridge deck is experiencing active heating or cooling, infrared thermography scanning can be an effective method for detecting delaminations when the environmental conditions are appropriate (Washer et al. 2010).

2.2.12.1 *Theory*

Variations in surface temperature across a bridge deck during heating or cooling can be associated with the occurrence of delaminations (Manning 1985). Delaminations minimize heat transfer through the deck because of the insulating air space between the separated layers of concrete, causing the concrete layer above the delamination to become hotter than intact concrete, in which heat is transferred throughout the entire deck thickness (Manning 1985, Maser et al. 2001). Thus, during times of heating, the surface temperature of a delamination is higher than that of surrounding intact concrete. Similarly, in the evening when heat is being discharged from the concrete, the surface temperature of delaminations is lower than that of the adjacent concrete.

2.2.12.2 *Procedures*

A thermographic scan is performed with sensitive infrared equipment, as shown in Figure 2-18. The components of a thermographic system include an infrared scanner, a control unit, a battery pack, and a display screen (Manning 1985). The system receives infrared data from the scanner and produces a two-dimensional image on the display screen (Clark et al. 2002, Maser et al. 2001). The data are used to create a temperature map for qualitative data analysis (Gucunski et al. 2013, Maser et al. 2001). Since an infrared thermography scan is generally performed with vehicle-mounted equipment, this method of analysis is fast and does not require traffic control.

2.2.12.3 *Data Interpretation*

The main result of a thermographic scan is a temperature map, such as that shown in Figure 2-19, that indicates the locations of possible delaminations. Unfortunately, these results can sometimes be inconclusive. For instance, a positive result from a thermographic scan, which

Figure 2-18 Vehicle-mounted infrared thermography scanning (Ruohonen 2013).

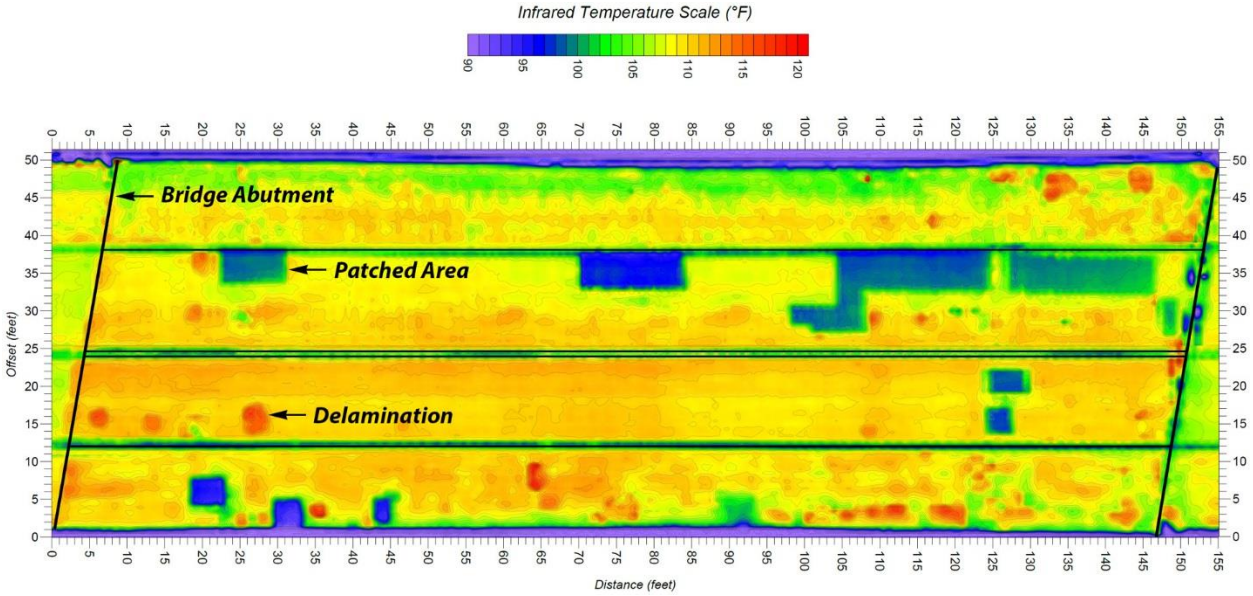

Figure 2-19 Infrared thermography map of a concrete bridge deck (Penetradar Corporation 2017).

is manifest as a temperature difference of at least 1°C between delaminated and intact sections of concrete, implies that a delamination is present in the bridge deck (Manning 1985, Washer et al. 2010); however, a negative result suggests that no delamination is present in the deck or that the

thermographic scan was unable to detect a delamination (Manning 1985). For this reason, additional testing is often performed to supplement the results of infrared thermography scanning.

2.2.12.4 *Considerations*

Infrared thermography scanning is typically used to identify delaminations on concrete bridge decks before a preservation or rehabilitation project. Infrared thermography can be used to quickly assess the condition of a deck and then determine if a more detailed evaluation is necessary (Manning 1985).

One limitation of infrared thermography scanning is that the scanner is sensitive to both infrared radiation emitted from the deck and solar radiation reflected onto or diverted from the deck (Clark et al. 2002, Maser et al. 2001). Therefore, the scanner is sensitive to glare from passing vehicles, shadows from fixed overhead structures, cloud cover, and other objects that may either reflect or divert solar radiation. In addition, wind can influence the results of a thermographic scan since it causes momentary variations in deck surface temperature (Clark et al. 2002, Gucunski et al. 2013, Manning 1985). Also, when moisture is present on the bridge deck, a thermographic scan should not be performed because of the high emissivity of water, where emissivity is the relative power of a surface to emit heat by radiation (Clark et al. 2002, Manning 1985). In general, the results of infrared thermography scanning can be adversely affected by debris on the surface, boundary conditions, and other surface anomalies (Gucunski et al. 2013).

Another limitation is that, although this method can detect flaws in a bridge deck, determining information about the depth of a flaw requires additional testing, and detection of deep flaws may not be possible. In particular, although infrared thermography can be used on asphalt-overlaid decks, increasing asphalt overlay thickness leads to decreasing sensitivity of the method to the presence of delaminations in the underlying concrete (Manning 1985).

2.2.13 Linear Polarization Testing

Linear polarization testing, also called linear polarization resistance testing, is a nondestructive method of measuring the resistance of the reinforcing steel to polarization (So

and Millard 2007). This method is used to estimate the corrosion current density of the reinforcing steel (Andrade and Alonso 2004). Figure 2-20 shows linear polarization testing of a concrete bridge deck.

2.2.13.1 *Theory*

During testing, voltage is applied to the reinforcing steel in order to shift the potential of the steel slightly below its free corrosion, or half-cell, potential. The voltage is then slowly increased until it is slightly above the free corrosion potential of the steel. The change in current is measured along with the change in potential. Polarization resistance is then computed as the ratio of the change in current to the corresponding change in potential (Andrade and González 1978). The polarization resistance can be used to calculate the corrosion current density of the steel (Andrade and Alonso 2004).

2.2.13.2 *Procedures*

At each testing location, the rebar must be located with a cover meter (Andrade and Alonso 2004). As with the GPM or the HCP method, part of the rebar must be exposed so that a

Figure 2-20 Linear polarization testing.

direct electrical connection between the rebar and the testing instrument can be made, and the surface should be pre-wetted. For a stable corrosion potential, a current is applied to the rebar, and the voltage shift is measured by the apparatus. Several measurements are commonly obtained at one location to ensure reliability (Andrade and Alonso 2004). Linear polarization testing requires stationary traffic control.

2.2.13.3 *Data Interpretation*

Corrosion current densities can be used to assess the corrosion activity, identify areas of a bridge deck at risk of corrosion, or evaluate the effectiveness of maintenance efforts (Andrade and Alonso 2004). The corrosion current densities can be correlated with corrosion rates to determine reinforcing steel condition, as shown in Table 2-2.

2.2.13.4 *Considerations*

Much like the GPM or the HCP method, linear polarization is useful for on-site evaluation of the condition of embedded reinforcing steel (So and Millard 2007). One limitation of linear polarization testing is that environmental factors, such as ambient temperature and concrete moisture, can influence the instantaneous measurement of the corrosion rate and therefore must be taken into account (So and Millard 2007). Regarding moisture, although the concrete surface to be tested should always be pre-wetted, excessive water will cause the measurements to be unreliable; therefore, linear polarization testing is not recommended for testing of submerged structures. Linear polarization testing is also not recommended during freezing conditions when water applied to the bridge deck may change to ice.

Variable conditions often require more than 10 measurements at a given location to achieve repeatable corrosion current density results. In addition, in the case of localized

Table 2-2 Interpretation of Corrosion Current Density Measurements (Andrade and Alonso 2004)

I_{corr} ($\mu A/cm^2$)	Corrosion Rate
$\leq$ 0.1	Negligible
0.1 to 0.5	Low
0.5 to 1.0	Moderate
> 1.0	High

corrosion, an error in the estimated corrosion density, which is an error proportional to the ratio of the corroding area to the total area, must be accounted for by multiplying the average corrosion rate by a pitting factor, commonly assumed to be 10 (Andrade and Alonso 2004).

2.2.14 Petrographic Analysis

Petrography is the evaluation and assessment of the microstructure and composition of a material (Manning 1985, Poole and Sims 2016). Because a sample of concrete must be removed from a concrete bridge deck in order for a petrographic analysis to be performed in the laboratory, petrography is considered to be a destructive test. A petrographic analysis includes both visual and microscopy techniques to identify the constituents of concrete, detect performance problems, and/or assess the integrity of concrete (Manning 1985). This method is extremely useful in identifying concrete construction problems, as well as mechanisms of deterioration such as freeze-thaw cycling and chloride infiltration.

2.2.14.1 *Theory*

According to ASTM C856, petrographic analysis of concrete is essentially a more detailed visual analysis that is performed by a qualified technician using various instruments to evaluate specimen composition, air content, surface hardness, cracking, and other physical properties. ASTM C856 provides numerous tables for the inspector to reference when determining the condition of a concrete specimen.

2.2.14.2 *Procedures*

Specimens can be prepared in different ways for evaluation in a petrographic analysis (Manning 1985). Specimens can have polished or etched surfaces, or they can be thinly sliced. The thinly sliced sample, also known as a thin-section, is often a cross-sectional slice of a concrete core. The analysis begins with a visual examination of the concrete sample in order to gather information concerning construction practices, unique characteristics of the specimen, or noticeable deterioration. Occasionally, the information gathered during a visual inspection is sufficient to meet the needs of the investigation. However, when a more thorough examination of the specimen is necessary, stereo microscopy, transmitted-light microscopy, reflected-light

microscopy, or scanning-electron microscopy may be used (Poole and Sims 2016). These tests are highly specialized and are usually performed by an expert petrographer (Manning 1985).

Petrographic image analysis (PIA) requires the use of advanced equipment, such as the petrographic microscope shown in Figure 2-21 (Poole and Sims 2016). The equipment is completely automated and uses digital image acquisition to obtain quantitative information about sizes, shapes, and numbers of pores in a given thin-section. PIA yields a high-resolution scan of thin-sections, cuttings, and core samples in true color. PIA also provides details concerning texture and composition of concrete constituents, including specific textural parameters such as pore size and geometry. The time needed to conduct a PIA is considerably reduced since the equipment can detect characteristics and make classifications of concrete properties at a faster rate than a traditional petrographic analysis (Poole and Sims 2016). Obtaining concrete core samples to test in the laboratory requires stationary traffic control.

2.2.14.3 *Data Interpretation*

Similar to a visual inspection, the results of a petrographic analysis typically include photographs, diagrams, and descriptions of the specimens. Table 2-3 presents several possible results of a petrographic analysis, as well as the type of microscope that can be used for the

Figure 2-21 Petrographic microscope (Poole and Sims 2016).

Table 2-3 Characteristics of Concrete Observed Using Microscopes (ASTM C856)

	Characteristic	Type of Microscope	
		Stereomicroscope	Petrographic
Aggregate	Shape	X	X
	Grading	X	-
	Distribution	X	-
	Texture	X	X
	Composition	X	X
	Rock types	X	X
	Degree of alteration	X	X
	Alteration products	X	X
	Coatings	X	X
	Rims	X	X
	Internal cracking	X	X
	Contamination	X	X
Concrete	Air-entrained or not	X	X
	Shape of air voids	X	X
	Size of air voids	X	X
	Distribution of air voids	X	-
	Bleeding	X	-
	Segregation	X	-
	Aggregate-paste bond	X	X
	Fractures	X	X
	Size of embedded items	X	-
	Shape of embedded items	X	-
	Location of embedded items	X	-
	Type of embedded items	X	-
	Degree and type of alteration	X	X
	Location of reaction products	X	X
	Identification of reaction products	X	X
	Nature and condition of surface treatments	X	X
Paste	Color	X	X
	Hardness	X	-
	Porosity	X	-
	Carbonation	X	X
	Distribution of residual cement	-	X
	Particle size of residual cement	-	X
	Abundance of residual cement	-	X
	Composition of residual cement	-	X
	Size of supplementary cementitious materials	-	X
	Abundance of supplementary cementitious materials	X	X
	Identification of supplementary cementitious materials	X	X
	Compounds in hydrated cement	X	X
	Size of contamination	X	X
	Abundance of contamination	X	X
	Identification of contamination	-	X

analysis. A hyphen in Table 2-3 indicates that an analysis cannot be performed by the given type of microscope.

2.2.14.4 *Considerations*

A petrographic analysis is performed on hardened concrete, typically a core sampled from a deck of interest. According to ASTM C856, this type of analysis is often required to address concerns about the integrity of the concrete, such as the extent of fire damage or alkali-silica reaction. Care must be taken during sample collection to retrieve intact, representative samples that can be used in the analysis.

2.2.15 Radiography

Radiography (also called x-ray inspection) is a nondestructive testing method used for the evaluation of internal characteristics of concrete bridge decks. Radiography can be used to locate reinforcing steel, voids, and honeycombing (McGormley et al. 2013, Rehman et al. 2015).

2.2.15.1 *Theory*

Radiography is a nuclear method in which electromagnetic radiation, in the form of either X-rays or higher-energy gamma rays, is transmitted from a radioactive source on the surface of the bridge deck through the bridge deck and recorded on collection screens placed on the underside of the bridge deck (McGormley et al. 2013, Rehman et al. 2015). High-density materials, such as reinforcing steel, block radiation from reaching the collection screen, so that a two-dimensional image, or radiograph, of the interior of the bridge deck can be created, as shown in Figure 2-22. Conventional radiographic testing uses photographic film as the collection screen, while digital radiographic testing uses digital X-ray sensors (McGormley et al. 2013).

2.2.15.2 *Procedures*

Radiography is performed by placing a radioactive source on the surface of the bridge deck and collection screens on the underside of the bridge deck and then exposing the bridge deck to radiation (McGormley et al. 2013, Rehman et al. 2015). The precise locations of the screens must be recorded so that the locations of reinforcement, voids, and honeycombing can be correctly marked.

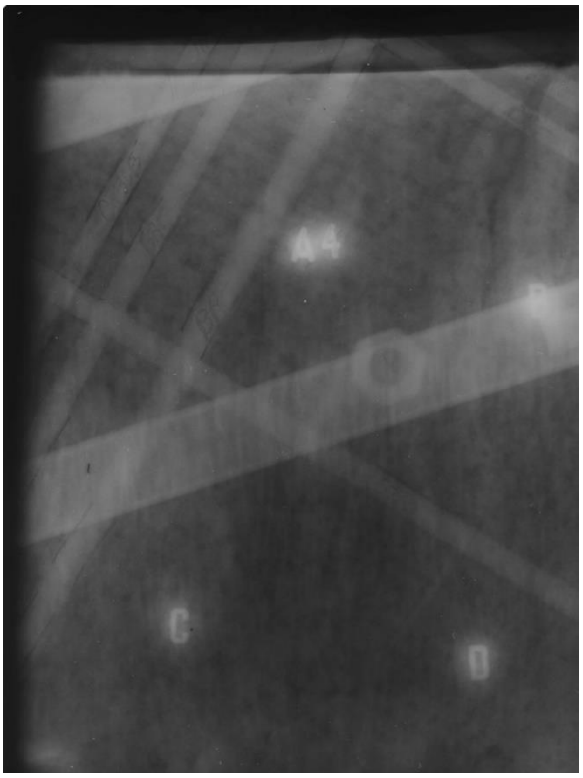

Figure 2-22 Radiograph showing reinforcing steel and conduit (Digital Concrete Scanning 2020).

2.2.15.3 *Data Interpretation*

When conventional radiographic testing is used, the film must be developed in a dark room after radiation exposure. The results of digital radiographic testing can be post-processed and filtered to provide more accurate, enhanced images. Reading a radiograph and processing the data requires experience and skill (Digital Concrete Scanning 2020).

2.2.15.4 *Considerations*

Radiography can be more precise than GPR for locating reinforcement and can produce clearer results than GPR. One major limitation of radiography is the safety concern associated with radiation, requiring highly specialized safety training and licensing (McGormley et al. 2013, Rehman et al. 2015). Another limitation of radiography is that access to both the surface and underside of the bridge deck is required (McGormley et al. 2013).

2.2.16 Rapid Chloride Permeability Testing

RCP testing is a method that measures the chloride permeability of concrete in coulombs (Elsener and Bohni 1990, Stanish et al. 2004). The RCP test can be considered either destructive or nondestructive, depending on how the sample is obtained. Figure 2-23 shows an RCP test in progress.

2.2.16.1 *Theory*

Chloride permeability is determined with the RCP test by applying a voltage across a concrete specimen and measuring the electrical charge that passes through the specimen during a 6-hour period, as described in ASTM C1202 (Standard Test Method for Electrical Indication of Concrete's Ability to Resist Chloride Ion Penetration) (Mindess et al. 2003), where a higher value indicates a higher chloride permeability. Measuring the chloride permeability of concrete is one way to determine the risk of deterioration. Low-permeability concrete generally possesses high strength and is resistant to the infiltration of water and chlorides (Elsener and Bohni 1990). Conversely, high-permeability concrete allows water, salts, and oxygen to more easily reach the reinforcing steel, which accelerates corrosion of the reinforcement. Through measurement of the chloride permeability of concrete, durability problems can be detected early in the service life of a concrete bridge deck so that timely and cost-effective protective measures can be implemented

Figure 2-23 RCP testing.

before the occurrence of any significant corrosion or deterioration of the concrete (Elsener and Bohni 1990).

2.2.16.2 *Procedures*

The RCP test is performed on concrete specimens that are 4.0 in. in diameter and 2.0 in. in thickness, which can be obtained by cutting a core sample from a concrete bridge deck or from a cylinder cast at the time of construction (Elsener and Bohni 1990, Stanish et al. 2004). The specimen must undergo a vacuum-saturation conditioning procedure before the RCP test can be performed. After the conditioning, one side of the specimen is immersed in a sodium chloride (NaCl) solution, while the other side is immersed in a sodium hydroxide solution (NaOH) (Stanish et al. 2004). An electrical voltage of 60 V DC is then applied to the specimen to facilitate migration of the chloride ions into the concrete. Electrical current readings are taken at least every 30 minutes during the 6-hour test and then plotted as a function of time. Obtaining concrete core samples to test in the laboratory requires stationary traffic control.

2.2.16.3 *Data Interpretation*

From the plot of electrical current readings as a function of time, the area under the curve indicates the total charge passed through a specimen during the 6-hour test, which is a measure of the chloride-ion permeability of the concrete. A high charge indicates a high permeability to chloride ions, or poor-quality concrete. Table 2-4 provides values that relate the charge passed to chloride-ion penetrability (Elsener and Bohni 1990).

Table 2-4 Interpretation of Chloride-Ion Penetrability Measurements (Elsener and Bohni 1990)

Charge Passed (Coulombs)	Chloride Ion Penetrability
> 4,000	High
2,000 to 4,000	Moderate
1,000 to 2,000	Low
100 to 1,000	Very Low
< 100	Negligible

2.2.16.4 *Considerations*

The RCP test can be used to evaluate both cores and cast concrete specimens. When the test is performed on cast concrete samples, the test is usually scheduled to take place after a specified curing time.

Several researchers have criticized the accuracy of the RCP test even though the method has been adopted as a standard by both ASTM and AASHTO (Elsener and Bohni 1990). One of the main criticisms is that the electrical current passed through the specimen is a measure of all ions in the pore solution, not solely the chloride ions. Critics also suggest that measurements are made prematurely, before steady-state migration rates are attained. In addition, the high voltage passed through a high-permeability specimen, typical of poor-quality concrete, can cause an increase in the temperature of the concrete, which increases the electrical current flow compared to the flow that would occur if the specimen were to remain at a constant temperature. Therefore, the RCP test results may indicate that poor-quality concrete appears to be worse than it actually is. Additionally, the accuracy and precision of the RCP test is poor. ASTM C1202 requires that the average value of three samples cannot differ by more than 29 percent between two independent laboratories, which is viewed by many researchers as excessive. Furthermore, the method depends on a relationship between the conductivity of concrete and the chloride-ion permeability. Consequently, if conductive materials, such as reinforcing steel, carbon fiber, or corrosion-inhibiting admixtures, are present within the specimen, the test results may be uninterpretable.

2.2.17 Resistivity Testing

Resistivity testing is a nondestructive method that measures the electrical resistivity of concrete. It is used to assess the resistance of concrete to current flow that may lead to reinforcing steel corrosion and can also be useful for isolating areas of deteriorating concrete (Whiting and Naji 2003).

2.2.17.1 *Theory*

Electrical resistivity measurements are based on Ohm's law, which states that the direct current through a conductor is directly proportional to the applied potential and inversely

proportional to the resistance of the conductor (Malhotra and Carino 1991, Monfore 1968). Electrical resistivity is the resistance per unit length of a material to the flow of an electrical current through a defined cross-sectional area (Whiting and Naji 2003). Resistivity is directly proportional to the cross-sectional area of a material and inversely proportional to its effective length. The electrical resistivity of concrete is largely a function of the properties of the concrete matrix and the pore water (Brameshuber and Raupach 2003). A concrete matrix with high porosity, characterized by high interconnectivity and low tortuosity, allows for the passage of high amounts of electrical current and would have a lower resistivity than a concrete matrix with low porosity, characterized by low interconnectivity and high tortuosity, all other factors constant (Malhotra and Carino 1991, Mindess et al. 2003). Regarding pore water, high ion concentrations and high temperatures allow for the passage of high amounts of electrical current through the concrete due to the high abundance and mobility of current carriers (Brameshuber and Raupach 2003); as temperature increases, the activity of the ions increases and the viscosity of the pore solution within the concrete decreases, causing an increase in ion mobility that corresponds to lower concrete resistivity measurements (Malhotra and Carino 1991, Mindess et al. 2003).

Two devices commonly used to measure resistivity are the two-prong and four-prong resistivity instruments (Giatec 2013, Pullar-Strecker 2002, Song and Saraswathy 2007, Whiting and Naji 2003). Both the two-prong and four-prong instruments operate by passing an alternating current between the prongs, or electrodes, measuring the corresponding potential drop, and then computing the resistance of the concrete (Guthrie and Tuttle 2006, Hema et al. 2004). Alternating current, instead of direct current, is used for resistivity measurements to minimize polarization at the electrode tips (Böhni 2005, Pullar-Strecker 2002, Song and Saraswathy 2007). For the four-prong instrument, a known alternating current is applied to the two outer prongs, and the resulting potential drop is measured between the spring-loaded inner prongs for calculation of resistivity (Böhni 2005, Broomfield 1997, Bungey and Millard 1996, Malhotra 1976, Malhotra and Carino 1991, Morris et al. 1996, Pullar-Strecker 2002, Song and Saraswathy 2007). The resistivity values measured using this method represent the average concrete resistivity at a depth approximately equivalent to the probe spacing (Malhotra 1976, Song and Saraswathy 2007). Typically, the prongs are uniformly spaced 1.2 to 2.0 in. apart (Malhotra 1976, Morris et al. 1996).

2.2.17.2 *Procedures*

When either the two-prong or the four-prong resistivity instruments are used, the concrete surface should be void of any standing water; however, assuming that condition is met, the concrete surface should not be deliberately dried or pre-wetted, which could change the test results. The probes for both the two-prong and four-prong instruments should be oriented parallel to the tines of the concrete, as applicable, avoiding the groves and exposed aggregate. Prongs should also be placed away from the location of reinforcing steel, which can be determined using a cover meter. Readings are generally obtained within a few seconds after placing the probes in the desired location on the bridge deck.

For use of the two-prong probe, two holes are pre-drilled into the deck surface for placement of the prongs. Because the ends of the prongs typically rest on the bottom of these drilled holes, the depth of the holes should be controlled. The concrete powder is removed from the holes with a vacuum or compressed air, and the holes are then partially filled with a conductive fluid, such as liquid soap. The prongs of the probe are then inserted into the holes, and a reading is taken, as shown in Figure 2-24. The probe may then be removed, rotated 180 degrees, and re-inserted for a second reading if an average of more than one reading per location is desired.

Figure 2-24 Two-prong resistivity testing.

For use of the four-prong probe, pre-drilled holes are not required. Instead, the probe is positioned directly on the deck surface, as shown in Figure 2-25. The resistivity value should stabilize before being recorded. The probe may then be rotated 180 degrees for a second reading at the same location if an average is needed. Resistivity testing requires stationary traffic control.

2.2.17.3 *Data Interpretation*

Table 2-5 shows the interpretation of resistivity measurements with respect to the potential risk of corrosion of reinforcing steel in the concrete (Brameshuber and Raupach 2003, James Instruments, Inc. 2004, Song and Saraswathy 2007, Whiting and Naji 2003).

2.2.17.4 *Considerations*

Resistivity testing is an appropriate method for estimating the likelihood of reinforcing steel corrosion because the development of corrosion currents in concrete is also largely a

Figure 2-25 Four-prong resistivity testing (Giatec 2013).

Table 2-5 Interpretation of Resistivity Measurements (Guthrie and Tuttle 2006)

Resistivity (kohm-cm)	Corrosion Risk
> 20	Low
10 to 20	Low to Moderate
5 to 10	High
< 5	Very High

function of the properties of the concrete matrix and the pore water (Bungey and Millard 1996, CNS Farnell Limited 2008, Whiting and Naji 2003). Higher porosities, moisture contents, chloride concentrations, and temperatures are all consistently correlated with higher corrosion rates and are manifest by lower resistivity values (Bungey and Millard 1996, CNS Farnell Limited 2008, Guthrie and Mazzeo 2015, Guthrie et al. 2018, Whiting and Naji 2003).

One limitation of resistivity testing is that, although it measures the likelihood of corrosion to occur, it does not measure actual corrosion rates or the amount of corrosion that has already occurred (CNS Farnell Limited 2008). In addition, concrete surface conditions such as laitance and carbonation can affect four-prong resistivity measurements (Broomfield 1997, CNS Farnell Limited 2008). Resistivity measurements have been shown to be sensitive to factors such as concrete age, moisture content, curing method, temperature, cement type, additives, resistivity probe orientation relative to the reinforcing steel, and chloride concentration (Böhni 2005, Brameshuber and Raupach 2003, Broomfield 1997, Malhotra and Carino 1991, Mindess et al. 2003, Monfore 1968, Sengul and Gjorv 2009, Song and Saraswathy 2007, Whiting and Naji 2003).

2.2.18 Schmidt Rebound Hammer Testing

The Schmidt rebound hammer test, also known as the Swiss hammer test, is a nondestructive test that measures the rebound of a spring-loaded plunger, which has been empirically correlated to concrete strength (Fanous et al. 2000, Moore 1975). The Schmidt rebound hammer test is useful in determining the uniformity of concrete with a focus on identifying areas that require further investigation (Kosmatka and Panarese 1988, Manning 1985).

2.2.18.1 *Theory*

The rebound number is determined by measuring the rebound of a spring-loaded plunger as a percentage of the initial length of the spring (Fanous et al. 2000, Moore 1975). When the plunger rod is pushed against a hard surface, a spring inside the device tightens until a latch is released, and the spring then propels the internal hammer into the plunger tip. The rebound of the internal steel hammer is recorded by a slide indicator on the outside of the device. This result is

called a rebound number. A harder surface will generate a higher rebound number (Cemex 2013). Figure 2-26 shows a Schmidt rebound hammer in use.

2.2.18.2 *Procedures*

According to ASTM C805 (Standard Test Method for Rebound Number of Hardened Concrete), the Schmidt hammer must be held perpendicular to the surface being tested to produce accurate results. The hammer is then pushed slowly toward the surface until the hammer impacts, and the impact number is then recorded. Ten readings spaced at least 1.0 in. apart and at least 2.0 in. from the edge of any members should be obtained in each test area, which may take a few minutes per test area. Concrete elements should be at least 4.0 in. thick and fixed within a structure, unless supported rigidly, with a 6.0-in.-wide testing surface. Concrete surfaces that are soft, are heavily textured, or have loose mortar present should be avoided or ground flat with a grinding stone, and direct contact with coarse aggregate particles should be avoided to improve accuracy. Concrete having a compressive strength of less than 1,000 psi should not be evaluated

Figure 2-26 Schmidt rebound hammer testing.

by this method, as the hammer may cause damage to the concrete (Kosmatka and Panarese 1988, Manning 1985). Schmidt rebound hammer testing requires stationary traffic control.

2.2.18.3 *Data Interpretation*

The Schmidt rebound hammer readings collected in each test area should be averaged after outliers are removed. Specifically, according to ASTM C805, any readings differing from the average by more than six units should be excluded, and the remaining readings should be averaged. No fewer than eight readings should be averaged for the impact number; therefore, if more than two readings differ from the average of 10 readings by more than six units, additional readings should be obtained within the test area.

As described previously, Schmidt rebound hammer test results can be affected by aspects of concrete mixture design, operator practices, and instrument calibration. Therefore, when the objective of Schmidt rebound hammer testing is to estimate the in-place concrete strength, the relationship between rebound number and strength should be established for each concrete mixture design and instrument. To establish this relationship, ASTM C805 states that rebound numbers measured at various locations on the structure should be correlated to concrete strength measurements obtained from core samples taken at corresponding locations. At least six locations with different rebound numbers should be included, with at least two cores per location, in this process. A general correlation between rebound number and concrete strength is shown in Figure 2-27.

2.2.18.4 *Considerations*

Schmidt rebound hammer testing can be performed in any eligible areas of interest. A limitation of the Schmidt rebound hammer test is that the results are affected by several factors, including the angle of testing, concrete surface smoothness, concrete mixture proportions, concrete coarse aggregate type, concrete moisture content, concrete surface carbonation, concrete age, proximity of near-surface steel reinforcement, concrete air voids, temperature of the concrete surface and/or the Schmidt rebound hammer device, and instrument calibration (Manning 1985, Cemex 2013). Calibration techniques should be used to ensure that the readings are accurate, especially regarding the angle of test. Because the angle of the test will affect any

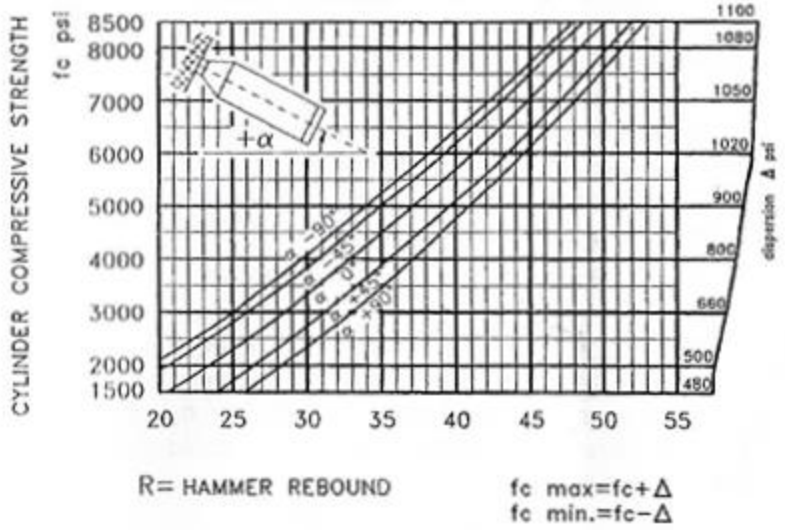

Figure 2-27 Schmidt rebound hammer strength correlation (James Instruments Inc. 2010).

strength correlation, placement of the instrument in vertically up, vertically down, or horizontal positions should be noted during testing (Kosmatka and Panarese 1988, Manning 1985).

2.2.19 Skid Resistance Testing

Skid resistance testing is a nondestructive method for determining the resistance to slipping and skidding of a tire traversing a bridge deck surface. Two tests that are commonly used for measuring skid resistance are the British pendulum test (BPT) and the locked-wheel skid trailer test.

2.2.19.1 *Theory*

The BPT apparatus, shown in Figure 2-28, is comprised of a pendulum arm that is attached to a vertical support (Mitchell 1987). On the bottom end of the pendulum is a weighted head with a rubber slider. The opposite end of the pendulum is allowed to rotate freely around a spindle. A skid resistance test is conducted by placing the apparatus on the concrete surface to be tested, and, after performing a calibration procedure, raising the pendulum arm to a horizontal position and then releasing it. The pendulum swings freely downward to the bridge deck surface, which is generally soaked with water to achieve a worst-case scenario before the test is performed. Friction between the rubber slider and the deck surface causes a reduction in the

Figure 2-28 Skid resistance testing using the BPT apparatus.

speed of the pendulum as the slider travels across the deck surface, which in turn reduces the height of the swing that occurs after the slider contacts the deck. A pointer that moves with the pendulum arm reports the surface resistance on a scale from 0 to 150. This value is used to calculate a skid number.

Testing with a locked-wheel skid trailer involves measurement of skid resistance of a deck surface with a specified full-scale automotive tire. The test apparatus, as shown in Figure 2-29, is comprised of a trailer that is towed behind a vehicle. The trailer includes a test wheel, a transducer, instrumentation, a water supply and dispensing system, and actuation controls for braking of the test wheel. The measurement represents the steady-state friction force on a locked test wheel as it is dragged over a wetted deck surface under constant load and at a constant speed. The skid resistance of the paved surface is determined from the resulting force or torque and is reported as a skid number (SN). For more conservative measurements, water is applied in front of the test wheel before locking it, similar to the process of wetting a bridge deck surface before performing a BPT (Smith et al. 2016).

2.2.19.2 *Procedures*

The procedure for the BPT is described in ASTM E303 (Standard Test Method for Measuring Surface Frictional Properties Using the British Pendulum Tester). The BPT apparatus

Figure 2-29 Locked-wheel trailer test apparatus (Smith 2016).

must first be calibrated to the proper strike distance of 5.0 in. The surface is wetted, a test swing is performed, and then four more swings are performed and recorded. The surface should be re-wetted before each swing. The temperature of the surface should also be measured and recorded at each test location. Each test takes approximately 5 to 10 minutes. This method of skid resistance testing requires stationary traffic control.

The procedure for testing with the locked-wheel skid trailer is described in ASTM E274 (Standard Test Method for Skid Resistance of Paved Surfaces Using a Full-Scale Tire). The testing apparatus is a trailer that is towed across the bridge deck of interest. The vehicle is maintained at a constant speed of 40 mph while water is applied to the deck surface directly in front of the test wheel. Brakes are then applied to the test wheel so that the wheel locks and begins to skid for 1.0 to 3.0 seconds. At this point, the horizontal and vertical forces are recorded and correlated to a measurement called the friction number or skid number. This method of skid resistance testing does not require traffic control.

2.2.19.3 *Data Interpretation*

BPT results can be used to calculate a skid number (Huang 2004). Corrections for temperature are needed since vehicle tires are typically at a higher temperature than that of the rubber slider (Mitchell 1987). A skid number can also be calculated from the results of testing using a locked-wheel skid trailer using relationships given in ASTM E274. A higher skid number

indicates a lower risk of slipping. Skid numbers can be compared to a minimum value to determine the acceptability of the skid resistance of a given deck surface. An interpretation of skid number measurements is shown in Table 2-6, but different agencies may have different minimum skid number requirements.

2.2.19.4 *Considerations*

Skid resistance tests are generally performed on high-risk areas to determine if the surface condition is safe. These tests can also be performed to determine the effectiveness of seals and overlays or to regularly monitor surface condition.

The friction value of dry surfaces is relatively high, which aids in preventing crashes. However, moisture on surfaces causes a loss of friction, which can be potentially dangerous to motor vehicles, especially those with tires in poor condition. Skid resistance testing enables identification of surfaces that are hazardous in the presence of moisture (Smith et al. 2016).

The BPT is useful for smaller areas, where driving at 40 mph is impossible, or where the distance to be tested is less than the minimum skid distance that can be tested using a locked-wheel skid trailer. The BPT also provides a more localized SN, allowing for a more detailed analysis. The locked-wheel skid trailer is used for longer decks where driving at 40 mph is appropriate and safe.

Table 2-6 Interpretation of Skid Number Measurements (Wambold et al. 1990)

Skid Number	Recommendation
Less than 30	Take measures to correct
Greater than 30	Acceptable for low-volume roads
31 to 34	Monitor pavement frequently
Greater than 35	Acceptable for heavily-traveled roads

2.2.20 Ultrasonic Pulse Echo Testing

The ultrasonic pulse echo test is a nondestructive method that uses ultrasonic waves, which are high-frequency acoustic waves, to detect internal anomalies, objects, and interfaces in concrete (Gucunski et al. 2013). These acoustic waves are transmitted and received by

transducers, and the time required for the waves to travel through the medium between the transducers is measured.

2.2.20.1 *Theory*

An ultrasonic pulse echo, or ultrasonic pulse velocity, test uses vibration frequencies in the range of 20 to 150 Hz to detect voids in concrete, although frequencies of 150 Hz have only been used in laboratory studies (Bindal et al. 1996, Manning 1985). The vibration frequencies are generated by electronic pulses and then converted into mechanical energy by a transducer. Although higher frequencies are more sensitive to smaller voids and can be used with much thinner specimens, they are also subject to greater attenuation (Manning 1985).

Two different types of transducers are used during an ultrasonic pulse echo test. One is a transmitting transducer, and the other is a receiving transducer (Manning 1985). For testing, the transducers are positioned on the surface of the concrete deck at a specified distance from each other, as shown in Figure 2-30 (Manning 1985). Electronic pulses are generated by the transmitting transducer and recorded by the receiving transducer, and the travel time between the two transducers is measured electronically. As the pulse passes through concrete, its velocity decreases due to the presence of voids associated with porosity and internal cracking. Cracks that are nearly perpendicular to the direction of wave propagation and large enough to disrupt the

Figure 2-30 Ultrasonic pulse echo testing (Hema et al. 2004).

normal transmission path are most easily detected (Manning 1985). Such cracks are detected because they cause an unusually long transit time or a decrease in the amplitude of the received waves. A particular implementation of ultrasonic pulse echo principles, MIRA tomography uses an array of 40 to 48 point transducers acting as transmitters and receivers in a sequential mode to create a three-dimensional representation, or tomogram, of internal defects that may be present in a concrete bridge deck (Germann Instruments 2020, Khazanovich and Hoegh 2016).

2.2.20.2 *Procedures*

An ultrasonic pulse echo test is performed by sending electronically generated mechanical pulses through the bridge deck with an ultrasonic transducer unit and measuring the transit time of the pulse with a digital meter or a cathode-ray oscilloscope (Gucunski et al. 2013, Manning 1985). The technician takes point measurements, typically in a grid pattern, and the measurements are recorded by the device or noted manually. The recorded data include the transit time or velocity, which directly correlates with the concrete quality (Gucunski et al. 2013). Ultrasonic pulse echo testing requires stationary traffic control.

2.2.20.3 *Data Interpretation*

The main result of an ultrasonic pulse echo test is the transit time of the ultrasonic waves (Gucunski et al. 2013). Transit times are longer in the presence of internal defects such as delaminations, voids, or cracking (Gucunski et al. 2013), and they can be correlated with concrete strength (Mindess et al. 2003). The data can be compiled into a map that reflects the presence of internal defects in a concrete bridge deck.

2.2.20.4 *Considerations*

Pulse velocity measurements are reliable for assessing concrete quality and uniformity, as well as detecting voids and cracks in concrete. Some limitations associated with the ultrasonic pulse echo method should be considered during testing. Closely spaced test points are required to produce ultrasonic pulse echo maps of the deck. Therefore, the testing can be time-consuming. Also, good mechanical coupling of the sensor to the deck surface must be achieved, which can prove difficult on rough surfaces. Another limitation is that shallow defects may not be detectable when testing at lower frequencies (Gucunski et al. 2013). Overall, ultrasonic pulse

echo test results are affected by the transmission path length, temperature, moisture content, the presence of reinforcing steel, and concrete strength (Mindess et al. 2003).

2.2.21 Ultrasonic Surface Waves Measurement

The USW test is a nondestructive method that uses the velocity of surface waves to identify anomalies within a material (Gucunski et al. 2013). The USW test can be used in condition assessment to evaluate probable material damage from alkali-silica reaction, delayed ettringite formation, freeze-thaw cycling, and other deterioration processes (Gucunski et al. 2013).

2.2.21.1 *Theory*

The USW test is a technique based on the phenomenon of surface wave dispersion. The USW test is related to the spectral analysis of surface waves method, which uses frequency and wave length to determine layer thickness and elastic moduli of a multi-layered system. However, the USW test is limited to a high frequency range so that the surface waves do not penetrate to a depth greater than the thickness of the object being tested. In this near-surface zone, the USW test can be used to evaluate material properties, such as the elastic modulus of concrete (Gucunski et al. 2013). The velocity of surface waves in bridge decks that are sound and homogeneous will not vary significantly with frequency; however, significant variation in wave velocity will occur in the presence of a delamination or other anomalies (Gucunski et al. 2013).

The measured or assumed mass density or Poisson's ratio of a material can be used to relate the surface wave velocity to the elastic modulus of a concrete bridge deck (Gucunski et al. 2013). The condition of the concrete beneath the surface can be inferred from wave velocity and wave frequency, or the dispersion of the wave propagation as evaluated using spectral analysis (Gucunski et al. 2013).

2.2.21.2 *Procedures*

Automated projectile sources or solenoid-type impactors are used to generate an impact, which produces elastic waves that propagate through the tested medium (Gucunski et al. 2013). The response of the near-surface material is recorded at two receiver locations (Azari et al. 2014, Gucunski et al. 2013). Figure 2-31 shows a USW apparatus, which includes two adjustable feet

Figure 2-31 Ultrasonic surface wave equipment (Gucunski et al. 2013).

(left) to ensure that the apparatus is level, a point of impact (middle), and two receivers (right) (Gucunski et al. 2013). The velocity of the surface waves is determined, and then the modulus of the material is calculated (Azari et al. 2014). Data are typically collected in a grid pattern along the section to be tested, the data collection process at each point taking about 15 seconds (Nazarian 2005). USW testing requires stationary traffic control.

2.2.21.3 *Data Interpretation*

The USW test uses the time computed from two accelerometers at different distances from the source of impact to determine the shear wave velocity or shear modulus of the top layer of the material being tested (Nazarian et al. 1995). Each test results in a modulus value. Very low modulus values often indicate the presence of delamination or cracking (Azari et al. 2014, Gucunski et al. 2013)

2.2.21.4 *Considerations*

While the USW test can be useful for detecting deterioration, it cannot provide reliable modulus values for deteriorated sections of a concrete deck, such as debonded or delaminated sections. In addition, the USW method is significantly more complicated when modulus values must be determined for layered systems, such as asphalt-overlaid decks, where the moduli of the layers differ significantly (Gucunski et al. 2013).

2.2.22 Vertical Electrical Impedance Testing

VEI testing is a nondestructive method of measuring the electrical impedance, or resistance to electrical current flow, of the concrete in a direction perpendicular to the surface of a concrete bridge deck when an alternating electrical potential is applied. VEI can be used to quantify the level of protection against water and chloride ion ingress in concrete bridge decks because the same factors that increase the VEI of concrete also increase the resistance of the concrete to the ingress of those corrosive elements. Increased VEI, which would be expected from the application of a bridge deck surface treatment, for example, is therefore desirable, as it indicates increased protection from corrosion (Argyle 2014).

2.2.22.1 *Theory*

For applications to reinforced concrete, VEI testing is performed by applying alternating electrical potentials at a specific frequency, typically around 200 Hz, between the embedded reinforcing steel, which behaves as the working electrode, and a metal testing probe, or counter electrode, that is placed on the concrete surface; the impedance of the system is then measured at the specified frequency (Bartholomew et al. 2012, Ismail and Ohtsu 2006, Krauss et al. 1996). This approach allows interrogation of all materials between the two electrodes; therefore, on a bridge deck with an asphalt overlay system, for example, VEI measurements reflect the total protection against chloride ingress provided by the asphalt layer, the membrane, the concrete cover, and any reinforcing steel coatings (Guthrie and Mazzeo 2015). A multi-channel VEI bridge deck testing apparatus towed behind a vehicle is shown in Figure 2-32 (Barton et al. 2019a).

Electrical impedance and the rate of corrosion have an inverse relationship. If electrical impedance is high, the movement of corrosive ions is more restricted, which decelerates the corrosion reaction. Conversely, if electrical impedance is low, the movement of corrosive ions is less restricted, which accelerates the reaction (Bentur et al. 1997). Therefore, higher impedance in a particular region of a bridge deck should theoretically signify higher resistance to the movement and accumulation of corrosive chloride ions in the vicinity of the reinforcing steel in that region compared to a region with lower impedance.

Figure 2-32 VEI testing apparatus (Barton et al. 2019a).

2.2.22.2 *Procedures*

A direct or indirect electrical connection to the reinforcing steel is necessary to perform VEI testing. The VEI apparatus is connected to the top mat of rebar directly with a wire or indirectly with a large-area electrode that slides along the concrete deck surface with the VEI apparatus (Barton et al. 2019a, Barton et al. 2019b).

The VEI testing apparatus is towed over the deck area to be tested, and water is sprayed onto the surface of the bridge deck to improve the electrical connection of the probes to the deck surface. The apparatus collects data at a rate of 98 samples per second while being towed along the length of the bridge deck at a target speed of about 5.0 to 9.0 ft per second (Guthrie et al. 2014). VEI testing may or may not require stationary traffic control, depending on the speed of traffic within the test area.

2.2.22.3 *Data Interpretation*

Table 2-7 shows the interpretation of VEI measurements with respect to the protection offered to the reinforcing steel in the concrete. One example of an analysis of the results of a VEI test is shown in Figure 2-33 in the form of a heat map (Guthrie et al. 2014). This particular example is from a highly deteriorated bridge, and the areas of concern, or the areas with low impedance, are shown in red.

Table 2-7 Interpretation of VEI Measurements (Guthrie et al. 2019b)

Impedance Magnitude	Protection Rating
< 4.0	Low
4.0 to 5.0	Medium
> 5.0	High

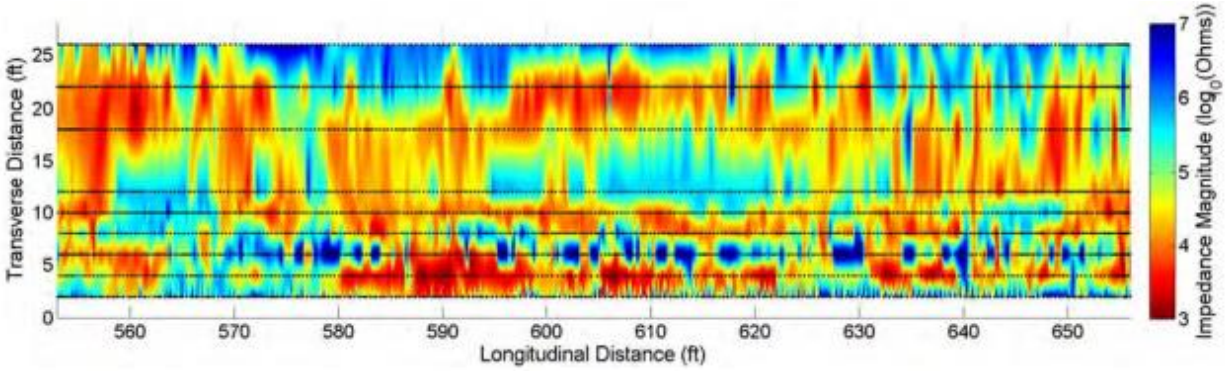

Figure 2-33 VEI map of a highly deteriorated concrete bridge deck (Guthrie et al. 2014).

2.2.22.4 *Considerations*

VEI measurements are appropriate for quantifying the level of protection against water and chloride ion ingress in concrete bridge decks because the same factors that increase the VEI of concrete also increase the resistance of the concrete to the ingress of those corrosive elements. For example, studies have shown that the electrical impedance of concrete is influenced by surface treatments, curing period, temperature, moisture content, cover depth, water-to-cementitious materials ratio, composition of the pore water solution, chloride concentration, and reinforcing steel coatings, which are all factors that affect the rate of the corrosion reaction (Bartholomew et al. 2012, Hope and Ip 1985, Mindess et al. 2003, Saleem et al. 1996).

2.2.23 Visual Inspection

Visual inspection is a nondestructive method that is usually the first step in assessing the condition of a bridge deck (Manning 1985, Shin and Grivas 2003). Inspectors generally look for bridge deck distress and deterioration, drainage issues, and safety hazards. While some of these can be quantified or assigned a standardized rating, many are subjective observations that are simply noted.

2.2.23.1 *Theory*

When conducting a visual inspection, an inspector may identify distresses such as cracking, scaling, rust stains, spalling, and surficial delaminations in a bridge deck as possible indicators of deck deterioration. Another good indicator of deck deterioration is the distress manifested on the underside of a deck. The bridge should also be inspected for damage caused by collisions, excessive deflections, vibrations, or deformations because the deck near or at the location of these occurrences may have suffered accelerated deterioration (Manning 1985).

Cracks are the precursors of deck deterioration and are the most important feature to document when conducting a visual bridge deck condition assessment. Cracks should be identified by their size, location, and orientation (Manning 1985). The depth of a crack is also important, especially if the crack intersects the reinforcing steel, because this information can be used to assess the risk of chloride-induced corrosion, sulfate attack, and freeze-thaw deterioration. However, the depth of a crack cannot be measured unless cores are taken or the crack propagates through the entire deck cross-section. The orientation of a deck crack is identified as longitudinal, transverse, diagonal, or random (Manning 1985). Crack widths can be measured with a ruler or a crack width comparator card (Hasan et al. 1995), as shown in Figure 2-34. Hand-held crack comparator microscopes are available for inspecting extremely small cracks (Manning 1985) but are not commonly used.

Scaling is another distress that needs to be considered in visual inspections and should be reported with respect to its location and severity. Four general categories of scaling have been established: light, medium, heavy, and severe (Manning 1985). Light scaling is when the top 0.00 to 0.25 in. of surface concrete has flaked off without exposing any coarse aggregate. Medium scaling is characterized by the flaking off of the top 0.25 to 0.50 in. of surface concrete and the exposure of coarse aggregates. Scaling is considered heavy when the top 0.50 to 1.0 in. of surface concrete has flaked off and coarse aggregates are projecting from the surface. Severe scaling is distinguished by the flaking off of over 1.0 in. of concrete and the loss of coarse aggregate particles.

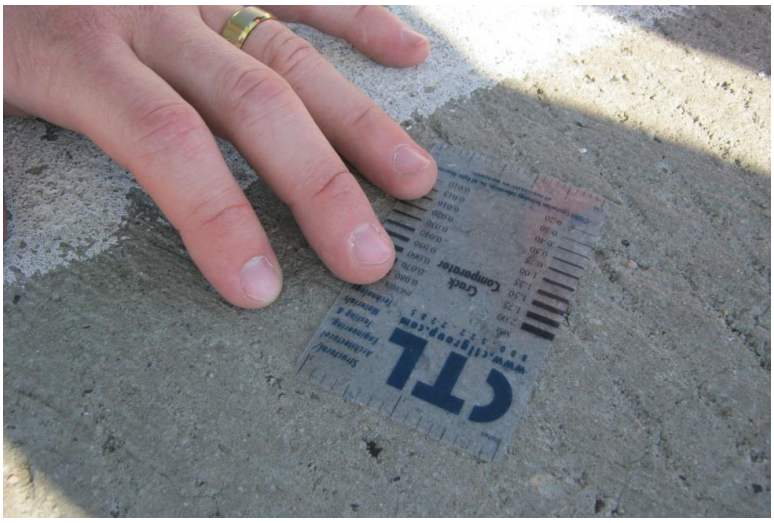

Figure 2-34 Crack comparator card.

In addition, rust stains are often good indicators of reinforcing steel corrosion (Manning 1985). Sometimes, however, ferrous sulfide inclusions in the aggregate or the corrosion of form ties may be mistaken for the corrosion of reinforcing steel.

The development of spalls and potholes on bridge decks is especially problematic and can lead to reduced structural capacity and safety concerns for drivers (Manning 1985). When the depth of spalls and potholes extends to the top mat of reinforcing steel, these distresses can be indicators of advanced corrosion-induced damage.

2.2.23.2 *Procedures*

As required by the National Bridge Inspection program, bridge inspections are conducted by state DOTs at least every 2 years. In Utah, data collected from the inspections are compiled into two documents, including the Structural Inventory and Appraisal Sheet and the UDOT Bridge Inspection Report (BIR). According to the UDOT Bridge Inspection Report, bridge deck condition assessment addresses the wearing surface, structural condition, expansion joints, railing, fencing, sidewalks, curbs, and median. Evaluation of the wearing surface includes determining the surface type, top surface condition, and overall thickness. The structural condition assessment considers the condition of the top and bottom surfaces of the deck and the overhangs, which may require the use of special equipment as shown in Figure 2-35. Assessment of the expansion joints includes reporting the joint type and the occurrence of any leakage.

Figure 2-35 Visual inspection of a reinforced concrete bridge deck (Hema et al. 2004).

Stationary traffic control may or may not be required for visual inspection, depending on the scope of work.

2.2.23.3 *Data Interpretation*

During visual inspection, various observations are photographed, noted, and/or quantified, where possible. These observations may include cracking, spalling, wear, scaling, deflection, surficial deposits, patches, and other forms of distress or damage. These data are typically used to assign condition ratings to the inspected bridges. As an example, the NBI rating scale, which is commonly used, is shown in Table 2-8. In addition to a condition rating, the type and extent of deterioration may be assessed through consideration of the distresses observed during visual inspection (UDOT 2017).

2.2.23.4 *Considerations*

One major disadvantage of the visual inspection method is that it is subjective (Moore et al. 2001) and may not provide an accurate assessment of the bridge deck condition (Manning 1985, Shin and Grivas 2003). Furthermore, the method is slow, qualitative, and potentially hazardous for the inspector, as closure of the full bridge to traffic may not be possible (Shubinsky 1994).

Table 2-8 Interpretation of NBI Deck Condition Ratings (USDOT 1995)

Rating	Description
9	Excellent
8	Very Good
7	Good
6	Satisfactory
5	Fair
4	Poor
3	Serious
2	Critical
1	Imminent Failure
0	Failed

Although some bridge decks may not exhibit any significant visible distress, the reinforcing steel in the concrete decks may be actively corroding. In these cases, the appropriate time for application of preventive maintenance treatments has passed, as the corroding reinforcement will inevitably lead to future distress regardless of any treatment applied to the deck; the engineers responsible for maintaining such bridges should then focus on potential rehabilitation or replacement strategies instead. In order to optimize applications of preventive maintenance treatments to bridge decks, engineers must monitor internal deck conditions and initiate preventive action before corrosion of the reinforcing steel begins. For this reason, visual inspection should be supplemented with other test methods.

For bridge decks overlaid with an asphalt wearing surface, in particular, the apparent condition of the overlay may not give an adequate representation of the actual deck condition. For example, when a waterproofing membrane is used beneath an asphalt overlay, the concrete deck may be in excellent condition while the wearing surface may exhibit extensive deterioration (Manning 1985). Conversely, when a waterproofing membrane is not used, the asphalt wearing surface may be in good condition while the concrete deck is heavily deteriorated. For these reasons, visual inspection may be ineffective for condition assessment of bridge decks with asphalt overlays. However, other forms of nondestructive testing, such as VEI testing, can be considered. Visual inspection is often used to determine the scope of supplemental testing that may be required to more fully investigate the condition of the bridge deck.

2.3 Bridge Deck Preservation and Rehabilitation Methods

After the condition of a bridge deck has been determined through appropriate assessment methods and tools, the proper preservation, rehabilitation, or reconstruction method can be determined. The FHWA defines bridge preservation as "action or strategies that prevent, delay, or reduce deterioration of bridges or bridge elements, restore the function of existing bridges, keep bridges in good condition, and extend their life" (FHWA 2018). Adding a surface treatment to a concrete bridge deck is an effective and economical method of preservation that reduces the ingress of water and chloride ions (Swamy and Tanikawa 1993). Although the properties and performance of surface treatments can vary, the products are usually intended to serve as barriers to the ingress of both water and chloride ions.

The FHWA states that rehabilitation "involves major work required to restore the structural integrity of a bridge, as well as work necessary to correct major safety defects" (FHWA 2018). Rehabilitation generally involves higher costs and more work than bridge deck preservation. Removal and replacement of deteriorated concrete is a common motivation for rehabilitation (Hema et al. 2004).

Preservation treatments are typically performed on bridge decks in good condition and generally result in comparatively small improvements in condition, while rehabilitation treatments are typically performed on bridges in fair condition and result in larger improvements in condition. Preservation treatments are typically less expensive than rehabilitation treatments and can therefore help reduce the overall life-cycle cost of a bridge deck. The following sections describe some of the available preservation and rehabilitation methods, including sealant application, polymer overlay application, membrane system installation, scarification and overlay, delamination and pothole repair, and partial-depth deck replacement. For each method, information about theory, considerations, procedures, and benefits is presented.

2.3.1 Sealant Application

A sealant is a preservation treatment comprising an adhesive resin that bonds to the concrete bridge deck, creating a layer that can seal cracks and prevent water and chloride ions from entering the concrete and thereby inhibiting corrosion of the reinforcing steel in the bridge

deck (Cuelho and Stephens 2013, Filice and Wong 2001, O'Connell 1995). An effective sealant resists water absorption, prevents chloride ion penetration, does not stain surfaces to which it is applied, functions over long periods of time in alkaline environments, and does not pose a significant threat to human health or the environment (McGettigan 1992).

Some sealants are also used for aesthetic purposes. When rehabilitation of a bridge deck involves partial patching of the deck, for example, a coating may be applied to mask the repair work (O'Connell 1995).

2.3.1.1 *Theory*

Two main types of sealants include surface sealants and penetrating sealants. Surface sealants, or coatings, are products like linseed oil or epoxy that adhere to the surface of the concrete and form a waterproofing film (Filice and Wong 2001, Weyers et al. 1993). These sealers are generally used when the appearance of a bridge deck is of concern, and they do not provide as much protection against water and chloride ions as penetrating sealants (O'Connell 1995).

Penetrating sealants are products that are absorbed into concrete surfaces, where they chemically react to form a hydrophobic, water-repelling surface (Filice and Wong 2001, O'Connell 1995, Paul 1998, Weyers et al. 1993). Sealants that penetrate the concrete are better protected from harmful UV rays and traffic (McGettigan 1992). Factors that control the depth to which a sealant will penetrate a substrate include porosity, moisture content, pH, and silica content of the substrate (McGettigan 1992). Sealers that penetrate deeply into the substrate last longer because they do not as quickly degrade under UV exposure and are not subject to abrasion (McGettigan 1992, O'Connell 1995, Paul 1998).

Both surface sealants and penetrating sealants are available in many different compositions. While acrylic, epoxy, gum resin, rubber, urethane, silicone resin, silane, siloxane, high-molecular-weight methacrylate (HMWM), and hydraulic cement can be used (Sprinkel et al. 1993), silicon- and methacrylate-based sealants are most common.

A few examples of hydrophobic, silicon-based sealants include silane, siloxane, silicates, and siliconates (McGettigan 1992). When under alkaline conditions, silanes chemically react

with water to form a hydrophobic, silicone resin film (Kepler et al. 2000, Sprinkel et al. 1993). Silanes offer the most uniform level of protection, penetrate deeper than other silicon-based sealants, and are more commonly used (Attanayake et al. 2006, Concrete Sealer Reviews 2014, McGettigan 1992). Siloxanes are silanes that have polymerized, making the molecules larger in size (Kepler et al. 2000); therefore, siloxanes do not penetrate deeply, lack any significant resistance to alkali, do not last long when applied to concrete, and are best used in a blend with silanes (Attanayake et al. 2006, Concrete Sealer Reviews 2014, McGettigan 1992).

HMWM sealants consist of liquid methacrylate monomers that form an adhesive resin. The resin is applied directly onto the bridge deck surface and, because of its low viscosity and surface tension, can readily penetrate cracks, sealing them against water and chloride ion ingress (Cuelho and Stephens 2013, Liang et al. 2014). HMWM sealants have been used to seal cracks ranging in width from 0.002 in. to 0.50 in. (Cuelho and Stephens 2013). In addition to sealing cracks, HMWM sealants bond to the concrete and can restore flexural stiffness to a cracked bridge deck (Cuelho and Stephens 2013, Liang et al. 2014).

2.3.1.2 *Considerations*

Sealants are best used within a year after deck construction or before the chloride concentration at the top mat of reinforcement reaches the corrosion initiation threshold (Cuelho and Stephens 2013). Once the corrosion initiation threshold has been reached, preventing further chloride ion ingress is no longer beneficial (Weyers et al. 1993).

The primary limitations of surface sealants include degradation from UV exposure, surface abrasion from traffic loads (Paul 1998), and prevention of water vapor transmission out of the deck, since the coatings seal the pore openings (Attanayake et al. 2003). Therefore, if appearance of the bridge deck is not a concern, penetrating sealants may be preferred over surface sealants since penetrating sealants provide better protection against water and chloride ions (O'Connell 1995).

A primary limitation of penetrating sealants is that, because they do not substantially alter the appearance of treated concrete, they are unable to conceal concrete repairs (O'Connell 1995, Paul 1998). Additionally, penetrating sealants cannot prevent water intrusion through open cracks (Paul 1998).

2.3.1.3 *Procedures*

In the case of new decks, applying sealants 3 to 6 months after construction, or prior to the first exposure to deicing salts, is recommended for preventing the ingress of chloride ions. Sealant applications on older decks that do not yet have excessive chloride concentrations is also recommended. In all cases, the deck surface must first be prepared so the sealant can properly bond to the surface (Cuelho and Stephens 2013). The prepared surface must be free of contaminants and moisture, and it must consist of sound concrete (O'Connell 1995, Weyers et al. 1993). Beyond construction quality, factors like temperature, moisture, crack width, and concrete condition can influence the quality of the final product (Cuelho and Stephens 2013).

Sealants can be applied using sprayers, rollers, brushes, or squeegees (Weyers et al. 1993). Figure 2-36 shows a methacrylate sealant being applied with a squeegee. Silicon-based sealants can be dissolved in a carrier such as alcohol and sprayed onto the deck to improve penetration into the concrete and to reduce the effect of any moisture in the concrete pores (Attanayake et al. 2006).

2.3.1.4 *Benefits*

The expected service life of a surface sealant under normal conditions is about 3 years, while the expected service life of a penetrating, silicon-based sealant is 5 to 7 years (Weyers et

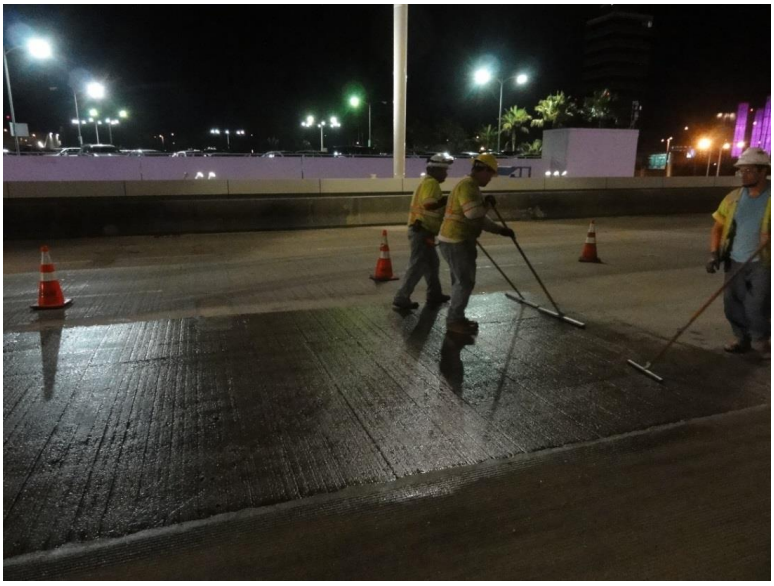

Figure 2-36 Methacrylate sealant application process.

al. 1993). Since methacrylate sealants are generally thicker than other types of sealant, they have an estimated service life of about 7 years (Weyers et al. 1993). The extent of possible bridge deck service life extension derived from sealant applications was not documented in the literature reviewed for this research but can be assumed to be correlated to the degree to which the sealant prevents the ingress of chloride ions into the deck.

2.3.2 Polymer Overlay Application

A polymer overlay is a preservation treatment comprising natural aggregate and a polymer binder (Kepler et al. 2000). Although the chemical composition of polymer overlays varies, the products are usually intended to serve as barriers to the ingress of both water and chloride ions (Tabatabai et al. 2016). In practice, the timing of initial polymer overlay applications varies widely, ranging from 1 year to 25 years from the date of deck construction, with similar variability in the frequency of repeated applications (Guthrie et al. 2005). However, for protection against chloride ion ingress, in particular, placement of polymer overlays within 1 to 11 years, depending on the cover depth, is recommended (Birdsall et al. 2007).

2.3.2.1 *Theory*

Polymer overlays are designed to seal the surface of a bridge deck, preventing water and chloride ions from penetrating the concrete (Sprinkel et al. 1993, Tabatabi et al. 2016). Some types of polymer binders in use include acrylic, methacrylate, HMWM, epoxy, epoxy-urethane, polyester styrene, polyurethane, and sulfur (Guthrie et al. 2005, Sprinkel et al. 1993). Polymer overlays can be applied in multiple layers, in a premixed layer, or as a slurry (Sprinkel et al. 1993). One example of a polymer overlay is shown in Figure 2-37; this particular polymer overlay has begun to fail, exhibiting poor bonding with the concrete bridge deck.

2.3.2.2 *Considerations*

Polymer overlays should be applied before significant distresses have developed in the bridge deck (Guthrie et al. 2005). The success of a polymer overlay can be influenced by the quality of construction, materials selection, mixture design, bond strength, and application techniques (Ramey and Derickson 2003, Stenko and Chawalwala 2001, Tabatabai et al. 2016).

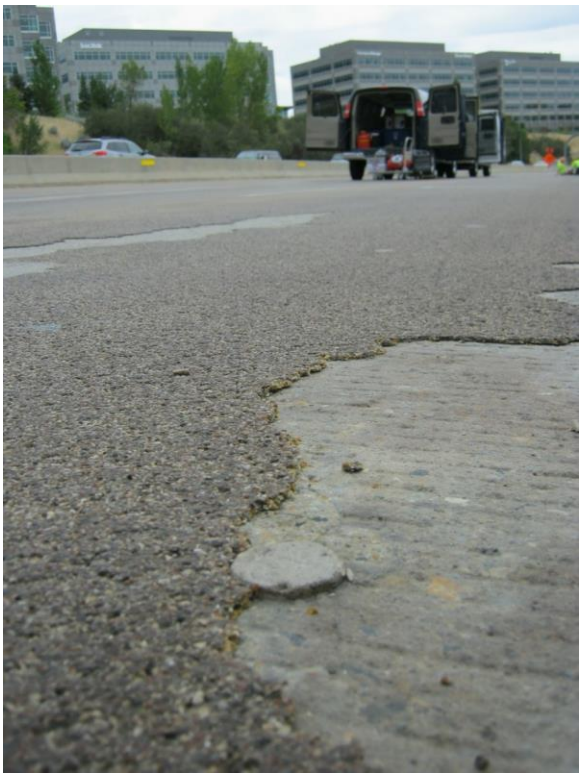

Figure 2-37 Failing polymer overlay.

Some bridge decks may be unsuitable for a polymer overlay, limiting potential candidates for the procedure. For example, a bridge deck with chloride concentrations near or above 2.0 lb Cl^-/yd^3 of concrete at the depth of the top mat of reinforcement is unsuitable because the deck has a high probability of steel corrosion in the near future, if corrosion has not already begun. Excessively distressed or deteriorated concrete is also unsuitable, as applying a polymer overlay directly over damaged concrete will severely diminish the life expectancy of the overlay (Guthrie et al. 2005). Distresses must be repaired, or milled off if the distress is surficial, before the overlay can be placed (Guthrie et al. 2005, Stenko and Chawalwala 2001). Concrete with excessive moisture is also unsuitable, as excessive moisture can weaken the bond between the concrete and the overlay and contribute to early failure of the overlay (Guthrie et al. 2005, O'Donoghue et al. 1998).

2.3.2.3 *Procedures*

Polymer overlays are supplied by various manufacturers. Construction procedures specified by the manufacturer should be followed to ensure proper placement. However, regardless of which application method or product is used, the first step of polymer overlay

application is surface preparation. Surface preparation is the most important part of applying a polymer overlay (Stenko and Chawalwala 2001); without sufficient surface preparation, the polymer overlay may not bond to the concrete bridge deck, and delamination of the overlay from the concrete may result. Preparation typically involves patching any deteriorated concrete and cleaning the surface with shot-blasting (O'Donoghue et al. 1998, Stenko and Chawalwala 2001, Tabatabai et al. 2016). Alternatively, the top 0.50 to 1.5 in. of the concrete deck is scarified, or milled, to remove any damaged or deteriorated concrete, and the milled surface is then cleaned (Ramey and Derickson 2003).

For multi-layer overlays, the polymer binder is mixed with a hardener and applied in lifts using a sprayer, brush, roller, or squeegee (Stenko and Chawalwala 2001, Tabatabai et al. 2016). Good-quality aggregate is often broadcast onto the binder before it hardens, and excess aggregate is removed before another lift is placed (Tabatabai et al. 2016). Polymer overlay materials should set quickly, with a gel time between 15 and 45 minutes, but it should also give workers enough time for application (Guthrie et al. 2005). Multi-layer overlays are typically 0.25 to 0.75 in. thick (Tabatabai et al. 2016).

For premixed overlays, the binder, initiator, and aggregates are mixed in a mixer, placed on the deck, and finished using a vibrating screed. Premixed overlays are typically 0.50 to 1.0 in. thick (Tabatabai et al. 2016). Figure 2-38 shows placement of a pre-mixed polyester polymer concrete (PPC) overlay.

For slurry overlays, a flowable polymer mortar is mixed and then placed on a primed deck surface, and then good-quality aggregate is broadcast onto the slurry before it hardens. Excess aggregate is removed after the slurry hardens, and sometimes a seal coat is applied. Slurry overlays are typically 0.25 to 0.50 in. thick (Tabatabai et al. 2016).

2.3.2.4 *Benefits*

Polymer overlays have a number of advantages over other protection methods involving conventional portland cement concrete mixtures. Although polymer overlays are typically very thin, they can be used to effectively repair spalls and other shallow defects in a bridge deck surface. Another benefit of a thin overlay is that it contributes minimal dead load to the overall

Figure 2-38 PPC overlay placement.

weight of the bridge deck (Tabatabai et al. 2016). Furthermore, because polymer overlays are flexible, they are less likely than standard concrete mixtures to crack and delaminate if applied correctly. Polymer overlays can also improve skid resistance and ride quality on a bridge deck (Guthrie et al. 2005, Ramey and Derickson 2003, Tabatabai et al. 2016). The benefits of any polymer overlay will depend on factors such as material viscosity, quality of application, bond quality, concrete condition, and curing quality (O'Donoghue et al. 1998).

Some reports claim that a polymer overlay can last between 15 and 30 years depending on traffic conditions (Sprinkel 2003), but a service life of 10 to 15 years is more realistic (Tabatabai et al. 2016). The extent of possible bridge deck service life extension derived from polymer overlay applications was not documented in the literature reviewed for this research but

can be assumed to be correlated to the degree to which the overlay prevents the ingress of chloride ions into the deck.

2.3.3 Asphalt Overlay with Membrane Application

An asphalt overlay with a membrane is a preservation treatment that prevents reinforcing steel corrosion in concrete bridge decks by inhibiting the penetration of moisture and chloride ions (Al-Qadi et al. 1993, Guthrie et al. 2005). In the installation process, a membrane is applied directly to the surface of the bridge deck and then overlaid with an asphalt layer, which protects the membrane and provides a wearing course on the bridge deck.

2.3.3.1 *Theory*

Membrane systems are designed to seal the surface of a bridge deck, preventing water and chloride ions from penetrating the concrete (Al-Qadi et al. 1993, Guthrie et al. 2005). Two main types of membranes include preformed membranes and spray-applied membranes.

Preformed membranes are made of fiber-mesh fabric impregnated with polymer-modified or rubberized asphalt (Eriksson 2001). These membranes have a sticky surface on one side that allows them to adhere to bridge deck surfaces. The application of a hot asphalt overlay causes the asphalt impregnated within the membrane to melt, consequently filling surface voids and tightly bonding the asphalt overlay to the bridge deck surface. The bond is often improved through the use of a concrete sealer placed prior to the installation of the membrane (Eriksson 2001). Upon completion of the process, a waterproof seal is created that limits the ingress of water and other harmful chemicals into the bridge deck.

Spray-applied membranes are elastomeric coatings made of polymers that can be sprayed directly onto the concrete bridge deck or onto an epoxy or sealant (Bridge Preservation 2016, Guthrie et al. 2005). Spray-applied membranes cure quickly and are able to accept asphalt overlays within an hour (Bridge Preservation 2016). These elastomeric, spray-applied membranes are waterproof and are fully bonded to the concrete (Mays 1992).

2.3.3.2 *Considerations*

An asphalt overlay with a membrane should be applied while chloride concentrations within the bridge deck are still low. Like most other preservation treatments, early application is most effective for maintaining low chloride concentrations (Guthrie et al. 2005). Any distresses should be repaired before placement of a membrane system. Spray-applied membranes are often used for bridges with curbs, expansion joints, horizontal curvature, or rough surfaces, and preformed membranes are used when thickness control is more important (Manning 1995).

Protecting the underlying concrete from water is certainly a benefit of a membrane system; however, if water is allowed to accumulate above the membrane, the asphalt layer on top of the membrane can begin to strip, and the bond between the membrane and the asphalt overlay can deteriorate (Al-Qadi et al. 1993). Membrane systems also limit visual inspection quality. For example, when a waterproofing membrane is used, the concrete deck may be in excellent condition while the wearing surface may exhibit extensive deterioration; conversely, when a waterproofing membrane is not used, the asphalt wearing surface may be in good condition while the concrete deck is heavily deteriorated (Manning 1985). Because the membrane generally lasts longer than the asphalt overlay that protects it, removal and replacement of the asphalt can be required for maintenance of a membrane system (Al-Qadi et al. 1993, Babaei and Hawkins 1987).

A few additional limitations of membrane systems may also apply, depending on the project. Relating to phased construction of bridge decks, placing a section of new membrane later than that placed on an adjacent section, which may already have an asphalt overlay in place, can lead to difficulty in sealing the joint (C. Hersh Simmons, personal communication, November 5, 2020). Other limitations of asphalt overlays with membranes relate to the construction and maintenance of the adjacent pavement. In some cases, an asphalt overlay applied to improve the structural capacity of the adjacent pavement may be inadvertently extended across the deck, which results in an increased dead load on the bridge deck that could affect the load rating of the bridge. An increased overlay thickness also results in a reduction of the barrier height, which is a safety concern (T. Pinkerton, personal communication, November 5, 2020).

2.3.3.3 *Procedures*

As with other preservation treatments, surface preparation of the bridge deck prior to applying the membrane is the most important part of the process. The deck must be completely repaired to ensure good bonding and the absence of air voids under the membrane (Manning 1995). The deck must be cleaned of all dirt, grease, oil, and other materials that may inhibit proper bonding or damage the membrane, and the bridge deck surface should then be allowed to dry before the membrane is applied (Manning 1995, Sprinkel et al. 1993). Typically, a primer or tack coat is added before membrane application to improve the bond between the membrane and the deck (Kepler et al. 2000). Applications of preformed membranes and spray-applied membranes are shown in Figures 2-39 and Figure 2-40, respectively (Mays 1992).

Following the application of the membrane, a protective overlay, typically asphalt, is also applied to the bridge deck. If the asphalt overlay needs to be replaced earlier than the membrane, only the upper 75 percent of the overlay should be milled off; the lower 25 percent should be left in place to preserve the membrane (Al-Qadi et al. 1993, Babaei and Hawkins 1987).

Figure 2-39 Preformed membrane application process.

Figure 2-40 Spray-applied membrane application process (Bridge Preservation 2016).

2.3.3.4 *Benefits*

Asphalt overlays with membranes are relatively inexpensive and have been shown to improve rideability. If applied correctly, asphalt overlays with membranes can also seal cracks in the concrete (Guthrie et al. 2005).

One study found that asphalt overlays with membranes have a service life of up to 20 years, depending on the condition of the deck prior to placement (Russell 2012). Asphalt overlays with membranes can extend the life of a bridge deck by 25 years in some cases (Al-Qadi et al. 1993).

2.3.4 Scarification and Overlay

Scarification and overlay is a preservation treatment where a shallow depth of chloride-contaminated and/or deteriorated concrete, above the top mat of reinforcement, is uniformly removed from the surface of a bridge deck and replaced with high-performance concrete (HPC). HPC overlays are intended to serve as barriers to the ingress of both water and chloride ions (Nolan 2008, Sprinkel et al. 1993, Weyers et al. 1994). Additionally, concrete overlays can be placed to strengthen the deck and improve ride quality, skid resistance, and drainage on the deck (Sprinkel et al. 1993, Sprinkel 1998).

2.3.4.1 *Theory*

HPC meets special requirements based on strength or durability, or both (Goodspeed et al. 1996). HPC is usually denser and has fewer interconnected pores than typical bridge deck concrete, which increases its resistance to diffusion of chloride ions (Bentz 2000, Hansson et al. 2006, Ismail and Soleymani 2002, Marcotte and Hansson 2003, Nolan 2008, Sanford 2008, Sprinkel et al. 1993, Sprinkel 1998, Sun 2004). Some types of HPC include latex-modified concrete (LMC), microsilica concrete (MSC) (also known as silica-fume-modified concrete), low-slump dense concrete, and fiber-reinforced concrete (Nolan 2008, Sprinkel et al. 1993, Sprinkel 1998, Sun 2004, Weyers et al. 1994). LMC and MSC are the most commonly used types of HPC for bridge deck overlays (Nolan 2008, Sprinkel 2003).

LMC includes a latex emulsion that replaces some of the cement and mix water in the concrete; the latex collects in the capillary pores during hydration, increasing density and creating a film that reduces the permeability of the concrete (Nolan 2008, Sprinkel 1998, Sprinkel 1999). Modifications can be made to the mixture design of LMC to increase early strength, making it a good option for highly trafficked bridge decks that can only be closed for a short period of time (Sprinkel 1998, Sprinkel 1999). MSC includes silica fume, which replaces some of the cement in the mixture design and increases the production of calcium silicate hydrate (C-S-H); increasing the amount of C-S-H typically decreases the interconnectivity of the pores in the concrete and provides better protection against water and chloride ion ingress (Nolan 2008).

2.3.4.2 *Considerations*

Scarification and overlay should be used when the chloride concentration at the depth of the top mat of reinforcing steel is near or above the corrosion initiation threshold, so that a preservation treatment would no longer be effective in extending the bridge deck service life, and removal and replacement of a portion of the concrete above the top mat would be expected to reduce the chloride concentration at the top mat to a level below the threshold in an acceptable period of time. Furthermore, scarification and overlay should be applied to bridge decks that exhibit little to no deterioration (Sprinkel et al. 1993). If the depth of required concrete removal

extends below the top mat of reinforcement, scarification and overlay should not be specified; instead, partial-depth deck replacement may be appropriate.

One limitation of this treatment is the long curing time typical of concrete overlays. Without the use of admixtures to increase early strength, many concrete overlays can require several days to reach sufficient strength to withstand traffic loading, requiring bridge closures during that time (Sun 2004). Another limitation of some concrete overlays is their tendency to crack. Plastic shrinkage and drying cracking can be especially pronounced in overlays with high cement contents (Sprinkel 1999, Sun 2004). While it can be avoided with proper surface preparation, poor bonding to the substrate can also be a limiting factor of concrete overlays (Nolan 2008, Sprinkel et al. 1993).

2.3.4.3 *Procedures*

Regardless of the type of concrete used in the overlay, the surface must be prepared for the overlay. In this process, the surface is first scarified, sandblasted, or shot blasted to remove any surface contamination and any deteriorated concrete and also to create a rough surface for bonding, as shown in Figure 2-41 (Nolan 2008, Sprinkel et al. 1993). Scarification depths ranging from 0.25 in. to just above the top mat of the reinforcement are commonly attained using a milling machine or a hydrodemolition jet (Nolan 2008). The surface is then cleaned and sprayed with water to achieve a saturated-surface-dry condition. After placement on the prepared

Figure 2-41 Surface prepared for concrete overlay (Nolan 2008).

deck surface, the overlay is consolidated using internal and surface vibration and struck off with a mechanical screed. LMC and MSC overlays are typically at least 1.25 in. thick (Nolan 2008, Sprinkel et al. 1993).

2.3.4.4 *Benefits*

In addition to inhibiting the ingress of water and chloride ions, LMC is more resistant to freeze-thaw damage and has higher tensile, compressive, and flexural strengths than conventional concrete (Sprinkel 1998, Sun 2004). According to one study, concrete overlays placed following scarification had a service life of 18 to 29 years. The same study estimated that LMC overlays placed following scarification could extend the service life of a bridge deck by 10 to 15 years (Weyers et al. 1994). According to another study, if the scarification and overlay process takes place before the chloride concentration at the top mat of reinforcement exceeds the corrosion threshold, the chloride concentration should remain below the threshold for at least a 50-year service life, assuming that an impermeable surface treatment is maintained on the deck surface after the scarification and overlay process is complete (Guthrie et al. 2011).

2.3.5 Delamination and Pothole Repair

Delamination and pothole repair can be considered to be preservation or rehabilitation actions, depending on the extent of damage and the purpose of the repair. If the deteriorated area is small and the structural integrity of the bridge is not a concern, this treatment may be considered to be a preservation action. However, if the deteriorated area is large and the structural integrity of the bridge is in question, this treatment may be considered to be a rehabilitation action.

2.3.5.1 *Theory*

Delaminations and potholes in concrete bridge decks are usually caused by corrosion of the reinforcing steel. Chloride ions can destroy the passive oxide film on steel and initiate corrosion (Mindess et al. 2003). Because corrosion products are expansive, the corrosion process can lead to the development of tensile stresses in the concrete, eventually leading to cracking, delamination, spalling, and potholes. To properly repair a delamination or pothole, all deteriorated concrete must be removed and replaced. The most common method of delamination

and pothole repair includes saw-cutting around the damaged area and removing the deteriorated concrete with jackhammers, but hydrodemolition may also be used (Hema et al. 2004).

While patching a pothole temporarily restores rideability, installing a proper patch is not always sufficient to prevent further damage, which can develop if the "halo effect" occurs. The "halo effect" can occur when a pothole or delamination is patched, resulting in new concrete around the reinforcing steel and a reversal of the anode and cathode in the corrosion circuit. That is, the steel within the patch, which was previously an anode, becomes a cathode, and the steel adjacent to the patch now becomes an anode, initiating new corrosion and corrosion-induced damage in the area surrounding the patch (Mindess et al. 2003). The halo effect can be prevented by using cathodic protection, such as sacrificial anodes (Mindess et al. 2003, Page and Sergi 2000). Sacrificial anodes, depicted in Figure 2-42, are typically made of zinc, which is lower than steel on the galvanic series and therefore behaves as an anode when in electrical contact with steel. As the anode, zinc then experiences the corrosion, and the steel, acting as the cathode, is protected. Because zinc is comparatively much less expansive than steel upon corroding, the formation of zinc corrosion products does not lead to the development of further distress at the repair site.

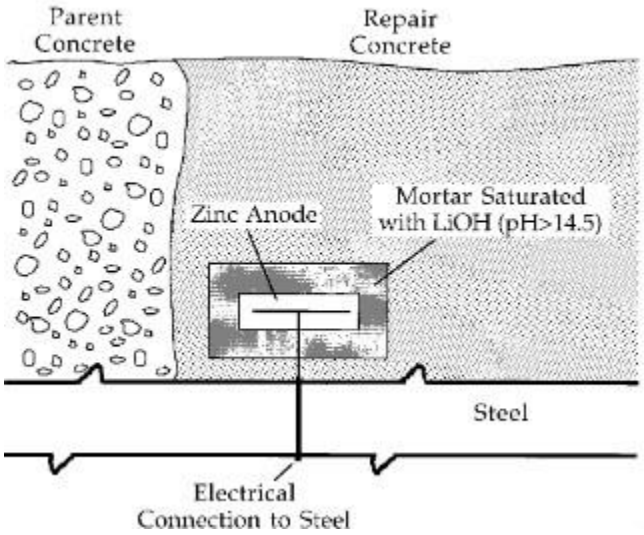

Figure 2-42 Depiction of pothole repair using a sacrificial anode (Page and Sergi 2000).

2.3.5.2 *Considerations*

To provide a smooth driving surface for the public and to prevent critical loss of structural integrity, delamination and pothole repair should occur throughout the life of a bridge deck. However, once the damage affects a certain percentage of the deck area, a more aggressive bridge deck treatment may not only become necessary but may also be more cost-efficient.

One major limitation of delamination and pothole repair is the possibility of causing collateral damage to adjacent intact concrete when jackhammering is used to remove deteriorated concrete. When a jackhammer strikes reinforcing steel, the vibrations can propagate to areas of intact concrete and cause microcracking in the concrete and debonding of the concrete and reinforcing steel. Another limitation of delamination and pothole repair is the possibility of poor bonding between the repair material and the concrete substrate (Weyers et al. 1993). If the substrate is not thoroughly cleaned and texturized, proper bonding cannot occur. Jackhammering is also a time-consuming method of concrete removal (Hema et al. 2004).

When hydrodemolition is used to remove deteriorated concrete, environmental and safety concerns must be considered. Environmental concerns arise when even small quantities of the waste water, which has high levels of alkalinity and harmful solutes, bypass the water collection and treatment system and enter the surrounding landscape (Roper 2018). Because of the possibility of waste water leakage and falling debris, blow-throughs, which occur when the full thickness of the deck breaks apart under the pressure of a hydrodemolition jet, pose both environmental and safety problems if special precautions are not taken (Roper 2018).

2.3.5.3 *Procedures*

The process of repairing delaminations and potholes requires that the damaged areas be located and marked using chain dragging, hammer sounding, impact-echo testing, and/or visual inspection. To ensure that all deteriorated concrete is removed, an extra 6.0 in. of concrete is commonly removed from around the edge of a delamination or pothole. A saw is used to cut around the boundary, typically to the depth of the top mat of reinforcement, and jackhammers are used to remove the damaged concrete, sometimes to a specified depth below the top mat, before the area is cleaned with sandblasting (Hema et al. 2004, Weyers et al. 1993). Figure 2-43 shows a saw-cut and jackhammered area before the repair concrete was placed.

Figure 2-43 Cover concrete removal.

Alternatively, hydrodemolition can be used to remove deteriorated concrete from the top surface of a concrete bridge deck using a high-pressure water jet. This method can be applied only to damaged areas, or it can be applied to the entire deck. When hydrodemolition is applied to an entire deck, knowledge of the location of the delaminated areas is not necessary, as calibrated hydrodemolition equipment can automatically remove any deteriorated concrete while leaving sound concrete intact. Hydrodemolition also effectively cleans the reinforcement and substrate in preparation for placement of repair concrete, such that no sandblasting or shot blasting is required (Wenzlick 2002).

If sacrificial anodes are to be installed as part of the repair, the concrete must be removed to a depth of at least 0.50 in. below the bottom of the top mat of reinforcement to allow for anode installation. The sacrificial anode is placed so that it is in electrical contact with the reinforcement, and then repair concrete is placed around the sacrificial anode, as shown in Figure 2-42 (Page and Sergi 2000). Sacrificial anode spacing depends on manufacturer and reinforcement density but typically ranges from 13 to 30 in. The repair concrete is typically made of a rapid-setting material to allow traffic to be returned to the bridge deck as quickly as possible.

2.3.5.4 *Benefits*

Patching delaminations and potholes can restore rideability immediately at a relatively low cost. Depending on a number of project-specific factors, a patch can provide only 1 to 2 years of service life (Hema et al. 2004, Weyers et al. 1994), or it can provide a service life of 25 years when all chloride-contaminated concrete is removed (Weyers et al. 1993). Sacrificial anodes have a life expectancy of about 10 years (Wilson et al. 2013). Patching adds very little, if any, service life to a bridge deck.

2.3.6 Partial-Depth Deck Replacement

Partial-depth deck replacement is a rehabilitation treatment in which hydrodemolition is used to remove all deck concrete to a specified depth, such as 0.50 in., below the top mat of reinforcement and new concrete is placed (Roper 2018, Wenzlick 2002).

2.3.6.1 *Theory*

When chloride-induced corrosion causes widespread damage to a bridge deck, repairs must sometimes extend below the top mat of reinforcement. In this situation, hydrodemolition can be used to remove all deteriorated concrete from above and around the top mat. Subsequent placement of new concrete then restores or increases the structural integrity of the bridge deck (Roper 2018).

2.3.6.2 *Considerations*

Partial-depth deck replacement should be used when the chloride concentration at the depth of the top mat of reinforcement reaches or exceeds the corrosion threshold over a significant area of the deck, beyond the area that could be economically repaired using standard patching techniques, and the depth of required repair extends below the top mat of reinforcement, such that a scarification and overlay treatment would no longer be effective in extending the bridge deck service life. Partial-depth deck replacement can be a viable option as long as the chloride concentration at the bottom mat of reinforcement has not reached the corrosion threshold and less than approximately 10 percent of the underside of the deck exhibits damage (Wenzlick 2002).

Limitations of partial-depth deck replacement are associated with the hydrodemolition process. All water used in hydrodemolition must be treated to remove any contaminants before it can be returned to the local water system (Roper 2018). If the underside of the deck is deteriorated, so that blow-throughs occur, debris may fall onto property below the deck, and contaminated water may bypass the water collection and treatment system; in this situation, repair of the blow-throughs requires additional formwork and concrete during replacement of the upper half of the deck (Roper 2018). Because hydrodemolition typically removes any epoxy coatings from the top mat of rebar, the corrosion initiation threshold for black bar of 2.0 lb Cl^- /yd^3 of concrete should be used for future evaluation of decks that have received this treatment.

2.3.6.3 *Procedures*

The first step in partial-depth deck replacement is a shallow scarification of the surface of the bridge deck using a milling machine. The rough surface allows the jets to more effectively initiate concrete removal (Wenzlick 2002). After the surface has been milled, hydrodemolition is performed using a jet that sprays water at a constant pressure, sometimes in excess of 20,000 psi, to remove the concrete from above and around the top mat of reinforcement, as shown in Figure 2-44 (Roper 2018). Concrete is typically removed to a depth of 0.50 in. below the bottom of the

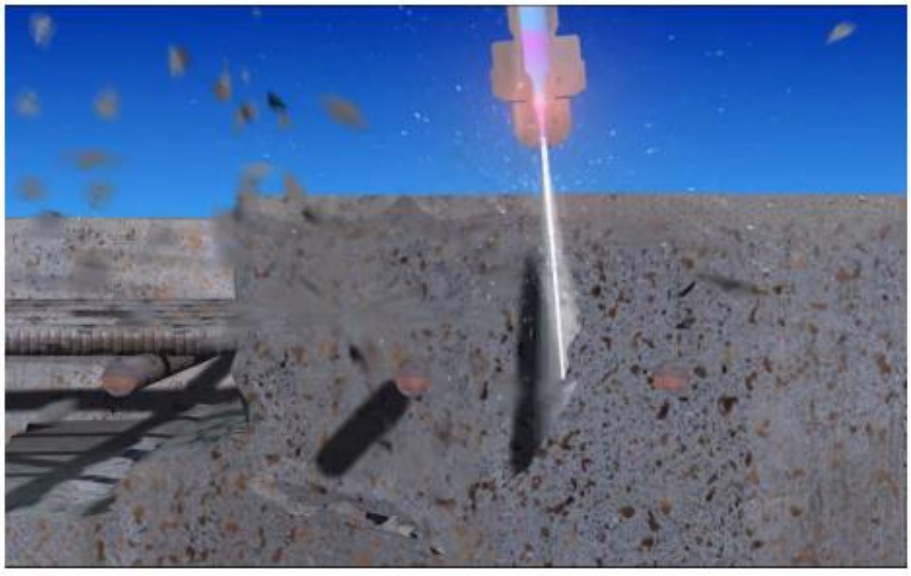

Figure 2-44 Schematic of concrete removal below the top mat of reinforcing steel using hydrodemolition equipment (Roper 2018).

reinforcement, which provides sufficient clear space for the replacement concrete to flow under and interlock with the reinforcement.

The next step is to wash all debris from the deck and replace or supplement any deteriorated reinforcement (Wenzlick 2002). New concrete can then be placed to restore or increase the original strength or deck thickness. The use of hydrodemolition removes the need for any additional concrete surface preparation or cleaning of the reinforcement (Wenzlick 2002).

Partial-depth deck replacement removes all chloride ions from the upper portion of the deck, where chloride concentrations are typically highest, thus effectively restoring the deck to a nearly-new condition. If a surface treatment is placed shortly after partial-depth deck replacement, the deck could last an additional 50 or more years (Roper 2018).

2.4 Bridge Deck Reconstruction Methods

When a bridge deck exhibits extensive deterioration, preservation and rehabilitation treatments are no longer effective at restoring the deck to good condition, and reconstruction must take place. The following sections describe common construction and reconstruction methods, including stay-in-place metal form installation, precast half-deck panel usage, internally cured concrete usage, and accelerated bridge construction. For each method, information about theory, considerations, procedures, and benefits is presented.

2.4.1 Stay-in-Place Metal Form Installation

Stay-in-place metal forms (SIPMFs) are permanent formwork made of thin, corrugated sheets of galvanized steel (Grace et al. 2004). They are used in cast-in-place concrete bridge deck construction and reconstruction.

2.4.1.1 *Theory*

Formwork for concrete construction is necessary to provide control of shape, position, and alignment of the concrete structure. The formwork must support its own weight, the weight of freshly placed concrete, and live loads associated with construction activity and equipment

while the concrete gains strength (Grace et. al 2004). SIPMFs are designed to be left in place after construction of a bridge deck and become part of the permanent bridge deck structure. Construction can be accelerated using SIPMFs since the formwork is lightweight, generally prefabricated, simple to construct, and does not require removal after construction (Grace et al. 2004). SIPMFs are galvanized to inhibit corrosion of the panels.

Research has shown that decks with SIPMFs are characterized by higher moisture contents than those constructed with conventional formwork; the increase in moisture results from the reduction in exposed deck surface area from which moisture may evaporate (Carrier et al. 1975). One study showed that decks with SIPMFs exhibited diffusion coefficients approximately twice as high as those associated with decks without SIPMFs (Birdsall et al. 2007). Therefore, because different diffusion coefficients would result in different rates of chloride penetration, different bridge deck rehabilitation practices may be required depending on the presence or absence of SIPMFs.

2.4.1.2 *Considerations*

SIPMFs are advantageous in a number of bridge deck construction applications, such as in high-traffic areas and over deep ravines (Guthrie et al. 2006). In these situations, eliminating the need to remove forms decreases the exposure of construction workers to elevated levels of risk.

Although the use of SIPMFs has some advantages, several limitations also exist. The presence of SIPMFs obstructs access to the undersides of bridge decks by bridge inspectors, and the presence of SIPMFs may exacerbate deck deterioration by causing higher moisture contents and chloride concentrations within the deck (Guthrie et al. 2006). Specifically, decks with SIPMFs may require earlier maintenance and rehabilitation procedures than those without SIPMFs. Higher moisture contents also increase the probability of frost damage to bridge decks in cold climates (Cady and Renton 1976, Carrier et al. 1975, Mindess et al. 2003) and increase the rate at which chloride ions diffuse into the concrete (Xi and Bazant 1999). Perhaps for this reason, acceptance of SIPMFs for deck construction in southern states is higher than in northern states, where deicing salts are routinely applied to bridge decks as part of winter maintenance activities (Grace et al. 2004).

2.4.1.3 *Procedures*

SIPMFs are placed between girders and act as formwork for concrete placement. Figure 2-45 shows an SIPMF installed on a bridge deck (Guthrie et al. 2006).

2.4.1.4 *Benefits*

SIPMFs accelerate the construction process because they are prefabricated, are easy to install, and do not require removal (Guthrie et al. 2006). SIPMFs also decrease the exposure of construction workers to elevated levels of risk (Guthrie et al. 2006).

Figure 2-45 Bottom view of SIPMF (Guthrie et al. 2006).

2.4.2 Precast Half-Deck Panel Usage

Precast half-deck panels are permanent formwork made of precast, prestressed reinforced concrete (Guthrie and Yaede 2014). Precast half-deck panels can be used in concrete bridge deck construction and reconstruction.

2.4.2.1 *Theory*

Precast half-deck panels are used to accelerate the bridge construction process by eliminating the need for conventional formwork between the bridge girders during placement of the concrete bridge deck (Guthrie and Yaede 2014). The pre-stressed concrete panels together

with the cast-in-place concrete surface are designed to act compositely with the pre-stressed girders and behave similarly to a monolithic concrete deck (Buth et al. 1972).

2.4.2.2 *Considerations*

Similar to SIPMFs, precast half-deck panels can be used when speed of construction is important and when removal of temporary formwork would be difficult (Guthrie and Yaede 2014). Several reports have noted that the use of precast panels has led to transverse cracking in the concrete bridge deck, where the cracks in the cast-in-place deck surface are reflected from the butt joints between adjacent underlying panels (Guthrie and Yaede 2014, Medlock et al. 2001, Precast/Prestressed Concrete Institute 1987). Although these cracks are not believed to significantly affect the structural performance of the deck (Medlock et al. 2001, Precast/Prestressed Concrete Institute 1987), such cracking may accelerate deck deterioration by allowing moisture and chloride ions to penetrate the concrete and initiate corrosion of the embedded reinforcing steel (Spraggs et al. 2012). Reflection cracking from the butt joints between underlying precast half-deck panels has been documented on bridges constructed using conventional concrete, internally cured concrete, and fiber-reinforced concrete (Guthrie and Yaede 2014, Hebdon et al. 2020).

2.4.2.3 *Procedures*

Precast half-deck panels rest on the top flanges of the bridge girders and span between girders, as shown in Figure 2-46. A layer of reinforcement is configured above the panels, and then the upper half of the deck is cast directly on top of the panels and girders (Guthrie and Yaede 2014).

2.4.2.4 *Benefits*

Precast half-deck panels are advantageous because they minimize traffic interruption, lower construction time, improve construction safety, and are less disruptive to the environment (Fowler 2006).

Figure 2-46 Precast half-deck panels.

2.4.3 Internally Cured Concrete Usage

Internally cured concrete is a concrete bridge deck construction or reconstruction option. Pre-wetted lightweight fine aggregate (LWFA) is incorporated in the concrete mixture to increase internal moisture within the concrete during curing (Guthrie and Yaede 2013).

2.4.3.1 *Theory*

Maintaining sufficient internal moisture during curing is critical in the development of concrete strength and durability. During the curing process, water reacts with the cementitious materials in concrete to form two main hydration products, including C-S-H and calcium hydroxide (CH) (Mindess et al. 2003). C-S-H is the primary source of concrete strength and durability. A sufficient amount of water well distributed throughout the concrete matrix is necessary to ensure a high degree of cement hydration (Guthrie and Yaede 2013).

While external curing of concrete can prevent evaporation of water from the concrete surface and replenish some water near the concrete surface, internal curing provides small reservoirs of additional water, as illustrated in Figure 2-47, inside the concrete (De la Varga et al. 2012). This additional water, which is above and beyond the free water necessary to achieve the specified water-cementitious materials ratio for the given concrete mixture, is located within the water-permeable pores of the LWFA and allows the cement to continue to hydrate for a longer

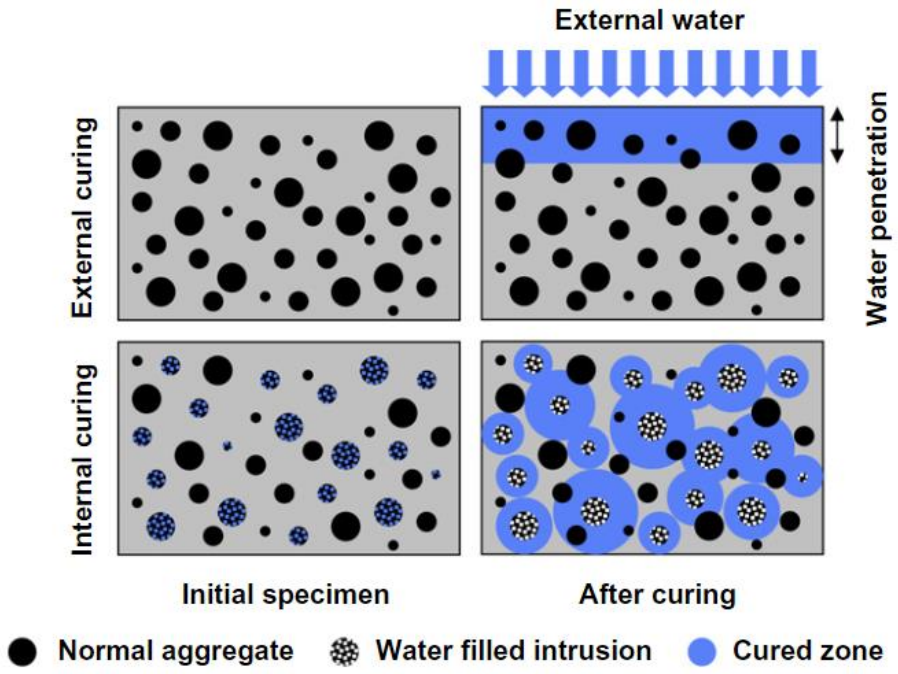

Figure 2-47 Comparison of external and internal curing (De la Varga et al. 2012).

period of time. Through this process, the concrete gains strength and becomes less permeable while also exhibiting less shrinkage (Bentz et al. 2006, De la Varga et al. 2012, Mindess et al. 2003).

2.4.3.2 *Considerations*

Internally cured concrete can be used in any construction or reconstruction application (Guthrie and Yaede 2013). One limitation of internally cured concrete is that the aggregate tends to crush more easily, limiting the ultimate compressive strength to around 6,000 psi (Guthrie and Yaede 2013). Additionally, research has found that internally cured concrete allows faster chloride penetration than conventional concrete (Bitnoff 2014).

2.4.3.3 *Procedures*

Internally cured concrete is batched and placed the same way as conventional concrete, with the exception that pre-wetted LWFA is incorporated into the mixture. Pre-wetting of the LWFA in the concrete batching process allows the LWFA to absorb the required water before being mixed with the other concrete ingredients (Guthrie and Yaede 2013).

2.4.3.4 *Benefits*

In some studies, the use of pre-wetted LWFA has been shown to densify the microstructure of concrete, reduce permeability, and reduce shrinkage cracking, thereby extending deck service life (Castro et al. 2012, De la Varga et al. 2012). In a case study to determine the benefits of internal curing, the use of LWFA was projected to extend the life of high-performance concrete bridge decks by more than 20 years. The research proposed that a conventional concrete deck would have a service life of 22 years, a high-performance concrete deck without pre-wetted LWFA would have a service life of 40 years, and a high-performance concrete deck with pre-wetted LWFA to promote internal curing would have a service life of 63 years (Cusson et al. 2010). By increasing the service life of a deck, agencies can significantly lower the overall life-cycle cost of a bridge through reductions in maintenance requirements and rehabilitation efforts.

2.4.4 Accelerated Bridge Construction

Accelerated bridge construction (ABC) is a method for reconstruction of bridges in which the new bridge is constructed near or parallel to the existing bridge site and then moved into place after the existing bridge is demolished (Culmo 2011, FHWA 2017, Guthrie et al. 2015). The new bridge can be moved using mobile transporters, or it can be slid into place.

2.4.4.1 *Theory*

In the ABC method, because the new bridge must sometimes be lifted and moved into place, the use of lightweight concrete is prevalent. Because lightweight concrete bridge decks weigh less than normal-weight concrete bridge decks, fewer mobile transporters are required to move the bridges into place (Medeiros 2010).

2.4.4.2 *Considerations*

ABC can be used when sufficient space exists in a nearby gore area or in a location immediately adjacent to the existing bridge for the new bridge to be constructed while the existing bridge remains in service. Because the new bridge can be installed comparatively quickly after it is constructed, ABC should be considered for replacement of bridges with high traffic on or below the bridge.

2.4.4.3 *Procedures*

In one ABC technique, the new bridge is constructed in a gore area adjacent to or near the existing bridge that warrants replacement, as shown in Figure 2-48. After construction of the new bridge is complete, mobile transporters are often used to lift and carry the existing bridge to a nearby demolition yard and then to lift and move the new bridge into place, as shown in Figure 2-49 (Culmo 2011).

Figure 2-48 ABC taking place in the gore area.

Figure 2-49 Movement of a bridge using mobile transporters.

Another technique is slide-in bridge construction, in which a new bridge is built on temporary supports parallel to the existing bridge. After construction of the new bridge is complete, the existing bridge is demolished or removed, and the new bridge is slid into place (FHWA 2017).

2.4.4.4 *Benefits*

The main benefits for ABC include increased safety and decreased traffic congestion. Safety is increased because construction takes place off of the roadway in the gore area, protecting both drivers and construction workers, and traffic congestion is decreased because normal trafficking of the existing bridge and roadway can continue during construction of the new bridge. Once the new bridge is completed, removal of the old bridge and installation of the new bridge can be completed in the course of one or two nights, depending on the project, requiring lane closures only during that time (Culmo 2011, FHWA 2017).

2.5 Estimating Remaining Service Life Using Computer Models

Another important aspect of maintaining a network of bridge decks is estimating remaining service life. A primary method of estimating remaining service life involves the use of chloride concentration profile modeling (Bentz 2007, Ehlen 2018, Samson 2014, Violetta 2002). As one example, models can simulate the effect of equilibration after sealing the surface of a deck with an overlay, ensuring that the chloride concentration at the depth of the top mat of reinforcement never reaches the corrosion initiation threshold (Birdsall 2007). As another example, the effect of removing chloride-contaminated concrete and replacing it with new, uncontaminated concrete, as is the case with scarification and overlay and partial-depth deck replacement, can also be simulated, ensuring that, during equilibration, the chloride concentration at the top mat of reinforcement is reduced to a level below the corrosion initiation threshold in an acceptable period of time following treatment (Nolan 2008, Roper 2018).

Software can also be used for predicting the time interval from construction to the initiation of corrosion, predicting the time interval from initiation of corrosion to the time of the first repair (or the time at which an unacceptable damage level is reached), determining the repair schedule for the life of the structure, and/or estimating life-cycle costs (Violetta 2002). Most

models use Fick's second law of diffusion to model the ingress of chloride ions under different types of environmental conditions; an assumed or measured diffusion coefficient can typically be used in these analyses (Bentz 2007, Ehlen 2018). Other models use ionic transport and reaction modeling for conditions representing saturated or unsaturated concrete (SIMCO Technologies undated). Software packages are available commercially, such as Life-365 and STADIUM, or through government agencies such as the National Institute of Standards and Technology.

2.6 Summary

This chapter provided a detailed summary of information available in the literature about concrete bridge decks, focusing on condition assessment; bridge deck preservation and rehabilitation; bridge deck reconstruction; and estimating remaining service life using computer models. Condition assessment can be performed using many different test methods, both destructive and nondestructive, to assess the state of deterioration of a bridge deck. Many different preservation and rehabilitation techniques can be applied to extend the service life of a bridge deck. Several options for reconstruction are also available. In addition, a few computer models are available for predicting the service life of a bridge deck subject to specific conditions.

3.0 BRIDGE DECK TESTING

3.1 Overview

This chapter addresses objective 2 of this research, for which field data from representative concrete bridge decks in Utah were collected and analyzed to investigate the effects of selected bridge deck features, including polymer overlay application, deck age at polymer overlay application, overlay age, asphalt overlay application with and without a membrane, SIPMFs, SIPMF removal, internally cured concrete, and use of an automatic deck deicing system. These features, which are all related to concerns about protecting decks against rebar corrosion, were selected in consultation with UDOT bridge engineers. The procedures and results are presented in the following sections.

3.2 Procedures

The following sections describe the procedures used in bridge deck selection, bridge deck testing, and statistical analyses.

3.2.1 Bridge Deck Selection

Fifteen concrete bridge decks were strategically selected for testing from a list of "typical" bridges owned by UDOT, with parameters defining a typical bridge provided in an earlier study (Guthrie and De Leon 2020). Five bridge decks had bare concrete surfaces, five bridge decks had asphalt overlays, and five bridge decks had polymer overlays. Where possible, bridges with varying deck ages and overlay ages were selected. The 15 selected bridges are presented in alphabetical order in Table 3-1, which gives summary information about each bridge deck.

Further information about each of the tested decks is summarized in the following sections. A hyphen in Table 3-1 indicates that the given deck property is not applicable. Each section includes inventory data as well as information summarized from the UDOT BIRs associated with each bridge. During bridge inspections by UDOT personnel, observations

Table 3-1 Bridge Deck Summary

Deck ID	Surface Type	Bar Type	Construction Year	Deck Age at Testing	Deck Age at Overlay	Overlay Age at Testing	Date(s) of Testing	Selection Criteria
C-460	Asphalt Overlay with Membrane	Epoxy-Coated	1988	28	21	7	August 22, 2016	Asphalt overlay placed at a deck age of > 20 years, SIPMFs
C-698	Asphalt Overlay with Membrane	Epoxy-Coated	1987	29	22	7	August 22, 2016	Asphalt overlay placed at a deck age of > 20 years, SIPMF removal at deck age of > 18 years
C-725	Bare Concrete	Epoxy-Coated	1984	32	-	-	August 25, 2016	Bare deck with a high deck age
C-757	Polymer Overlay	Black	1989	27	16	11	August 17, 2016	Polymer overlay placed at a deck age of 10-20 years, automatic deck deicing system
C-759	Polymer Overlay	Black	1989	27	13	14	August 17, 2016	Polymer overlay placed at a deck age of 10-20 years, SIPMF removal at deck age of < 18 years
C-760	Bare Concrete	Epoxy-Coated	1989	27	-	-	September 21, 2016	Bare deck with a high deck age, SIPMF removal at deck age of < 19 years
C-794	Asphalt Overlay with Membrane	Epoxy-Coated	1996	20	0	20	November 5, 2016	Asphalt overlay placed immediately after construction
C-931	Polymer Overlay	Epoxy-Coated	2004	12	0	12	October 15, 2016	Polymer overlay placed immediately after construction

Table 3-1 Bridge Deck Summary, Continued

Deck ID	Surface Type	Bar Type	Construction Year	Deck Age at Testing	Deck Age at Overlay	Overlay Age at Testing	Date(s) of Testing	Selection Criteria
C-953	Polymer Overlay	Epoxy-Coated	2007	9	5	4	October 15, 2016	Polymer overlay placed at a deck age of 1-10 years
F-53	Asphalt Overlay with Membrane	Epoxy-Coated	2001	16	0	16	September 29, 2016	Asphalt overlay placed immediately after construction, SIPMFs
F-476	Asphalt Overlay without Membrane	Epoxy-Coated	1983	33	12	21	August 19, 2016	Asphalt overlay placed at a deck age of 10-20 years
F-562	Bare Concrete	Epoxy-Coated	1989	27	-	-	September 16 and 23, 2016	Bare deck with a high age, scheduled to be treated with PPC, SIPMFs
F-738	Polymer Overlay	Epoxy-Coated	2008	8	0	8	August 23, 2016	Polymer overlay placed immediately after construction, requested by UDOT
F-799	Bare Concrete	Epoxy-Coated	2012	4	-	-	August 13, 2016	Bare deck with a low deck age, internally cured concrete
F-800	Bare Concrete	Epoxy-Coated	2012	4	-	-	August 13, 2016	Bare deck with a low deck age

regarding the condition of the decks were documented. The notes contain comments about the visible distresses and appearance of each deck, as well as the most recent preservation and reconstruction actions in progress or completed. Because the reports contain notes only from 1991 to the present, complete histories were not available for bridge decks constructed prior to 1991. BIRs were not obtained for bridges F-799 and F-800, which were extensively studied in previous research (Bitnoff 2014).

3.2.1.1 *Bridge C-460*

Bridge C-460 is a three-span bridge with a total span length of 227 ft. It is located in Salt Lake City on the Interstate 215 (I-215) corridor just south of the Interstate 80 (I-80) interchange and spans Indiana Avenue and the Union Pacific railroad (UPRR), as shown in Figure 3-1. The bridge was constructed using SIPMFs in 1988. The BIR indicates that the deck had a series of full-depth transverse cracks in 1991. The underside of the deck was not visible due to the presence of SIPMFs, which were still in place during the field testing performed for this research. The bridge deck surface was bare concrete until 2009, when potholes on the deck

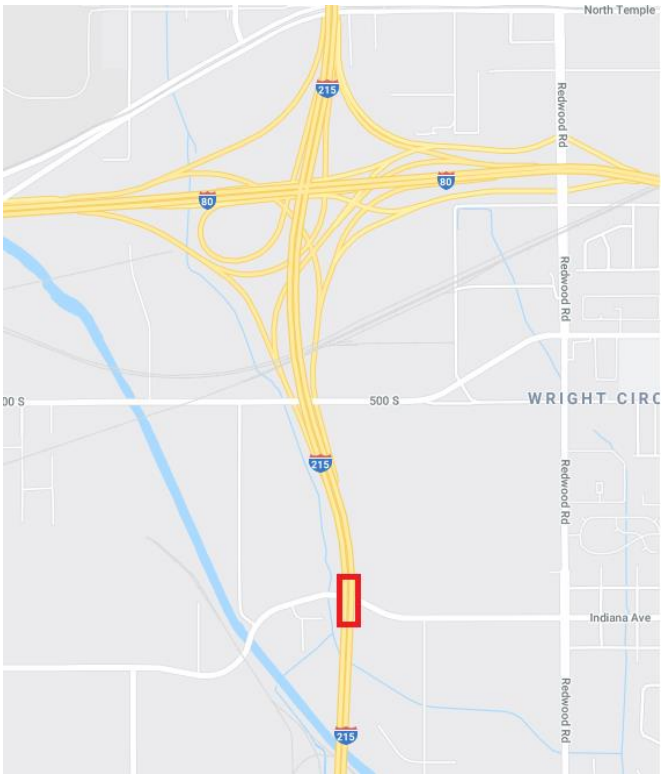

Figure 3-1 Map location of bridge C-460.

surface were repaired and a waterproofing membrane and an asphalt overlay were installed. The asphalt overlay was still in place during the field testing performed for this research.

3.2.1.2 *Bridge C-698*

Bridge C-698 is a single-span bridge with a total span length of 152 ft. It is an off-ramp located in Salt Lake City on the northbound I-215 to I-80 interchange and spans 500 South, as shown in Figure 3-2. The bridge was constructed using SIPMFs in 1987. The BIR indicates that the deck had some potholes beginning in 2005. The 2007 notes indicate that SIPMFs were in place until sometime between March 2005 and February 2007, when they were removed. The bridge deck surface was bare concrete until 2009, when potholes on the deck surface were repaired and a waterproofing membrane and an asphalt overlay were installed. The asphalt overlay was still in place during the field testing performed for this research.

3.2.1.3 *Bridge C-725*

Bridge C-725 is a two-span bridge with a total span length of 288 ft. It is located in Salt Lake City on 700 East and spans I-215, as shown in Figure 3-3. The bridge was constructed in

Figure 3-2 Map location of bridge C-698.

Figure 3-3 Map location of bridge C-725.

1984. The BIR indicates that the deck had a series of full-depth transverse cracks and efflorescence from 1991 to the time of testing. Potholes began forming in 2007 and were occasionally repaired. The bridge deck surface was bare concrete from construction until the time of field testing performed for this research.

3.2.1.4 *Bridge C-757*

Bridge C-757 is a three-span bridge with a total span length of 465 ft. It is located in Holladay on I-215 and spans 6200 South (Big Cottonwood Road), as shown in Figure 3-4. The bridge was constructed in 1989. The BIR first mentions a polymer overlay in the 2005 notes, and the BIR also indicates that SIPMFs were removed prior to the 2005 inspection. The polymer overlay remained in good condition until 2010. However, by 2012, potholes had formed on the deck surface, and cracking had developed on the underside of the deck. The polymer overlay was still in place during the field testing performed for this research. The bridge has an automatic deicing system installed in the deck.

3.2.1.5 *Bridge C-759*

Bridge C-759 is a single-span bridge with a total span length of 189 ft. It is located in Holladay on I-215 and spans Big Cottonwood Creek and a bike path, as shown in Figure 3-5.

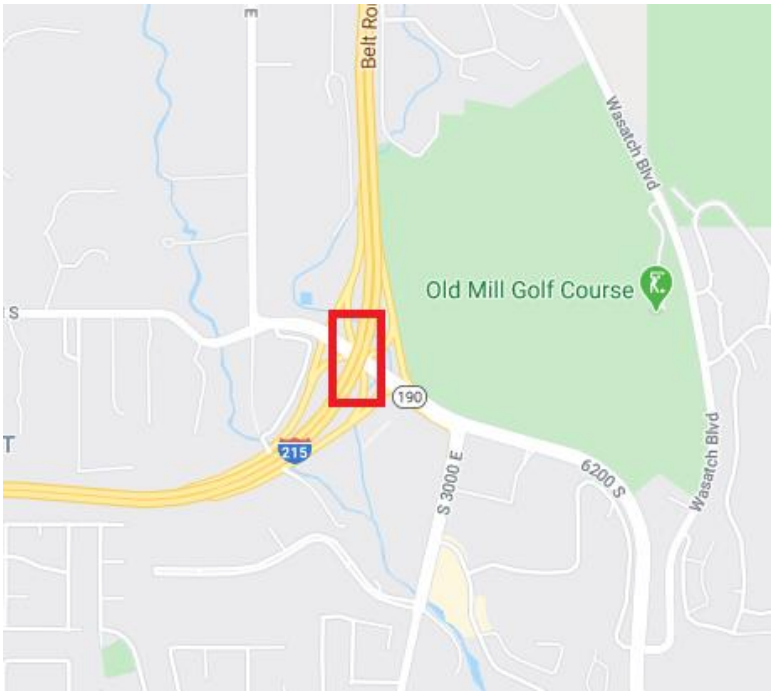

Figure 3-4 Map location of bridge C-757.

Figure 3-5 Map location of bridge C-759.

The bridge was constructed in 1989. The BIR first mentions a polymer overlay in the 2002 notes, which indicate that the overlay was already in poor condition in some areas at that time. A new polymer overlay was placed and the SIPMFs were removed sometime between June 2005 and

January 2007. The polymer overlay began debonding by 2010, and up to 25 percent of the overlay exhibited delamination and/or was worn thin by 2012. The polymer overlay was still in place during the field testing performed for this research.

3.2.1.6 *Bridge C-760*

Bridge C-760 is a single-span bridge with a total span length of 171 ft. It is an on-ramp from 6200 South to westbound I-215 in Holladay and spans Big Cottonwood Creek and a bike path, as shown in Figure 3-6. The bridge was constructed in 1989. As early as 1996, the deck surface began spalling, and potholes began forming. The deck had some potholes continuously from then until the time of field testing performed for this research. SIPMFs were removed from this deck sometime before 2008. The bridge deck surface was bare concrete from construction until the time of field testing performed for this research.

3.2.1.7 *Bridge C-794*

Bridge C-794 is a single-span bridge with a total span length of 163 ft. It is located in Myton on United States Route 40 and spans the Duchesne River, as shown in Figure 3-7. The bridge was constructed in 1996. The BIR first mentions an asphalt overlay in the 2003 notes, but

Figure 3-6 Map location of bridge C-760.

Figure 3-7 Map location of bridge C-794.

a UDOT bridge engineer confirmed that an asphalt overlay was placed within one year of construction. The asphalt overlay and underside of the deck remained in good condition. The asphalt overlay was still in place during the field testing performed for this research.

3.2.1.8 *Bridge C-931*

Bridge C-931 is a single-span bridge with a total span length of 108 ft. It is located in Salt Lake City on I-215 and spans 3800 South (Upland Drive), as shown in Figure 3-8. The bridge

Figure 3-8 Map location of bridge C-931.

was constructed in 2004, and a polymer overlay was placed within a year of construction. The BIR notes that transverse cracking on the surface began by 2005, and cracking and efflorescence on the underside of the deck began by 2008. The polymer overlay was still in place during the field testing performed for this research.

3.2.1.9 *Bridge C-953*

Bridge C-953 is a single-span bridge with a total span length of 175 ft. It is located in Salt Lake City on 4500 South and spans I-215, as shown in Figure 3-9. The bridge was constructed in 2007. The BIR first mentions a polymer overlay in good condition in 2012. The polymer overlay was still in place during the field testing performed for this research.

3.2.1.10 *Bridge F-53*

Bridge F-53 is a four-span bridge with a total span length of 213 ft. It is an off-ramp located in Salt Lake City on the westbound I-80 to I-215 interchange and spans I-215, as shown in Figure 3-10. The bridge was reconstructed using SIPMFs in 2001, and a waterproofing membrane and asphalt overlay were placed within one year after reconstruction. The SIPMFs and the asphalt overlay were still in place during the field testing performed for this research.

3.2.1.11 *Bridge F-476*

Bridge F-476 is a single-span bridge with a total span length of 128 ft. It is located in Salt Lake City on State Route 190 (SR-190) (Cottonwood Canyon Road) and spans Big Cottonwood

Figure 3-9 Map location of bridge C-953.

Figure 3-10 Map location of bridge F-53.

Creek, as shown in Figure 3-11. The bridge was constructed in 1983. The BIR notes that both transverse cracking and efflorescence had developed on the underside of the deck by 1991. The BIR does not clearly indicate when the asphalt overlay was placed, but it was in place by 1995 at the latest. The asphalt overlay was still in place during the field testing performed for this research.

Figure 3-11 Map location of bridge F-476.

3.2.1.12 *Bridge F-562*

Bridge F-562 is a single-span bridge with a total span length of 133 ft. It is located in Cottonwood Heights on SR-190 (Wasatch Boulevard) and spans Big Cottonwood Creek, as shown in Figure 3-12. The bridge was constructed using SIPMFs in 1989. The BIR notes that cracking began by 1998 but that the deck remained in good condition until 2014, when some potholes were observed. The bridge deck surface was bare concrete, and the SIPMFs were still in place at the time of field testing performed for this research.

3.2.1.13 *Bridge F-738*

Bridge F-738 is a two-span bridge with a total span length of 191 ft. It is located in Ogden on Interstate 15 and spans State Route 53 (Pennsylvania Avenue) and the UPRR, as shown in Figure 3-13. It was constructed in 2008. The BIR notes that a polymer overlay was placed less than a year after construction. Both transverse cracking and efflorescence had developed on the underside of the deck by 2011. The polymer overlay was still in place during the field testing performed for this research.

3.2.1.14 *Bridge F-799*

Bridge F-799 is a single-span bridge with a total span length of 122 ft. It is located in West Jordan on State Route 85 (SR-85) (Mountain View Corridor) and spans 8200 South, as shown in Figure 3-14. It was constructed using internally cured concrete in 2012. Research previously conducted by Brigham Young University (BYU) indicates that transverse and map

Figure 3-12 Map location of bridge F-562.

Figure 3-13 Map location of bridge F-738.

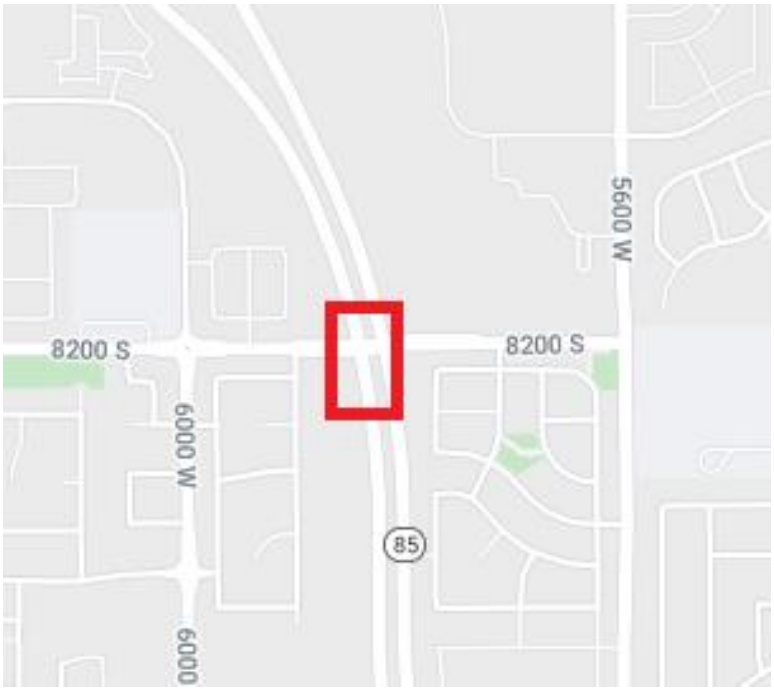

Figure 3-14 Map location of bridge F-799.

cracking had occurred over a majority of the deck surface by 2014. The bridge deck surface was bare concrete from construction until the time of field testing performed for this research.

3.2.1.15 *Bridge F-800*

Bridge F-800 is a single-span bridge with a total span length of 128 ft. It is located in West Jordan on SR-85 (Mountain View Corridor) and spans Dannon Way, as shown in Figure 3-15. It was constructed in 2012. Research previously conducted by BYU indicates that transverse and map cracking had occurred over a majority of the deck surface by 2014. The bridge deck surface was bare concrete from construction until the time of field testing performed for this research.

Figure 3-15 Map location of bridge F-800.

3.2.2 Bridge Deck Testing

Among the many condition assessment methods described in Chapter 2, several were available for use in this research. The methods were specifically selected to identify corrosion activity, delamination, concrete quality, and construction quality. The following sections describe site layout, cover depth measurement, chloride concentration testing, chain dragging, HCP testing, Schmidt rebound hammer testing, impact-echo testing, and VEI testing.

3.2.2.1 *Site Layout*

Because of limited access associated with traffic control constraints, the testing area on each bridge deck consisted of one lane and the adjacent shoulder in most cases. Full access was available for bridges C-725, C-757, C-759, F-53, and F-562.

For determining the coordinates of eight test locations on each of the 15 bridge decks, a set of six random number pairs, shown in Table 3-2, was consistently used. The full bridge length was multiplied by the first number in each pair to generate the longitudinal coordinate, and the width of the testing area was multiplied by the second number in each pair to generate the transverse coordinate. The test locations were then marked on the bridge. (The origin was typically defined as the corner of the deck next to the parapet on the approach side of the deck, so that the longitudinal stationing increased in the direction of trafficking). As shown in Table 3-2, test locations 1 and 2 were co-located, and test locations 7 and 8 were also co-located. A schematic of each bridge deck, including test locations, is provided in Appendix A.

3.2.2.2 *Cover Depth Measurement*

At each test location, a cover meter was used to measure the concrete cover depth and identify the locations of nearby reinforcing steel, as shown in Figure 3-16. Four measurements corresponding to two adjacent longitudinal bars and two adjacent transverse bars were recorded and averaged at each test location to obtain an overall characterization of the deck. Because the transverse reinforcement is typically placed above the longitudinal reinforcement in the top mat of reinforcing steel, the average cover depth was approximately equal to the depth of the interface between the longitudinal and transverse bars.

Table 3-2 Random Number Pairs

Testing	Random Numbers	
Location	Longitudinal	Transverse
1, 2	0.139	0.068
3	0.174	1.00
4	0.347	0.332
5	0.417	0.532
6	0.833	0.932
7, 8	0.972	0.268

Figure 3-16 Cover depth measurement.

3.2.2.3 *Chloride Concentration Testing*

Chloride concentration sampling was performed by pulverizing and collecting concrete powder directly from the bridge deck, as shown in Figure 3-17. On the five decks with an asphalt overlay, a 6-in.-diameter core of the overlay was first removed to expose the concrete bridge deck surface; chloride concentration sampling could then be performed at each test location. Test locations 1 and 2, as well as 7 and 8, were deliberately co-located for the purpose of comparing chloride profiles obtained from the two locations. At test locations 1 and 8, chloride concentration sampling was performed immediately over a reinforcing bar, usually close to an intersection of transverse and longitudinal bars, while at test locations 2 and 7 chloride concentration sampling was performed between bars but within approximately 4 in. of the sampling location immediately over a bar. Samples were collected on 0.5-in. depth intervals to a depth of 4 in. at test locations 2, 4, 5, and 7; 0.5-in. depth intervals until the top mat of reinforcing steel was reached at test locations 1 and 8; and 1-in. depth intervals to a depth of 7 in. at test locations 3 and 6. At locations 3 and 6, the lower mat of reinforcing steel was encountered on some decks, causing a shallower sampling depth at those locations. Because F-562 was

Figure 3-17 Chloride concentration sampling.

scheduled to receive a PPC overlay shortly after testing, samples were collected on 1-in. depth intervals to a slightly greater depth of 8 in. at test locations 3, 4, 5, and 6 to better understand the pre-overlay deck condition in support of a related research effort (Stevens and Guthrie 2020); however, sampling at test locations 1, 2, 7, and 8 was consistent with the procedures used at the other decks. Each sampling hole was patched with rapid-setting, air-entrained grout. On decks with asphalt overlays, a bituminous sealant was applied to seal the bottom of each core hole, and an asphalt repair material was then compacted into the holes. Chloride concentration testing was performed in the BYU Highway Materials Laboratory using the acid-soluble chloride testing method in general accordance with ASTM C1152.

3.2.2.4 *Chain Dragging*

Chain dragging was performed in general accordance with ASTM D4580 to identify any occurrence of delamination at each testing location, as shown in Figure 3-18. When delaminations were identified within 3 in. of the testing location, the test location was recorded as being delaminated. Chain dragging was not performed on the five bridge decks that had an asphalt overlay.

Figure 3-18 Chain dragging.

3.2.2.5 *Half-Cell Potential Testing*

HCP testing was performed on bridge decks with uncoated, or black, bar in general accordance with ASTM C876. The reinforcing steel was first tapped at test locations 1 and 8 to measure the electrical resistance of the top mat of reinforcement within the test area; for the two bridge decks with black bar, the transverse distance between test locations 1 and 8 was 4 ft, requiring electrical current to pass through at least one junction between longitudinal and transverse rebar. After verifying that the top mat of reinforcement was electrically continuous, the HCP apparatus was connected to one of the taps, and a reading was obtained at each test location, as shown in Figure 3-19.

3.2.2.6 *Schmidt Rebound Hammer Testing*

Schmidt rebound hammer testing was performed in general accordance with ASTM C805, as shown in Figure 3-20. Before testing, the concrete surface was smoothed using a masonry grinding wheel mounted to an angle grinder. When a polymer overlay was present, the grinding wheel was also used to grind through the overlay to expose and smooth the bare

Figure 3-19 HCP testing.

Figure 3-20 Schmidt rebound hammer testing.

concrete bridge deck. When an asphalt overlay was present, testing was performed through a 6-in.-diameter core hole on the exposed concrete bridge deck surface following removal of any membrane materials and after smoothing the concrete with the grinding wheel. Three readings within an approximately 2-in.-diameter area were recorded and averaged at each test location. The hammer was held perpendicular to the deck surface in each case.

3.2.2.7 *Impact-Echo Testing*

Impact-echo testing was performed on the 10 bridge decks that did not have an asphalt overlay. The full width of the testing area was scanned using a multi-channel, mallet-based, impact-echo apparatus, as shown in Figure 3-21. The spatial resolution of data collected using the impact-echo apparatus was 2 ft in the transverse direction and approximately 1 ft in the longitudinal direction (Larsen et al. 2020).

3.2.2.8 *Vertical Electrical Impedance Testing*

VEI testing was performed on all 15 bridge decks. The full width of the testing area was scanned using a multi-channel VEI apparatus, as shown in Figure 3-22. The VEI apparatus required an electrical connection to a rebar tap, which was available at either test location 1 or 8 on each bridge deck. The spatial resolution of data collected using the VEI apparatus was 2 ft in the transverse direction and approximately 1 ft in the longitudinal direction (Baxter et al. 2020).

Figure 3-21 Impact-echo testing.

Figure 3-22 VEI testing.

3.2.3 Statistical Analyses

Data from bridge deck testing were compiled into a spreadsheet for analysis. Two-sample *t*-tests were performed to investigate the effects of selected bridge deck features, including polymer overlay application, deck age at polymer overlay application, overlay age, asphalt overlay application with and without a membrane, SIPMFs, SIPMF removal, internally cured concrete, and use of an automatic deck deicing system. Specifically, comparisons were considered only when the deck ages at the time of testing were different by less than 5 years, which minimized temporal variability between the decks, and all of the primary features of the bridge decks were similar except for the feature of interest. This approach resulted in a total of 11 comparisons involving all 15 decks. In each comparison, the null hypothesis was that no difference existed between the two bridge decks, and the alternative hypothesis was that a difference existed between the two bridge decks. A two-sided *p*-value was used to determine if the selected bridge deck feature had a significant effect on the measured properties. A *p*-value less than or equal to 0.05 was used to establish statistical significance at a 95 percent confidence level.

Table 3-3 shows the bridge comparisons for which statistical analyses were performed. In each comparison, one deck was designated as the control deck while the other was designated as the comparison deck. In Table 3-3 the comparisons are presented in groups based on the

Table 3-3 Bridge Deck Comparisons

Control Deck	Comparison Deck	Similarities	Comparison Feature
F-800	F-738	Deck age of 4-8 years	Polymer overlay
F-738	C-953	Deck age of 8-9 years	Deck age at polymer overlay
C-760	C-759	Deck age of 27 years	Polymer overlay
F-738	C-931	Deck age of 8-12 years, polymer overlay placed immediately after deck construction	Treatment age
C-760	C-698	Deck age of 27-28 years, SIPMF removal at deck age of > 18 years	Asphalt overlay
C-725	F-476	Deck age of 32-33 years	Asphalt overlay (no membrane)
C-794	F-53	Deck age of 16-20 years, asphalt overlay placed immediately after construction	SIPMFs
C-460	C-698	Deck age of 28-29 years, asphalt overlay placed at a deck age of > 20 years	SIPMF removal at deck age of > 18 years
F-562	C-760	Deck age of 27 years, bare concrete	SIPMF removal at deck age of < 19 years
F-800	F-799	Deck age of 4 years, bare concrete	Internally cured concrete
C-759	C-757	Deck age of 27 years, polymer overlay placed at a deck age of 10-20 years	Automatic deck deicing system

comparison feature; four comparisons relate to polymer overlays, two relate to asphalt overlays, three relate to SIPMFs, one relates to internally cured concrete, and one relates to automatic deck deicing systems.

3.3 Results

The following sections discuss the results of bridge deck testing and statistical analyses. All results presented in this chapter are limited in their application to the bridge designs, material types, construction techniques, environmental conditions, and trafficking levels associated with the bridges studied in this research.

3.3.1 Bridge Deck Testing

Table 3-4 shows the results of bridge deck testing. All values represent an average of the measurements obtained at the test locations on each deck. The chloride concentration data include only the results from testing between reinforcing bars. For each deck, chloride concentrations at typical cover depths of 2.0, 2.5, and 3.0 in. were computed using linear interpolation from the chloride concentration profile measured at each location, and the values for a given depth were then averaged across the deck. In addition, the chloride concentration at the cover depth measured at each location was computed, and these values were also averaged across each deck. VEI and impact-echo maps, as well as data for each test location, are provided in Appendix B. Hyphens in the columns of Table 3-4 showing relative energy of echo and percent delaminated indicate that the data were not measured, while hyphens in the column of Table 3-4 showing VEI magnitude and percent with low VEI indicate that the data were not valid; invalid data may have resulted from apparatus malfunction, insufficient soaking time, and/or high electrical resistance in the top mat of rebar; high electrical resistance is typical of bridge decks for which the epoxy coating on the top mat of reinforcing steel is generally intact. (After these data were collected for the current research, development of an improved VEI apparatus using a large-area electrode has eliminated many of these issues (Mazzeo and Guthrie 2019).) In Table 3-4, percent with low VEI was calculated by dividing the area with a VEI magnitude less than or equal to 4.0 (Guthrie et al. 2019b) by the total test area, and percent delaminated was calculated by dividing the area with a relative energy of echo less than 225,000 (Larsen et al. 2020) by the total test area.

Table 3-5 compares delamination data and chloride concentrations at the depth of the top mat of rebar for bridge decks with epoxy-coated rebar and bare concrete or polymer overlay surfaces; chloride concentrations at the depth of the top mat of rebar were calculated using cover depth and chloride concentration data from Tables B-1 to B-15. These data support previously published information indicating that epoxy-coated rebar can withstand chloride concentrations up to 4.6 times higher than uncoated reinforcing steel before corrosion is initiated (Bentz et al. 2014). Based on these data, a corrosion initiation threshold of 8.0 lb Cl^-/yd^3 of concrete is recommended in this research for bridge decks with intact epoxy-coated rebar; damage to the epoxy coating, such as rib scrapes, plier strikes, and end cuts, may reduce the corrosion

Table 3-4 Bridge Deck Testing Results

Deck ID	Cover Depth (in.)	Chloride Concentration at Indicated Depth (lb Cl^-/yd^3 Concrete)				Schmidt Rebound Number	Half-Cell Potential (V)	VEI Magnitude (log_{10}(ohms))	Percent with Low VEI (%)	Relative Energy of Echo	Percent Delaminated (%)
		2.0 in.	2.5 in.	3.0 in.	Top Mat of Rebar						
C-460	2.5	11.7	8.7	6.8	8.7	50	-	5.35	0.5	-	-
C-698	2.9	13.4	12.2	10.3	11.0	51	-	5.45	5.7	-	-
C-725	2.6	10.2	8.2	6.6	7.7	54	-	4.62	10.8	119480	2.0
C-757	3.4	14.9	11.5	12.0	9.8	52	-0.498	-	-	105300	0.0
C-759	3.0	10.9	8.9	7.4	8.3	56	-0.275	4.04	47.5	103809	0.0
C-760	2.3	20.9	16.5	11.7	20.7	52	-	3.47	87.6	153227	8.5
C-794	3.0	1.1	0.5	0.3	0.4	49	-	6.00	0.0	-	-
C-931	2.7	0.2	0.2	0.2	0.2	55	-	-	-	72743	0.0
C-953	3.8	1.6	1.3	1.2	3.2	54	-	5.31	0.2	72235	0.0
F-53	2.1	0.4	0.4	0.4	0.3	52	-	5.24	0.0	-	-
F-476	2.5	9.9	8.8	7.4	8.6	46	-	4.73	13.5	-	-
F-562	2.4	6.0	2.6	1.7	5.1	52	-	4.48	0.8	125069	0.2
F-738	3.3	0.2	0.2	0.2	0.2	52	-	5.50	0.1	106766	0.0
F-799	2.5	0.5	0.2	0.2	0.3	58	-	-	-	114450	0.0
F-800	3.1	0.3	0.2	0.1	0.1	57	-	-	-	116482	0.0

Table 3-5 Chloride Concentration and Delamination Data

Chloride Concentration at Depth of Top Mat of Rebar (lb Cl^-/yd^3 Concrete)	Number of Samples	Percent Delaminated (%)
0.0-2.0	26	0.0
2.0-4.0	1	0.0
4.0-6.0	3	0.0
6.0-8.0	1	0.0
8.0+	11	27.3

protection offered to the rebar (Pinkerton 2007). Insufficient data were available in this research to independently evaluate the typical corrosion initiation threshold of 2.0 lb Cl^-/yd^3 of concrete for black bar with respect to the occurrence of delamination.

Beyond consideration of corrosion initiation thresholds, the issue of chloride concentration sampling was investigated. While the chloride concentration data presented in Tables 3-4 and 3-5 are the results of testing between reinforcing bars, so that samples below the top mat of reinforcing steel could be obtained, Figure 3-23 includes chloride concentration data from directly above the top mat of rebar, as measured at test locations 1 and 8 on each deck. To compare the results of sampling directly above and between reinforcing bars, Figure 3-23 presents a ratio of the former to the latter at the depth of the top mat of rebar. With the majority of the ratios exceeding a value of 1.0, the effect of the rebar itself on the accumulation of chloride ions becomes apparent. Because chloride ions are unable to pass through the rebar, they accumulate immediately above the rebar, which causes a higher chloride concentration at that depth than would be measured in the absence of rebar, all other factors held constant. (Ratios less than 1.0 may have been influenced by heterogeneity in the concrete matrix.)

To quantify the relationship between the calculated ratio and the chloride concentration between reinforcing bars, linear regression was used to develop a best-fit line for a selected range of 1 to 20 lb Cl^-/yd^3 of concrete as measured between reinforcing bars. The results, which are shown in Figure 3-24, suggest that chloride concentration values directly above rebar may be up to 70 percent greater, on average, than values measured between reinforcing bars at the same depth. As would be expected, the ratio decreases, approaching 1.0, with increasing chloride

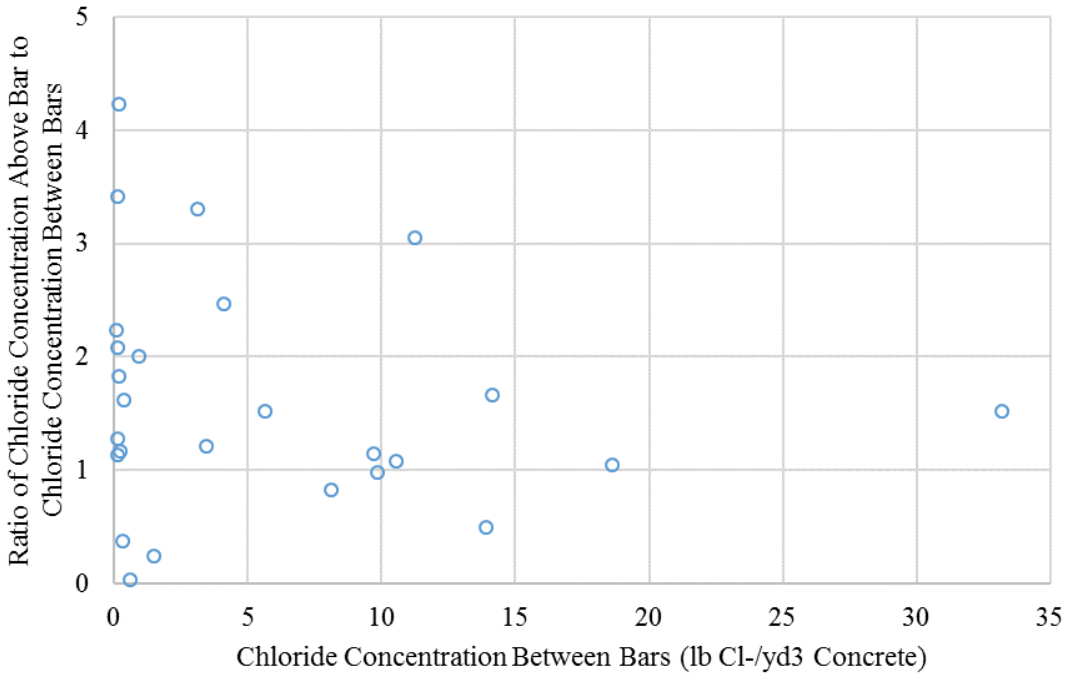

Figure 3-23 Chloride concentrations directly above and between reinforcing bars at the depth of the top mat of rebar.

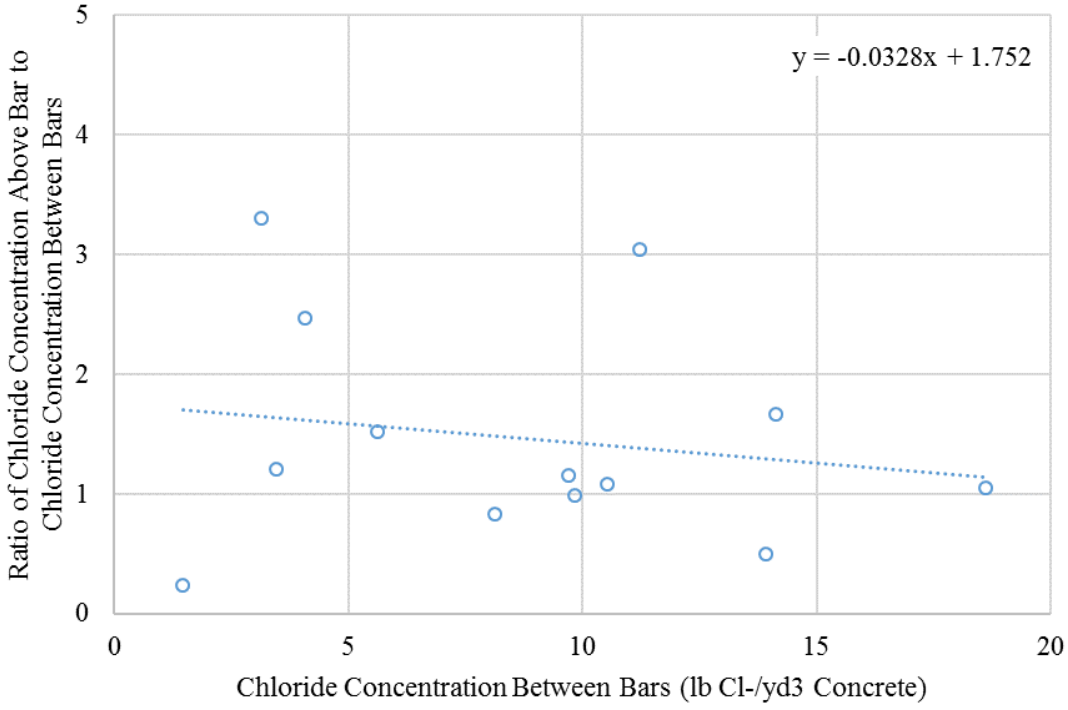

Figure 3-24 Linear regression for selected chloride concentrations directly above and between reinforcing bars at the depth of the top mat of rebar.

concentration; therefore, at chloride concentrations exceeding about 20 lb Cl^-/yd^3 of concrete as measured between reinforcing bars, chloride ion concentrations above and between reinforcing bars would be expected to be approximately equal. This analysis indicates that chloride concentrations measured between reinforcing bars should be increased by up to 70 percent to estimate chloride concentrations directly above the rebar, which should then be compared with the corrosion initiation threshold for the type of reinforcement in the bridge deck (black or epoxy-coated bar).

3.3.2 Statistical Analyses

Results from two-sample *t*-tests performed to evaluate specific bridge deck features, as previously described in Table 3-3, are presented in Tables 3-6 to 3-16. Cover depth; chloride concentration at depths of 2.0, 2.5, and 3.0 in.; Schmidt rebound number; HCP (only for bridge decks with black bar); VEI magnitude; and relative energy of echo were included in the comparisons, with cover depth being included only because of its potential role in analyzing HCP and VEI data. *P*-values less than or equal to 0.05 indicate statistically significant differences, while *p*-values greater than 0.05 indicate statistically insignificant differences. In Tables 3-6 to 3-16, *p*-values associated with statistically significant differences are presented in bold-faced font. Because only two decks were included in each comparison, the results are limited by the possibility that factors not measured or considered, such as deicing salt application frequency, in the comparisons may mask the effects of the feature of interest despite the careful selection of the decks included in this research. A hyphen in Tables 3-6 to 3-16 indicates that the data were not measured, that only one measurement was available (so that a standard deviation could not be computed), and/or that the *t*-test could not be performed because of insufficient data. (In some cases, the standard deviation is greater than the average; for measurements limited to only positive values, this occurrence indicates a long tail in the distribution).

Bridges F-800 and F-738, which were respectively 4 and 8 years old at the time of testing, were compared to evaluate the effects of placing a polymer overlay immediately after deck construction. The results shown in Table 3-6 indicate that the chloride concentrations at a depth of 3.0 in. are significantly different, with F-738 unexpectedly exhibiting a higher value despite the presence of the polymer overlay on that deck. However, because the observed

Table 3-6 Statistical Results for Comparison of F-800 and F-738

Measured Property	F-800 (Bare Concrete)		F-738 (Polymer Overlay Placed Immediately After Deck Construction)		*p*- value
	Avg.	St. Dev.	Avg.	St. Dev.	
Cover Depth (in.)	3.1	0.3	3.3	0.4	0.257
Chloride Concentration at Depth of 2.0 in. (lb Cl^-/yd^3 Concrete)	0.3	0.4	0.2	0.1	0.496
Chloride Concentration at Depth of 2.5 in. (lb Cl^-/yd^3 Concrete)	0.2	0.1	0.2	0.1	0.454
Chloride Concentration at Depth of 3.0 in. (lb Cl^-/yd^3 Concrete)	0.1	0.0	0.2	0.1	**0.024**
Schmidt Rebound Number	57	3	52	6	0.119
VEI Magnitude (log_{10}(ohms))	-	-	5.50	0.16	-
Relative Energy of Echo	116482	14024	106766	9585	0.289

difference is very small, it is considered to be practically unimportant in this research. Indeed, given that the chloride concentrations analyzed in this comparison are similar to those previously reported for new concrete bridge decks in Utah (Guthrie et al. 2020), these data suggest that additional time may be required to observe the benefits of placing a polymer overlay immediately after deck construction.

Bridges F-738 and C-953, which were respectively 8 and 9 years old at the time of testing, were compared to evaluate the effects of placing a polymer overlay 5 years after deck construction. The results shown in Table 3-7 indicate no statistically significant differences among the evaluated properties. Nonetheless, the chloride concentrations at depths of 2.0, 2.5, and 3.0 in. for C-953 are all higher than those reported for F-738 at the same depths; the absence of statistically significant differences is likely attributable to the relatively high standard deviations associated with the chloride concentrations measured for C-953.

Bridges C-760 and C-759, which were both 27 years old at the time of testing, were compared to evaluate the effects of placing a polymer overlay 13 years after deck construction. The results shown in Table 3-8 indicate that, although the chloride concentrations at a depth of

Table 3-7 Statistical Results for Comparison of F-738 and C-953

Measured Property	F-738 (Polymer Overlay Placed Immediately After Deck Construction)		C-953 (Polymer Overlay Placed 5 Years After Deck Construction)		*p* -value
	Avg.	St. Dev.	Avg.	St. Dev.	
Cover Depth (in.)	3.3	0.4	3.8	0.9	0.273
Chloride Concentration at Depth of 2.0 in. (lb Cl^-/yd^3 Concrete)	0.2	0.1	2.4	3.7	0.145
Chloride Concentration at Depth of 2.5 in. (lb Cl^-/yd^3 Concrete)	0.2	0.1	2.0	3.2	0.161
Chloride Concentration at Depth of 3.0 in. (lb Cl^-/yd^3 Concrete)	0.2	0.1	1.9	3.2	0.169
Schmidt Rebound Number	52	6	54	6	0.719
VEI Magnitude (log_{10}(ohms))	5.50	0.16	5.31	0.15	0.088
Relative Energy of Echo	106766	9585	72235	31181	0.067

Table 3-8 Statistical Results for Comparison of C-760 and C-759

Measured Property	C-760 (Bare Concrete)		C-759 (Polymer Overlay Placed 13 Years After Deck Construction)		*p* -value
	Avg.	St. Dev.	Avg.	St. Dev.	
Cover Depth (in.)	2.3	0.3	3.0	0.5	**0.016**
Chloride Concentration at Depth of 2.0 in. (lb Cl^-/yd^3 Concrete)	24.4	12.8	11.1	1.3	**0.033**
Chloride Concentration at Depth of 2.5 in. (lb Cl^-/yd^3 Concrete)	16.5	9.0	8.8	1.7	0.090
Chloride Concentration at Depth of 3.0 in. (lb Cl^-/yd^3 Concrete)	11.7	6.5	7.3	2.1	0.165
Schmidt Rebound Number	52	5	56	5	0.149
VEI Magnitude (log_{10}(ohms))	3.47	0.23	4.04	0.24	**0.004**
Relative Energy of Echo	153227	32882	103809	16801	**0.012**

2.0 in. are significantly different, with C-759 having the lower value as expected, all of the chloride concentrations are well above the corrosion initiation thresholds for both black and

epoxy-coated bar. These data therefore suggest that waiting 13 years before placing a polymer overlay may be too late to prevent chloride-induced corrosion. Nonetheless, some benefits from the overlay placed on C-759 include a lower relative energy of echo value, which indicates less delamination, and a higher VEI magnitude, which indicates greater protection against water and chloride ion ingress, compared to C-760. The higher cover depth on C-759 may have also contributed to the higher VEI magnitude.

Bridges F-738 and C-931, which were respectively 8 and 12 years old at the time of testing and had polymer overlays placed immediately after deck construction, were compared to evaluate the effects of a higher overlay age. The results shown in Table 3-9 indicate that the difference in cover depth between the two decks is statistically significant; however, variation in cover depth itself is not related to treatment age. The data suggest that a higher overlay age does not have a measurable effect when both treatments are in good condition, as evidenced by the low chloride concentrations in both decks.

Bridges C-760 and C-698, which were respectively 27 and 29 years old at the time of testing and had SIPMFs removed at a deck age greater than 18 years, were compared to evaluate the effects of placing an asphalt overlay with a membrane 22 years after deck construction. The results shown in Table 3-10 indicate that the values of VEI magnitude are significantly different

Table 3-9 Statistical Results for Comparison of F-738 and C-931

Measured Property	F-738 (Overlay Age of 8 Years)		C-931 (Overlay Age of 12 Years)		*p* -value
	Avg.	St. Dev.	Avg.	St. Dev.	
Cover Depth (in.)	3.3	0.4	2.7	0.1	**0.012**
Chloride Concentration at Depth of 2.0 in. (lb Cl^-/yd^3 Concrete)	0.2	0.1	0.3	0.2	0.187
Chloride Concentration at Depth of 2.5 in. (lb Cl^-/yd^3 Concrete)	0.2	0.1	0.2	0.1	0.254
Chloride Concentration at Depth of 3.0 in. (lb Cl^-/yd^3 Concrete)	0.2	0.1	0.2	0.1	0.916
Schmidt Rebound Number	52	6	55	4	0.486
VEI Magnitude (log_{10}(ohms))	5.50	0.16	-	-	-
Relative Energy of Echo	106766	9585	72743	40835	0.098

Table 3-10 Statistical Results for Comparison of C-760 and C-698

Measured Property	C-760 (Bare Concrete)		C-698 (Asphalt Overlay Placed 22 Years After Deck Construction)		*p* -value
	Avg.	St. Dev.	Avg.	St. Dev.	
Cover Depth (in.)	2.3	0.3	2.9	0.3	0.100
Chloride Concentration at Depth of 2.0 in. (lb Cl^-/yd^3 Concrete)	24.4	12.8	14.3	6.4	0.093
Chloride Concentration at Depth of 2.5 in. (lb Cl^-/yd^3 Concrete)	16.5	9.0	11.8	5.9	0.300
Chloride Concentration at Depth of 3.0 in. (lb Cl^-/yd^3 Concrete)	11.7	6.5	10.3	4.6	0.677
Schmidt Rebound Number	52	5	51	6	0.748
VEI Magnitude (log_{10}(ohms))	3.47	0.23	5.45	0.82	**0.004**
Relative Energy of Echo	153227	32882	-	-	-

for C-760 and C-698, with a higher VEI magnitude resulting from the application of the asphalt overlay with a membrane on C-698 as expected. However, despite the apparent improvement in protection against further water and chloride ion ingress, the chloride concentrations are all well above the corrosion initiation thresholds for both black and epoxy-coated bar, suggesting that waiting 22 years before placing an asphalt overlay with a membrane may be too late to prevent chloride-induced corrosion.

Bridges C-725 and F-476, which were respectively 32 and 33 years old at the time of testing, were compared to evaluate the effects of placing an asphalt overlay without a membrane 12 years after deck construction. Although the results shown in Table 3-11 indicate that Schmidt rebound numbers are significantly different for C-725 and F-476, variation in Schmidt rebound number itself is not related to placement of an asphalt overlay. Given the absence of any significant improvement in deck condition for F-476 compared to C-725, the data suggest that placing an asphalt overlay without a membrane 12 years after deck construction is not an effective practice for protecting against rebar corrosion.

Bridges C-794 and F-53, which were respectively 20 and 16 years old at the time of testing and had asphalt overlays with membranes placed immediately after construction, were

Table 3-11 Statistical Results for Comparison of C-725 and F-476

Measured Property	C-725 (Bare Concrete)		F-476 (Asphalt Overlay without Membrane Placed 12 Years After Deck Construction)		*p* -value
	Avg.	St. Dev.	Avg.	St. Dev.	
Cover Depth (in.)	2.6	0.3	2.5	1.4	0.943
Chloride Concentration at Depth of 2.0 in. (lb Cl^-/yd^3 Concrete)	10.7	4.4	8.9	6.9	0.565
Chloride Concentration at Depth of 2.5 in. (lb Cl^-/yd^3 Concrete)	8.2	3.9	7.8	6.5	0.898
Chloride Concentration at Depth of 3.0 in. (lb Cl^-/yd^3 Concrete)	6.6	3.8	6.4	5.7	0.968
Schmidt Rebound Number	54	6	46	5	**0.032**
VEI Magnitude (log_{10}(ohms))	4.619	0.450	4.73	0.23	0.594
Relative Energy of Echo	119480	17290	-	-	-

compared to evaluate the effects of SIPMFs on bridge decks with asphalt overlays with membranes placed immediately after construction. The results shown in Table 3-12 indicate that the values of VEI magnitude are significantly different, with C-794 having a higher value than that of F-53. This result may be more related to potential differences in asphalt overlay quality than the effects of SIPMFs, however. Beyond the evaluation of the effects of SIPMFs, these data also demonstrate the effectiveness of placing asphalt overlays with membranes immediately after construction; consistent with previous research (Sumsion 2013), the chloride concentrations are extremely low, indicating that excellent protection against chloride ion ingress can be achieved when the overlays are installed properly.

Bridges C-460 and C-698, which were respectively 28 and 29 years old at the time of testing and had asphalt overlays with membranes placed at a deck age greater than 20 years, were compared to evaluate the effects of removing SIPMFs 18 years after deck construction. The results shown in Table 3-13 indicate that, given the absence of any significant improvement in deck condition for C-698 compared to C-460, removing SIPMFs after a deck age greater than 18

Table 3-12 Statistical Results for Comparison of C-794 and F-53

Measured Property	C-794 (No SIPMFs)		F-53 (SIPMFs)		*p* -value
	Avg.	St. Dev.	Avg.	St. Dev.	
Cover Depth (in.)	3.0	0.5	2.1	0.9	0.212
Chloride Concentration at Depth of 2.0 in. (lb Cl^-/yd^3 Concrete)	0.8	1.1	0.4	0.1	0.288
Chloride Concentration at Depth of 2.5 in. (lb Cl^-/yd^3 Concrete)	0.4	0.5	0.4	0.1	0.745
Chloride Concentration at Depth of 3.0 in. (lb Cl^-/yd^3 Concrete)	0.3	0.3	0.4	0.3	0.561
Schmidt Rebound Number	49	11	52	6	0.592
VEI Magnitude (log_{10}(ohms))	6.00	0.11	5.24	0.18	**0.006**
Relative Energy of Echo	-	-	-	-	-

Table 3-13 Statistical Results for Comparison of C-460 and C-698

Measured Property	C-460 (SIPMFs)		C-698 (SIPMFs Removed)		*p* -value
	Avg.	St. Dev.	Avg.	St. Dev.	
Cover Depth (in.)	2.5	-	2.9	0.3	-
Chloride Concentration at Depth of 2.0 in. (lb Cl^-/yd^3 Concrete)	11.1	3.0	14.3	6.4	0.219
Chloride Concentration at Depth of 2.5 in. (lb Cl^-/yd^3 Concrete)	8.6	3.0	11.8	5.9	0.227
Chloride Concentration at Depth of 3.0 in. (lb Cl^-/yd^3 Concrete)	6.9	2.3	10.3	4.6	0.138
Schmidt Rebound Number	50	5	51	6	0.866
VEI Magnitude (log_{10}(ohms))	5.35	0.45	5.45	0.82	0.821
Relative Energy of Echo	-	-	-	-	-

years is not likely to be effective at reversing the adverse effects of the SIPMFs on bridge deck condition.

Bridges F-562 and C-760, which were both 27 years old and had bare concrete surfaces at the time of testing, were compared to evaluate the effects of removing SIPMFs 18 years after deck construction. The results shown in Table 3-14 indicate that chloride concentrations at depths of 2.0, 2.5, and 3.0 in. and values of VEI magnitude are significantly different for F-562

Table 3-14 Statistical Results for Comparison of F-562 and C-760

Measured Property	F-562 (SIPMFs)		C-760 (SIPMFs Removed)		*p* -value
	Avg.	St. Dev.	Avg.	St. Dev.	
Cover Depth (in.)	2.4	0.6	2.3	0.3	0.613
Chloride Concentration at Depth of 2.0 in. (lb Cl^-/yd^3 Concrete)	5.2	4.5	24.4	12.8	**0.006**
Chloride Concentration at Depth of 2.5 in. (lb Cl^-/yd^3 Concrete)	2.2	2.3	16.5	9.0	**0.010**
Chloride Concentration at Depth of 3.0 in. (lb Cl^-/yd^3 Concrete)	1.4	1.4	11.7	6.5	**0.011**
Schmidt Rebound Number	52	2	52	5	0.960
VEI Magnitude ($\log_{10}$(ohms))	4.48	0.17	3.47	0.23	**0.000**
Relative Energy of Echo	125069	18114	153227	32882	0.144

and C-760; unexpectedly, C-760 has higher chloride concentration and lower VEI magnitude even though the SIPMFs were removed from that deck. Because F-562 has such a steep chloride concentration profile, with high chloride concentrations near the surface and much lower chloride concentrations deeper in the deck as shown in Table B-27, the concrete in bridge deck F-562 may have a lower diffusion coefficient than C-760. In that case, the effect of a lower diffusion coefficient likely masked any potential effect of removing SIPMFs (Guthrie et al. 2006).

Bridges F-800 and F-799, which were both 4 years old and had bare concrete surfaces at the time of testing, were compared to evaluate the effects of internally cured concrete. The results shown in Table 3-15 indicate that the difference in cover depth between the two decks is statistically significant; however, variation in cover depth itself is not related to a change in curing method. Given the absence of any significant improvement in deck condition for F-799 compared to F-800, the data suggest that bridge deck construction using internally cured concrete is not an effective practice for protecting against rebar corrosion.

Bridges C-759 and C-757, which were both 27 years old at the time of testing and had polymer overlays placed at a deck age between 10 and 20 years, were compared to evaluate the effects of an automatic deck deicing system. The results shown in Table 3-16 indicate that

Table 3-15 Statistical Results for Comparison of F-800 and F-799

Measured Property	F-800 (Conventionally Cured Concrete)		F-799 (Internally Cured Concrete)		*p* -value
	Avg.	St. Dev.	Avg.	St. Dev.	
Cover Depth (in.)	3.1	0.3	2.5	0.3	**0.005**
Chloride Concentration at Depth of 2.0 in. (lb Cl^-/yd^3 Concrete)	0.3	0.4	0.8	0.8	0.164
Chloride Concentration at Depth of 2.5 in. (lb Cl^-/yd^3 Concrete)	0.2	0.1	0.5	0.6	0.172
Chloride Concentration at Depth of 3.0 in. (lb Cl^-/yd^3 Concrete)	0.1	0.0	0.4	0.6	0.224
Schmidt Rebound Number	57	3	58	4	0.719
VEI Magnitude (log_{10}(ohms))	-	-	-	-	-
Relative Energy of Echo	116482	14024	114450	6724	0.803

Table 3-16 Statistical Results for Comparison of C-759 and C-757

Measured Property	C-759 (No Automatic Deck Deicing System)		C-757 (Automatic Deck Deicing System)		*p* -value
	Avg.	St. Dev.	Avg.	St. Dev.	
Cover Depth (in.)	3.0	0.5	3.4	0.4	0.114
Chloride Concentration at Depth of 2.0 in. (lb Cl^-/yd^3 Concrete)	11.1	1.3	14.4	3.0	**0.021**
Chloride Concentration at Depth of 2.5 in. (lb Cl^-/yd^3 Concrete)	8.8	1.7	11.5	1.9	**0.012**
Chloride Concentration at Depth of 3.0 in. (lb Cl^-/yd^3 Concrete)	7.3	2.1	11.5	4.3	**0.048**
Schmidt Rebound Number	56	5	52	9	0.312
HCP (V)	-0.275	0.042	-0.498	0.081	**0.000**
VEI Magnitude (log_{10}(ohms))	4.04	0.24	-	-	-
Relative Energy of Echo	103809	16801	105300	8090	0.850

chloride concentrations at depths of 2.0, 2.5, and 3.0 in. are significantly different for C-759 and C-757, with C-757 having higher concentrations. HCP values are also significantly different, with C-759 being categorized as uncertain and C-757 being categorized as having a probability greater than 90 percent that corrosion is occurring. These data suggest that automatic deicing

systems can lead to higher chloride concentrations at typical cover depths, which can in turn lead to increased corrosion potential.

3.4 Summary

Fifteen bridge decks were strategically selected for testing in this research. Five bridge decks had bare concrete surfaces, five bridge decks had asphalt overlays, and five bridge decks had polymer overlays. Bridge deck testing included site layout, cover depth measurement, chloride concentration testing, chain dragging, HCP testing, Schmidt rebound hammer testing, impact-echo testing, and VEI testing. Two-sample *t*-tests were performed to investigate the effects of selected bridge deck features, including polymer overlay application, deck age at polymer overlay application, overlay age, asphalt overlay application with and without a membrane, SIPMFs, SIPMF removal, internally cured concrete, and use of an automatic deck deicing system.

Based on the results of field work and statistical analyses, placing an overlay within a year after construction is recommended. Removing SIPMFs after a deck age greater than 18 years is not likely to be effective at reversing the adverse effects of the SIPMFs on bridge deck condition and is not recommended. Bridge deck construction using internally cured concrete is not recommended for protecting against rebar corrosion. To the extent that excluding an automatic deck deicing system does not compromise public safety, automatic deck deicing systems are not recommended.

To supplement the typical corrosion initiation threshold of 2.0 lb Cl^-/yd^3 of concrete for black bar, a corrosion initiation threshold of 8.0 lb Cl^-/yd^3 of concrete is recommended in this research for bridge decks with intact epoxy-coated rebar. For chloride concentrations less than 20 lb Cl^-/yd^3 of concrete as measured between reinforcing bars, an increase of up to 70 percent should be applied to estimate the corresponding chloride concentration of the concrete in direct contact with the rebar.

4.0 DECISION TREE FOR CONCRETE BRIDGE DECK MANAGEMENT

4.1 Overview

This chapter addresses objective 3 of this research, for which a decision tree for concrete bridge deck management in Utah was developed. The data from Chapter 3 were supplemented with information about current bridge deck management practices and treatment costs obtained from UDOT, as well as information about condition assessment and expected treatment service life reported in Chapter 2, to develop a decision tree for concrete bridge deck management. The development process was iterative and benefited from intermediate feedback from UDOT about the sequence of decisions, the desired options, and the decision criteria. Revisions were incrementally incorporated with the goal of developing a concise, user-friendly decision tree for concrete bridge deck management. As stated in Chapter 2, this research is not intended to promote any specific product or manufacturer; prices and performance may vary among the available options. The following sections describe condition assessment methods; bridge deck preservation, rehabilitation, and reconstruction methods; and the decision tree.

4.2 Condition Assessment Methods

Condition assessment methods described in Chapter 2 are summarized in Table 4-1, which includes information about test type, factors evaluated, equipment cost, data collection speed, required expertise, and traffic control for each method. Test type differentiates between destructive and nondestructive methods. Factors that can be evaluated include concrete quality, construction quality, corrosion activity, cracking, delamination, and overlay quality. In addition, information about equipment cost, data collection speed, and required expertise reflect information obtained during this research and may vary among models of similar equipment. Equipment cost and required expertise were obtained by studying the literature, reviewing websites, contacting equipment suppliers, and relying on personal experience, where applicable. For the estimation of data collection speed for a typical bridge deck, six test locations per bridge deck were assumed for methods involving collection of static point measurements, while scanning of the full length of the bridge deck across a substantial portion of the width of each lane and shoulder was assumed for methods involving data collection from a continuously

Table 4-1 Condition Assessment Methods

Condition Assessment Method	Test Type	Factor(s) Evaluated	Equipment Cost	Data Collection Speed	Required Expertise	Traffic Control Required
Chain Dragging	Nondestructive	Delamination	Low	High	Low	Yes
Chloride Concentration Testing	Destructive	Concrete quality	High	Medium	Medium	Yes
Coring	Destructive	Delamination, construction quality	Medium	Medium	Low	Yes
Cover Depth Measurement	Nondestructive	Construction quality	Medium	Low	Low	Yes
Dye Penetration Testing	Nondestructive	Cracking	Low	Medium	Low	Yes
Embedded Sensor Monitoring	Nondestructive	Concrete quality, corrosion activity	Low	Low	Medium	No
Galvanostatic Pulse Measurement	Nondestructive	Corrosion activity	High	Medium	Medium	Yes
Ground-Penetrating Radar Scanning	Nondestructive	Delamination, construction quality	High	Low	High	No
Half-Cell Potential Testing	Nondestructive	Corrosion activity	Medium	Medium	Low	Yes
Hammer Sounding	Nondestructive	Delamination	Low	High	Low	Yes
Impact-Echo Testing	Nondestructive	Delamination	High	Low	High	No
Infrared Thermography Scanning	Nondestructive	Delamination	High	Low	High	No
Linear Polarization Testing	Nondestructive	Corrosion activity	High	Medium	Medium	Yes
Petrographic Analysis	Destructive	Cracking, concrete quality, construction quality	High	Medium	High	Yes
Radiography	Nondestructive	Concrete quality	High	Low	High	Yes
Rapid Chloride Permeability Testing	Destructive	Concrete quality	Medium	Medium	Medium	Yes
Resistivity Testing	Nondestructive	Concrete quality	Medium	Medium	Low	Yes
Schmidt Rebound Hammer Testing	Nondestructive	Concrete quality	Low	Low	Low	Yes
Skid Resistance Testing	Nondestructive	Construction quality, overlay quality	Medium	Medium	Medium	No
Ultrasonic Pulse Echo Testing	Nondestructive	Cracking, delamination, construction quality	High	Medium	Medium	Yes
Ultrasonic Surface Waves Measurement	Nondestructive	Cracking, delamination, construction quality	High	Medium	Medium	Yes
Vertical Electrical Impedance Testing	Nondestructive	Concrete quality, overlay quality	High	Low	High	Yes
Visual Inspection	Nondestructive	Cracking, overlay quality	Low	Low	Medium	Yes

moving platform. When more than one option for testing equipment was available for a given method, the equipment already familiar to UDOT was selected. If an option for testing was available that did not require traffic control, traffic control was indicated as not being required.

In Table 4-1, equipment cost ratings of low, medium, and high represent less than $1,000, between $1,000 and $10,000, and greater than $10,000, respectively. Data collection speeds of low, medium, and high represent less than 1 hour per bridge, between 1 and 4 hours per bridge, and greater than 4 hours per bridge, respectively, and include any applicable laboratory work. A required expertise rating of low indicates that the condition assessment method does not require knowledge of contextual information or the use of complex equipment or software. A required expertise rating of medium indicates that the condition assessment method requires knowledge of some contextual information and the use of moderately complex equipment or software. A required expertise rating of high indicates that the condition assessment method requires potentially extensive knowledge of contextual information and the use of complex equipment or software. As the required expertise rating increases, the results are expected to be increasingly sensitive to deviations in proper procedures or data analysis.

4.3 Bridge Deck Preservation, Rehabilitation, and Reconstruction Methods

Table 4-2 lists unit costs, expected treatment service life estimates, and factors addressed for the preservation, rehabilitation, and reconstruction methods most commonly used by UDOT (T. Pinkerton, personal communication, July 20, 2020). Unit costs include materials and labor but do not include equipment mobilization or traffic control. Equipment mobilization and traffic control costs are typically estimated by UDOT to be 10 and 5 percent of material and labor costs, respectively, but may be adjusted based on location, traffic, or other factors. User costs, which are much more difficult to define, were not directly addressed in this research. Treatment service life estimates were determined using information from the literature presented in Chapter 2 and the results of bridge deck testing presented in Chapter 3.

Table 4-2 Bridge Deck Preservation, Rehabilitation, and Reconstruction Methods

Treatment	Unit Cost ($/ft^2)	Expected Treatment Service Life (years)	Factor(s) Addressed
High-Molecular-Weight Methacrylate Sealant Application	3.55	7	Cracking, concrete quality
Thin-Bonded Polymer Overlay Application	7.25	8 to 12	Cracking, concrete quality
Polyester Polymer Concrete Overlay Application (0.75 in.)	36.25	15 to 20	Cracking, concrete quality
Asphalt Overlay with Membrane Application (3 in.)	7.15	15 to 20	Cracking, concrete quality
Scarification and Overlay	25.00	18 to 29	Concrete quality, construction quality
Delamination and Pothole Repair without Galvanic Anode	43.50	1 to 10	Delamination
Delamination and Pothole Repair with Galvanic Anode	65.25	1 to 10	Delamination, corrosion activity
Partial-Depth Concrete Deck Replacement Using Hydrodemolition	38.05	30 to 35	Corrosion activity, concrete quality, construction quality, delamination
Full-Depth Cast-in-Place Concrete Deck Replacement	241.00	30 to 35	Cracking, corrosion activity, concrete quality, construction quality, delamination

4.4 Decision Tree

Figures 4-1 to 4-4 show the concrete bridge deck decision tree. The decision tree includes 10 junctions, labeled A to J, and seven recommended treatments, labeled 1 to 7. The junctions, shown as rectangles in the decision tree, require the user to address questions about surface type, degree of protection against water and chloride ion ingress, degree of deterioration, and years of additional service life needed; the answers, shown as diamonds in the decision tree, lead to selection of treatment options ranging from repairing an overlay to full-depth bridge deck reconstruction. The decision tree process ends when a treatment recommendation is reached. A

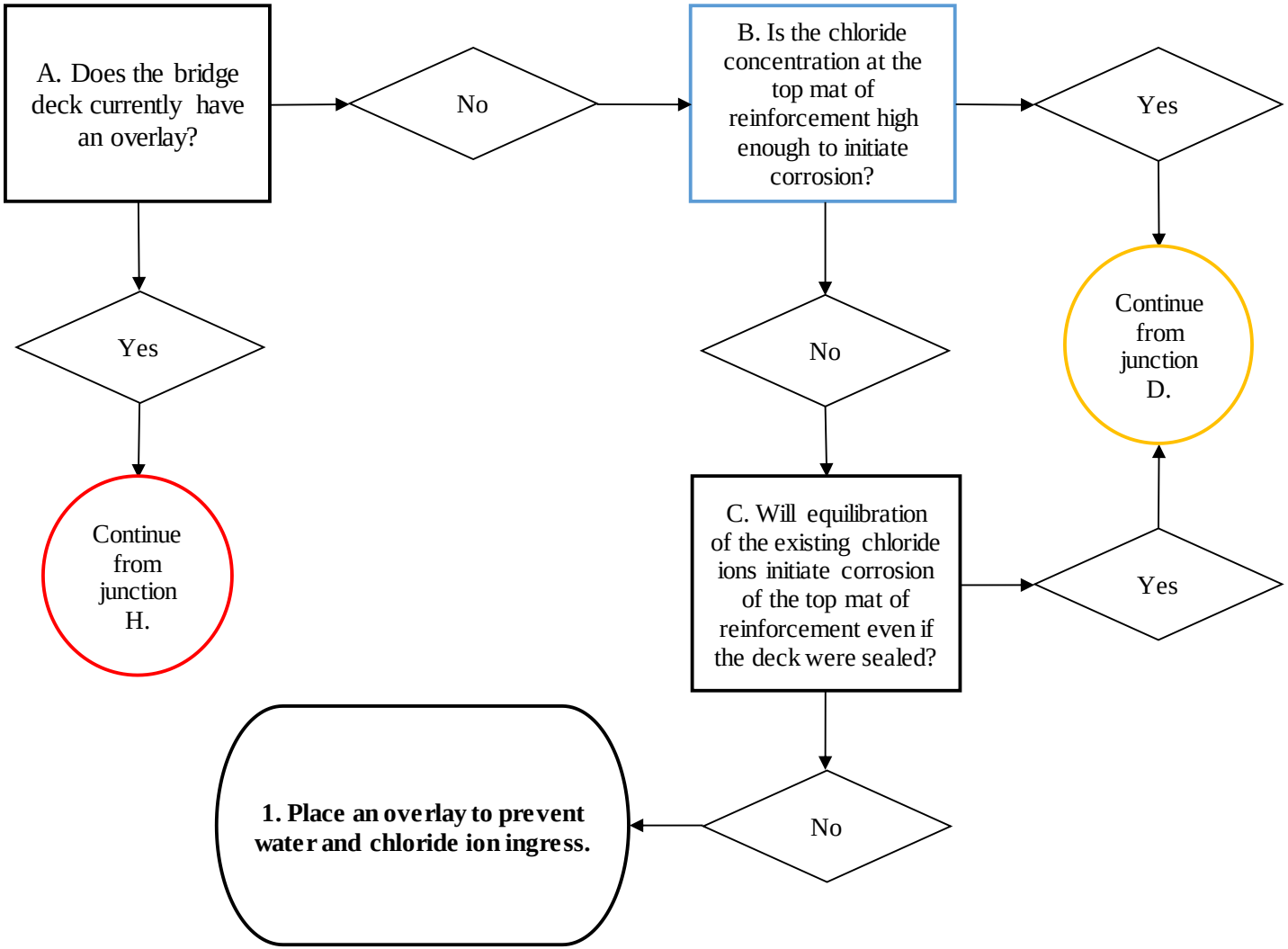

Figure 4-1 Decision tree (junctions A to C).

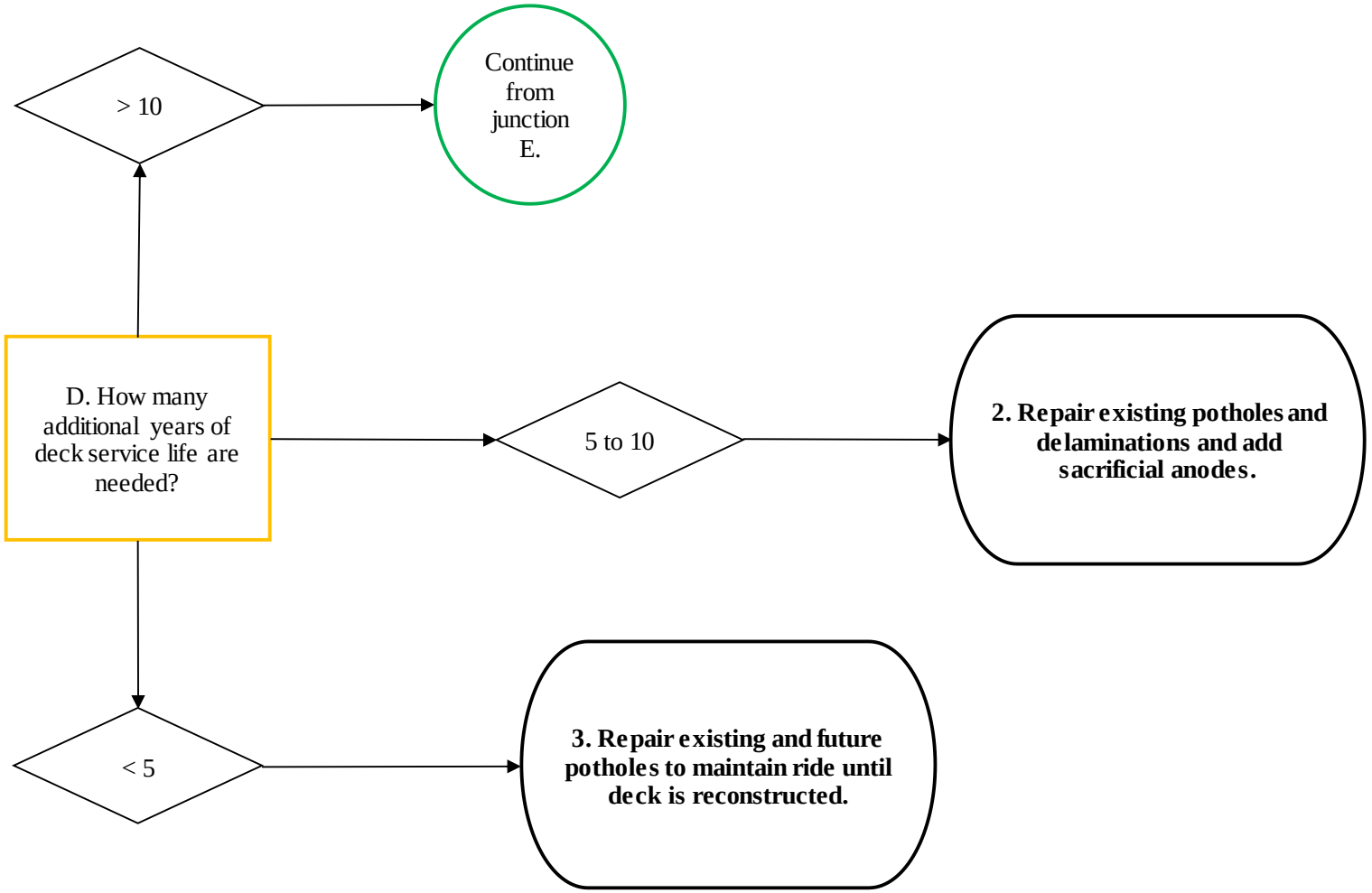

Figure 4-2 Decision tree (junction D).

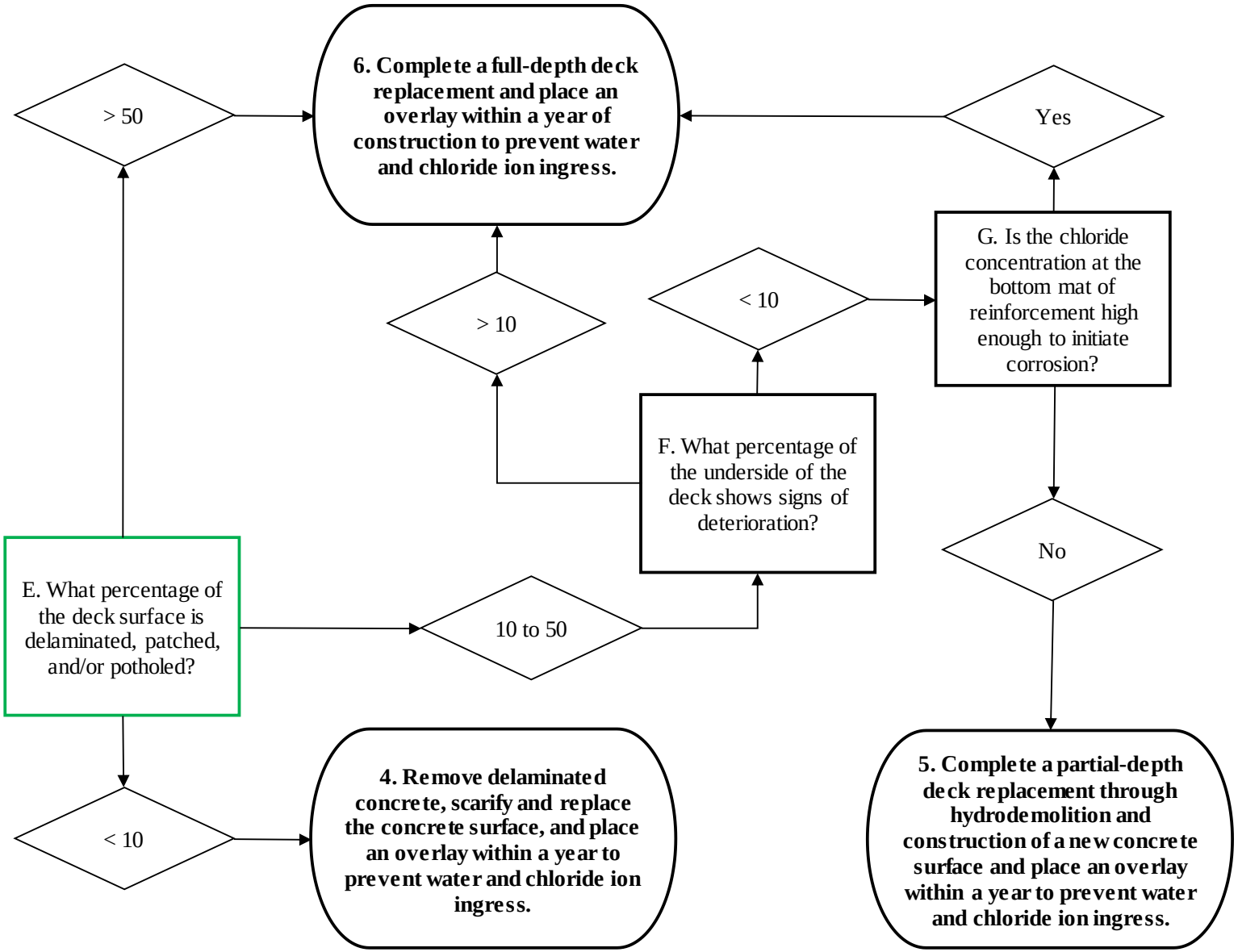

Figure 4-3 Decision tree (junctions E to G).

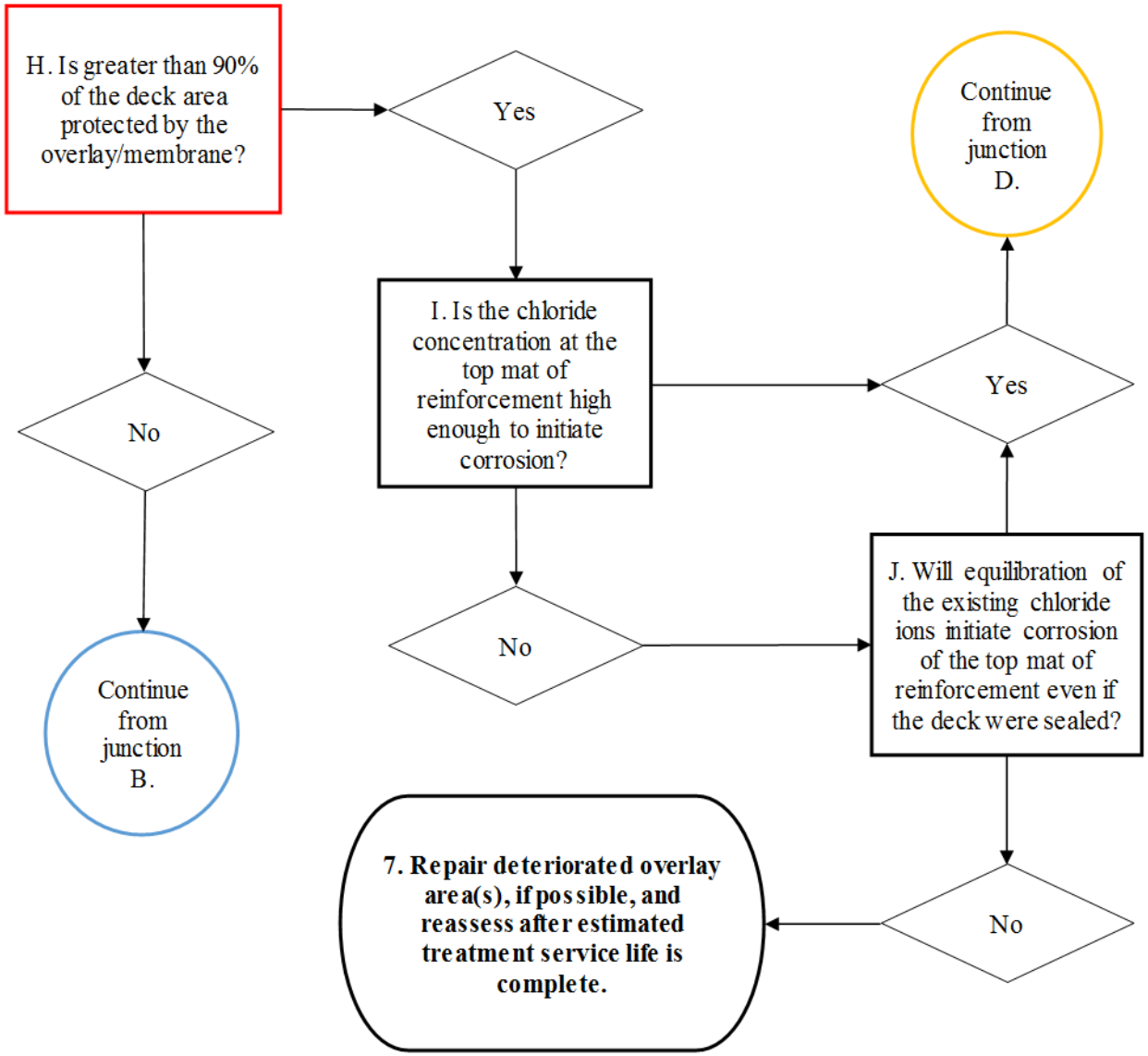

Figure 4-4 Decision tree (junctions H to J).

circle in the decision tree requires the user to move to a junction, which is outlined in the same color as the circle for convenience, in a different figure. The junctions and treatments are discussed in the following sections.

4.4.1 Junctions

Junction A, shown in Figure 4-1, involves using visual inspection or inventory records to determine the bridge deck surface type. Bridge decks with overlays are then evaluated in the decision tree differently than bare concrete bridge decks.

Junction B, shown in Figure 4-1, involves using chloride concentration testing to evaluate the chloride concentration at the top mat of reinforcement. Chloride concentration sampling should be performed to a depth just below the bottom mat of reinforcement to also enable evaluation of the chloride concentration at the bottom mat, as potentially required for junction G. As suggested in Figure 3-23, chloride concentrations measured between bars should be increased by up to 70 percent to better estimate the chloride concentration of the concrete in direct contact with the rebar. As suggested in Chapter 3, corrosion initiation thresholds of 2.0 and 8.0 lb Cl^-/yd^3 of concrete should be used for decks with black and epoxy-coated bar, respectively.

Junction C, shown in Figure 4-1, involves using chloride concentration testing to determine the chloride concentration profile and computer modeling software to evaluate the possibility of corrosion initiation in the future. For example, the chloride concentration profile may be such that the chloride concentration at the top mat of reinforcement is not yet higher than the corrosion initiation threshold at the time that an overlay is placed but will later exceed the threshold when chloride ions in the overlying concrete nearer the surface diffuse downwards over time as equilibration occurs, even though the overlay prevents new chloride ion ingress. An illustration of this possibility, based on previous research (Birdsall 2007), is presented in Figure 4-5, in which the solid gray line represents a cover depth of 2.5 in. and the dashed red line represents the corrosion initiation threshold for black bar of 2.0 lb Cl^-/yd^3 of concrete. The chloride concentration at the top mat of reinforcement is less than the corrosion initiation threshold immediately before treatment but reaches the corrosion initiation threshold 5 years after treatment and remains just above the corrosion initiation threshold 10 years after treatment. However, the chloride profile may also be such that the chloride concentration at the top mat of

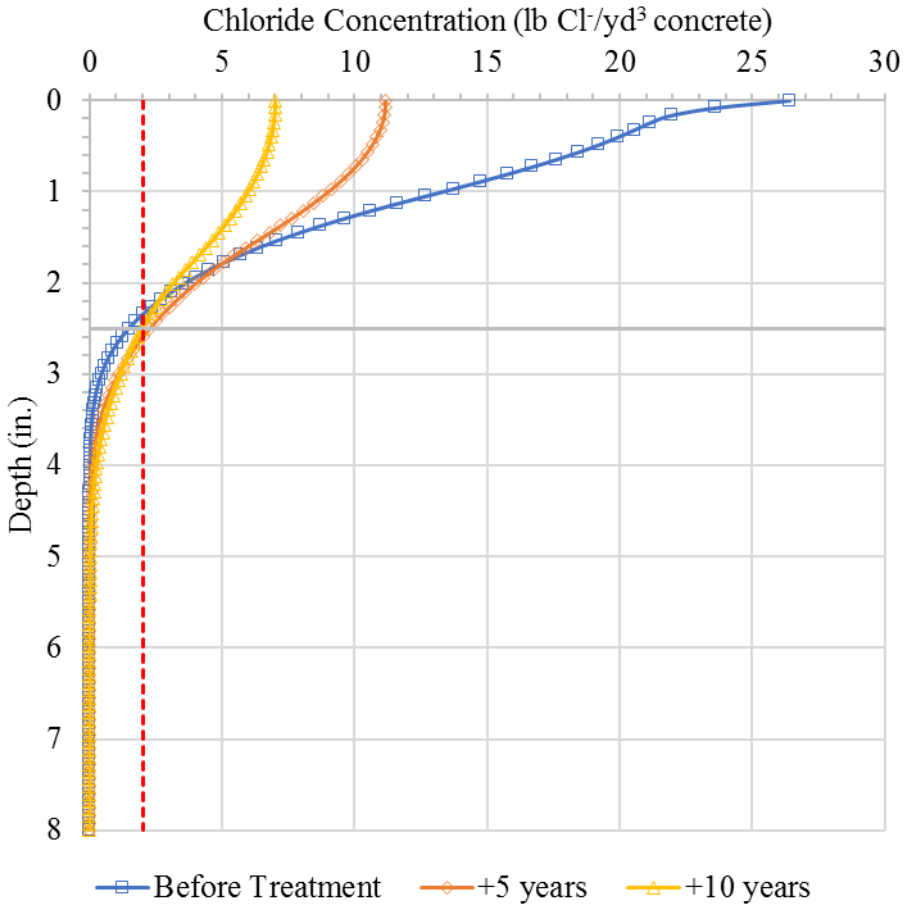

Figure 4-5 Chloride concentration profiles for a scenario in which an overlay is applied and the corrosion initiation threshold is reached after equilibration.

reinforcement will never reach the corrosion initiation threshold, even after chloride ion equilibration. This possibility, also based on previous research (Birdsall 2007), is illustrated in Figure 4-6, in which the solid gray line again represents a cover depth of 2.5 in. and the dashed red line represents the corrosion initiation threshold for black bar of 2.0 lb Cl^-/yd^3 of concrete. The chloride concentration at the top mat of reinforcement is less than the corrosion initiation threshold before treatment and remains below the corrosion initiation threshold for at least 10 years after treatment. Computer modeling software can be used to simulate the equilibration process and determine if rebar corrosion is likely to be initiated after the deck surface is sealed. Removal of contaminated concrete may be required to reduce high chloride concentrations near the surface and prevent corrosion initiation after equilibration, and computer modeling software can also be used to simulate this option. Again, chloride concentrations measured between bars

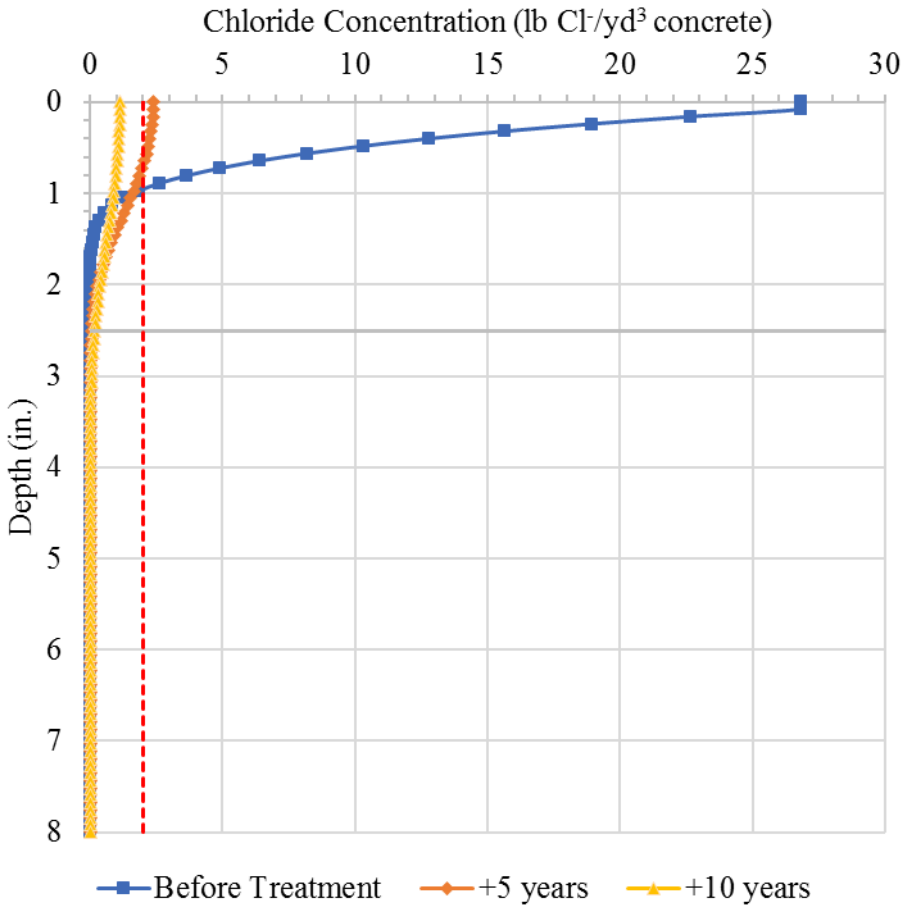

Figure 4-6 Chloride concentration profiles for a scenario in which an overlay is applied and the corrosion initiation threshold is not reached after equilibration.

should be increased by up to 70 percent, as suggested in Figure 3-23, to better estimate the chloride concentration of the concrete in direct contact with the rebar. As suggested in Chapter 3, corrosion initiation thresholds of 2.0 and 8.0 lb Cl^-/yd^3 of concrete should be used for decks with black and epoxy-coated bar, respectively.

Junction D, shown in Figure 4-2, involves indicating how many additional years of deck service life are needed. The number of additional years of service life that are needed can be informed by asset management plans developed for a given corridor, in which structural, functional, and political aspects of bridge management may be considered. A more expensive and/or more complex treatment is typically required for a greater extension in deck service life.

Junction E, shown in Figure 4-3, involves using visual inspection and delamination surveys to evaluate the percentage of the deck area that exhibits delamination, patching, and/or potholing. While windshield surveys may be suitable for some decks, other decks may warrant a more detailed visual inspection, possibly even requiring lane closures. Delamination surveys can be conducted using chain dragging, GPR scanning, hammer sounding, impact-echo testing, and/or infrared thermography scanning as described in Chapter 2. Because most methods for detecting delaminations on bridge decks with polymer overlays cannot differentiate between corrosion-induced concrete delamination and overlay debonding, coring should be used to determine the delamination depth when delamination is detected. Under some circumstances, such as when an asphalt overlay has been in place for several years and localized deterioration of the overlay has led to corresponding deterioration of the underlying concrete at the same locations, VEI results can be effectively substituted for delamination data (Guthrie and Mazzeo 2015). Deck inspection notes from BIRs can also be useful for estimating the extent of patching that may have occurred prior to overlay placement.

Junction F, shown in Figure 4-3, involves using visual inspection to evaluate the percentage of the area of the underside of the deck that exhibits deterioration. Signs of deterioration include cracking, efflorescence, staining, and spalling. As an example, Figure 4-7 shows significant cracking and efflorescence on the underside of a bridge deck. Deterioration of the underside of the bridge deck can be a predictor for especially the occurrence of blow-throughs during hydrodemolition (Roper 2018). A deterioration threshold of 10 percent is recommended to avoid extensive blow-throughs and differentiate between partial- and full-depth deck replacement.

Junction G, shown in Figure 4-3, involves using chloride concentration testing to evaluate the chloride concentration at the bottom mat of reinforcement, also to differentiate between partial- and full-depth deck replacement. As suggested in Figure 3-23, chloride concentrations measured between bars should be increased by up to 70 percent to better estimate the chloride concentration of the concrete in direct contact with the rebar. As suggested in Chapter 3, corrosion initiation thresholds of 2.0 and 8.0 lb Cl^-/yd^3 of concrete should be used for decks with black and epoxy-coated bar, respectively.

Figure 4-7 Significant cracking and efflorescence on the underside of a bridge deck.

Junction H, shown in Figure 4-4, involves using VEI or visual inspection to evaluate the percentage of a bridge deck protected by an overlay or membrane. VEI is preferred because some overlay deterioration cannot be determined using visual inspection, such as the example polymer overlay shown in Figure 4-8; under trafficking, this polymer overlay had worn thin in

Figure 4-8 Polymer overlay deterioration.

some places, leaving holes that were not visible without a light source behind the overlay. When less than 90 percent of the deck area has an impedance magnitude greater than or equal to 4.0, the deck should be treated as if it were bare concrete.

Junction I, shown in Figure 4-4, involves using chloride concentration testing to evaluate the chloride concentration at the top mat of reinforcement to determine the average chloride concentration profile. Chloride concentration sampling should be performed to a depth just below the bottom mat of reinforcement to also enable evaluation of the chloride concentration at the bottom mat, as potentially required for junction G. As suggested in Figure 3-23, chloride concentrations measured between bars should be increased by up to 70 percent to better estimate the chloride concentration of the concrete in direct contact with the rebar. As suggested in Chapter 3, corrosion initiation thresholds of 2.0 and 8.0 lb Cl^-/yd^3 of concrete should be used for decks with black and epoxy-coated bar, respectively. If the chloride concentration at the top mat of reinforcement is higher than the corrosion initiation threshold, the deck should be treated as if it were bare concrete.

Junction J, shown in Figure 4-4, involves using chloride concentration testing to determine the chloride concentration profile and computer modeling software to evaluate the possibility of corrosion initiation in the future. For example, the chloride concentration profile may be such that the chloride concentration at the top mat of reinforcement is not yet higher than the corrosion initiation threshold at the time that an overlay is placed but will later exceed the threshold when chloride ions in the overlying concrete nearer the surface diffuse downwards over time as equilibration occurs, even though the overlay prevents new chloride ion ingress. An illustration of this possibility, based on previous research (Birdsall 2007), was presented previously in Figure 4-5, in which the solid gray line represents a cover depth of 2.5 in. and the dashed red line represents the corrosion initiation threshold of 2.0 lb Cl^-/yd^3 of concrete. The chloride concentration at the top mat of reinforcement is less than the corrosion initiation threshold immediately before treatment but reaches the corrosion initiation threshold 5 years after treatment and remains just above the corrosion initiation threshold 10 years after treatment. However, the chloride profile may also be such that the chloride concentration at the top mat of reinforcement will never reach the corrosion initiation threshold, even after chloride ion equilibration. This possibility was illustrated in Figure 4-6, in which the solid gray line again

represents a cover depth of 2.5 in. and the dashed red line represents the corrosion initiation threshold of 2.0 lb Cl^-/yd^3 of concrete. The chloride concentration at the top mat of reinforcement is less than the corrosion initiation threshold before treatment and remains below the corrosion initiation threshold for at least 10 years after treatment. Computer modeling software can be used to simulate the equilibration process and determine if rebar corrosion is likely to be initiated after the deck surface is sealed. Removal of contaminated concrete may be required to reduce high chloride concentrations near the surface and prevent corrosion initiation after equilibration, and computer modeling software can also be used to simulate this option. Again, chloride concentrations measured between bars should be increased by up to 70 percent, as suggested in Figure 3-23, to better estimate the chloride concentration of the concrete in direct contact with the rebar. As suggested in Chapter 3, corrosion initiation thresholds of 2.0 and 8.0 lb Cl^-/yd^3 of concrete should be used for decks with black and epoxy-coated bar, respectively. If the chloride concentration at the top mat of reinforcement will be higher than the corrosion initiation threshold after equilibration, the deck should be treated as if it were bare concrete. Under some circumstances, such as when an asphalt overlay has been in place for several years and localized deterioration of the overlay has led to corresponding deterioration of the underlying concrete at the same locations, VEI results can be effectively substituted for delamination data (Guthrie and Mazzeo 2015).

4.4.2 Treatment Recommendations

Treatment recommendation 1, shown in Figure 4-1, involves placing an overlay to prevent water and chloride ion ingress. Overlay options include HMWM sealants, thin-bonded polymer overlays, PPC overlays, and asphalt overlays with membranes. In addition to the cost and service life information provided in Table 4-2, traffic levels and surrounding pavement types should be considered when selecting an overlay. HMWM sealants are typically best suited for bridge decks with low traffic, such as non-highway bridges. Thin-bonded polymer overlays are typically best suited for bridge decks with medium traffic, such as non-mainline and rural highway bridges. PPC overlays are typically best suited for bridge decks with high traffic, such as urban highways and freeways. Asphalt overlays with membranes can be used for any traffic level and are typically best suited for bridge decks whose surrounding pavement is asphalt, although current UDOT policy reserves asphalt overlay applications only for older bridge decks

that are approaching the end of their service life. Regardless of the type, overlays should be maintained through future years and replaced as necessary. Maintenance for asphalt overlays could include sealing cracks, milling and filling the surface while retaining an intact membrane, and adding a surface treatment, such as those used on asphalt pavement (Nykänen et al. 2013). Second-generation thin-bonded polymer overlays can be placed on existing polymer overlays when the existing overlay has worn thin from trafficking and when no spalls, potholes, or delaminations exist on the deck (Balakumaran and Weyers 2019).

Treatment recommendation 2, shown in Figure 4-2, involves repairing existing delaminations and potholes and adding sacrificial anodes. To ensure that all deteriorated concrete is removed, an extra 6.0 in. of concrete is commonly removed from around the edge of a delamination or pothole. A concrete saw is used to cut around the boundary, typically to the depth of the top mat of reinforcement, after which jackhammers are used to remove the damaged concrete before the area is cleaned with sandblasting. Alternatively, hydrodemolition can be used to remove deteriorated concrete from the top surface of a concrete bridge deck using a high-pressure water jet (Roper 2018). Repair concrete is typically made of a rapid-setting material to allow traffic to be returned to the bridge deck as quickly as possible. As described in Chapter 2, sacrificial anodes prevent the halo effect from occurring. When sacrificial anodes are installed as part of the repair, the concrete must be removed to a depth of at least 0.50 in. below the bottom of the top mat of reinforcement to allow for anode installation. The sacrificial anodes are then placed around the perimeter of the patch. Electrical connection to the rebar is required, so any rebar coatings must be removed where a sacrificial anode is attached to the rebar. Sacrificial anode spacing depends on manufacturer and reinforcement density but typically ranges from 13 to 30 in.

Treatment recommendation 3, shown in Figure 4-2, involves repairing existing and future potholes to maintain ride until the bridge deck is reconstructed. The same procedures given for treatment 2 should be used to repair potholes for this treatment recommendation. This treatment recommendation is most similar to a “do-nothing” approach; the potholes are repaired for safety purposes only, without sacrificial anodes to reduce cost, while plans for reconstruction are being developed.

Treatment recommendation 4, shown in Figure 4-3, involves removing delaminated concrete and scarifying and replacing the concrete surface. An overlay should be placed within a year and maintained through future years to prevent water and chloride ion ingress, as previously described in the discussion of treatment 1. Scarification depths ranging from 0.25 in. to just above the top mat of the reinforcement are commonly attained using a milling machine, and the thickness of the new concrete is typically at least 1.25 in. (Nolan 2008). Computer modeling software should be used to ensure that sufficient contaminated concrete will be removed to prevent corrosion initiation after equilibration. For example, the chloride profile on a bridge deck may be such that removing 0.5 to 1.0 in. of concrete will reduce the chloride concentration at the top mat of reinforcement to below the corrosion initiation threshold in an acceptable period of time after treatment. An illustration of this possibility, based on previous research (Nolan 2008), is presented in Figure 4-9, in which the solid gray line represents an original cover depth of 2.5

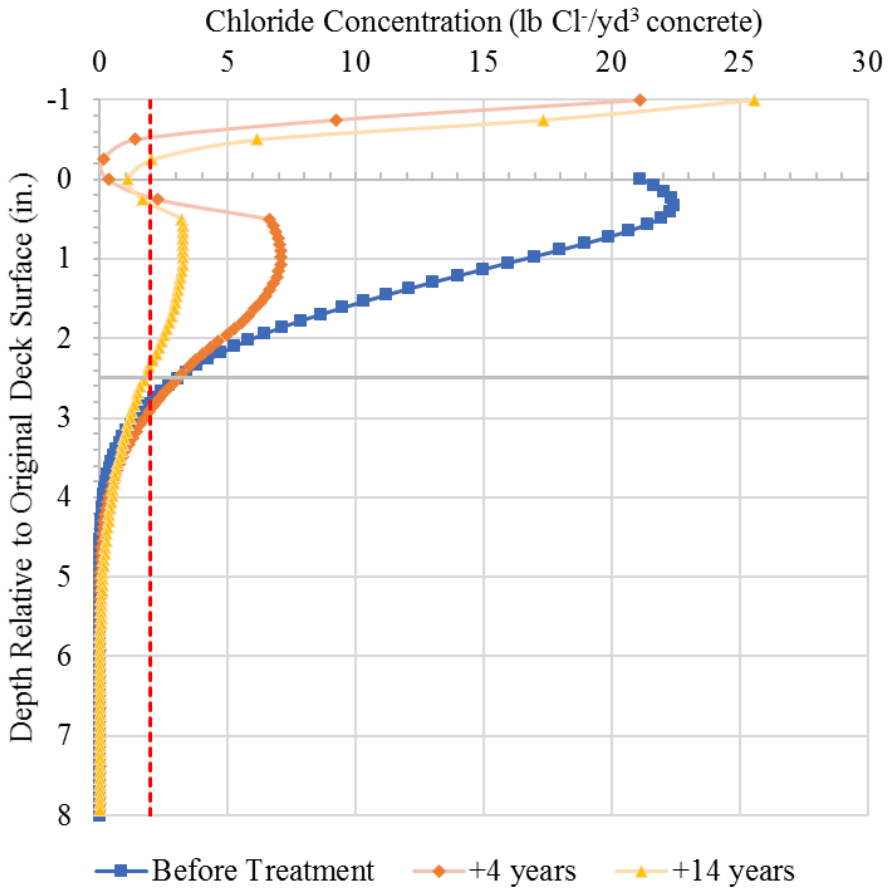

Figure 4-9 Chloride concentration profile for a scenario in which a 0.5-in. scarification and 1.5-in. overlay is applied.

in. and the dashed red line represents the corrosion initiation threshold for black bar of 2.0 lb Cl^-/yd^3 of concrete. In Figure 4-9, the y-axis represents the depth relative to the original deck surface, with negative values representing the newly placed overlay. The chloride concentration at the top mat of reinforcement is greater than the corrosion initiation threshold before scarification of 0.5 in. and placement of 1.0 in. of new concrete, but the chloride concentration at the top mat of reinforcement is reduced to below the corrosion initiation threshold sometime between 4 and 14 years after treatment. Because the new concrete thickness is greater than the scarification depth, the cover depth increases after the treatment. However, the chloride profile on a bridge deck may be such that removing 1.5 to 2.0 in. of concrete is necessary to reduce the chloride concentration at the top mat of reinforcement to below the corrosion initiation threshold in an acceptable period of time after treatment. This possibility, also based on previous research (Nolan 2008), is illustrated in Figure 4-10, in which the solid gray line represents a cover depth

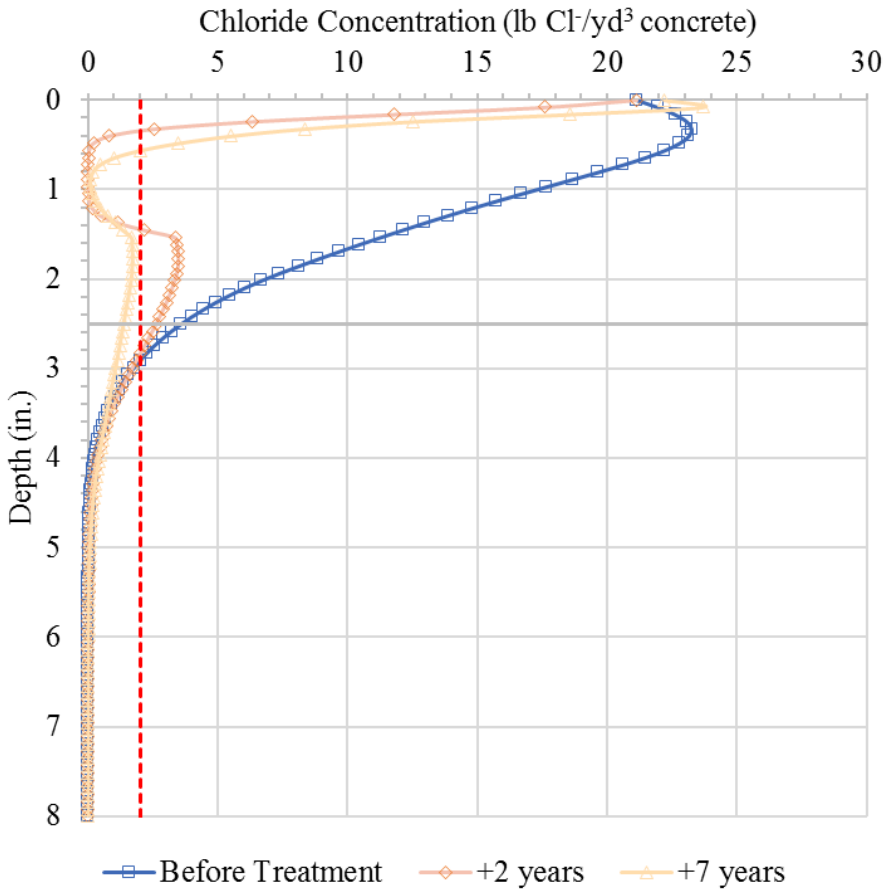

Figure 4-10 Chloride concentration profile for a scenario in which a 1.5-in. scarification and 1.5-in. overlay is applied.

of 2.5 in. and the dashed red line represents the corrosion initiation threshold for black bar of 2.0 lb Cl^-/yd^3 of concrete. The chloride concentration at the top mat of reinforcement is greater than the corrosion initiation threshold before scarification of 1.5 in. and placement of 1.5 in. of new concrete, but the chloride concentration at the top mat of reinforcement is reduced to below the corrosion initiation threshold sometime between 2 and 7 years after treatment.

Treatment recommendation 5, shown in Figure 4-3, involves partial-depth deck replacement through hydrodemolition and construction of a new concrete surface. An overlay should be placed within a year and maintained through future years to prevent water and chloride ion ingress, as previously described in the discussion of treatment 1. Partial-depth deck replacement can be used as long as the chloride concentration at the depth of the bottom mat of reinforcement has not reached a threshold of corrosion and less than approximately 10 percent of the underside of the deck exhibits damage (Wenzlick 2002). Factors to consider to prevent blow-throughs include transverse rebar spacing, concrete compressive strength, depth of removal below the bottom of the top mat of reinforcement, and hydrodemolition orifice size, water pressure, and jet angle (Roper 2018). Contaminated concrete should be removed to a depth below the top mat of reinforcement, and a new concrete surface should be constructed. Water management is another important factor to consider with hydrodemolition; a sufficient water source is necessary, and all water used in hydrodemolition must be treated to remove any contaminants before it can be returned to the local water system (Roper 2018). As described in Chapter 2, hydrodemolition typically removes any epoxy coatings from the top mat of rebar; therefore, the corrosion initiation threshold for black bar of 2.0 lb Cl^-/yd^3 of concrete should be used for future evaluation of decks that have received this treatment.

Treatment recommendation 6, shown in Figure 4-3, involves full-depth deck reconstruction. An overlay should be placed within a year and maintained through future years to prevent water and chloride ion ingress, as previously described in the discussion of treatment 1. Chapter 2 describes options available for reconstruction. Results from Chapter 3 discourage the use of automatic deck deicing systems, SIPMFs, and internally cured concrete when pre-cast half-deck panels are also used.

Treatment recommendation 7, shown in Figure 4-4, involves repairing deteriorated overlay area(s), if possible. Repairs could include overlay patching, crack sealing, or asphalt surface treatments, for example. Bridge deck condition should be reassessed when the overlay reaches its estimated service life.

4.4.3 Applications

Tables 4-3 to 4-5 document the application of the decision tree to each of the 15 bridge decks tested in this research. The tables are organized into steps involving the applicable junctions. A hyphen in Tables 4-3 to 4-5 indicates that no additional steps are required to determine the recommended treatment. If junction C or J was reached in the analysis of a given deck, the chloride concentration at the depth of the rebar after equilibration was estimated using numerical modeling; chloride concentration profiles from locations 3 and 6 were linearly extrapolated to model equilibration of a full-depth chloride concentration profile. Where applicable, corrosion initiation thresholds of 2.0 and 8.0 lb Cl^-/yd^3 of concrete were used for bridge decks with black and epoxy-coated bar, respectively. If junction D was reached in the analysis of a given deck, a value of greater than 10 years of needed service life was assumed because a value of less than 5 years always leads to a recommendation of treatment 3 and a value of 5 to 10 years always leads to a recommendation of treatment 2. When necessary, delamination data were supplemented with visual inspection using photographs to estimate a total percentage of deteriorated area for bare decks. When necessary, the percentage of deteriorated area for decks with asphalt overlays was estimated from VEI results. Photos were available to estimate the percentage of deteriorated area on the underside of the deck for C-760 but not for F-476; the percentage of deteriorated area on the underside of the deck was subsequently assumed to be less than 10 percent for F-476. Because VEI results were not available for C-931, the percentage of deteriorated area was also assumed to be less than 10 percent for that bridge deck.

While the 15 decks were not randomly selected and are therefore not representative of the entire UDOT bridge network, the decks include a variety of features present within the network. With the exception of treatments 2 and 3, which were deliberately avoided as described previously, each treatment is included as a recommendation at least once in Tables 4-3 to 4-5. Treatment 7 was recommended the most often, five times, suggesting within the context of this

Table 4-3 Decision Tree Examples for Decks with Bare Concrete

Deck ID	Step 1		Step 2		Step 3		Step 4	
	Junction	Necessary Information	Junction	Necessary Information	Junction	Necessary Information	Junction	Necessary Information
C-725	A	Surface Type: Bare Concrete	B	Chloride Concentration at Top Mat of Rebar: 7.9 lb Cl^-/yd^3 concrete	C	Corrosion Initiation after Equilibration: Yes	D	Additional Deck Service Life Needed: > 10 years
C-760	A	Surface Type: Bare Concrete	B	Chloride Concentration at Top Mat of Rebar: 24.8 lb Cl^-/yd^3 concrete	D	Additional Deck Service Life Needed: > 10 years	E	Percent Deteriorated: 15.0%
F-562	A	Surface Type: Bare Concrete	B	Chloride Concentration at Top Mat of Rebar: 4.4 lb Cl^-/yd^3 concrete	C	Corrosion Initiation after Equilibration: Yes	D	Additional Deck Service Life Needed: > 10 years
F-799	A	Surface Type: Bare Concrete	B	Chloride Concentration at Top Mat of Rebar: 0.6 lb Cl^-/yd^3 concrete	C	Corrosion Initiation after Equilibration: No	-	-
F-800	A	Surface Type: Bare Concrete	B	Chloride Concentration at Top Mat of Rebar: 0.1 lb Cl^-/yd^3 concrete	C	Corrosion Initiation after Equilibration: No	-	-

Table 4-3 Decision Tree Examples for Decks with Bare Concrete, Continued

Deck ID	Step 5		Step 6		Recommended Treatment
	Junction	Necessary Information	Junction	Necessary Information	
C-725	E	Percent Deteriorated: 5.0%	-	-	4
C-760	F	Underside Percent Deteriorated: 2.0%	G	Chloride Concentration at Bottom Mat of Rebar: 1.4 lb Cl^-/yd^3 concrete	5
F-562	E	Percent Deteriorated: 0.2%	-	-	4
F-799	-	-	-	-	1
F-800	-	-	-	-	1

Table 4-4 Decision Tree Examples for Decks with Asphalt Overlays

Deck ID	Step 1		Step 2		Step 3		Step 4	
	Junction	Necessary Information	Junction	Necessary Information	Junction	Necessary Information	Junction	Necessary Information
C-460	A	Surface Type: Asphalt Overlay	H	Percent Low VEI: 0.5%	I	Chloride Concentration at Top Mat of Rebar: 8.8 lb Cl^-/yd^3 concrete	D	Additional Deck Service Life Needed: > 10 years
C-698	A	Surface Type: Asphalt Overlay	H	Percent Low VEI: 5.7%	I	Chloride Concentration at Top Mat of Rebar: 11.7 lb Cl^-/yd^3 concrete	D	Additional Deck Service Life Needed: > 10 years
C-794	A	Surface Type: Asphalt Overlay	H	Percent Low VEI: 0.0%	I	Chloride Concentration at Top Mat of Rebar: 0.3 lb Cl^-/yd^3 concrete	J	Corrosion Initiation after Equilibration: No
F-53	A	Surface Type: Asphalt Overlay	H	Percent Low VEI: 0.0%	I	Chloride Concentration at Top Mat of Rebar: 0.4 lb Cl^-/yd^3 concrete	J	Corrosion Initiation after Equilibration: No
F-476	A	Surface Type: Asphalt Overlay	H	Percent Low VEI: 13.5%	B	Chloride Concentration at Top Mat of Rebar: 7.0 lb Cl^-/yd^3 concrete	C	Corrosion Initiation after Equilibration: Yes

Table 4-4 Decision Tree Examples for Decks with Asphalt Overlays, Continued

Deck ID	Step 5		Step 6		Step 7		Step 8		Recommended Treatment
	Junction	Necessary Information	Junction	Necessary Information	Junction	Necessary Information	Junction	Necessary Information	
C-460	E	Percent Deteriorated: 0.5%	-	-	-	-	-	-	4
C-698	E	Percent Deteriorated: 5.7%	-	-	-	-	-	-	4
C-794	-	-	-	-	-	-	-	-	7
F-53	-	-	-	-	-	-	-	-	7
F-476	D	Additional Deck Service Life Needed: > 10 years	E	Percent Deteriorated: 13.5%	F	Underside Percent Deteriorated: Assume < 10.0%	G	Chloride Concentration at Bottom Mat of Rebar: 6.5 lb Cl^-/yd^3 concrete	6

Table 4-5 Decision Tree Examples for Decks with Polymer Overlays

Deck ID	Step 1		Step 2		Step 3		Step 4	
	Junction	Necessary Information	Junction	Necessary Information	Junction	Necessary Information	Junction	Necessary Information
C-757	A	Surface Type: Polymer Overlay	H	Percent Low VEI: Assume > 10.0%	B	Chloride Concentration at Top Mat of Rebar: 10.0 lb Cl^-/yd^3 concrete	D	Additional Deck Service Life Needed: > 10 years
C-759	A	Surface Type: Polymer Overlay	H	Percent Low VEI: 47.5%	B	Chloride Concentration at Top Mat of Rebar: 8.5 lb Cl^-/yd^3 concrete	D	Additional Deck Service Life Needed: > 10 years
C-931	A	Surface Type: Polymer Overlay	H	Percent Low VEI: Assume < 10.0%	I	Chloride Concentration at Top Mat of Rebar: 0.3 lb Cl^-/yd^3 concrete	J	Corrosion Initiation after Equilibration: No
C-953	A	Surface Type: Polymer Overlay	H	Percent Low VEI: 0.2%	I	Chloride Concentration at Top Mat of Rebar: 3.2 lb Cl^-/yd^3 concrete	J	Corrosion Initiation after Equilibration: No
F-738	A	Surface Type: Polymer Overlay	H	Percent Low VEI: 0.1%	I	Chloride Concentration at Top Mat of Rebar: 0.2 lb Cl^-/yd^3 concrete	J	Corrosion Initiation after Equilibration: No

Table 4-5 Decision Tree Examples for Decks with Polymer Overlays, Continued

Deck ID	Step 5		Step 6		Step 7		Recommended Treatment
	Junction	Necessary Information	Junction	Necessary Information	Junction	Necessary Information	
C-757	E	Percent Deteriorated: Assume > 10.0%	F	Underside Percent Deteriorated: Assume < 10.0%	G	Chloride Concentration at Bottom Mat of Rebar: 6.1 lb Cl^-/yd^3 concrete	6
C-759	E	Percent Deteriorated: 47.5%	F	Underside Percent Deteriorated: Assume < 10.0%	G	Chloride Concentration at Bottom Mat of Rebar: 0.4 lb Cl^-/yd^3 concrete	5
C-931	-	-	-	-	-	-	7
C-953	-	-	-	-	-	-	7
F-738	-	-	-	-	-	-	7

study that placing an overlay within a year after bridge deck construction will lead to less expensive and/or less complex treatments in future years. Treatment 4 was recommended four times, suggesting that waiting too long to place on overlay, or not placing one at all, will necessitate removing chloride-contaminated concrete at some point during the life of the bridge deck. In each case where treatment 4 was recommended, a 1-in. scarification and overlay will remove sufficient chloride-contaminated concrete to prevent future rebar corrosion. Treatment 1 was recommended twice, suggesting that some bridge decks only need an overlay placement. Treatment 5 was also recommended twice, suggesting that a major rehabilitation will be required at some point during the life of the bridge deck. Finally, Treatment 6 was recommended twice, suggesting that reconstruction will eventually be necessary during the life of the bridge deck and that placing an asphalt overlay without a membrane is not an effective practice for preventing the ingress of water and chloride ions.

4.5 Summary

Condition assessment methods presented in Chapter 2 were described in terms of test type, factors evaluated, equipment cost, data collection speed, required expertise, and traffic control for each method. Unit costs, expected treatment service life estimates, and factors addressed for the preservation, rehabilitation, and reconstruction methods most commonly used by UDOT were also summarized. The data from Chapter 3 were supplemented with information about current bridge deck management practices and treatment costs obtained from UDOT, as well as information about condition assessment and expected treatment service life reported in Chapter 2, to develop a decision tree for concrete bridge deck management. The decision tree includes 10 junctions and seven recommended treatments. The junctions require the user to address questions about surface type, degree of protection against water and chloride ion ingress, degree of deterioration, and years of additional service life needed; the answers lead to selection of treatment options ranging from repairing an overlay to full-depth bridge deck reconstruction.

5.0 CONCLUSION

5.1 Summary

Despite many efforts to mitigate chloride-induced corrosion in concrete bridge decks, the rate of structural deterioration of bridge decks throughout the United States appears to be increasing, most likely due to the expanding use of deicing salts in cold regions. The corrosion epidemic yields two major objectives for bridge managers: 1) slow the rate of corrosion that will eventually result in costly repairs and 2) prioritize individual bridges so that they are repaired before costly rehabilitation or reconstruction is required (Carter 1989).

Although useful information has been published about selected aspects of bridge deck management, a comprehensive guide describing bridge deck management processes is not currently available in the industry. Furthermore, the effects of specific deck treatment types and timing on bridge deck performance have not been fully quantified. Given the continuing challenges of preserving concrete bridge decks in Utah, UDOT requested development of a concrete bridge deck management guide specific to the design, construction, environmental conditions, and deterioration mechanisms typical of concrete bridge decks in Utah. To address this request, three objectives were developed for this research:

1. Investigate bridge deck condition assessment methods used in the field and laboratory, methods of managing bridge decks, and methods for estimating remaining bridge deck service life using computer models through a comprehensive literature review on these subjects.
2. Collect and analyze field data from representative concrete bridge decks in Utah.
3. Develop a decision tree for concrete bridge deck management in Utah.

These three objectives were necessarily completed in numerical order; information about possible condition assessment methods was required before bridge deck testing was completed. Additionally, information about possible preservation and rehabilitation methods, as well as the results from bridge deck testing, were required to inform the development of the decision tree and test the efficacy of the recommended treatments.

Objective 1 was summarized in Chapter 2, which provided a detailed summary of information available in the literature about concrete bridge decks, focusing on condition assessment; bridge deck preservation and rehabilitation; bridge deck reconstruction; and estimating remaining service life using computer models. Condition assessment can be performed using many different test methods, both destructive and nondestructive, to assess the state of deterioration of a bridge deck. Many different preservation and rehabilitation techniques can be applied to extend the service life of a bridge deck. Several options for reconstruction are also available. In addition, a few computer models are available for predicting the service life of a bridge deck subject to specific conditions.

Objective 2 was summarized in Chapter 3, which described bridge deck testing. Fifteen bridge decks were strategically selected for testing in this research. Five bridge decks had bare concrete surfaces, five bridge decks had asphalt overlays, and five bridge decks had polymer overlays. Bridge deck testing included site layout, cover depth measurement, chloride concentration testing, chain dragging, HCP testing, Schmidt rebound hammer testing, impact-echo testing, and VEI testing. Two-sample *t*-tests were performed to investigate the effects of selected bridge deck features, including polymer overlay application, deck age at polymer overlay application, overlay age, asphalt overlay application with and without a membrane, SIPMFs, SIPMF removal, internally cured concrete, and use of an automatic deck deicing system.

Objective 3 was summarized in Chapter 4, which included the decision tree. Condition assessment methods presented in Chapter 2 were described in terms of test type, factors evaluated, equipment cost, data collection speed, required expertise, and traffic control for each method. Unit costs, expected treatment service life estimates, and factors addressed for the preservation, rehabilitation, and reconstruction methods most commonly used by UDOT were also summarized. The data from Chapter 3 were supplemented with information about current bridge deck management practices and treatment costs obtained from UDOT, as well as information about condition assessment and expected treatment service life reported in Chapter 2, to develop a decision tree for concrete bridge deck management.

5.2 Findings and Recommendations

Based on the results of field work and statistical analyses, placing an overlay within a year after construction is recommended. Removing SIPMFs after a deck age greater than 18 years is not likely to be effective at reversing the adverse effects of the SIPMFs on bridge deck condition and is not recommended. Bridge deck construction using internally cured concrete is not recommended for protecting against rebar corrosion. To the extent that excluding an automatic deck deicing system does not compromise public safety, automatic deck deicing systems are not recommended.

To supplement the typical corrosion initiation threshold of 2.0 lb Cl^-/yd^3 of concrete for black bar, a corrosion initiation threshold of 8.0 lb Cl^-/yd^3 of concrete is recommended in this research for bridge decks with intact epoxy-coated rebar. For chloride concentrations less than 20 lb Cl^-/yd^3 of concrete as measured between reinforcing bars, an increase of up to 70 percent should be applied to estimate the corresponding chloride concentration of the concrete in direct contact with the rebar.

The decision tree developed in this research includes 10 junctions and seven recommended treatments. The junctions require the user to address questions about surface type, degree of protection against water and chloride ion ingress, degree of deterioration, and years of additional service life needed; the answers lead to selection of treatment options ranging from repairing an overlay to full-depth bridge deck reconstruction.

5.3 Future Research

Recommendations for future research include studying the service life of bridge deck overlays under environmental conditions and trafficking levels typical of Utah, further investigating corrosion initiation thresholds for black bar and epoxy-coated bar, measuring the ratio of chloride concentrations between and over bars in the lower mat of reinforcement, and quantifying the occurrence of damage to epoxy-coated rebar during concrete bridge deck construction. Additionally, revisions to the decision tree should be incorporated as additional methods, data, treatments, or other relevant information become available.

5.4 Main Contributions

This research has advanced the body of knowledge on concrete bridge deck management through bridge deck testing and data analysis. As a result of the literature review, a synthesis of existing information about condition assessment, bridge deck preservation and rehabilitation, bridge deck reconstruction, and estimating remaining service life using computer models was compiled. Findings and recommendations from bridge deck testing of 15 bridge decks were documented. These findings, along with information from the literature review, were used to develop a decision tree that allows users to determine an appropriate preservation, rehabilitation, or reconstruction action. In summary, this research provided one of the most comprehensive bridge deck management guides available.

REFERENCES

Al-Qadi, I. L., Weyers, R. E., and Cady, P.D. (1993). "Field Evaluation of Preformed Membranes." *Journal of Transportation Engineering,* 119(2), 284-300.

Alldred, J. C. (1995). "Quantifying Losses in Cover Meter Accuracy Due to Congestion of Reinforcement," *Construction Repair,* 9(1), 41-47.

Andrade, C., and Alonso, C. (2004). "Test Methods for On-Site Corrosion Rate Measurement of Steel Reinforcement in Concrete by Means of the Polarization Resistance Method." *Materials and Structures,* 37, 623-643.

Andrade, C., and González, J. A. (1978). "Quantitative Measurements of Corrosion Rate of Reinforcing Steels Embedded in Concrete Using Polarization Resistance Measurements." *Materials and Corrosion,* 29(8), 515-519.

Argyle, H. M. (2014). "Sensitivity of Electrochemical Impedance Spectroscopy Measurements to Concrete Bridge Deck Properties." M.S. thesis. Department of Civil and Environmental Engineering, Brigham Young University, Provo, UT.

Arora, P., Popov, B., Haran, B., Ramasubramanian, M., Popova, S., and White, R. (1997). "Corrosion Initiation Time of Steel Reinforcement in a Chloride Environment – A One Dimensional Solution." *Corrosion Science,* 39(4), 739-759.

ASCE (American Society of Civil Engineers). (2017). "2017 Infrastructure Report Card." American Society of Civil Engineers. < https://www.infrastructurereportcard.org/wp-content/uploads/2019/02/Full-2017-Report-Card-FINAL.pdf> (Nov. 8, 2017).

ASTM (American Society for Testing and Materials). (1978). "Significance of Tests and Properties of Concrete and Concrete-Making Materials." Committee C9 on Concrete and Concrete Aggregates, Baltimore, MD.

Attanayake, U., Duyar, O., Liang, X., Aktan, H., and Ng, K. (2003). "Fundamentals of Use of Penetrating Sealants for Concrete Bridge Deck Protection." *82nd Annual Meeting of the*

Transportation Research Board Meeting Compendium of Papers, Transportation Research Board of the National Academies, Washington, DC.

Attanayake, U., Liang, X., Ng, S., and Aktan, H. (2006). "Penetrating Sealants for Concrete Bridge Decks—Selection Procedure." *Journal of Bridge Engineering*, 11(5), 533-540.

Azari, H., Nazarian, S., and Yuan, D. (2014). "Assessing Sensitivity of Impact Echo and Ultrasonic Surface Waves Methods for Nondestructive Evaluation of Concrete Structures." *Construction and Building Materials*, 71, 384-391.

Babaei, K., and Hawkins, N. M. (1987). "Evaluation of Bridge Deck Protective Strategies." NCHRP Report 297, National Research Council, Washington, DC.

Balakumaran, S. S. G, and Weyers, R. E. (2019). "Performance of Bridge Deck Overlays in Virginia: Phase II: Service Life Performance." Report No. VTRC 20-R6, Virginia Department of Transportation, Richmond, VA.

Barnes, C. L., and Trottier, J.-F. (2000). "Ground Penetrating Radar for Network Level Concrete Deck Repair Management." *ASCE Journal of Transportation Engineering*, 126(3).

Barnes, C. L., and Trottier, J.-F. (2004). "Effectiveness of Ground Penetrating Radar in Predicting Deck Repair Quantities," *Journal of Infrastructure Systems*, 10(2).

Barnes, R., and Zheng, T. (2008). "Research on Factors Affecting Concrete Cover Measurement," *The e-Journal of Nondestructive Testing, NDT.net*, New South Wales, Australia.

Bartholomew, P. D., Guthrie, W. S., and Mazzeo, B. A. (2012). "Vertical Impedance Measurements on Concrete Bridge Decks for Assessing Susceptibility of Reinforcing Steel to Corrosion." *Review of Scientific Instruments*, 83.

Barton, J., Baxter, J., Guthrie, W. S., and Mazzeo, B. A. (2019a). "Vertical Electrical Impedance Scanner for Nondestructive Concrete Bridge Deck Assessment without a Direct Rebar Connection." *Materials Evaluation*, 77(10), 1258-1266.

Barton, J., Baxter, J., Guthrie, W. S., and Mazzeo, B. A. (2019b). "Large-Area Electrode Design for Vertical Electrical Impedance Scanning of Concrete Bridge Decks." *Review of Scientific Instruments*, 90(025101), 1-10.

Baxter, J. S., Hendricks, L. J., Guthrie, W. S, and Mazzeo, B. A. (2020). "Instrumentation for Multi-Channel Vertical Electrical Impedance Scanning of Concrete Bridge Decks." *Engineering Research Express*, 2 035010.

Bentur, A., Diamond, S., and Berke, N. S. (1997). *Steel Corrosion in Concrete: Fundamentals and Civil Engineering Practice,* 1st Ed., E & FN Spon, London, United Kingdom.

Bentz, D. P. (2000). "Influence of Silica Fume on Diffusivity in Cement-Based Materials, II. Multi-Scale Modeling of Concrete Diffusivity." *Cement and Concrete Research*, 30(7), 1121-1129.

Bentz, D. P. (2007). "Prediction of a Chloride Ion Penetration Profile for a Concrete." National Institute of Standards and Technology, Gaithersburg, MD. <http://ciks.cbt.nist.gov/ ~bentz/clpen2.html> (July 29, 2020).

Bentz, D., Halleck, P., Grader, A., and Roberts, J. (2006). "Water Movement During Internal Curing: Direct Observation Using X-Ray Microtomography." *Concrete International*, 28(10), 39-45.

Bentz, D. P., Guthrie, W. S., Jones, S. Z., and Martys, N. S. (2014). "Predicting Service Life of Steel-Reinforced Concrete Exposed to Chlorides." *Concrete International*, 36(9), 55-64.

Bindal, V. N., Jain, S. K., Krishna Mohan Rao, P. S., Rao, M. V. B., and Chandra, S. (1996). "Design Considerations of Low Frequency Transducers for the NDT Testing of Concrete, Timber and Like Materials." In *Proceedings of the 14th World Conference on Non-Destructive Testing: Trends in NDE Science & Technology*, New Delhi, 4, 2053-2056.

Birdsall, A. W., Guthrie, W. S., and Bentz, D. P. (2007). "Effects of Initial Surface Treatment Timing on Chloride Concentrations in Concrete Bridge Decks." *Transportation Research Record: Journal of the Transportation Research Board,* No. 2028, Transportation Research Board of the National Academies, Washington, DC.

Bitnoff, A. C. (2014). “Internal Curing of Concrete Bridge Decks in Utah: Two-Year Update for Mountain View Corridor Project.” M.S. project report. Department of Civil and Environmental Engineering, Brigham Young University, Provo, UT.

Böhni, H. (2005). *Corrosion in Reinforced Concrete Structures*. Woodhead, Cambridge, England.

Bolen, W. P. (2016). *2014 Minerals Yearbook*. United States Geological Survey.

Brameshuber, I. W., and Raupach, I. M. (2003). “Nondestructive Determination of the Water-Content in the Concrete Cover Using the Multiring-Electrode.” In *Proceedings of the International Symposium of Non-Destructive Testing in Civil Engineering*, Berlin, Germany.

Bridge Preservation. (2016). “Bridge Deck Membrane Spray Applied Waterproofing.” *Bridge Preservation LLC*, <https://bridgepreservation.com/bridge-deck-membrane/ > (Sep. 10, 2019).

Broomfield, J. P. (1997). *Corrosion of Steel in Concrete—Understanding, Investigation and Repair*. E&FN Spon, New York, NY.

Bungey, J. H., and Millard, S. G. (1996). *Testing of Concrete in Structures*. Chapman and Hall, Cambridge, United Kingdom.

Buth, E., Furr, H. L., and Jones, H. L. (1972). “Evaluation of a Pre-Stressed Panel, Cast-in-Place Concrete Bridge.” Research Report 145-3. Texas Transportation Institute, Texas A&M University, College Station, TX.

Cady, P. D. and Renton, J. B. (1976). “Durability of Steel-Formed and Sealed Bridge Decks.” *Transportation Research Record: Journal of the Transportation Research Board*, No. 613, Transportation Research Board of the National Academies, Washington, DC.

Cain, R., Carkhuff, B, Pandolfini, P., and Weiskopf, F. (2003). “Smart Aggregate Sensor Suite for Bridge Deck Measurements – Phase 1.” Report No. MD-04-SP107B46, Maryland State Highway Administration, Baltimore, MD.

Carkhuff, B. and Cain, R. (2003). “Corrosion Sensors for Concrete Bridges.” *IEEE Instrumentation and Measurement Magazine*, 6(2).

Carrier, R. E., Pu, D. C., Cady, and P. D. (1975). “Moisture Distribution in Concrete Bridge Decks and Pavements.” *Durability of Concrete.* American Concrete Institute, Detroit, MI.

Carter, P. D. (1989). “Preventive Maintenance of Concrete Bridge Decks.” *Concrete International*, 11(11), 33-36.

Castro, J., Spragg, R., and Weiss, J. (2012). “Water Absorption and Electrical Conductivity for Internally Cured Mortars with a W/C Between 0.30 and 0.45.” *Journal of Materials in Civil Engineering*, 24(2), 223-231.

Cemex. (2013). “Proper Use of the Rebound Hammer: Updated to reflect the changes to ASTM C805.” <http://www.cemexusa.com/ProductsServices/files/TechnicalServices/Proper_Use_of_the_Rebound_Hammer.pdf> (May 18, 2017).

Ceylan, H., Gopalakrishnan, K., Taylor, P., Shrotriya, P., and Kim, S. (2011). “A Feasibility Study on Embedded Micro-Electromechanical Sensors and Systems (MEMS) for Monitoring Highway Structures.” Project 09-356, Iowa Department of Transportation, Cedar Rapids, IA.

Clark, M. R., McCann, D. M., and Forde, M. C. (2002). “Infrared Thermographic Analysis of Bridges.” *Transportation Research Record: Journal of the Transportation Research Board*, No. 1813, Transportation Research Board of the National Academies, Washington, DC.

CNS Farnell Limited. (2008). “RM MK II Concrete Resistivity Meter Model U95 Manual.” CNS Farnell Limited, Hertfordshire, England.

Concrete Sealer Reviews. (2014). “The Truth About Concrete Waterproofing.” <http://concretesealerreviews.com/the-truth-about-concrete-waterproofing/> (June 29, 2017).

Cuelho, E., and Stephens, J. (2013). "Investigation of Methacrylate Rehabilitation Strategy to Extend the Service Life of Concrete Bridge Decks." Report No. CA13-1723, California Department of Transportation, Sacramento, CA.

Culmo, M. P. (2011). "Accelerated Bridge Construction – Experience in Design, Fabrication and Erection of Prefabricated Bridge Elements and Systems." Report No. FHWA-HIF-12-013, Office of Bridge Technology, Federal Highway Administration, McLean, VA.

Cusson, D., Lounis, Z., and Daigle, L. (2010). "Benefits of Internal Curing on Service Life and Life Cycle Cost of High-Performance Concrete Bridge Decks: A Case Study." *Cement and Concrete Composites*, 32(5), 339-350.

De la Varga, I., Castro, J., Bentz, D., and Weiss, J. (2012). "Application of Internal Curing for Mixtures Containing High Volumes of Fly Ash." *Cement and Concrete Composites*, 34(9), 1001-1008.

Digital Concrete Scanning. (2020). "Concrete X-Ray." Digital Concrete Scanning Services, Alameda, CA. <http://www.digitalconcretescanning.com/services/xray/> (September 21, 2020).

Ehlen, M. A. (2018). "Life-365 Service Life Prediction Model and Computer Program for Predicting the Service Life and Life-Cycle Cost of Reinforced Concrete Exposed to Chlorides." Life-365 Consortium III. <http://www.life-365.org/download/Life-365_v2.2.3_Users_Manual.pdf> (May 28, 2020).

Elsener B. and Bohni, H. (1990). "Potential Mapping and Corrosion of Steel in Concrete." *Corrosion Rates of Steel in Concrete*, 143-156.

Elsener, B., Klinghoffer, O., Frølund, T., Rislund, E., Shiegg, Y., and Böhni, H. (1997). "Assessment of Reinforcement Corrosion by means of Galvanostatic Pulse Technique." In *Proceedings of International Conference on Repair of Concrete Structures—From Theory to Practice in a Marine Environment*, Svolvaer, Norway, 391-400.

Elsener, B. (2001). "Half-Cell Potential Mapping to Assess Repair Work on RC Structures." *Construction and Building Materials*, 15(3).

Eriksson, M. (2001). “Considerations when Paving Treated Timber Bridge Decks.” *IABSE Symposium Report*, 85(10), 23-28.

Fanous, F., Wu, H., and Pape, J. (2000). “Impact of Deck Cracking on Durability.” Center for Transportation Research Education, Iowa State University, Ames, IA.

FHWA (Federal Highway Administration). (2010). “Bridge Management Questionnaire Report.” Office of Asset Management, Washington, DC. <https://www.fhwa.dot.gov/bridge/management/bms.pdf> (October 9, 2019).

FHWA (Federal Highway Administration). (2015). “Galvanostatic Pulse Measurement (GPM).” Federal Highway Administration, U.S. Department of Transportation, Washington, DC. <https://fhwaapps.fhwa.dot.gov/ndep/DisplayTechnology.aspx?tech_id=11> (July 22, 2020).

FHWA (Federal Highway Administration). (2017). “Slide-in Bridge Construction.” Federal Highway Administration, U.S. Department of Transportation, Washington, DC. <https://www.fhwa.dot.gov/construction/sibc/about.cfm> (July 17, 2020).

FHWA (Federal Highway Administration). (2018). *Bridge Preservation Guide*. Publication No. FHWA-HIF-18-022, Federal Highway Administration, U.S. Department of Transportation, Washington, DC.

Filice, J. and Wong, J. (2001). “Best Practice Guidelines for Selecting Concrete Bridge Deck Sealers.” *Alberta Transportation and Utilities*.

Finch, R., Fischer, R., Grimes, M., Stits, R., and Watkins, W. A. (1998). “Acceptable Methods, Techniques, and Practices—Aircraft Inspection and Repair, Chapter 5, Section 5”. Report No. AC 43.13-1B. Federal Aviation Administration, U.S. Department of Transportation, Washington, DC.

Fortner, B. (2003). “Embedded Miniature Sensors Detect Chloride in Bridge Decks.” *Civil Engineering*, 73(6).

Fowler, J. R. (2006). “Accelerated Bridge Construction.” In *Conference of the Transportation Association of Canada: Bridges of the 21st Century Session*, Charlottetown, Prince Edward Island, Canada. <http://www.tac-atc.ca/english/resourcecentre/readingroom/conference/conf2006/docs/s008/Fowler.pdf> (November 17, 2015).

Frølund, T., Jensen, F. M., and Bassler, R. (2002). “Determination of Reinforcement Corrosion Rate by Means of the Galvanostatic Pulse Technique.” In *Proceedings of the First International Conference on Bridge Maintenance, Safety and Management*, Barcelona, Spain.

Frølund, T., Klinghoffer, O. and Sorensen, H. E. (2003). “Pro’s and Con’s of Half-Cell Potentials and Corrosion Rate Measurements.” *Structural Faults + Repairs*, London, England.

Gamidi, S. H. (2009). “Non Destructive Testing of Structures.” Indian Institute of Technology, Bombay, India.

GeoModel, Inc. (2014). “What is Ground Penetrating Radar.” <https://geomodel.com/methods/ground-penetrating-radar/> (May 28, 2020).

Germann Instruments. (2016). “GalvaPulse.” <http://germann.org/products-by-application/corrosion-rate/galvapulse> (May 28, 2020).

Germann Instruments. (2020). “MIRA.” <http://germann.org/products-by-application/flaw-detection/mira> (September 3, 2020).

Giatec. (2013). “Surf™ Concrete Surface Resistivity.” <https://www.giatecscientific.com/products/concrete-ndt-devices/surf-surface-resistivity/> (May 29, 2020).

Giatec. (2020). “BlueRock™ Wireless Temperature and Relative Humidity Sensor.” <https://www.giatecscientific.com/products/concrete-sensors/bluerock-humidity-temperature-meter/> (August 27, 2020).

Goodspeed, C. H., Vanikar, S., and Cook, R. (1996). “High-Performance Concrete Defined for Highway Structures.” *Concrete International*, 18(2).

Grace, N., Hanson, J., and Abdel-Messih, H. (2004). “Inspection and Deterioration of Bridge Decks Constructed Using Stay-in-Place Metal Forms and Epoxy-Coated Reinforcement.” Department of Civil Engineering, Lawrence Technological University, Southfield, MI.

Grover, R. and Jackson, D. (1996). “New Test Provides Quick Assessment of Bridge Conditions.” Publication No. FHWA-SA-96-045 (CS044). Federal Highway Administration, Washington, DC.

Gu, P., and Beaudoin, J. J. (1998). “Obtaining Effective Half-Cell Potential Measurements in Reinforced Concrete Structures.” Construction Technology Update No. 18. National Research Council of Canada, Ottawa, Ontario, Canada.

Gucunski, N., Antoljak, S., and Maher, A. (2000). “Seismic Methods in Post Construction Condition Monitoring of Bridge Decks.” *Use of Geophysical Methods in Construction*, No. 108.

Gucunski, N., Imani, A., Romero, F., Nazarian, S., Yuan, D., Wiggenhauser, H., Shokouhi, P., Taffe, A., and Kutrubes, D. (2013). “Nondestructive Testing to Identify Concrete Bridge Deck Deterioration.” SHRP2 Report S2-R06A-RR-1. Transportation Research Board, Washington, DC.

Guthrie, W. S., Baxter, J. S., and Mazzeo, B. A. (2018). “Vertical Electrical Impedance Testing of a Concrete Bridge Deck Using a Rolling Probe.” *NDT&E International*, 95, 65-71.

Guthrie, W. S., and De Leon, J. T. (2020). “Effects of Surface Treatments on National Bridge Inventory Condition Ratings for Concrete Bridge Decks in Utah.” Final Report. Utah Department of Transportation, Salt Lake City, UT.

Guthrie, W. S., Flannery, D. L., Baxter, J. S., and Mazzeo, B. A. (2014). “Demonstration of Vertical Impedance and Acoustic Impact-Echo Testing for Condition Assessment of a Concrete Bridge Deck with a Concrete Overlay and a Polymer Surface Treatment.” Utah Department of Transportation, Salt Lake City, UT.

Guthrie, W. S., Frost, S. L., Birdsall, A. W., Linford E. T., Ross, L. A., Crane, R. A., Eggett, D. L. (2006). “Effect of Stay-in-Place Metal Forms on Performance of Concrete Bridge

Decks." *Transportation Research Record: Journal of the Transportation Research Board*, No. 1958, Transportation Research Board of the National Academies, Washington, DC.

Guthrie, W. S., Hebdon, A. L., and Smith, E. D. S. (2020). "Evaluation of Concrete Bridge Decks Comprising Twisted Steel Micro Rebar." Final Report. Utah Department of Transportation Research Division, Salt Lake City, UT.

Guthrie, W. S., Larsen, J. L., Baxter, J. S., and Mazzeo, B. A. (2019a). "Automated Air-Coupled Impact-Echo Testing of a Concrete Bridge Deck from a Continuously Moving Platform." *Journal of Nondestructive Evaluation*, 38(32), 1-8.

Guthrie, W. S., and Mazzeo, B. A. (2015). "Vertical Impedance Testing for Assessing Protection from Chloride-Based Deicing Salts Provided by an Asphalt Overlay System on a Concrete Bridge Deck." In *Proceedings of the American Society of Civil Engineers Sixteenth International Conference on Cold Regions Engineering*. (CD-ROM.) Salt Lake City, UT.

Guthrie, W. S., Nelsen, T., and Ross, L. A. (2005). "Performance of Concrete Bridge Deck Surface Treatments." Report No. UT-05.05. Utah Department of Transportation Research Division, Salt Lake City, UT.

Guthrie, W. S., Nolan, C. D., and Bentz, D. P. (2011). "Effect of Initial Scarification and Overlay Treatment Timing on Chloride Concentrations in Concrete Bridge Decks." *Transportation Research Record: Journal of the Transportation Research Board*, No. 2728, Transportation Research Board of the National Academies, Washington, DC.

Guthrie, W. S., and Tuttle, R. S. (2006). "Condition Analysis of Concrete Bridge Decks in Utah." Report No. UT-06.01. Utah Department of Transportation Research Division, Salt Lake City, UT.

Guthrie, W. S., Waters, T., Baxter, J. S., Hendricks, L., and Mazzeo, B. A. (2019b). "New Tools for Evaluating Concrete Bridge Decks: High-Speed Acoustic Impact-Echo and Vertical

Electrical Impedance Testing of Utah's Longest Bridge Deck." In *Proceedings of the Bridge Engineering Institute Conference*, Honolulu, HI.

Guthrie, W. S., Waters, T., and Reese, G. B. (2015). "Comparison of Moisture Content and Electrical Conductivity of Lightweight and Normal-Weight Concrete Bridge Decks: Instrumentation and Monitoring." In *Proceedings of the American Society of Civil Engineers Sixteenth International Conference on Cold Regions Engineering*. (CD-ROM.) Salt Lake City, UT.

Guthrie, W. S., and Yaede, J. M. (2013). "Internal Curing of Concrete Bridge Decks in Utah: Preliminary Evaluation." *Transportation Research Record: Journal of the Transportation Research Board*, No. 2342, Transportation Research Board of the National Academies, Washington, DC, 212-128.

Guthrie, W. S., and Yaede, J. M. (2014). "Evolution of Early-Age Cracking in Concrete Bridge Decks Incorporating Pre-Stressed Concrete Panels and Internally Cured Concrete." In *Transportation Research Board 93rd Annual Meeting Compendium of Papers*, Transportation Research Board of the National Academies, Washington, DC.

Hansson, C. M., Poursaee, A., and Laurent, A. (2006). "Macrocell and Microcell Corrosion of Steel in Ordinary Portland Cement and High Performance Concretes." *Cement and Concrete Research*, 36(11).

Hasan, H. O., Ramirez, J. A., and Cleary. D. B. (1995). "Indiana Evaluates Epoxy-Coated Steel Reinforcement." *Better Roads*, 65(5).

Hayes, C. (1998). "The ABC's of Nondestructive Weld Examination: Liquid Penetrant Inspection." *NDTnet*, 3(6).

Hebdon, A. L., Smith, E. D. S., and Guthrie, W. S. (2020). "Mitigation of Cracking in Concrete Bridge Decks Using Twisted Steel Micro-Rebar. In *Proceedings of Intermountain Engineering, Technology, and Computing (I-ETC) Conference*, Orem, UT.

Hema, J. H., Guthrie, W. S., and Fonseca, F. S. (2004). “Concrete Bridge Deck Condition Assessment and Improvement Strategies.” Report No. UT-04.16. Utah Department of Transportation Research Division, Salt Lake City, UT.

Henderson, M. E., Dion, G. N., and Costley, R. D. (1999). “Acoustic Inspection of Concrete Bridge Decks.” *SPIE Conference on Nondestructive Evaluation of Bridges and Highways III*, Newport Beach, CA, 219-227.

Hoki, J. R. (2011). “Analysis of Selected Factors Affecting Concrete Cover Measurements on Bridge Decks.” M.S. thesis. Department of Civil and Environmental Engineering, Brigham Young University, Provo, UT.

Hope, B. B., and Ip, A. K. (1985). “Corrosion and Electrical Impedance in Concrete.” *Cement and Concrete Research*, 15(3), 525-534.

Huang, Y. (2004). *Pavement Analysis and Design,* Second Edition. Prentice Hall, Upper Saddle River, NJ.

Hudson, S. W., Carmichael, R. F. III, Moser, L.O., Hudson, W.R., and Wilkes, W. J. (1987). “Bridge Management Systems.” *Transportation Research Record: Journal of the Transportation Research Board*, No. 300, Transportation Research Board of the National Academies, Washington, DC.

Hugenschmidt, J., and Mastrangelo, R. (2006). “GPR Inspection of Concrete Bridges.” *Cement & Concrete Composites*, 28, 384-392.

IAEA (International Atomic Energy Agency). (2002). *Guidebook on Non-Destructive Testing of Concrete Structures*. International Atomic Energy Agency, Vienna, Austria.

Impact-Echo Instruments. (2004). “The Impact-Echo Method.” *Impact-Echo Instruments, LLC*, <http://www.impact-echo.com/Impact-Echo/impact.htm> (November 27, 2019).

Ismail, M., and Ohtsu, M. (2006). “Corrosion Rate of Ordinary and High-Performance Concrete Subjected to Chloride Attack by AC Impedance Spectroscopy.” *Construction and Building Materials*, 20(7), 458-469.

Ismail, M. E., and Soleymani, H. R. (2002). "Monitoring Corrosion Rate for Ordinary Portland Concrete (OPC) and High-Performance Concrete (HPC) Specimens Subjected to Chloride Attack." *Canadian Journal of Civil Engineering*, 29.

James Instruments, Inc. (2004). "RM-8000 Resistivity Meter Instruction Manual." James Instruments, Inc., Chicago IL.

James Instruments Inc. (2010). "James Concrete Test Hammers." James Instruments, Inc., Chicago IL.

Khazanovich, L., and Hoegh, K. (2016). "Quantitative Ultrasonic Evaluation of Concrete Structures Using One-Sided Access." In *AIP Conference Proceedings: 42nd Annual Review of Progress in Quantitative Nondestructive Evaluation*, Minneapolis, MN.

Kee S., and N. Gucunski. (2016). "Interpretation of Flexural Vibration Modes from Impact-Echo Testing." *Journal of Infrastructure Systems*, 22(3), 1-10.

Kepler, J., Darwin, D., and Locke, C. (2000). "Evaluation of Corrosion Protection Methods for Reinforced Concrete Highway Structures." SM Report No. 58. University of Kansas Center for Research, Inc., Lawrence, KS.

Kosmatka, S. H. and Panarese, W. C. (1988). *Design and Control of Concrete Mixtures*, Thirteenth Edition. Portland Cement Association, Skokie, IL.

Krauss, P. D., McDonald, D. B., and Sherman, M. R. (1996). "Corrosion Investigation of Four Bridges Built between 1973 and 1978 Containing Epoxy-Coated Reinforcing Steel." Report No. MN/RC-96/25. Minnesota Department of Transportation, St. Paul, MN.

Larsen, J. L., McElderry, J., Guthrie, W. S., and Mazzeo, B. A. (2020). "Automated Sounding for Concrete Bridge Deck Inspection through a Multi-Channel, Continuously Moving Platform." *NDT&E International*, 109.

Larson, B. (2002). "Study of the Factors Affecting the Sensitivity of Liquid Penetrant Inspections: Review of Literature Published from 1970 to 1998." Report No.

DOT/FAA/AR-01/95. US Department of Transportation Federal Aviation Administration, Washington, DC.

Liang, Y., Gallaher, B., and Xi, Y. (2014). "Evaluation of Bridge Deck Sealers." Report No. CDOT-2014-6. Colorado Department of Transportation, Denver, CO.

Malhotra, V. M. (1976). *Testing Hardened Concrete: Nondestructive Methods*. American Concrete Institute, Detroit, MI.

Malhotra, V. M., and Carino, N. J. (1991). *Handbook on Nondestructive Testing of Concrete.* CRC Press, Inc., Boca Raton, FL.

Manning, D. G. (1985). "Detecting Defects and Deterioration in Highway Structures." NCHRP Report 118, National Research Council, Washington, DC.

Manning, D. G. (1995). "Waterproofing Membranes for Concrete Bridge Decks." NCHRP Report 220, National Research Council, Washington, DC.

Marcotte, T. D., and Hansson, C. M. (2003). "The Influence of Silica Fume on the Corrosion Resistance of Steel in High Performance Concrete Exposed to Simulated Sea Water." *Journal of Materials Science*, 38(23).

Maser, K. R., and Rawson, A. (1992). "Network Bridge Deck Surveys Using High Speed Radar: Case Studies of 44 Decks (Abridgement)." *Transportation Research Record: Journal of the Transportation Research Board*, No. 1347, Transportation Research Board of the National Academies, Washington, DC.

Maser, K. R., Tabrizi, K., and Gangi, V. (2001). "Use of Nondestructive Methods for Large Scale Bridge Deck Evaluation." In *Proceedings of the Second International Symposium on Maintenance and Rehabilitation of Pavements and Technological Control*, Auburn, AL.

Mauch, M., and Madanat, S. (2001). "Semiparametric Hazard Rate Models of Reinforced Concrete Bridge Deck Deterioration." *Journal of Infrastructure Systems*, 7(2).

Mays, G. C. (1992). *Durability of Concrete Structures: Investigation, Repair, Inspection.* E& FN Spon, London, England.

Mazzeo, B. M., and Guthrie, W. S. (2019). "Vertical Electrical Impedance Scanner for Concrete Bridge Deck Assessment without Direct Rebar Attachment." NCHRP-IDEA 202, Transportation Research Board, Washington, DC.

McGettigan, E. (1992). "Silicon-Based Weatherproofing Materials." *Concrete International*, 14(6), 52-56.

McGormley, J. C., Rende, N. S., and Krauss, P. D. (2013). "Nondestructive Evaluation and Assessment of Concrete Barriers for Defects and Corrosion." Report No. BARR-010. Iowa Department of Transportation, Ames, IA.

Medeiros, D. (2010). "Accelerated Bridge Construction = Lower Cost." Expanded Shale, Clay, and Slate Institute, Chicago, IL.

Medlock, R., Hyzak, M., and Wolf, L. (2001). "Innovative Prefabrication in Texas Bridges." <ftp://ftp.dot.state.tx.us/pub/txdot-info/library/pubs/bus/bridge/innovative_prefab.pdf> (November 17, 2015).

Melhem, H. G., and Cheng, Y. (2003). "Prediction of Remaining Service Life of Bridge Decks Using Machine Learning." *Journal of Computing in Civil Engineering*, 17(1).

Meter Group. (2017). "Advanced Soil Moisture + Temperature." <https://www.metergroup.com/environment/products/teros-11/> (October 10, 2019).

Mindess, S., Young, J. F., and Darwin, D. (2003). *Concrete*, Second Edition. Prentice Hall, Upper Saddle River, NJ.

Mitchell, T. (1987). "Improved Method for Measuring the Chloride Permeability of Concrete." *TR News*, No. 130.

Monfore, G. E. (1968). "The Electrical Resistivity of Concrete." *Journal of the PCA Research and Development Laboratories*, 10(2).

Montgomery, S. R. (2014). “Development of a Chloride Concentration Sampling Protocol for Concrete Bridge Decks.” M.S. thesis. Department of Civil and Environmental Engineering, Brigham Young University, Provo, UT.

Moore M., Phares, B., Graybeal, B., Rolander, D., and Washer, G. (2001). “Reliability of Visual Inspection for Highway Bridges Volume 1: Final Report,” Report No. FHWA-RD-01-020. Federal Highway Administration, Washington, DC.

Moore, W. (1975) “Detection of Bridge Deck Deterioration.” *Highway Research Record*, No. 451, National Research Council, Washington, DC.

Morris, W., Moreno, E. I., and Sagüés, A. A. (1996). “Practical Evaluation of Resistivity of Concrete in Test Cylinders Using a Wenner Array Probe.” *Cement and Concrete Research*, 26(12).

Nazarian, S. (2005). “Use of Active Sensors for Health Monitoring of Transportation Infrastructure.” *Sensing Issues in Civil Structural Health Monitoring,* 229-238.

Nazarian, S., Yuan, D., and Barker, M. (1995). “Rapid Determination of Pavement Moduli with Spectral-Analysis-of-Surface-Waves Method.” Report No. 1243-1. Center for Geotechnical and Highway Materials Research, University of Texas at El Paso, El Paso, TX.

Newman, J., and Choo, B. S. (2003). *Advanced Concrete Technology.* Butterworth-Heinemann, Oxford, United Kingdom.

Nolan, C. D. (2008). “Effect of Initial Scarification and Overlay Treatment Timing on Chloride Concentrations in Concrete Bridge Decks.” M.S. thesis. Department of Civil and Environmental Engineering, Brigham Young University, Provo, UT.

NEA (Nuclear Energy Agency). (2002). “Electrochemical Techniques to Detect Corrosion in Concrete Structures in Nuclear Installations.” Technical Note NEA/CSI/R(2002)21. Nuclear Energy Agency, Paris, France.

Nykänen, S., Uotila, J., Äijälä, M., Laaksonen, A., and Guthrie, W. S. (2013). "Special Inspections and Rehabilitation of Concrete Bridges in Finland." In *Proceedings of the 10th International Symposium on Cold Regions Development*, Anchorage, AK.

O'Connell, J. (1995). "Design Guidelines for the Use of Penetrating and Coating Type Sealers for Concrete." New York State Department of Transportation, Albany, NY.

O'Donohue, M., Garret, R., Datta, V. J., and Peer, L. (1998). "Penetrating Sealers: A Comparison of Epoxy, Moisture-Cured Urethane, and Siloxane Technology on Concrete, Rust, and an Inorganic Zinc Coating." *Journal of Protective Coatings & Linings*, 15.

Oh, T. K. (2012). "Defect characterization in concrete elements using vibration analysis and imaging." Ph.D. dissertation. Department of Civil Engineering, University of Illinois at Urbana-Champaign, Urbana, IL.

Olson Instruments. (2015). "Verify Concrete Slab Thickness and Integrity: CTG-2." Olson Instruments, Wheat Ridge, CO.

Page, C. and Sergi, G. (2000). "Developments in Cathodic Protection Applied to Reinforced Concrete." *Journal of Materials in Civil Engineering*, 12(1), 8-15.

Paul, J. (1998). "Extending the Life of Concrete Repairs." *Concrete International*, 20(3), 62-66.

Penetradar Corporation. (2017). "Technical Services—Bridge Deck Inspection." <http://penetradar.com/new/?page_id=359> (May 29, 2020).

Pinkerton, T. (2007). "Sensitivity of Half-Cell Potential Measurements to Properties of Concrete Bridge Decks." M.S. thesis. Department of Civil and Environmental Engineering, Brigham Young University, Provo, UT.

Poole, A. B., and Sims, I. (2016). *Concrete Petrography: A Handbook of Investigative Techniques*. CRC Press, Boca Raton, FL.

Popovics, J. (2010). “Investigation of a Full-Lane Acoustic Scanning Method for Bridge Deck Nondestructive Evaluation.” Highway IDEA Project 134, Transportation Research Board of the National Academies, Washington, DC.

Precast/Prestressed Concrete Institute. (1987). “Precast Prestressed Concrete Bridge Deck Panels.” Special Report. Precast/Prestressed Concrete Institute, Chicago, IL. <http://www.pci.org/view_file.cfm?file=JL-87-MARCH-APRIL-3.pdf> (August 1, 2013).

Pullar-Strecker, P. (2002). *Concrete Reinforcement Corrosion*. Thomas Telford Publishing, Heron Quay, London, United Kingdom.

Ramey, G. E., and Derickson, J. P. (2003). “Performance of Bonded Bridge Deck Overlays in Alabama.” *Practical Periodical on Structural Design and Construction*, 8(1).

Rehman, S. K. U., Ibrahim, Z., Memon, S. A., and Jameel, M. (2015). “Nondestructive Test Methods for Concrete Bridges: A Review.” *Construction and Building Materials*, 107, 58-86.

Robison, T. W., and Tanner J. E. (2012). “Bridge Deck Evaluation Using Nondestructive Test Methods.” Report No. FHWA-WY-10/07F. Wyoming Department of Transportation, Cheyenne, WY.

Roper, E. A. (2018). “Chloride Concentration and Blow-Through Analysis for Concrete Bridge Decks Rehabilitated Using Hydro-Demolition.” M.S. thesis. Department of Civil and Environmental Engineering, Brigham Young University, Provo, UT.

Ruohonen, D. (2013). “Infrared & Visible Bridge Scoping.” *Modern Contractor Solutions*, <https://mcsmag.com/infrared-visible-bridge-scoping/> (May 8, 2020).

Russell, H. G. (2012). “Waterproofing Membranes for Concrete Bridge Decks.” NCHRP Report 425, National Research Council, Washington, DC.

Rutgers. (2018). “RABIT Autonomous Bridge Deck Inspection Tool.” <https://cait.rutgers.edu/facilities-equipment/rabit-autonomous-bridge-deck-inspection-tool/> (October 23, 2019).

Saarenketo, T. and Soderqvist, M. K. (1994). “Ground Penetrating Radar Applications for Bridge Deck Evaluations in Finland.” *Insight*, 36(7).

Saleem, M., Shameem, M., Hussain, S. E., and Maslehuddin M. (1996). “Effect of Moisture, Chloride and Sulphate Contamination on the Electrical Resistivity of Portland Cement Concrete.” *Construction and Building Materials*, 10(3), 209-214.

Samson, E. (2014). “Stadium Software Overview.” <http://cementbarriers.org/wordpress/wp-content/uploads/2014/09/STADIUM-Overview-Durability-of-Concrete-Structures.pdf> (May 28, 2020).

Sanford, K. A. (2008). “Evaluation of Strength and Stiffness of Acrylic-Modified Mortar for Village of Hope Construction.” M.S. project report. Department of Civil and Environmental Engineering, Brigham Young University, Provo, UT.

Sansalone, M., and Carino, N. J. (1989). “Detecting Delaminations in Concrete Slabs with and without Overlays Using the Impact-Echo Method.” *ACI Materials Journal*, 86(2).

Sathiyanarayanan, S., Natarajan, P., Saravanan, K., Srinivasan, S., Venkatachari, G. (2006). “Corrosion Monitoring of Steel in Concrete by Galvanostatic Pulse Technique.” *Cement and Concrete Composites*, 28(7), 6330-637.

Scott, M., Rezaizadeh, A., Delahaza, A., Santos, C. G., Moore, M., Graybeal, B., and Washer, G. (2003). “A Comparison of Nondestructive Evaluation Methods for Bridge Deck Assessment.” *NDT&E International*, 36(6), 245-255.

Sengul, O., and Gjorv, O. (2009). “Effect of Embedded Steel on Electrical Resistivity Measurements on Concrete Structures.” *ACI Materials Journal*, 106.

Sharma, P. V. (1997) *Environmental and Engineering Geophysics*. Cambridge Printing Press, Cambridge, United Kingdom.

Shin, H. and Grivas, D. A. (2003). "How Accurate is Ground Penetrating Radar (GPR) for Bridge Deck Condition Assessment?" *Transportation Research Record: Journal of the Transportation Research Board*, No. 1845, Transportation Research Board of the National Academies, Washington, DC.

Shohet, I. M., Wang, C., and Warszawski, A. (2002). "Automated Sensor-Driven Mapping of Reinforcement Bars," *Automation in Construction*, 11.

Shubinsky, G. (1994). "Visual and Infrared Imaging for Bridge Inspection." Northwestern University Basic Industrial Research Laboratory, Evanston, IL.

SIMCO Technologies. (undated). "STADIUM® Overview." *SIMCO Technologies*, <https://www.simcotechnologies.com/what-we-do/stadium-technology-portfolio/stadium-overview/> (May 28, 2020).

Smith, A. (2016). "Correlation of Laboratory and Field Friction Measurements to Optimize Utilization of Bituminous Surface Aggregates." Report No. UT-16.03. Utah Department of Transportation Research Division, Salt Lake City, UT.

Smith, A. B., Knighton, J. T., and Guthrie, W. S. (2016). "A Statistical Analysis of Network-Level Skid Numbers for Asphalt Pavement Surfaces in Utah." In *95th Annual Meeting of the Transportation Research Board Meeting Compendium of Papers*, Transportation Research Board of the National Academies, Washington, DC.

Snell, L. M., Rutledge, R. B., and Wallace, N. D. (1985). "Reinforcement Locations in Masonry Reinforcement," In *Proceedings of the Third North American Masonry Conference*, Masonry Society, Denver, CO.

So, H. S., and Millard, S. G. (2007). "On-Site Measurements on Corrosion Rate of Steel in Reinforced Concrete." *ACI Materials Journal*, 104(6), 638-642.

Song, H. W., and Saraswathy, V. (2007). "Corrosion Monitoring of Reinforced Concrete Structures A Review." *International Journal of Electrochemical Science*, 2.

Spraggs, K. R., Sneed, L. H., Belarbi, A., and Anderson, N. L. (2012) “Field Investigation of Spalling in Partial-Depth Precast Concrete Bridge Decks Using Nondestructive Testing.” *PCI Journal*, Spring 2012, 80-93.

Sprinkel, M., Sellars, A., and Weyers, R. (1993). “Rapid Concrete Bridge Deck Protection, Repair, and Rehabilitation”. Report No. SHRP-S-344. National Research Council, Washington, DC.

Sprinkel, M. M. (1998). “High Early Strength Latex Modified Concrete Overlay.” *Transportation Research Record: Journal of the Transportation Research Board*, No. 1204, Transportation Research Board of the National Academies, Washington, DC.

Sprinkel, M. M. (1999). “Very-Early-Strength Latex-Modified Concrete Overlay.” *Transportation Research Record: Journal of the Transportation Research Board*, No. 1668, Transportation Research Board of the National Academies, Washington, DC.

Sprinkel, M. M. (2003). “Deck Protection Systems for Post Tensioned Segmental Concrete Bridges.” American Segmental Bridge Institute, Phoenix, AZ.

Stanish, K. D., Hooton, R. D., and Thomas, M. D. A. (2004). “Testing the Chloride Penetration Resistance of Concrete: A Literature Review.” Department of Civil Engineering, University of Toronto, Toronto, Ontario, Canada.

Stenko, M. S., and Chawalwala, A. J. (2001). “Thin Polysulfide Epoxy Bridge Deck Overlays.” *Transportation Research Record: Journal of the Transportation Research Board*, No. 1749, Transportation Research Board of the National Academies, Washington, DC.

Stevens, R. J., and Guthrie, W. S. (2020). “Polyester Polymer Concrete for Bridge Deck Overlays.” Final Report. Utah Department of Transportation Research Division, Salt Lake City, UT.

Stratfull, R. F. (1973a). “Corrosion Autopsy of a Structurally Unsound Bridge Deck.” *Highway Research Record*, No. 433, National Research Council, Washington, DC.

Stratfull, R. F. (1973b). “Half-Cell Potentials and the Corrosion of Steel in Concrete.” *Highway Research Record 433*, No. 433, National Research Council, Washington, DC.

Stratfull, R. F., Jurkovich, W. J., and Spellman. D. L. (1975). “Corrosion Testing of Bridge Decks.” *Transportation Research Record: Journal of the Transportation Research Board*, No. 539, Transportation Research Board of the National Academies, Washington, DC.

Sumsion, E. (2013). “Condition Assessment of Decommissioned Bridge Decks Treated with Waterproofing Membranes and Asphalt Overlays. M.S. thesis. Department of Civil and Environmental Engineering, Brigham Young University, Provo, UT.

Sun, Z. (2004). “Evaluation of Concrete Bridge Deck Overlays.” M.S. thesis. Department of Civil and Environmental Engineering, West Virginia University, Morgantown, West Virginia.

Swamy, R. N., and Tanikawa, S. (1993). “An External Surface Coating to Protect Concrete and Steel from Aggressive Environments.” *Materials and Structures*, 26(162).

Tabatabai, H., Sobolev, K., Ghorbanpoor, A., Lee, C., and Lind, M. (2016). “Evaluation of Thin Polymer Overlays for Bridge Decks.” Report No. 0092-12-06. Department of Civil and Environmental Engineering, University of Wisconsin-Milwaukee, Milwaukee, WI.

Tam, C. T. (1977). “Orthogonal Detection Techniques for Determination and Cover of Embedded Reinforcement,” *Journal of the Institute of Engineers*, Malaysia, 22.

Tinkey, Y., Olson, L. D., Miller, P. K., and Tanner, P. K. (2011). “Vehicle-mounted bridge deck scanner.” <http://www.olsoninstruments.com/newsletter_June2011/site/pdf_downloads/TRB%202011%20VehicleMounted-BridgeDeckScanner_LDO.pdf> (November 18, 2019).

Tuttle, R. S. (2005). “Condition Analysis of Concrete Bridge Decks in Utah.” M.S. thesis. Department of Civil and Environmental Engineering, Brigham Young University, Provo, Utah.

UDOT (Utah Department of Transportation). (2017). “Bridge Management Manual.” <https://www.udot.utah.gov/main/uconowner.gf?n=35942524323318753> (May 29, 2020).

USDOT (United States Department of Transportation). (1995). “Recording and Coding Guide for the Structure Inventory and Appraisal of the Nation’s Bridges.” Report No. FHWA-PD-96-001. Federal Highway Administration, Washington DC.

Violetta, B. (2002). “Life-365 Service Life Prediction Model.” *Concrete International*, 24(12), 53-67.

Wambold, J. C., Meyer, W. E., and Henry, J. J. (1990). “New-Generation Skid Testers for the 1990s.” *Surface Characteristics of Roadways: International Research and Technologies*, American Society for Testing and Materials, Philadelphia, PA, 138-153.

Washer, G., N. Bolleni, and R. Fenwick. (2010). “Thermographic Imaging of Subsurface Deterioration in Concrete Bridges.” *Transportation Research Record: Journal of the Transportation Research Board*, No. 2201, Transportation Research Board of the National Academies, Washington, DC, 27-33.

Watters, D. (2003). “Wireless Sensors Will Monitor Bridge Decks.” *Better Roads*, 73(2).

Watters, D. G., Bahr, A. J., Jayaweera, P., and Huestis, D. L. (2003). “SMART PEBBLES™: Passive Embeddable Wireless Sensors for Chloride Ingress Monitoring in Bridge Decks.” Report No. FHWA/CA/TL-2003/07. SRI International, Menlo Park, CA.

Wenzlick, J. D. (2002). “Hydrodemolition and Repair of Bridge Decks.” Report No. RDT02-002, Missouri Department of Transportation, Jefferson City, MO.

Weyers, R. E., Fitch, M. G., Larsen, E. P., Al-Qadi, I. L., Chamberlin, W. P., Hoffman, P. C. (1994). “Concrete Bridge Protection and Rehabilitation: Chemical and Physical Techniques.” Report No. SHRP-S-668. National Research Council, Washington, DC.

Weyers, R. E., Prowell, B. D., Sprinkel, M. M., and Vorster, M. (1993). “Concrete Bridge Protection, Repair, and Rehabilitation Relative to Reinforcement Corrosion: A Methods

Application Manual." Report No. SHRP-S-360. National Research Council, Washington, DC.

Whiting, D. A., and Naji, M. A. (2003). "Electrical Resistivity of Concrete—A Literature Review." *PCA R&D*, No. 2457, Portland Cement Association, Skokie, IL.

Wilson, K., Jawed, M., Ngala, V. (2013). "The Selection and Use of Cathodic Protection Systems for the Repair of Reinforced Concrete Structures." *Construction and Building Materials*, 39, 19-25.

Xi, Y., and Bazant, Z. P. (1999). "Modeling Chloride Penetration in Saturated Concrete." *Journal of Materials in Civil Engineering*, 11(1).

APPENDIX A: BRIDGE DECK SCHEMATICS

Figures A-1 to A-15 show schematics of each bridge deck, including testing locations.

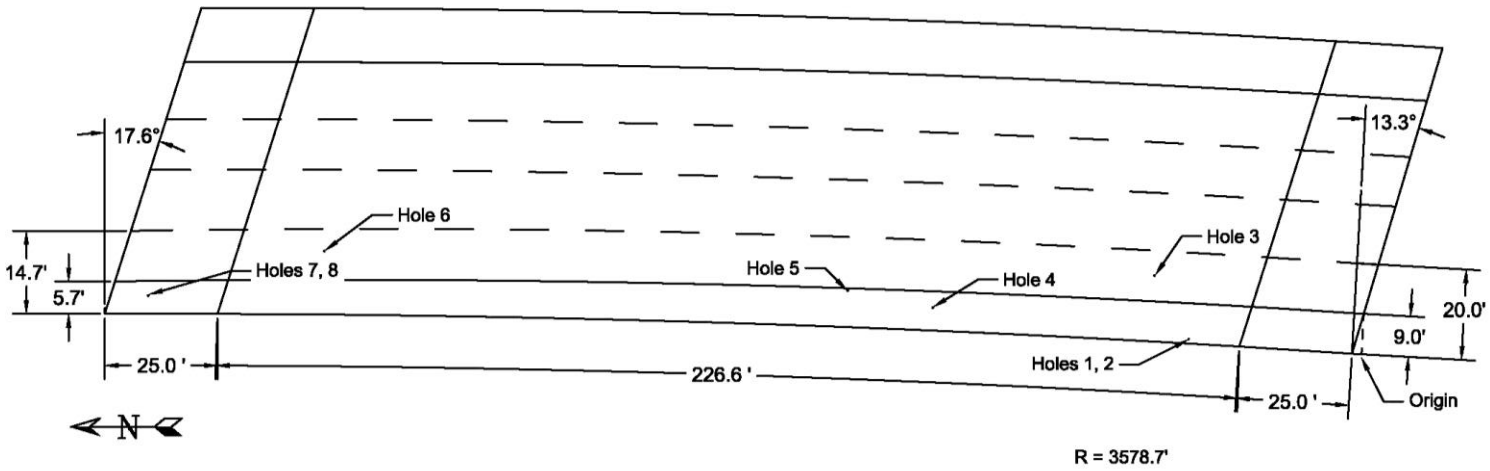

Figure A-1 Test locations for bridge C-460.

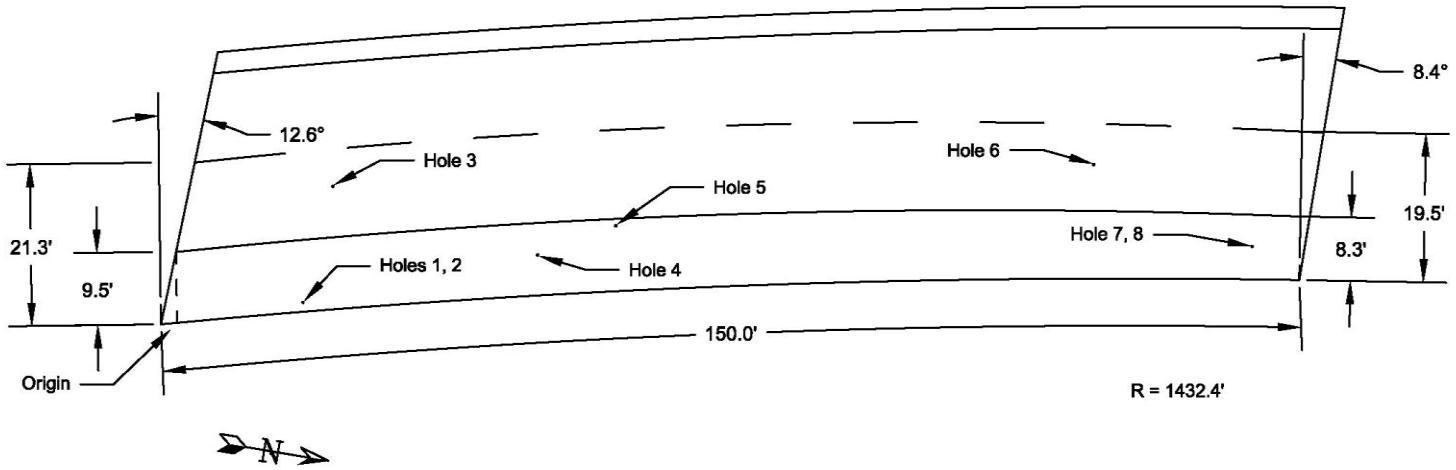

Figure A-2 Test locations for bridge C-698.

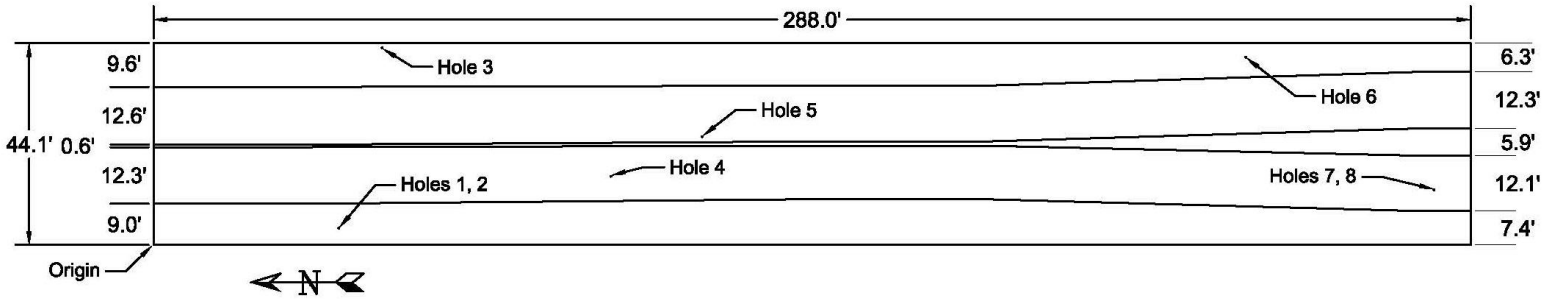

Figure A-3 Test locations for bridge C-725.

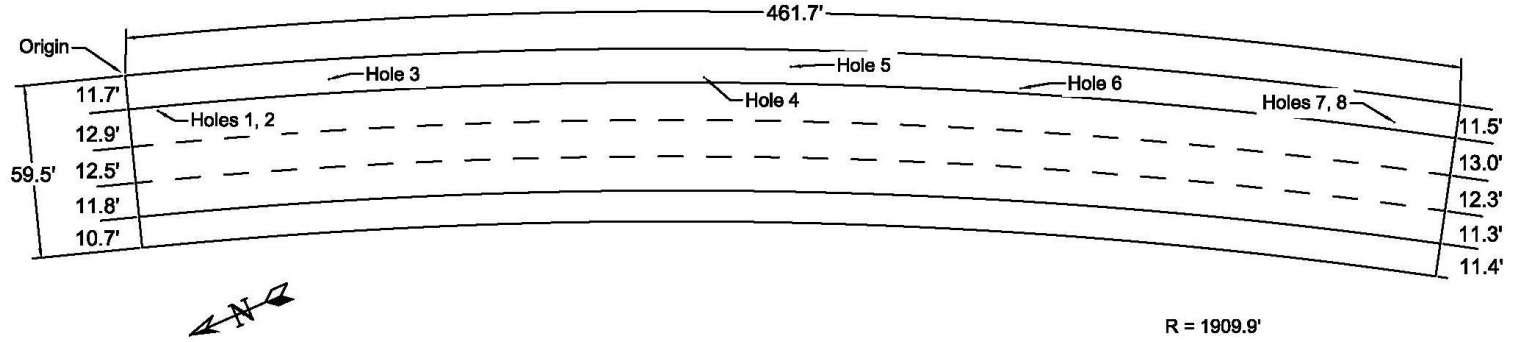

Figure A-4 Test locations for bridge C-757.

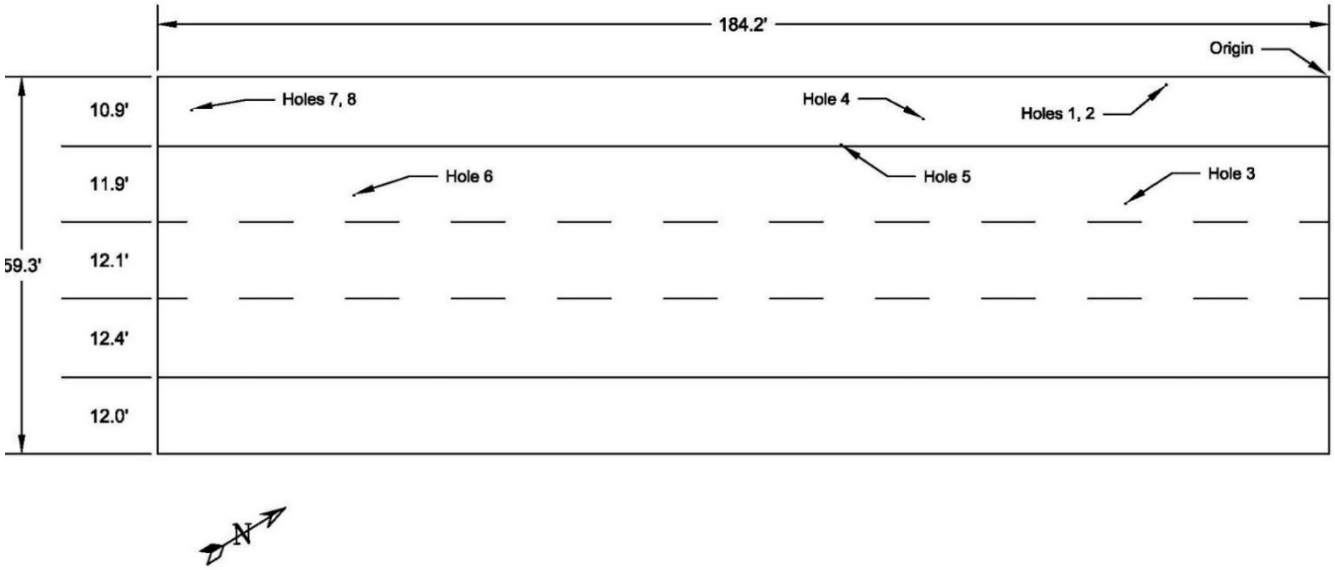

Figure A-5 Test locations for bridge C-759.

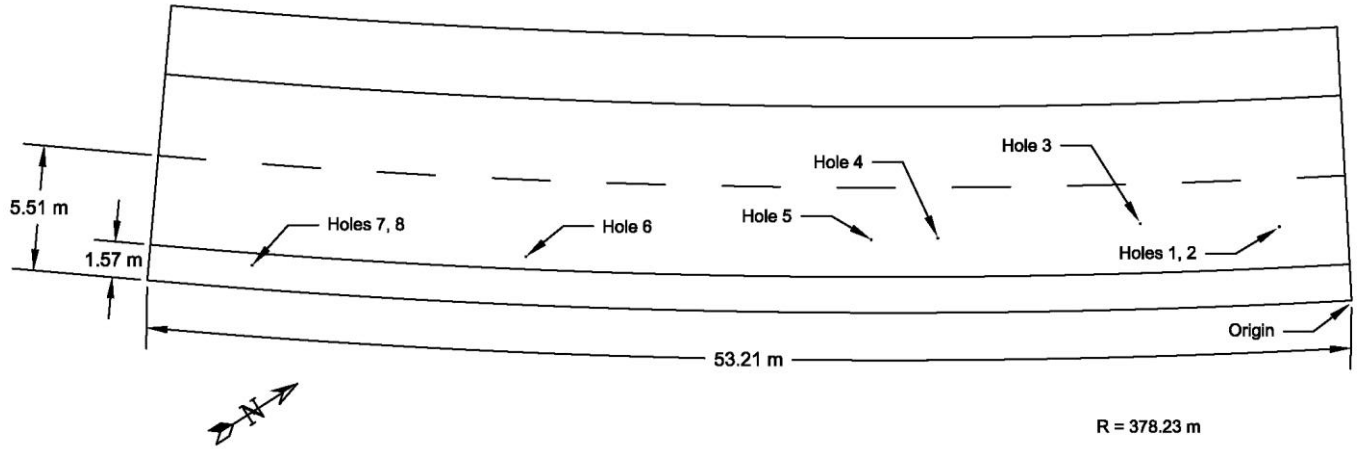

Figure A-6 Test locations for bridge C-760.

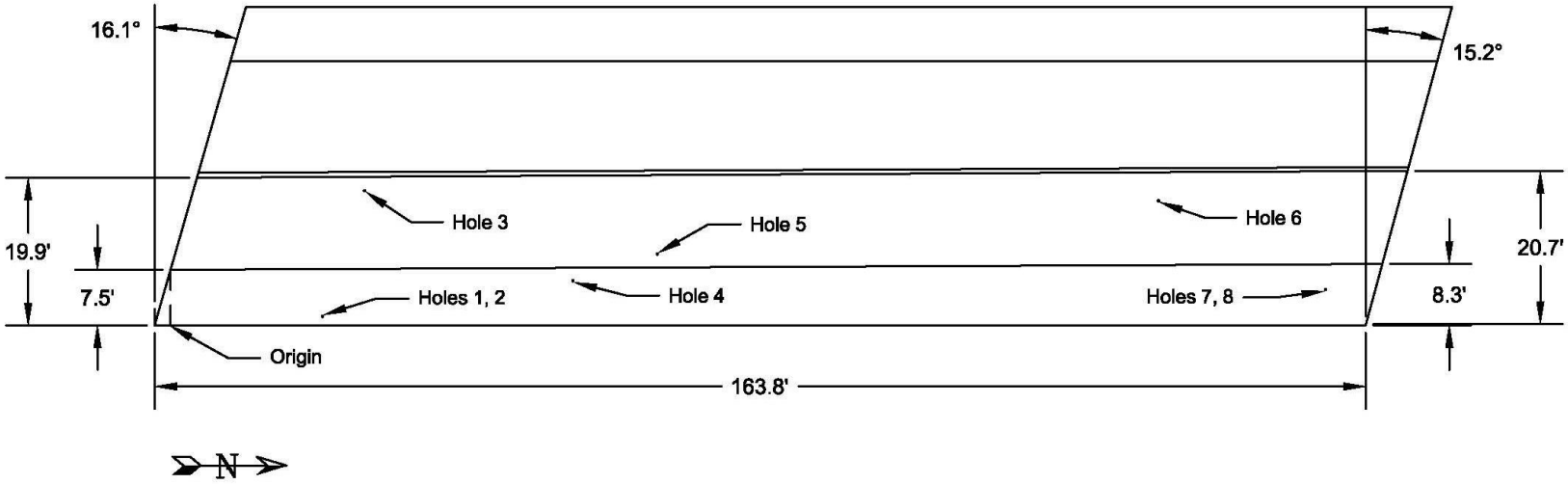

Figure A-7 Test locations for bridge C-794.

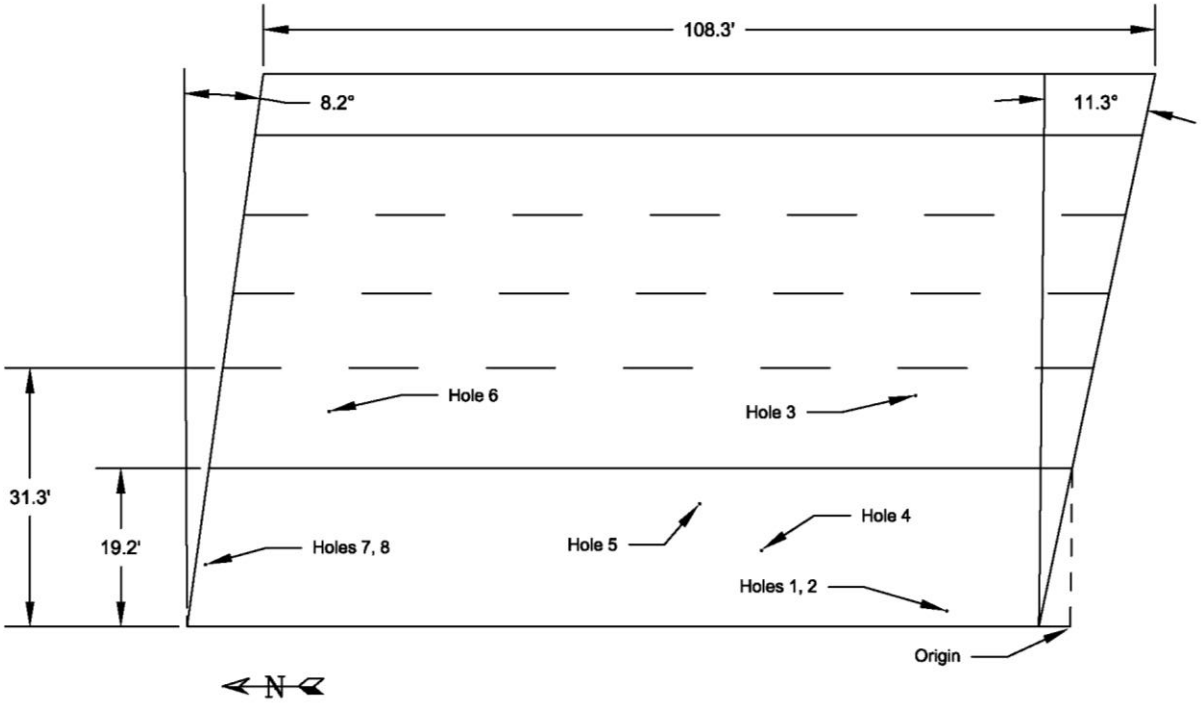

Figure A-8 Test locations for bridge C-931.

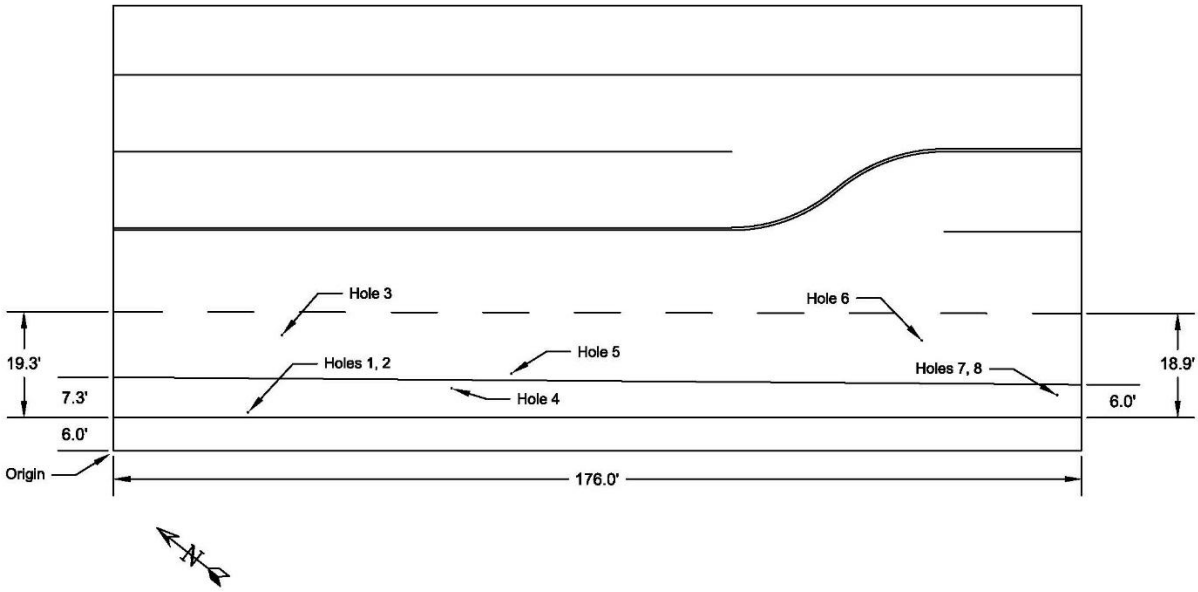

Figure A-9 Test locations for bridge C-953.

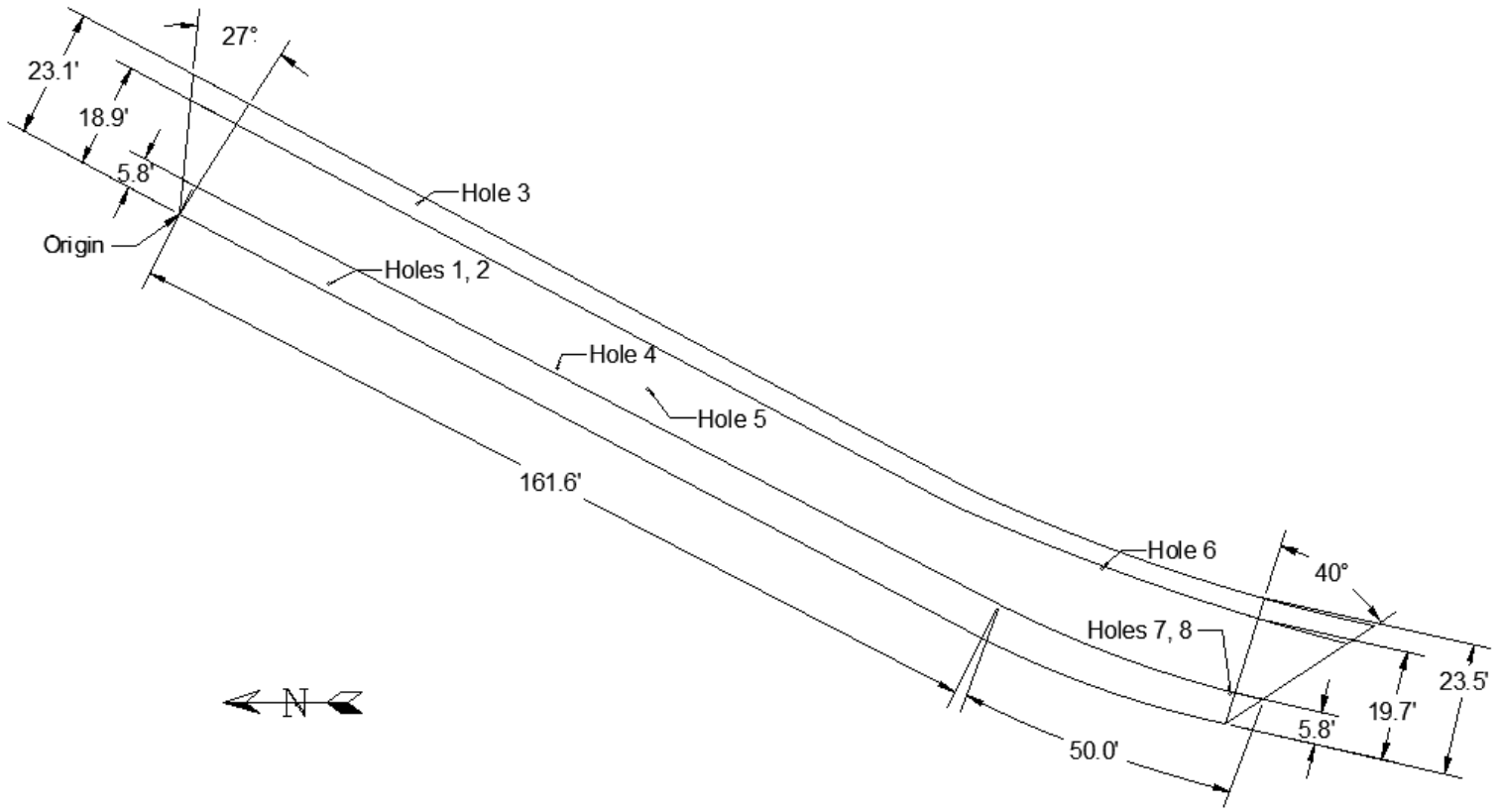

Figure A-10 Test locations for bridge F-53.

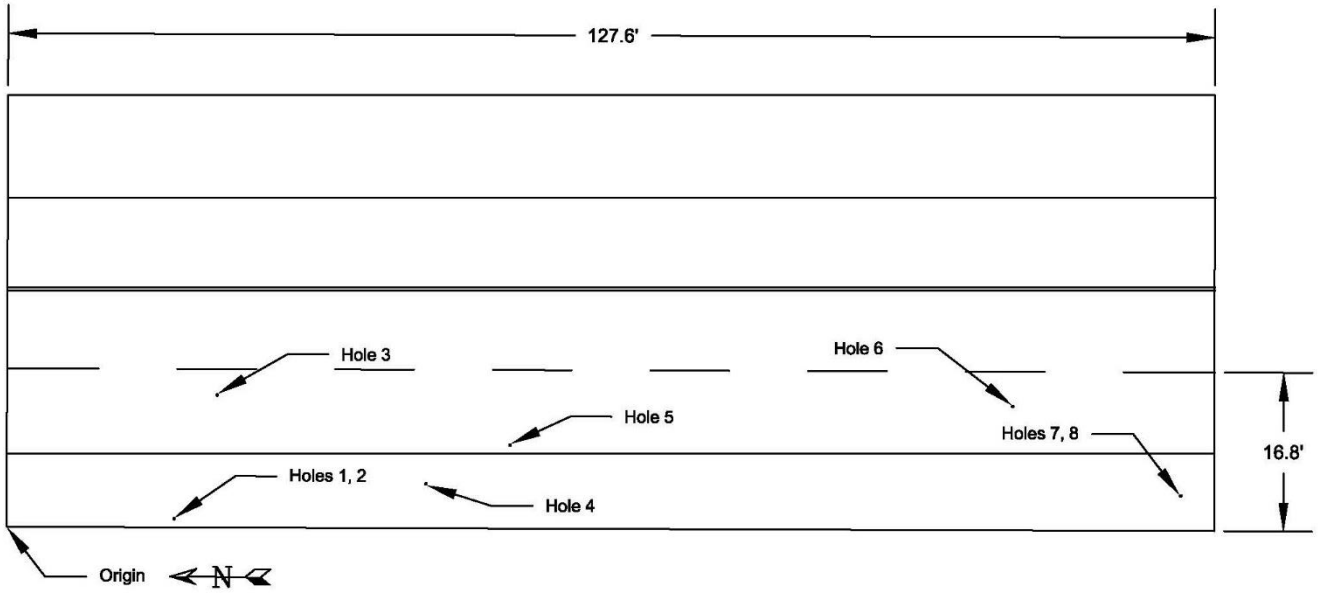

Figure A-11 Test locations for bridge F-476.

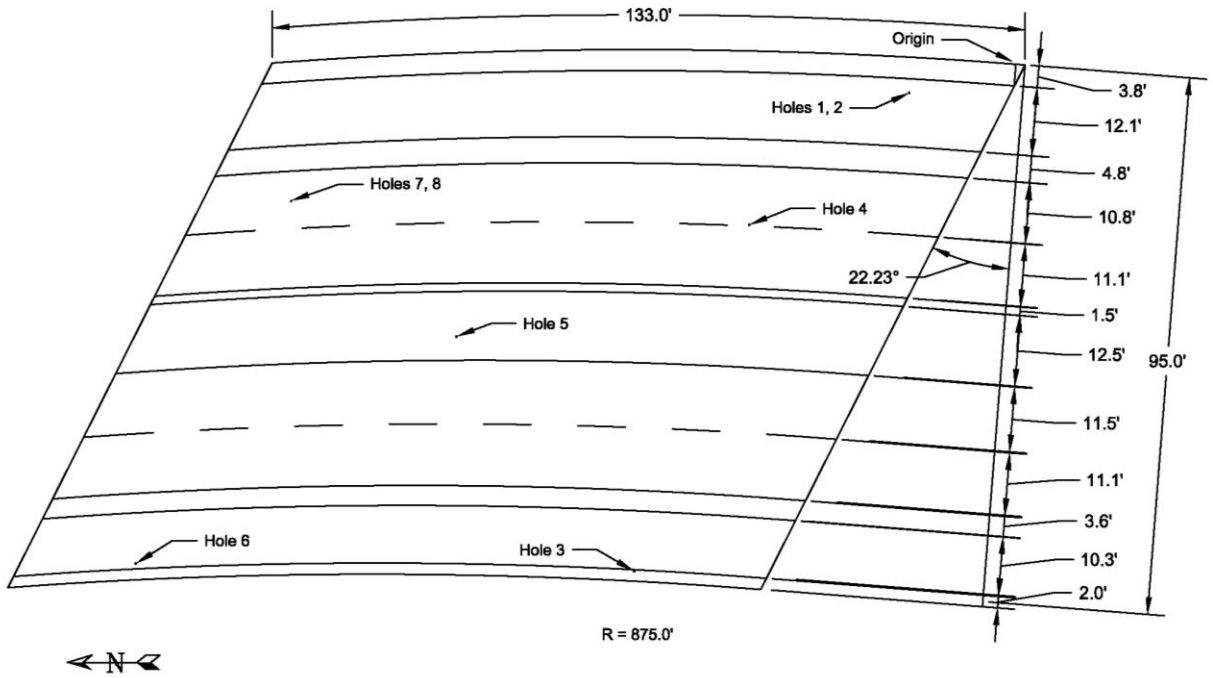

Figure A-12 Test locations for bridge F-562.

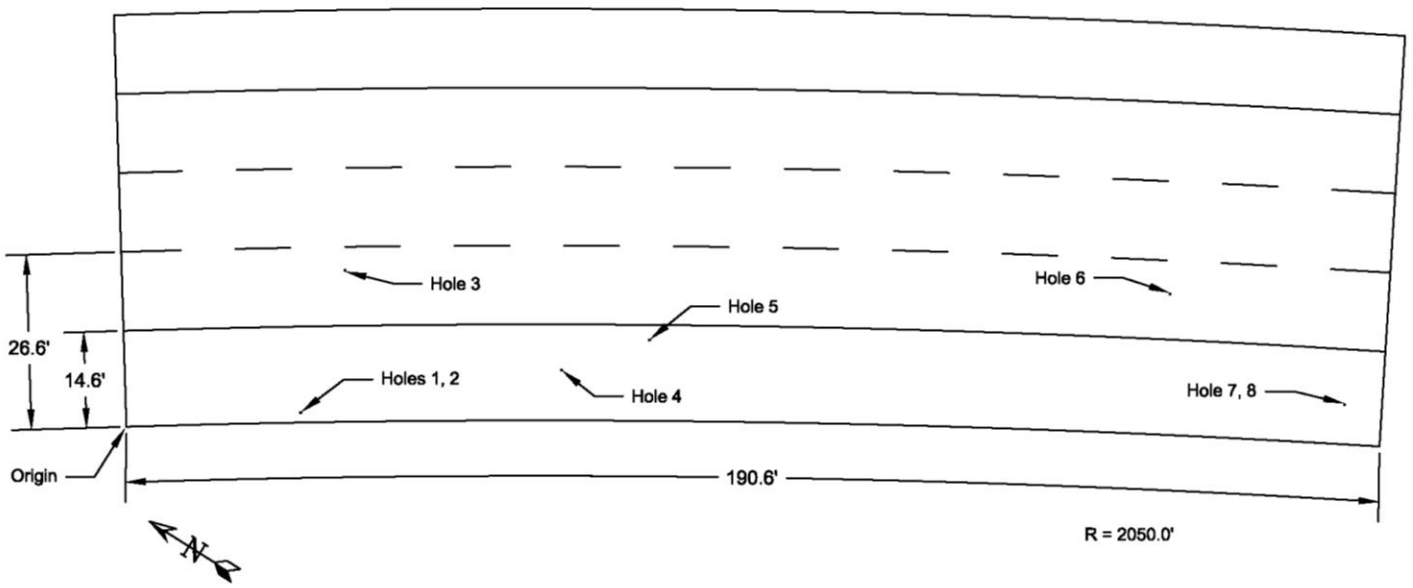

Figure A-13 Test locations for bridge F-738.

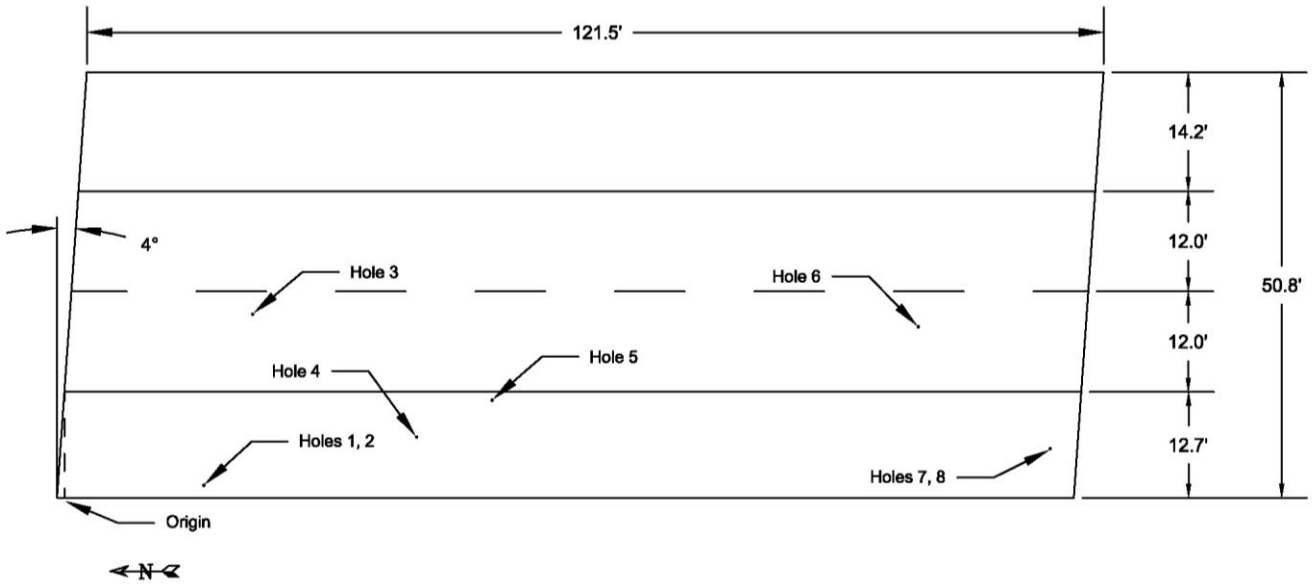

Figure A-14 Test locations for bridge F-799.

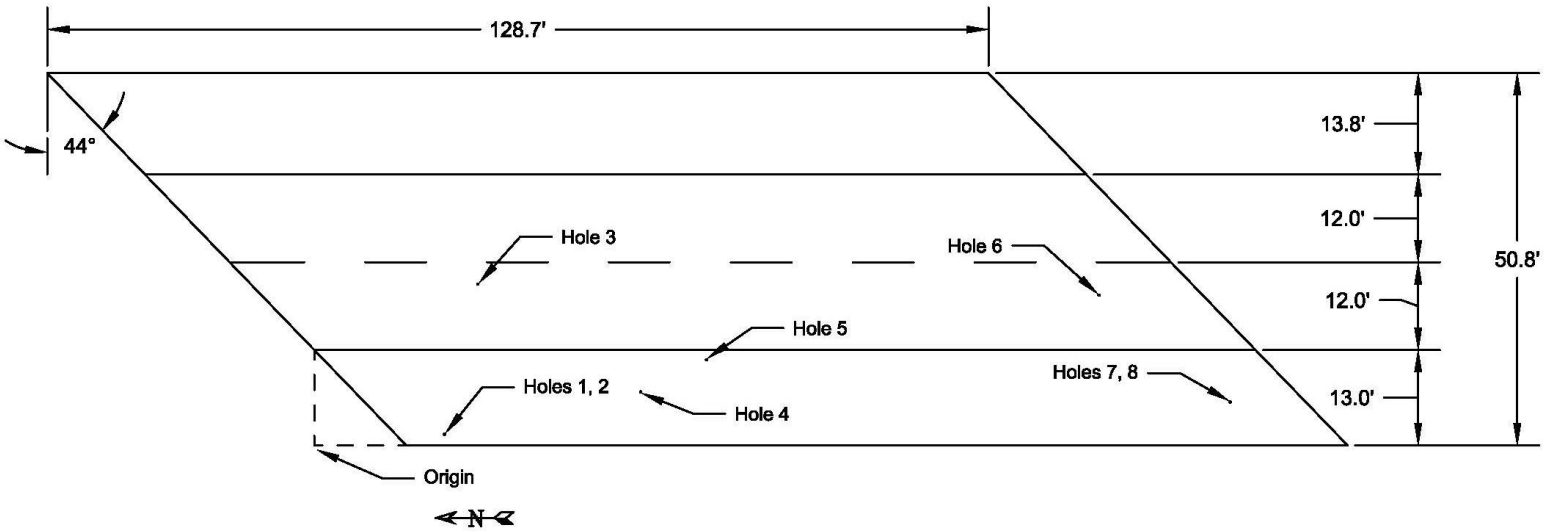

Figure A-15 Test locations for bridge F-800.

APPENDIX B: SUPPORTING FIELD DATA

Tables B-1 to B-15 show the results of bridge deck testing at each test location. In Tables B-1 to B-15, a hyphen indicates that the data were not measured. Tables B-16 to B-30 show the results of chloride concentration testing at each test location. In Tables B-16 to B-30, a hyphen indicates that the data were not measured, and an asterisk (*) or double asterisk (**) indicates that the top or bottom mat, respectively, of reinforcing steel was encountered during chloride concentration sampling; in these cases, the sampling depth may not have extended to the bottom of the indicated depth interval. Figures B-1 to B-21 show the results of VEI and impact-echo testing.

Table B-1 Data for Bridge C-460

Test Location	Station (x, y) (ft)	Cover Depth (in.)	Chloride Concentration at Indicated Depth (lb Cl^-/yd^3 Concrete)				Schmidt Rebound Number	Half-Cell Potential (V)	Delamination (Yes/No)	VEI Magnitude (log_{10}(ohms))	Relative Energy of Echo
			2.0 in.	2.5 in.	3.0 in.	Top Mat of Rebar					
1	(39, 1)	2.5	9.7	-	-	10.4	46	-0.533	-	-	-
2		-	6.2	3.1	2.1	3.1					
3	(48, 15)	-	10.9	8.1	6.6	8.1	59	-0.503	-	5.74	-
4	(96, 5)	-	15.6	12.0	8.6	12.0	51	-0.632	-	5.16	-
5	(115, 8)	-	14.5	11.7	9.3	11.7	46	-0.559	-	4.95	-
6	(231, 14)	-	11.9	8.7	7.7	8.7	50	-0.483	-	5.94	-
7	(269, 4)	-	10.9	8.7	6.6	8.7	49	-0.857	-	4.98	-
8		-	8.7	7.6	7.3	7.8					
Avg.	-	2.5	11.1	8.6	6.9	8.8	50	-0.595	-	5.35	-
St. Dev.	-	-	3.0	3.0	2.3	2.8	5	0.139	-	0.45	-

Table B-2 Data for Bridge C-698

Test Location	Station (x, y) (ft)	Cover Depth (in.)	Chloride Concentration at Indicated Depth (lb Cl^-/yd^3 Concrete)				Schmidt Rebound Number	Half-Cell Potential (V)	Delamination (Yes/No)	VEI Magnitude (log_{10}(ohms))	Relative Energy of Echo
			2.0 in.	2.5 in.	3.0 in.	Top Mat of Rebar					
1	(21, 1)	2.8	20.6	-	-	19.6	40	-0.480	-	-	-
2		-	18.7	18.2	15.3	18.6					
3	(26, 16)	-	14.1	13.0	9.3	9.7	50	-0.434	-	4.88	-
4	(52, 5)	-	21.4	18.8	14.0	14.8	54	-0.422	-	6.43	-
5	(63, 9)	-	12.5	12.6	13.2	13.4	50	-0.458	-	5.37	-
6	(125, 15)	-	1.2	1.7	3.8	3.5	54	-0.290	-	4.48	-
7	(146, 4)	-	12.5	9.0	6.5	5.6	57	-0.362	-	6.10	-
8		3.1	13.8	9.3	-	8.6					
Avg.	-	2.9	14.3	11.8	10.3	11.7	51	-0.408	-	5.45	-
St. Dev.	-	0.3	6.4	5.9	4.6	5.9	6	0.070	-	0.82	-

Table B-3 Data for Bridge C-725

Test Location	Station (x, y) (ft)	Cover Depth (in.)	Chloride Concentration at Indicated Depth (lb Cl^-/yd^3 Concrete)				Schmidt Rebound Number	Half-Cell Potential (V)	Delamination (Yes/No)	VEI Magnitude (log_{10}(ohms))	Relative Energy of Echo
			2.0 in.	2.5 in.	3.0 in.	Top Mat of Rebar					
1	(40, 3)	2.5	11.3	-	-	6.9	49	-0.327	Yes	5.23	119579
2			16.8	15.2	13.2	13.9					
3	(50, 45)	3.1	6.3	5.9	5.4	5.4	46	-0.354	No	4.49	107224
4	(100, 15)	2.2	5.1	4.4	3.6	3.5	63	-0.397	No	4.10	144889
5	(120, 24)	2.8	14.7	9.2	7.9	11.1	54	-0.395	Yes	4.76	134418
6	(240, 42)	2.5	12.5	10.3	6.8	8.5	58	-0.308	No	4.97	99125
7	(280, 12)	2.5	5.9	4.1	2.4	4.1	54	-0.384	No	4.17	111642
8			13.0	8.2	-	10.1					
Avg.	-	2.6	10.7	8.2	6.6	7.9	54	-0.361	-	4.62	119480
St. Dev.	-	0.3	4.4	3.9	3.8	3.6	6	0.037	-	0.45	17290

Table B-4 Data for Bridge C-757

Test Location	Station (x, y) (ft)	Cover Depth (in.)	Chloride Concentration at Indicated Depth (lb Cl^-/yd^3 Concrete)				Schmidt Rebound Number	Half-Cell Potential (V)	Delamination (Yes/No)	VEI Magnitude (log_{10}(ohms))	Relative Energy of Echo
			2.0 in.	2.5 in.	3.0 in.	Top Mat of Rebar					
1	(10, 13)	2.9	9.6	10.4	-	11.2	35	-0.562	Yes	-	91261
2			12.4	9.7	20.2	9.7					
3	(70, 7)	3.3	11.6	9.2	7.4	6.5	54	-0.363	No	-	113707
4	(200, 10)	3.3	18.9	14.5	13.2	12.2	51	-0.480	No	-	103279
5	(230, 6)	4.0	14.5	10.2	9.3	-	56	-0.479	No	-	112408
6	(310, 10)	3.5	15.2	13.2	12.0	10.8	58	-0.510	No	-	104034
7	(440, 9)	3.4	16.9	12.5	9.8	9.8	58	-0.596	No	-	107111
8			15.8	12.6	8.5	9.7					
Avg.	-	3.4	14.4	11.5	11.5	10.0	52	-0.498	-	-	105300
St. Dev.	-	0.4	3.0	1.9	4.3	1.8	9	0.081	-	-	8090

Table B-5 Data for Bridge C-759

Test Location	Station (x, y) (ft)	Cover Depth (in.)	Chloride Concentration at Indicated Depth (lb Cl^-/yd^3 Concrete)				Schmidt Rebound Number	Half-Cell Potential (V)	Delamination (Yes/No)	VEI Magnitude (log_{10}(ohms))	Relative Energy of Echo
			2.0 in.	2.5 in.	3.0 in.	Top Mat of Rebar					
1	(26, 1)	3.4	11.5	8.5	6.6	6.8	60	-0.318	No	-	81253
2			11.0	10.1	8.9	8.1					
3	(32, 20)	3.0	10.0	7.1	5.6	5.6	61	-0.256	No	3.89	111059
4	(64, 7)	3.1	13.5	11.5	10.6	10.3	57	-0.253	No	4.26	101826
5	(77, 11)	3.1	10.9	9.7	8.7	8.9	48	-0.250	No	4.15	104010
6	(153, 19)	3.0	9.6	7.3	6.2	6.1	58	-0.236	No	3.69	131063
7	(179, 5)	2.0	10.5	7.5	4.7	10.5	53	-0.339	No	4.22	93643
8			12.2	-	-	11.4					
Avg.	-	3.0	11.1	8.8	7.3	8.5	56	-0.275	-	4.04	103809
St. Dev.	-	0.5	1.3	1.7	2.1	2.2	5	0.042	-	0.24	16801

Table B-6 Data for Bridge C-760

Test Location	Station (x, y) (ft)	Cover Depth (in.)	Chloride Concentration at Indicated Depth (lb Cl^-/yd^3 Concrete)				Schmidt Rebound Number	Half-Cell Potential (V)	Delamination (Yes/No)	VEI Magnitude (log_{10}(ohms))	Relative Energy of Echo
			2.0 in.	2.5 in.	3.0 in.	Top Mat of Rebar					
1	(11, 11)	2.6	-	-	-	23.5	55	-0.386	No	3.75	121912
2			8.6	4.8	2.8	14.1					
3	(31, 13)	2.5	20.6	15.9	11.6	16.2	56	-0.368	No	3.72	130899
4	(60, 11)	2.0	16.7	11.8	7.3	16.4	46	-0.514	No	3.44	131277
5	(70, 11)	1.9	15.4	12.4	11.2	16.4	51	-0.512	No	3.22	163391
6	(120, 7)	2.4	29.6	27.3	21.6	27.8	46	-0.410	Yes	3.22	210449
7	(160, 3)	2.2	34.4	27.0	16.0	33.2	57	-0.457	No	3.46	161434
8			45.6	-	-	50.5					
Avg.	-	2.3	24.4	16.5	11.7	24.8	52	-0.441	-	3.47	153227
St. Dev.	-	0.3	12.8	9.0	6.5	12.4	5	0.063	-	0.23	32882

Table B-7 Data for Bridge C-794

Test Location	Station (x, y) (ft)	Cover Depth (in.)	Chloride Concentration at Indicated Depth (lb Cl^-/yd^3 Concrete)				Schmidt Rebound Number	Half-Cell Potential (V)	Delamination (Yes/No)	VEI Magnitude (log_{10}(ohms))	Relative Energy of Echo
			2.0 in.	2.5 in.	3.0 in.	Top Mat of Rebar					
1	(23, 1)	3.4	0.2	0.2	0.2	0.1	55	-0.516	-	-	-
2		-	0.1	0.1	0.1	0.1					
3	(28, 18)	-	3.1	1.3	1.0	1.0	37	-0.502	-	-	-
4	(57, 6)	-	0.1	0.1	0.1	0.1	35	-0.478	-	5.83	-
5	(68, 10)	-	0.1	0.0	0.0	0.0	46	-0.488	-	6.10	-
6	(136, 17)	-	1.6	0.7	0.4	0.4	61	-0.427	-	6.02	-
7	(158, 5)	-	1.5	0.8	0.3	0.6	58	-0.528	-	6.03	-
8		2.7	0.1	0.1	-	0.0					
Avg.	-	3.0	0.8	0.4	0.3	0.3	49	-0.490	-	6.00	-
St. Dev.	-	0.5	1.1	0.5	0.3	0.3	11	0.036	-	0.11	-

Table B-8 Data for Bridge C-931

Test Location	Station (x, y) (ft)	Cover Depth (in.)	Chloride Concentration at Indicated Depth (lb Cl^-/yd^3 Concrete)				Schmidt Rebound Number	Half-Cell Potential (V)	Delamination (Yes/No)	VEI Magnitude (log_{10}(ohms))	Relative Energy of Echo
			2.0 in.	2.5 in.	3.0 in.	Top Mat of Rebar					
1	(15, 2)	2.8	0.5	0.3	0.3	0.5	49	-0.169	No	-	90108
2			0.3	0.2	0.2	0.1					
3	(19, 28)	2.7	0.3	0.4	0.3	0.3	55	0.009	No	-	20347
4	(38, 9)	2.7	0.0	0.0	0.0	0.1	55	-0.043	No	-	103928
5	(45, 15)	2.6	0.3	0.3	0.3	0.3	52	0.113	No	-	43827
6	(90, 26)	2.7	0.2	0.3	0.3	0.3	54	0.084	No	-	50747
7	(105, 8)	2.7	0.1	0.1	0.2	0.2	62	0.039	No	-	127498
8			0.8	0.4	-	0.3					
Avg.	-	2.7	0.3	0.2	0.2	0.3	55	0.006	-	-	72743
St. Dev.	-	0.1	0.2	0.1	0.1	0.1	4	0.102	-	-	40835

Table B-9 Data for Bridge C-953

Test Location	Station (x, y) (ft)	Cover Depth (in.)	Chloride Concentration at Indicated Depth (lb Cl^-/yd^3 Concrete)				Schmidt Rebound Number	Half-Cell Potential (V)	Delamination (Yes/No)	VEI Magnitude (log_{10}(ohms))	Relative Energy of Echo
			2.0 in.	2.5 in.	3.0 in.	Top Mat of Rebar					
1	(25, 1)	5.2	9.1	7.6	7.9	-	51	-0.481	No	-	-
2			0.2	0.2	0.3	-					
3	(31, 15)	4.0	0.4	0.3	0.3	-	60	-0.377	No	5.29	92681
4	(62, 5)	2.9	0.3	0.2	0.2	0.2	61	-0.409	No	5.13	65055
5	(72, 8)	2.9	7.7	6.6	6.2	6.2	55	-0.395	No	5.39	97917
6	(147, 14)	3.6	0.7	0.2	0.2	-	50	-0.408	No	5.53	84394
7	(171, 4)	4.1	0.3	0.2	0.2	-	45	-0.511	No	5.21	21128
8			0.2	0.2	0.2	-					
Avg.	-	3.8	2.4	2.0	1.9	3.2	54	-0.430	-	5.31	72235
St. Dev.	-	0.9	3.7	3.2	3.2	4.3	6	0.053	-	0.15	31181

Table B-10 Data for Bridge F-53

Test Location	Station (x, y) (ft)	Cover Depth (in.)	Chloride Concentration at Indicated Depth (lb Cl^-/yd^3 Concrete)				Schmidt Rebound Number	Half-Cell Potential (V)	Delamination (Yes/No)	VEI Magnitude (log_{10}(ohms))	Relative Energy of Echo
			2.0 in.	2.5 in.	3.0 in.	Top Mat of Rebar					
1	(29, 1)	2.4	0.5	-	-	0.6	63	-1.032	-	-	-
2		2.8	0.4	0.4	0.3	0.4					
3	(37, 22)	-	0.4	0.4	0.3	0.4	53	-1.024	-	-	-
4	(73, 7)	-	0.3	0.3	0.2	0.3	51	-1.010	-	5.33	-
5	(88, 12)	-	0.2	0.2	0.2	0.2	50	-0.967	-	5.04	-
6	(176, 20)	-	0.4	0.5	1.1	0.4	47	-1.006	-	5.36	-
7	(206, 6)	-	0.4	0.5	0.4	0.3	47	-1.010	-	-	-
8		1.1	-	-	-	0.1					
Avg.	-	2.1	0.4	0.4	0.4	0.4	52	-1.008	-	5.24	-
St. Dev.	-	0.9	0.1	0.1	0.3	0.1	6	0.022	-	0.18	-

Table B-11 Data for Bridge F-476

Test Location	Station (x, y) (ft)	Cover Depth (in.)	Chloride Concentration at Indicated Depth (lb Cl^-/yd^3 Concrete)				Schmidt Rebound Number	Half-Cell Potential (V)	Delamination (Yes/No)	VEI Magnitude (log_{10}(ohms))	Relative Energy of Echo
			2.0 in.	2.5 in.	3.0 in.	Top Mat of Rebar					
1	(18, 1)	3.5	2.7	1.8	0.9	0.4	50	-0.379	-	4.79	-
2		-	4.5	3.1	2.1	1.5					
3	(22, 14)	-	20.4	18.2	15.5	18.2	48	-0.562	-	4.99	-
4	(44, 5)	-	6.2	5.2	4.3	5.2	48	-0.334	-	4.30	-
5	(53, 8)	-	8.5	7.9	6.3	7.9	43	-0.357	-	4.78	-
6	(106, 13)	-	16.6	15.4	13.3	15.4	38	-0.562	-	4.76	-
7	(124, 4)	-	3.2	3.0	2.7	3.5	51	-0.566	-	4.78	-
8		1.5	-	-	-	4.2					
Avg.	-	2.5	8.9	7.8	6.4	7.0	46	-0.460	-	4.73	-
St. Dev.	-	1.4	6.9	6.5	5.7	6.5	5	0.114	-	0.23	-

Table B-12 Data for Bridge F-562

Test Location	Station (x, y) (ft)	Cover Depth (in.)	Chloride Concentration at Indicated Depth (lb Cl^-/yd^3 Concrete)				Schmidt Rebound Number	Half-Cell Potential (V)	Delamination (Yes/No)	VEI Magnitude (log_{10}(ohms))	Relative Energy of Echo
			2.0 in.	2.5 in.	3.0 in.	Top Mat of Rebar					
1	(19, 6)	1.8	-	-	-	-	50	-0.390	No	4.40	126117
2			1.7	0.3	0.1	11.2					
3	(53, 92)	1.9	11.9	6.4	3.7	13.6	53	-0.512	No	4.64	-
4	(46, 31)	2.8	9.5	3.1	2.8	0.2	54	-0.368	No	4.39	106454
5	(86, 50)	2.9	6.6	2.6	1.5	0.1	49	-0.454	No	4.54	-
6	(141, 86)	2.1	5.9	2.9	1.6	5.5	53	-0.482	No	4.67	-
7	(129, 25)	3.1	0.5	0.1	0.1	0.1	53	-0.410	No	4.23	142636
8			0.5	0.3	0.2	0.2					
Avg.	-	2.4	5.2	2.2	1.4	4.4	52	-0.436	-	4.48	125069
St. Dev.	-	0.6	4.5	2.3	1.4	5.8	2	0.056	-	0.17	18114

Table B-13 Data for Bridge F-738

Test Location	Station (x, y) (ft)	Cover Depth (in.)	Chloride Concentration at Indicated Depth (lb Cl^-/yd^3 Concrete)				Schmidt Rebound Number	Half-Cell Potential (V)	Delamination (Yes/No)	VEI Magnitude (log_{10}(ohms))	Relative Energy of Echo
			2.0 in.	2.5 in.	3.0 in.	Top Mat of Rebar					
1	(27, 2)	3.5	0.1	0.2	0.2	0.3	49	-0.293	No	-	-
2			0.2	0.2	0.2	0.2					
3	(33, 23)	3.0	0.1	0.1	0.1	0.1	51	-0.279	No	5.38	118849
4	(66, 8)	2.9	0.2	0.2	0.3	0.3	62	-0.298	No	5.32	99693
5	(80, 12)	3.4	0.3	0.3	0.3	0.3	47	-0.259	No	5.61	108180
6	(159, 22)	3.1	0.1	0.2	0.2	0.2	57	-0.218	No	5.69	112179
7	(185, 6)	4.0	0.2	0.1	0.2	-	49	-0.298	No	5.52	94927
8			0.2	0.2	0.2	-					
Avg.	-	3.3	0.2	0.2	0.2	0.2	52	-0.274	-	5.50	106766
St. Dev.	-	0.4	0.1	0.1	0.1	0.1	6	0.031	-	0.16	9585

Table B-14 Data for Bridge F-799

Test Location	Station (x, y) (ft)	Cover Depth (in.)	Chloride Concentration at Indicated Depth (lb Cl^-/yd^3 Concrete)				Schmidt Rebound Number	Half-Cell Potential (V)	Delamination (Yes/No)	VEI Magnitude (log_{10}(ohms))	Relative Energy of Echo
			2.0 in.	2.5 in.	3.0 in.	Top Mat of Rebar					
1	(17, 2)	2.9	0.7	0.7	-	0.8	57	-0.527	No	-	-
2			1.4	0.6	0.2	0.2					
3	(21, 22)	2.3	0.6	0.0	0.0	0.2	57	-0.547	No	-	115602
4	(42, 7)	2.3	0.2	0.1	0.0	0.1	57	-0.487	No	-	116962
5	(50, 12)	2.4	0.2	0.2	0.3	0.2	54	-0.533	No	-	118362
6	(100, 21)	2.2	0.3	0.2	0.1	0.3	56	-0.488	No	-	118698
7	(117, 6)	2.7	0.2	0.2	0.7	0.9	65	-0.588	No	-	102624
8			2.5	2.0	1.7	1.9					
Avg.	-	2.5	0.8	0.5	0.4	0.6	58	-0.528	-	-	114450
St. Dev.	-	0.3	0.8	0.6	0.6	0.6	4	0.038	-	-	6724

Table B-15 Data for Bridge F-800

Test Location	Station (x, y) (ft)	Cover Depth (in.)	Chloride Concentration at Indicated Depth (lb Cl^-/yd^3 Concrete)				Schmidt Rebound Number	Half-Cell Potential (V)	Delamination (Yes/No)	VEI Magnitude (log_{10}(ohms))	Relative Energy of Echo
			2.0 in.	2.5 in.	3.0 in.	Top Mat of Rebar					
1	(18, 2)	3.2	0.1	0.1	0.1	0.2	60	-0.567	No	-	-
2			0.4	0.1	0.1	0.1					
3	(22, 22)	3.6	1.1	0.4	0.2	-	59	-0.357	No	-	104740
4	(45, 7)	3.0	0.2	0.2	0.1	0.1	57	-0.345	No	-	116737
5	(54, 12)	3.0	0.1	0.1	0.1	0.1	58	-0.343	No	-	136120
6	(107, 21)	2.9	0.2	0.1	0.1	0.1	56	-0.325	No	-	108332
7	(125, 6)	2.7	0.1	0.1	0.1	0.1	52	-0.409	No	-	-
8			0.1	0.1	-	0.2					
Avg.	-	3.1	0.3	0.2	0.1	0.1	57	-0.391	-	-	116482
St. Dev.	-	0.3	0.4	0.1	0.0	0.1	3	0.091	-	-	14024

Table B-16 Chloride Concentration Data for Bridge C-460

	Depth Interval (in.)											
Test Location	0-0.5	0.5-1.0	1.0-1.5	1.5-2.0	2.0-2.5	2.5-3.0	3.0-3.5	3.5-4.0	4.0-5.0	5.0-6.0	6.0-7.0	7.0-8.0
	Chloride Concentration (lb Cl^-/yd^3 Concrete)											
1*	27.5	43.1	13.7	9.0	10.4	-	-	-	-	-	-	-
2	-	15.7	10.8	8.7	3.8	2.5	1.8	1.9	-	-	-	-
3	13.3		13.6		8.1		5.1		1.2	0.2	0.2	-
4	11.5	26.3	21.2	17.3	13.9	10.1	7.2	5.1	-	-	-	-
5	13.2	22.2	19.5	15.6	13.4	10.0	8.6	5.5	-	-	-	-
6**	18.7		15.2		8.7		6.7		2.9	2.1	-	-
7	9.1	10.1	15.6	12.4	9.4	8.1	5.2	2.0	-	-	-	-
8	10.4	12.2	9.1	9.6	7.8	7.5	7.0	3.8	-	-	-	-
Average	17.6		13.8		8.8		5.1		2.0	1.1	0.2	-

Table B-17 Chloride Concentration Data for Bridge C-698

	Depth Interval (in.)											
Test Location	0-0.5	0.5-1.0	1.0-1.5	1.5-2.0	2.0-2.5	2.5-3.0	3.0-3.5	3.5-4.0	4.0-5.0	5.0-6.0	6.0-7.0	7.0-8.0
	Chloride Concentration (lb Cl^-/yd^3 Concrete)											
1*	12.8	19.1	21.9	21.6	19.6	-	-	-	-	-	-	-
2	10.3	20.2	22.6	19.5	17.9	18.6	12.0	11.2	-	-	-	-
3	11.7		15.3		13.0		5.5		1.6	-	-	-
4	15.2	24.4	25.4	22.5	20.3	17.2	10.8	6.7	-	-	-	-
5	5.4	11.4	12.7	13.9	11.1	14.1	12.4	9.1	-	-	-	-
6**	1.2		0.6		1.7		5.9		5.6	-	-	-
7	40.5	29.0	24.6	15.2	9.7	8.2	4.8	1.7	-	-	-	-
8*	21.7	32.8	22.3	17.6	10.0	8.6	-	-	-	-	-	-
Average	16.8		17.0		12.8		7.6		3.6	-	-	-

Table B-18 Chloride Concentration Data for Bridge C-725

Test Location	Depth Interval (in.) 0-0.5	0.5-1.0	1.0-1.5	1.5-2.0	2.0-2.5	2.5-3.0	3.0-3.5	3.5-4.0	4.0-5.0	5.0-6.0	6.0-7.0	7.0-8.0
	Chloride Concentration (lb Cl^-/yd^3 Concrete)											
1*	12.1	18.3	15.0	15.8	6.9	-	-	-	-	-	-	-
2	15.4	25.3	26.3	18.3	15.3	15.1	11.3	7.2	-	-	-	-
3	4.7		6.6		5.9		5.0		4.4	5.0	1.8	-
4	8.2	10.0	7.1	5.3	4.9	3.9	3.4	2.8	-	-	-	-
5	18.5	25.2	25.2	19.2	10.2	8.2	7.5	8.1	-	-	-	-
6	12.3		14.7		10.3		3.3		0.3	0.2	0.2	-
7	18.6	23.3	11.2	7.4	4.4	3.7	1.1	0.3	-	-	-	-
8*	21.7	20.9	23.7	16.0	10.1	6.4	-	-	-	-	-	-
Average	16.0		14.4		9.0		5.6		3.6	3.0	1.9	-

Table B-19 Chloride Concentration Data for Bridge C-757

Test Location	Depth Interval (in.) 0-0.5	0.5-1.0	1.0-1.5	1.5-2.0	2.0-2.5	2.5-3.0	3.0-3.5	3.5-4.0	4.0-5.0	5.0-6.0	6.0-7.0	7.0-8.0
	Chloride Concentration (lb Cl^-/yd^3 Concrete)											
1*	15.1	22.8	15.8	9.4	9.7	11.2	-	-	-	-	-	-
2	25.3	21.9	14.3	15.0	9.9	9.5	31.0	22.9	-	-	-	-
3**	15.7		14.0		9.2		5.6		2.8	1.5	0.4	-
4	17.6	22.3	22.8	23.0	14.8	14.2	12.2	9.5	-	-	-	-
5	14.7	17.8	15.6	18.4	10.7	9.8	8.9	8.3	-	-	-	-
6	44.5		17.3		13.2		10.8		9.0	10.7	12.3	-
7	14.3	21.2	19.0	18.9	15.0	10.0	9.6	7.8	-	-	-	-
8*	14.6	18.4	20.3	16.1	15.6	9.7	7.4	-	-	-	-	-
Average	23.0		16.7		11.5		10.8		5.9	6.1	6.4	-

Table B-20 Chloride Concentration Data for Bridge C-759

Test Location	Depth Interval (in.) 0-0.5	0.5-1.0	1.0-1.5	1.5-2.0	2.0-2.5	2.5-3.0	3.0-3.5	3.5-4.0	4.0-5.0	5.0-6.0	6.0-7.0	7.0-8.0
	Chloride Concentration (lb Cl^-/yd^3 Concrete)											
1*	7.4	11.6	14.2	13.0	10.0	7.0	6.1	6.8	-	-	-	-
2	6.3	11.0	13.8	11.0	10.9	9.3	8.4	6.7	-	-	-	-
3	38.0		12.8		7.1		4.1		1.2	0.3	0.2	-
4	8.5	14.1	17.0	15.6	11.5	11.6	9.6	10.7	-	-	-	-
5	7.0	15.4	15.2	10.7	11.1	8.3	9.1	6.3	-	-	-	-
6	13.8		12.0		7.3		5.1		1.6	0.6	0.2	-
7	7.1	14.6	15.1	11.5	9.5	5.6	3.9	2.2	-	-	-	-
8*	30.3	11.8	11.5	13.0	11.4	-	-	-	-	-	-	-
Average	15.5		13.2		9.1		6.3		1.4	0.4	0.2	-

Table B-21 Chloride Concentration Data for Bridge C-760

Test Location	Depth Interval (in.) 0-0.5	0.5-1.0	1.0-1.5	1.5-2.0	2.0-2.5	2.5-3.0	3.0-3.5	3.5-4.0	4.0-5.0	5.0-6.0	6.0-7.0	7.0-8.0
	Chloride Concentration (lb Cl^-/yd^3 Concrete)											
1*	30.2	27.2	23.5	-	-	-	-	-	-	-	-	-
2	34.8	19.7	17.6	10.7	6.5	3.0	2.7	2.3	-	-	-	-
3	31.9		25.4		15.9		7.2		4.0	1.2	0.4	0.2
4	33.0	27.8	18.6	18.4	15.0	8.5	6.0	4.5	-	-	-	-
5	20.5	25.9	20.1	17.1	13.7	11.2	11.2	9.1	-	-	-	-
6	39.3		31.9		27.3		15.8		6.4	1.6	-	-
7	59.7	48.0	38.0	34.1	34.7	19.3	12.7	8.7	-	-	-	-
8*	60.1	39.4	36.0	40.7	50.5	-	-	-	-	-	-	-
Average	35.0		26.2		22.0		10.0		5.2	1.4	0.4	0.2

Table B-22 Chloride Concentration Data for Bridge C-794

Test Location	Depth Interval (in.) 0-0.5	0.5-1.0	1.0-1.5	1.5-2.0	2.0-2.5	2.5-3.0	3.0-3.5	3.5-4.0	4.0-5.0	5.0-6.0	6.0-7.0	7.0-8.0
	Chloride Concentration (lb Cl^-/yd^3 Concrete)											
1*	0.6	0.2	0.2	0.2	0.2	0.2	0.1	-	-	-	-	-
2	0.1	0.2	0.1	0.1	0.1	0.1	0.1	0.1	-	-	-	-
3**	9.5		4.8		1.3		0.7		0.2	0.2	0.2	-
4	0.4	0.1	0.1	0.1	0.1	0.1	0.1	0.1	-	-	-	-
5	0.5	0.3	0.1	0.1	0.1	0.0	0.1	0.1	-	-	-	-
6	3.9		2.5		0.7		0.1		0.1	0.1	0.0	-
7	3.0	3.7	2.7	1.9	1.0	0.5	0.1	0.1	-	-	-	-
8*	0.5	0.3	0.1	0.1	0.1	0.0	-	-	-	-	-	-
Average	2.5		1.4		0.5		0.2		0.1	0.1	0.1	-

Table B-23 Chloride Concentration Data for Bridge C-931

Test Location	Depth Interval (in.) 0-0.5	0.5-1.0	1.0-1.5	1.5-2.0	2.0-2.5	2.5-3.0	3.0-3.5	3.5-4.0	4.0-5.0	5.0-6.0	6.0-7.0	7.0-8.0
	Chloride Concentration (lb Cl^-/yd^3 Concrete)											
1*	2.4	2.1	1.0	0.6	0.4	0.2	0.3	0.5	-	-	-	-
2	2.6	0.7	0.6	0.5	0.2	0.2	0.1	0.3	-	-	-	-
3	2.4		0.2		0.4		0.2		0.1	0.2	0.2	-
4	1.8	0.4	0.1	0.0	0.0	0.1	0.0	0.1	-	-	-	-
5	6.2	1.0	0.6	0.3	0.2	0.3	0.3	0.2	-	-	-	-
6	4.1		0.1		0.3		0.3		0.2	0.2	-	-
7	28.2	2.3	0.3	0.1	0.1	0.1	0.2	0.1	-	-	-	-
8*	4.9	6.2	3.1	1.1	0.4	0.3	-	-	-	-	-	-
Average	4.5		0.6		0.2		0.2		0.2	0.2	0.2	-

Table B-24 Chloride Concentration Data for Bridge C-953

Test Location	Depth Interval (in.) 0-0.5	0.5-1.0	1.0-1.5	1.5-2.0	2.0-2.5	2.5-3.0	3.0-3.5	3.5-4.0	4.0-5.0	5.0-6.0	6.0-7.0	7.0-8.0
	Chloride Concentration (lb Cl^-/yd^3 Concrete)											
1*	4.0	10.7	10.7	10.1	8.0	7.2	8.5	8.6	-	-	-	-
2	6.8	4.6	0.5	0.2	0.2	0.2	0.3	0.0	-	-	-	-
3	9.5		0.5		0.3		0.3		0.3	0.3	0.3	-
4	5.2	9.6	3.6	0.4	0.3	0.2	0.2	0.3	-	-	-	-
5	9.8	15.9	11.3	8.4	6.9	6.3	6.1	6.1	-	-	-	-
6	9.4		1.1		0.2		0.2		0.2	0.1	0.3	-
7	3.9	5.6	1.7	0.3	0.3	0.2	0.2	0.2	-	-	-	-
8*	4.2	8.0	3.8	0.3	0.2	0.2	0.2	0.3	-	-	-	-
Average	7.9		3.4		2.0		2.0		0.3	0.2	0.3	-

Table B-25 Chloride Concentration Data for Bridge F-53

Test Location	Depth Interval (in.) 0-0.5	0.5-1.0	1.0-1.5	1.5-2.0	2.0-2.5	2.5-3.0	3.0-3.5	3.5-4.0	4.0-5.0	5.0-6.0	6.0-7.0	7.0-8.0
	Chloride Concentration (lb Cl^-/yd^3 Concrete)											
1*	0.4	0.3	0.3	0.4	0.6	-	-	-	-	-	-	-
2	0.7	0.4	0.4	0.5	0.4	0.3	0.3	0.4	-	-	-	-
3	0.6		0.3		0.4		0.3		0.3	0.3	0.8	-
4	5.3	0.9	0.3	0.4	0.3	0.2	0.2	0.3	-	-	-	-
5	1.9	0.5	0.3	0.3	0.2	0.2	0.2	0.2	-	-	-	-
6**	1.0		0.3		0.5		1.7		5.2	-	-	-
7	0.5	0.4	0.3	0.4	0.4	0.5	0.3	0.4	-	-	-	-
8*	0.3	0.2	0.1	-	-	-	-	-	-	-	-	-
Average	1.1		0.5		0.4		0.5		2.8	0.3	0.8	-

Table B-26 Chloride Concentration Data for Bridge F-476

Test Location	Depth Interval (in.) 0-0.5	0.5-1.0	1.0-1.5	1.5-2.0	2.0-2.5	2.5-3.0	3.0-3.5	3.5-4.0	4.0-5.0	5.0-6.0	6.0-7.0	7.0-8.0
	Chloride Concentration (lb Cl^-/yd^3 Concrete)											
1*	7.0	4.7	4.5	3.3	2.1	1.4	0.4	-	-	-	-	-
2	9.6	7.8	6.0	5.2	3.9	2.4	1.7	0.6	-	-	-	-
3	22.5		22.5		18.2		12.8		8.3	6.1	5.8	-
4	7.4	7.6	7.0	6.7	5.8	4.6	4.0	2.9	-	-	-	-
5	12.9	9.8	9.1	9.0	8.0	7.9	4.7	6.7	-	-	-	-
6	22.3		17.8		15.4		11.3		8.4	6.9	5.3	-
7	4.8	4.7	3.7	3.2	3.2	2.7	2.7	2.2	-	-	-	-
8*	4.4	4.4	4.2	-	-	-	-	-	-	-	-	-
Average	10.9		9.2		7.8		5.3		8.3	6.5	5.5	-

Table B-27 Chloride Concentration Data for Bridge F-562

Test Location	Depth Interval (in.) 0-0.5	0.5-1.0	1.0-1.5	1.5-2.0	2.0-2.5	2.5-3.0	3.0-3.5	3.5-4.0	4.0-5.0	5.0-6.0	6.0-7.0	7.0-8.0
	Chloride Concentration (lb Cl^-/yd^3 Concrete)											
1*	41.8	23.6	35.0	34.2	-	-	-	-	-	-	-	-
2	35.6	42.7	19.6	2.9	0.5	0.1	0.2	0.1	-	-	-	-
3	30.5		17.5		6.4		1.1		0.2	0.3	0.2	0.2
4	37.2		15.9		3.1		2.5		2.0	0.9	-	-
5	33.7		10.6		2.6		0.4		0.2	0.3	0.2	0.4
6	25.0		9.0		2.9		0.4		0.2	0.2	0.2	0.1
7	41.3	31.7	10.3	0.8	0.1	0.1	0.1	0.0	-	-	-	-
8*	58.3	40.7	14.4	0.7	0.3	0.2	0.2	-	-	-	-	-
Average	35.5		14.0		2.2		0.7		0.6	0.4	0.2	-

Table B-28 Chloride Concentration Data for Bridge F-738

Test Location	Depth Interval (in.) 0-0.5	0.5-1.0	1.0-1.5	1.5-2.0	2.0-2.5	2.5-3.0	3.0-3.5	3.5-4.0	4.0-5.0	5.0-6.0	6.0-7.0	7.0-8.0
	Chloride Concentration (lb Cl^-/yd^3 Concrete)											
1*	2.2	1.0	0.2	0.2	0.1	0.2	0.3	-	-	-	-	-
2	2.1	1.1	0.2	0.3	0.2	0.2	0.3	0.2	-	-	-	-
3	2.1		0.1		0.1		0.1		0.1	0.0	0.1	-
4	3.1	0.8	0.2	0.3	0.2	0.3	0.3	0.4	-	-	-	-
5	4.0	2.0	0.6	0.3	0.3	0.3	0.3	0.3	-	-	-	-
6	1.5		0.0		0.2		0.2		0.2	0.2	0.3	-
7	2.2	0.6	0.1	0.2	0.2	0.0	0.3	0.3	-	-	-	-
8*	2.9	0.7	0.2	0.3	0.2	0.2	0.3	0.0	-	-	-	-
Average	1.9		0.2		0.2		0.2		0.1	0.1	0.2	-

Table B-29 Chloride Concentration Data for Bridge F-799

Test Location	Depth Interval (in.) 0-0.5	0.5-1.0	1.0-1.5	1.5-2.0	2.0-2.5	2.5-3.0	3.0-3.5	3.5-4.0	4.0-5.0	5.0-6.0	6.0-7.0	7.0-8.0
	Chloride Concentration (lb Cl^-/yd^3 Concrete)											
1*	14.7	5.7	2.0	0.9	0.5	0.8	-	-	-	-	-	-
2	15.9	10.2	3.6	1.8	0.9	0.3	0.2	0.1	-	-	-	-
3	15.8		1.2		0.0		0.0		0.0	0.0	0.0	-
4	22.8	7.1	0.6	0.2	0.1	0.0	0.0	0.1	-	-	-	-
5	25.3	12.0	1.0	0.2	0.2	0.2	0.4	0.3	-	-	-	-
6	14.6		0.4		0.2		0.0		0.3	0.3	-	-
7	19.3	11.0	0.4	0.0	0.3	0.1	1.3	0.0	-	-	-	-
8*	22.4	11.2	3.1	2.5	2.4	1.6	1.9	-	-	-	-	-
Average	14.9		1.2		0.5		0.4		0.1	0.1	0.0	-

Table B-30 Chloride Concentration Data for Bridge F-800

Test Location	Depth Interval (in.)											
	0-0.5	0.5-1.0	1.0-1.5	1.5-2.0	2.0-2.5	2.5-3.0	3.0-3.5	3.5-4.0	4.0-5.0	5.0-6.0	6.0-7.0	7.0-8.0
	Chloride Concentration (lb Cl^-/yd^3 Concrete)											
1*	13.0	4.0	0.3	0.1	0.1	0.1	0.2	-	-	-	-	-
2	11.3	3.5	1.0	0.6	0.2	0.1	0.1	0.1	-	-	-	-
3	10.1		1.9		0.4		0.1		0.1	0.2	0.3	-
4	15.3	4.8	0.2	0.1	0.2	0.1	0.1	0.1	-	-	-	-
5	15.4	2.6	0.2	0.1	0.1	0.1	0.1	0.1	-	-	-	-
6	5.3		0.2		0.1		0.0		0.0	0.0	0.0	-
7	18.5	5.6	0.2	0.1	0.1	0.1	0.1	0.2	-	-	-	-
8*	20.1	6.2	0.2	0.2	0.1	0.2	-	-	-	-	-	-
Average	9.4		0.5		0.2		0.1		0.1	0.1	0.1	-

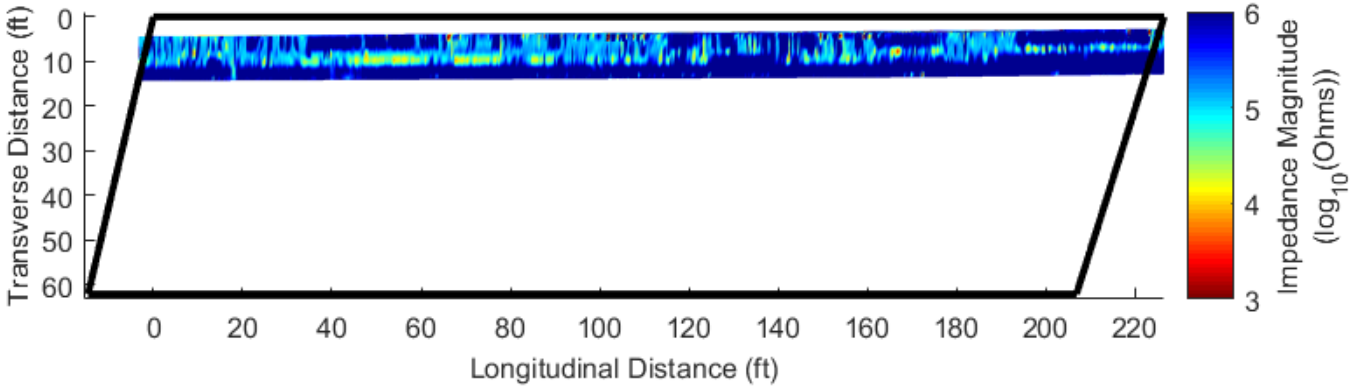

Figure B-1 VEI data for bridge C-460.

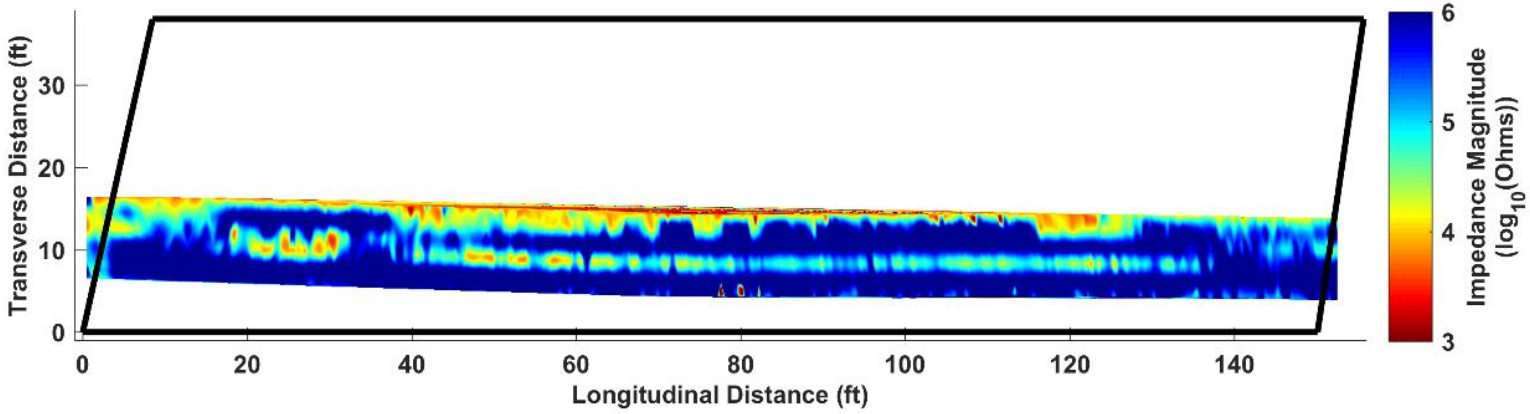

Figure B-2 VEI data for bridge C-698.

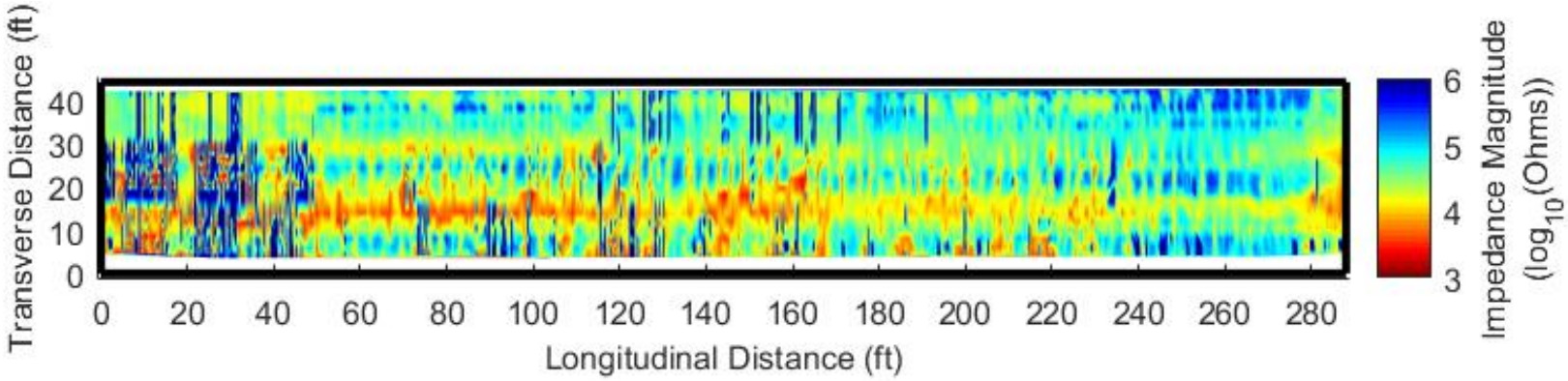

Figure B-3 VEI data for bridge C-725.

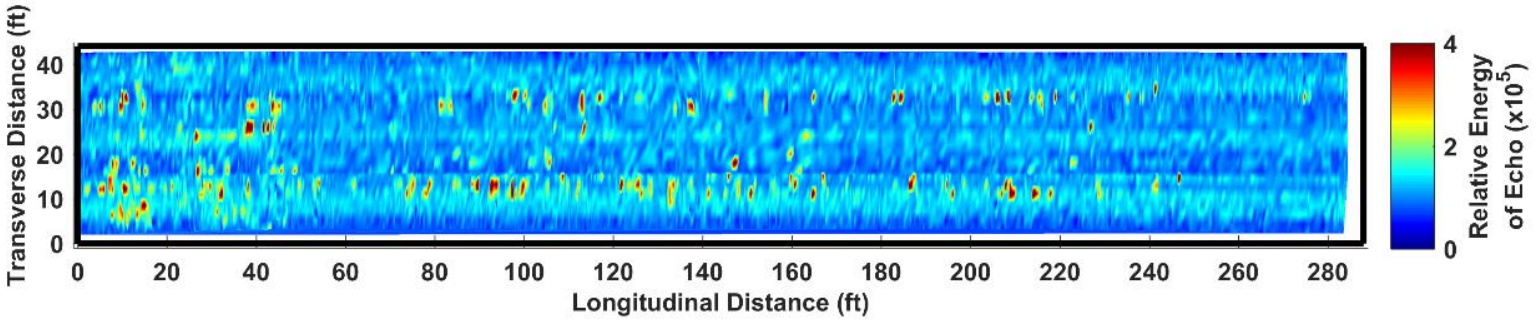

Figure B-4 Impact-echo data for bridge C-725.

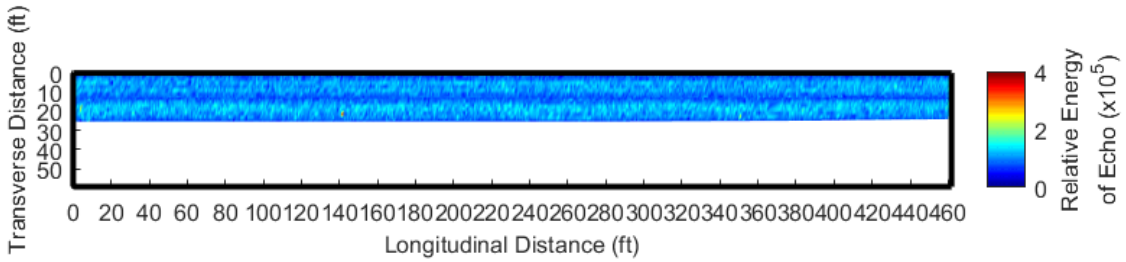

Figure B-5 Impact-echo data for bridge C-757.

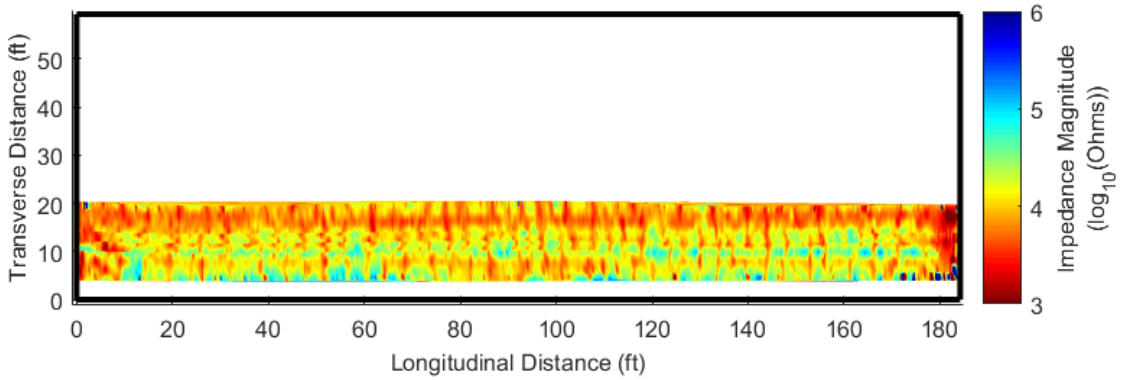

Figure B-6 VEI data for bridge C-759.

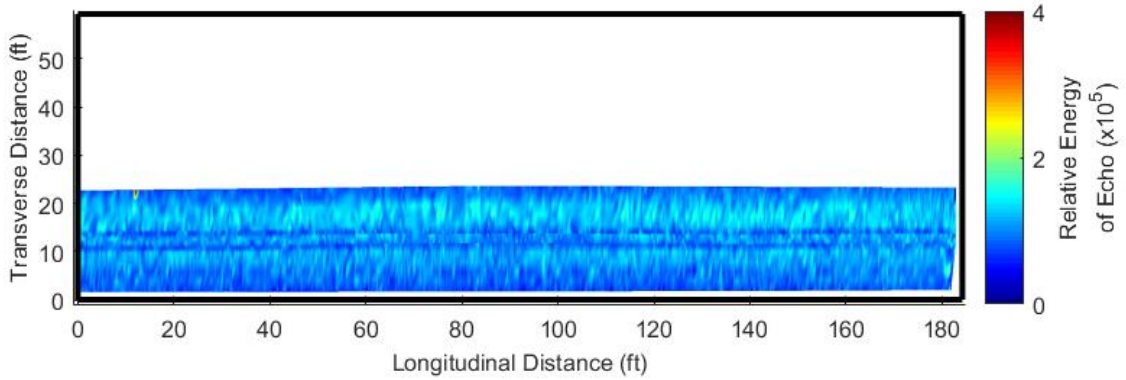

Figure B-7 Impact-echo data for bridge C-759.

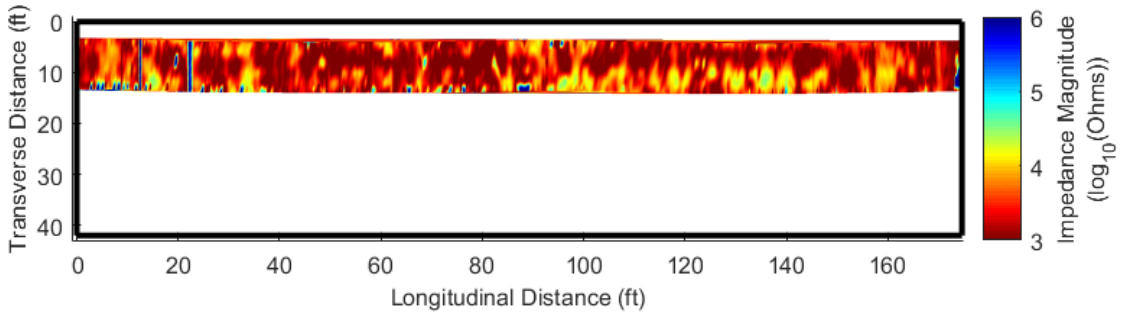

Figure B-8 VEI data for bridge C-760.

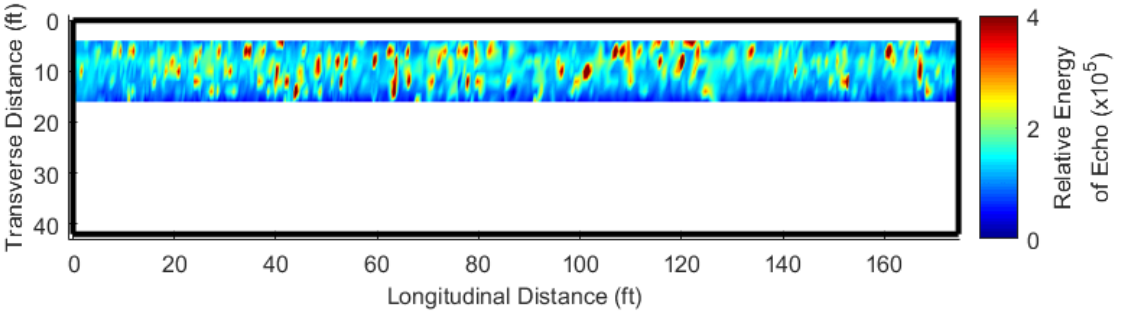

Figure B-9 Impact-echo data for bridge C-760.

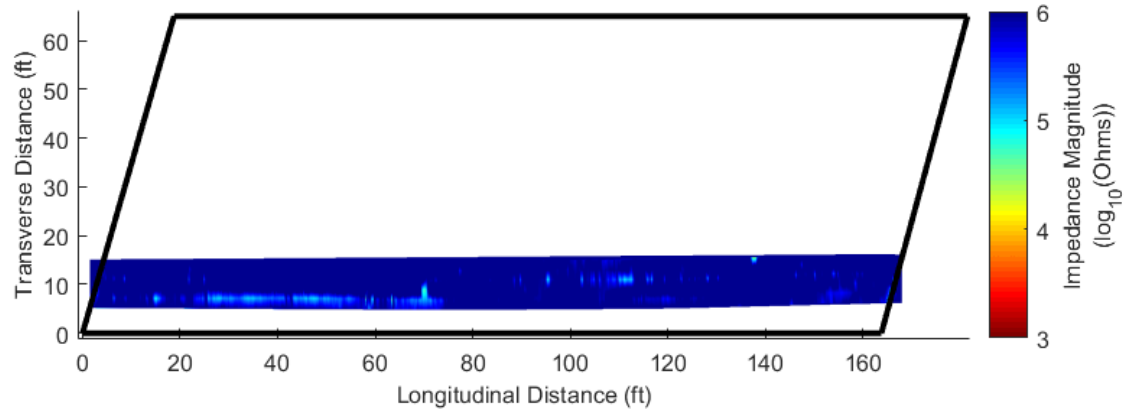

Figure B-10 VEI data for bridge C-794.

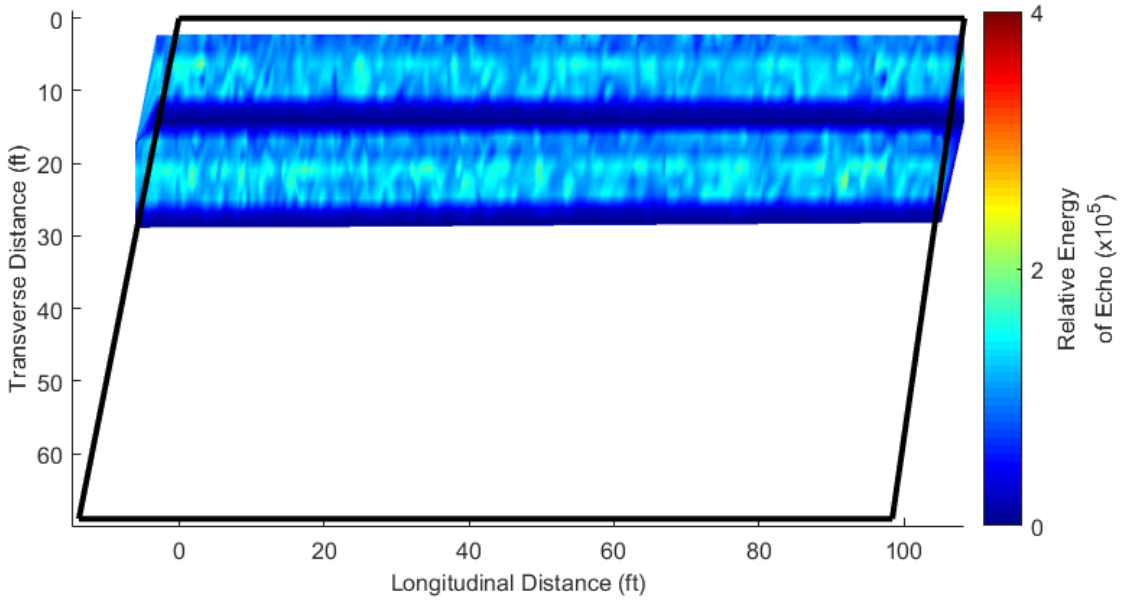

Figure B-11 Impact-echo data for bridge C-931.

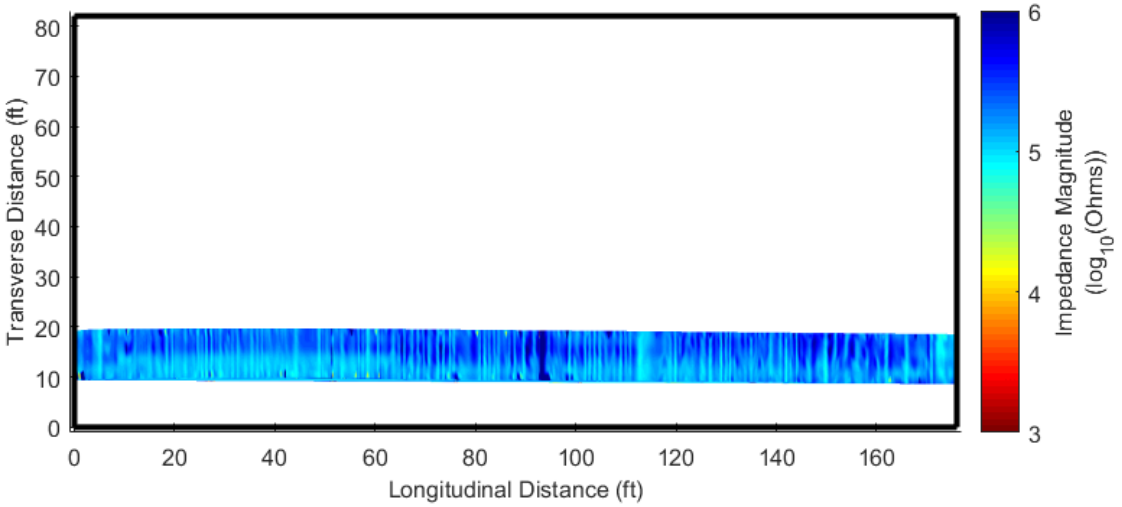

Figure B-12 VEI data for bridge C-953.

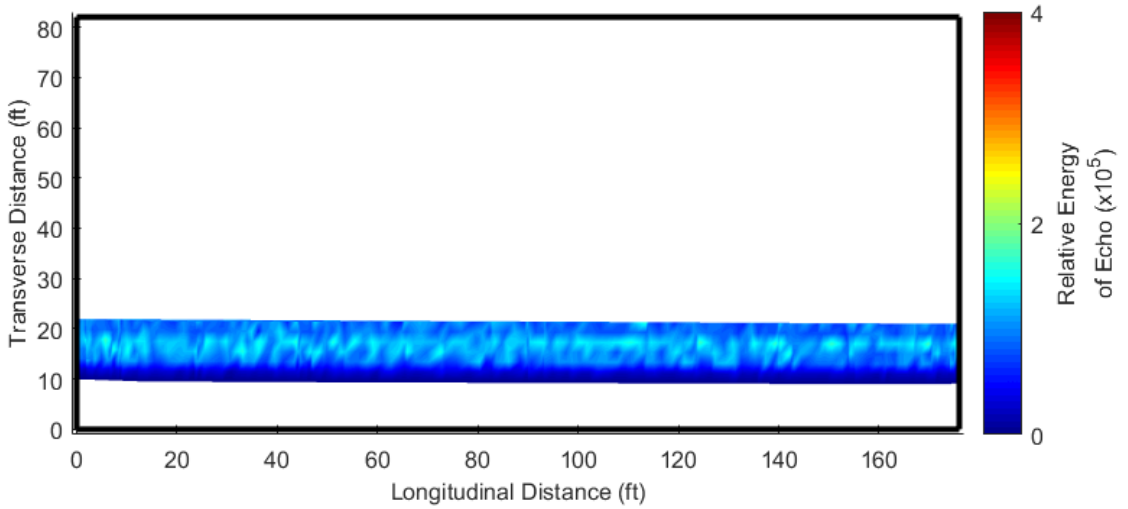

Figure B-13 Impact-echo data for bridge C-953.

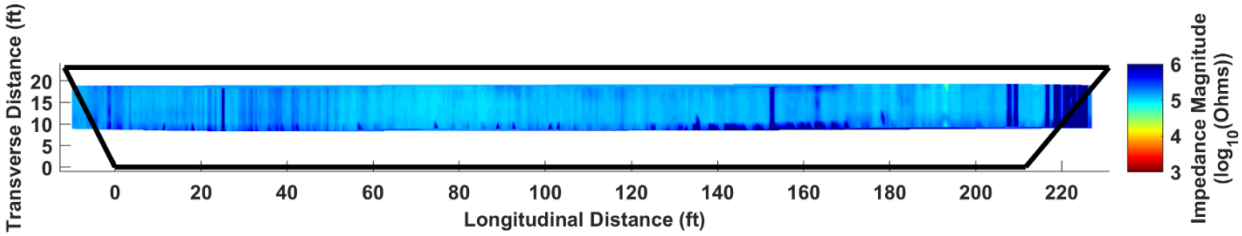

Figure B-14 VEI data for bridge F-53.

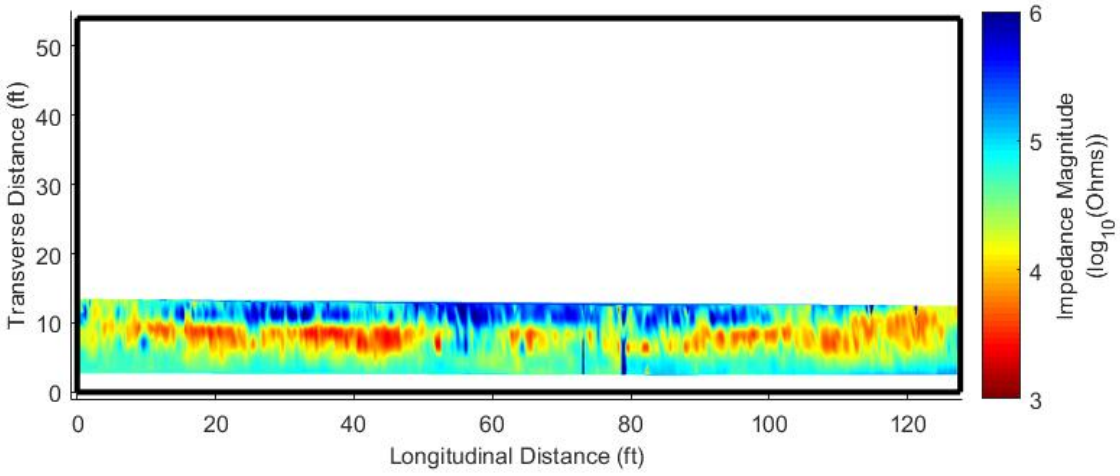

Figure B-15 VEI data for bridge F-476.

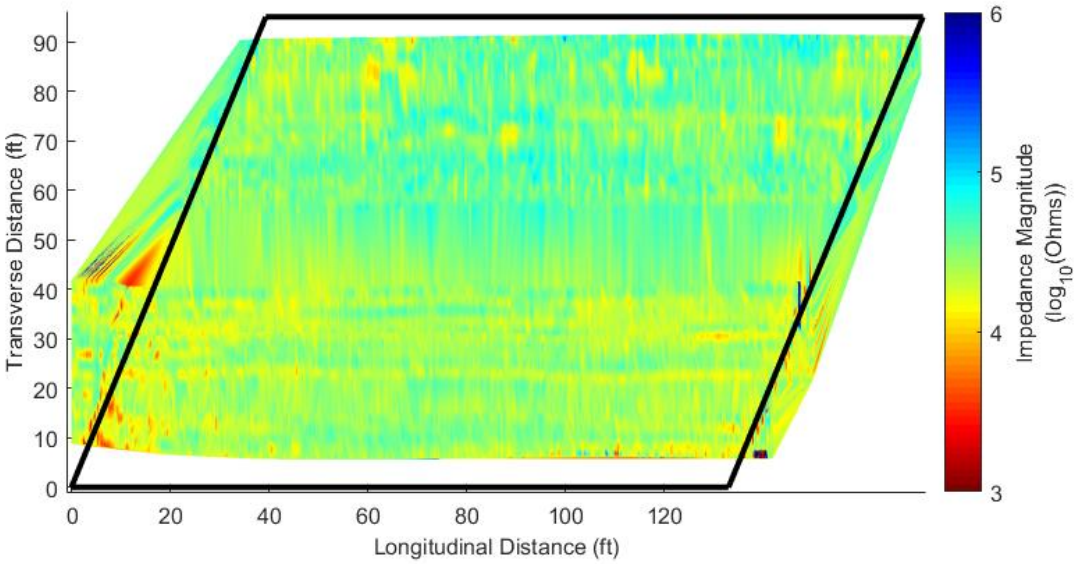

Figure B-16 VEI data for bridge F-562.

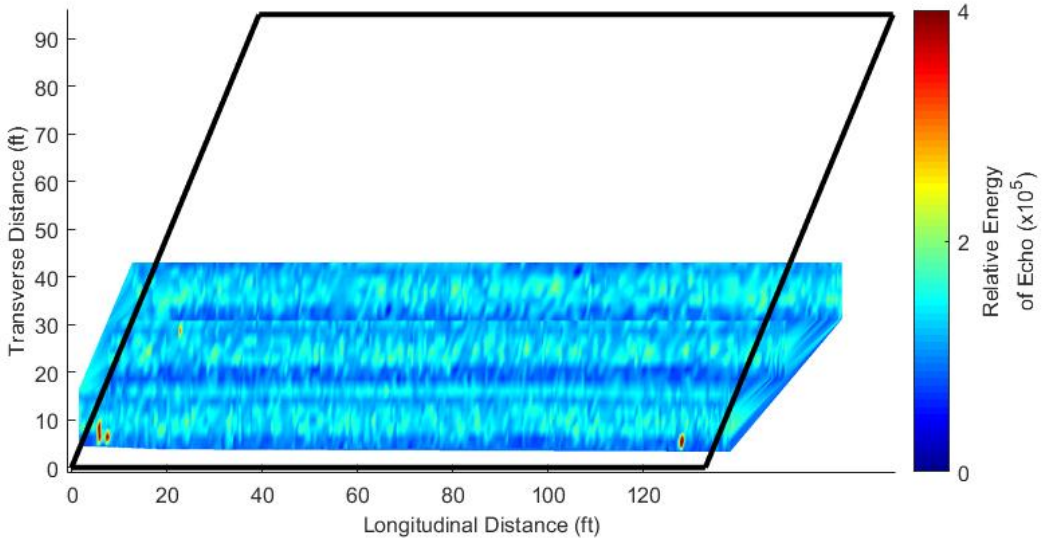

Figure B-17 Impact-echo data for bridge F-562.

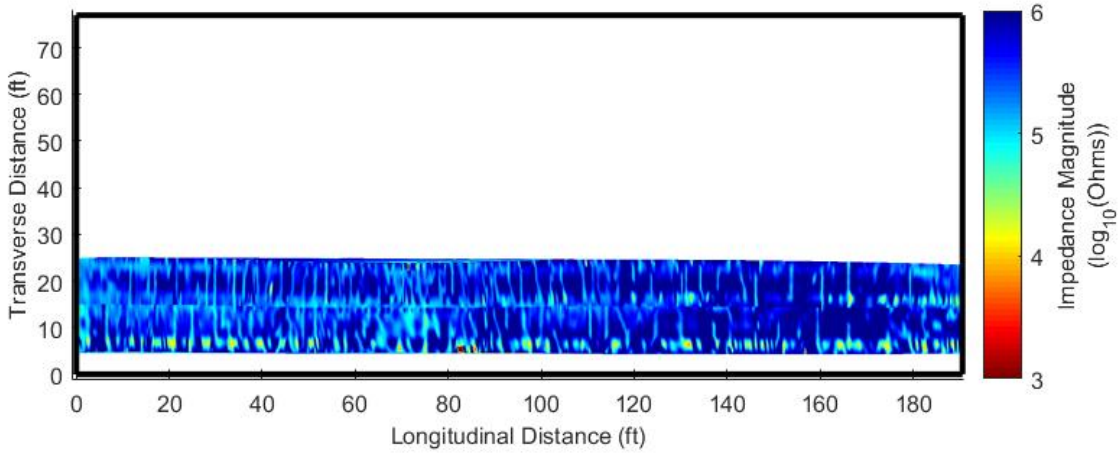

Figure B-18 VEI data for bridge F-738.

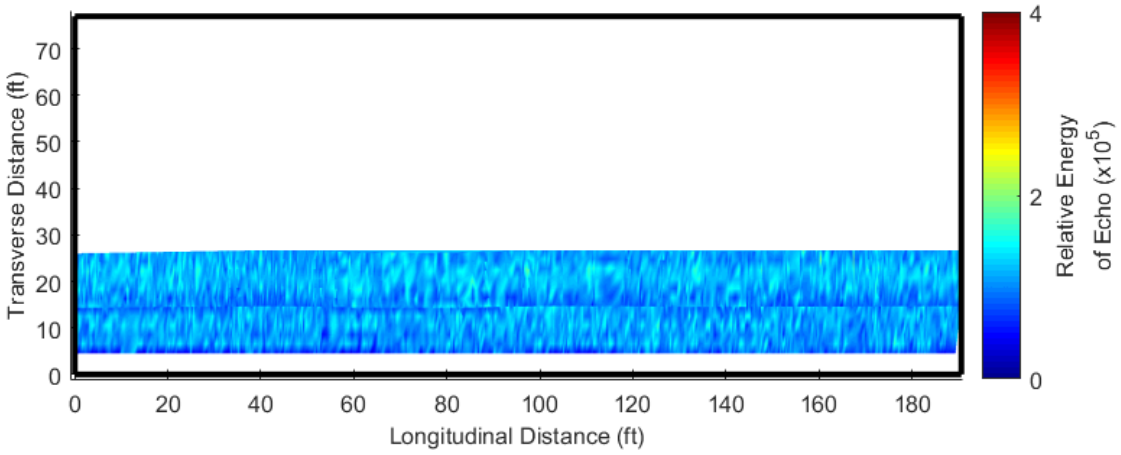

Figure B-19 Impact-echo data for bridge F-738.

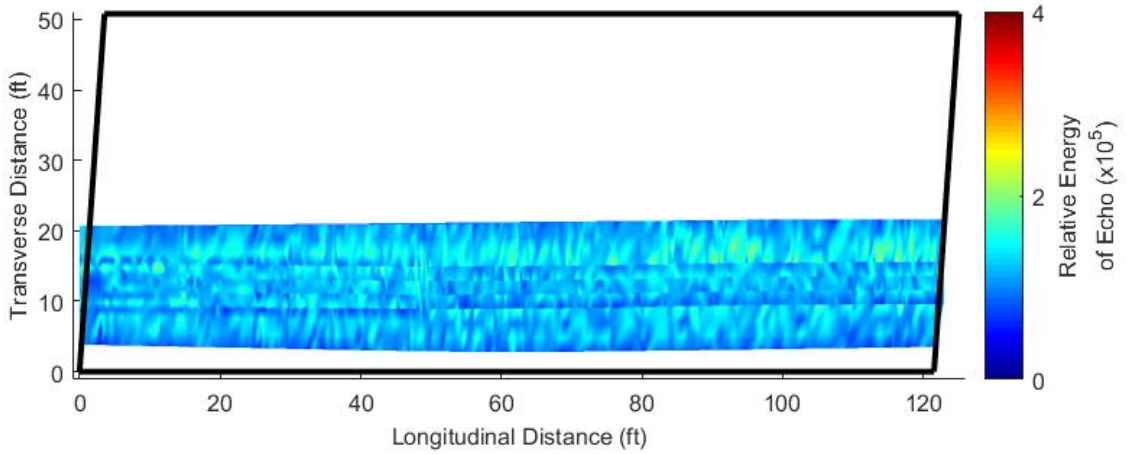

Figure B-20 Impact-echo data for bridge F-799.

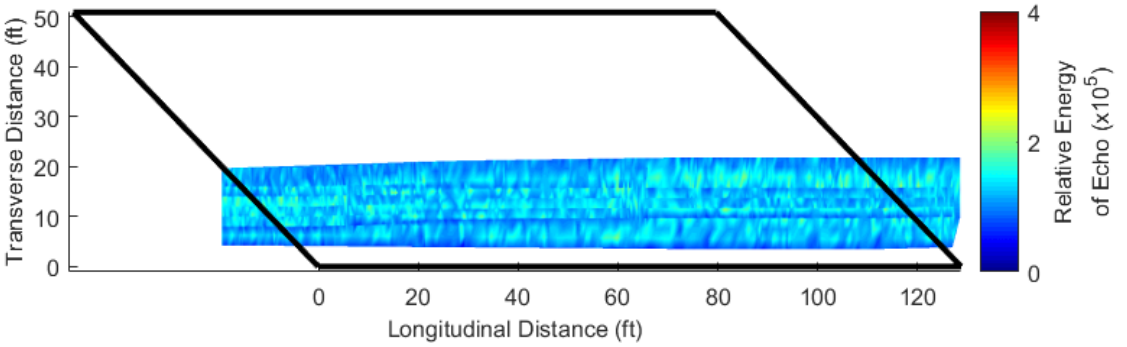

Figure B-21 Impact-echo data for bridge F-800.